CONDUCTIVE CURRENT EARTH MODE COMMUNICATIONS

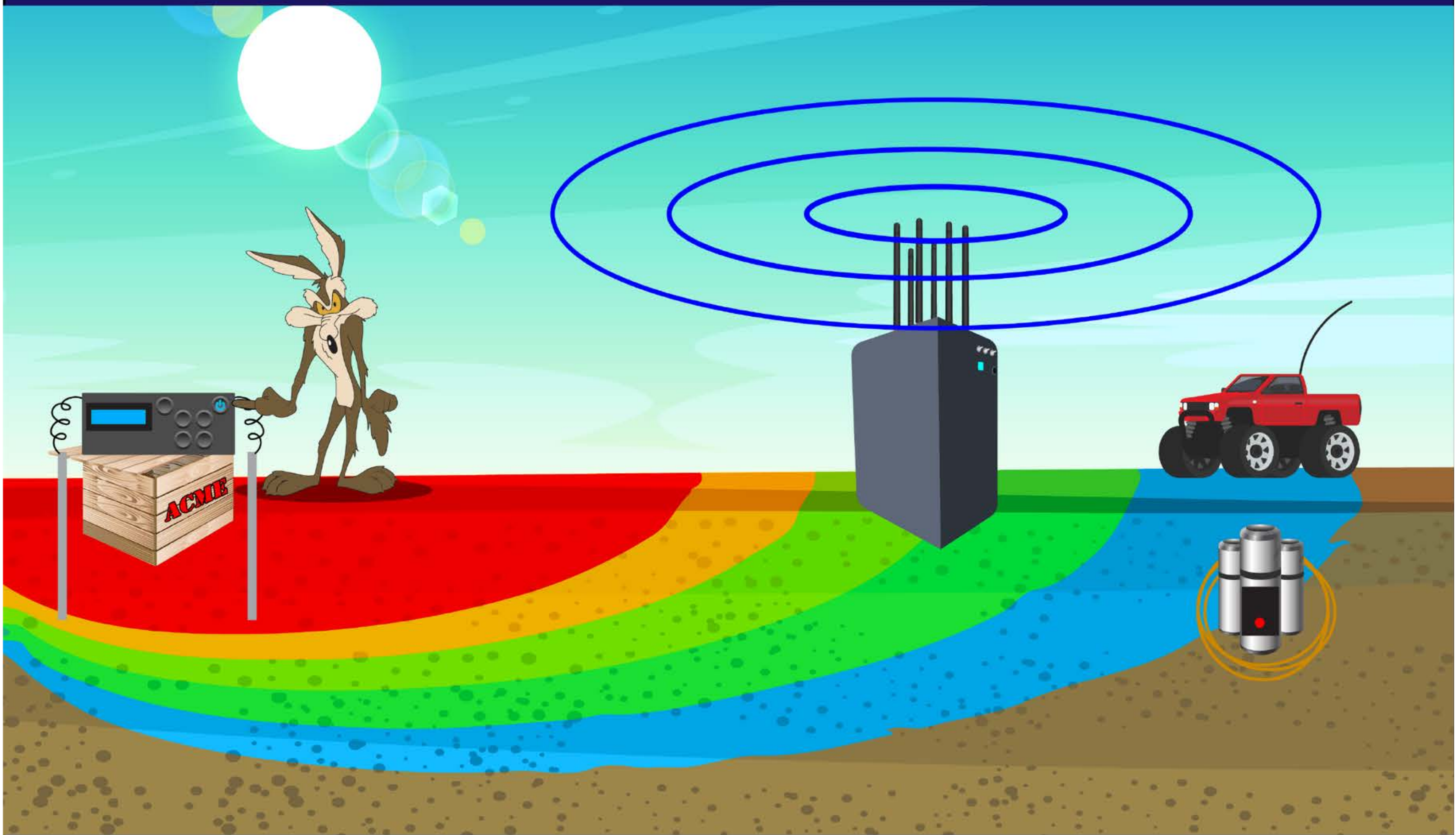

Radio Frequency Jammer
Electronic Counter Countermeasure

ISBN: 978-0-646-83750-5

Chris Rock

Table of Contents

Table of Figures

About the Author

Chris Rock is a Cyber Mercenary who has worked in the Middle East, US and Asia for the last 30 years working for both government and private organizations. He is the Chief Information Security Officer and co-founder of a SIEM platform, SIEMonster.

Chris is an Information Security researcher who specializes on vulnerabilities in global systems. He presented at the largest hacking conference in the world, "I Will Kill You". at DEFCON 23 in Las Vegas. Where he detailed how hackers could create fake people and kill them using vulnerabilities in the Birth and Death Registration systems around the world. Chris also presented "How to Overthrow a Government" at DEFCON 24, working with the coup mercenary Simon Mann.

Chris is also the author of the Baby Harvest, a book based on criminals and terrorists using virtual babies and fake deaths for financing. He has also been invited to speak at TED global.

Preface

This book focuses on Electronic Counter Countermeasures (ECCM) that defeat jammers in an IED setting. The technology also provides secure underground communications in a jammed environment for Underground Internet of things (UIOT) or a secret communications vector in a traditionally unused Near field H-Field spectrum at greater distances.

Our role as security researchers is to increase product security by studying flaws in these systems, no matter how sensitive the technology. In previous research, I focussed on the Birth and the Death Industry and well as targeting commercial and government systems to in effect a potential coup. This topic focuses on detonating an IED in a jammed environment but is more likely to be used in assassination of high value targets with commercial or military explosives. As we focus and identify flaws in systems whether technical or process, we thereby strengthen that system.

Far-Field communications using similar probes has been around for over a century to communicate between WWI trenches after comms lines were cut. However, research slowed down when wireless atmosphere communications at greater distances took the main stage. Using this previous research, we will extend and apply modern Signal to Noise Ratio equipment and apply Near Field Communications. Near Field Communications or NFC is used in phones or payment card systems for short-range communications; however, we will extend this range out to multi kilometres to provide secure underground communication techniques with advanced modulation techniques.

Before I entered Information Security and worked in physical security, a retail chain was dealing with the theft of popular clothing items. So, the countermeasure to theft was installing a fixed dye pack, that if pried off, covered the garment in dye and unwearable. The shoplifters would then steal the item and put the garment in the freezer to freeze the dye pack before prying it off to stop garment from spoiling. The store then placed anti-freeze in the dye packs to counter criminals from freezing the dye. This cat and mouse game further strengthens the original countermeasure to theft. This paper which focuses on Electronic Countermeasure (ECM) and Electronic Counter Countermeasure (ECCM). is like the above using modern electronic techniques. This paper aims to increase the security measures in jammer products.

The security researcher is starting to gain traction in our industry. As more and more security researchers start documenting and presenting their security findings, we must all rise to a more professional level than our predecessors in the material we release. If we are to call ourselves researchers, we need to apply what other industries do, for example, in science or medicine. We must draw in academic, government and industry experts' books or papers to support or complement our own findings. We must work together with additional evidence, proving or disproving our research in a supportive way. I hope the next generation of researchers contribute and better this research with their ideas and fieldwork.

Introduction

Improvised Explosive Devices (IEDs) account for over 70% of modern battlefield casualties. (URSANO 2018) Electronic Countermeasure (ECM) departments within the military spend billions of dollars annually developing solutions to counter the IED threat and other adversary systems like radar and anti-missile technology. Jammers are one example of ECM against IEDs.

While IEDs can be triggered by the Victim, Timer, and Command, this paper will focus on the command remote control (RC) method for precise assassinations.

Terrorists detonate RC-IEDs using cell phones and other radio frequency devices like garage door openers, children's toys, and doorbells to initiate the IED from a safe distance. To combat the growing threat of wirelessly detonated explosives jammers, military jam these frequency jamming ranges from 0.1 MHz to 6,500 MHz preventing the IED from receiving the RC signal to detonate. Jammer technology is designed to flood the desired frequency to block technologies such as cell phone 3G/4G/5G signals in prisons and movie theatres and blocking IED remote detonation signals, protecting military convoys and VIPs as well as communications in the commercial sector. Jammers operate in the Far Field zone.

The frequency bands under 20 MHz are not seen as a risk because of the large antenna requirements. Very low frequency (VLF) and extra low frequency (ELF) frequencies require large antennas, 180ft-3000ft arrays because of the wavelength size. There are however jammers dedicated for 100 kHz to 20 MHz spectrums operating in far field zones.

However using earth mode communications, we can create a magnetic field in these low frequencies and communicate over near field region instead of far field.

The payment industry uses Near field communication (NFC) technology for short range tap and go payment methods and many organizations use NFC in proximity cards to enter buildings. NFC uses Near field magnetic fields at 13.65MHz with a short communication range of 1-5cm. But at 2kHz the Near field zone is extends theoretically to 75km.

Using a custom-built VLF/ULF transmitter (Tx) and receiver (Rx), we will look at using the earth's crust as a conductive current as an antenna. The Tx/Rx uses advanced modulation techniques in Near-Field, H instead of Far-Field E and communicate through the ground securely from 1-11km away in the sub 9 kHz range. Using this technology, we will trigger an RC-IED device in a jammed environment to detonate the IED at a distance.

Building on this research, we will use the Tx to send encrypted data messages to the Rx and decrypt the message, using the earth's crust as a secure transmission medium between 30-300 baud rates. This technology can also be used for underground mining communications as the signal transmit through the earth to communicate with trapped miners or used in underground IOT applications like temperature and water sensors in agriculture. Because NFC has a radiative/reactive zone we can also transmit power through the earth to a waiting RX to power this device at shorter distances.

Improvised Explosive Device

An *IED* is an effective tool used against the larger, more equipped enemy with modern military force such as tanks, artillery, and aerial bombers. The *IED* gives the smaller force the ability to cause casualties against the superior force without direct engagement.

The *IED* is cheap to build and can be used to kill and maim soldiers on patrol, in a bar. or a convoy driving down a road. Military ordnance such as artillery shells that are modified into an IED as well as manufacturing chemicals that are in easy supply provide the adversary with most of the equipment, they need to manufacture the *IED*.

IEDs are also used to target civilian targets for political purposes. According to a report by the United Nations (U.N) in 2014, 4300 IEDs caused over 65,000 casualties and three quarters of these were civilian. (United Nations 2014.)

The purpose of this chapter is to understand the make-up of an explosive or *IED* and how the remote-controlled (RC) switch fits in from the adversary. *IEDs* are triggered by timers or pressure plates for example, but the focus of this paper is on the remote-controlled RCIED component triggered by using the RF spectrum.

Anatomy of an IED

An IED is compromised of the following components.

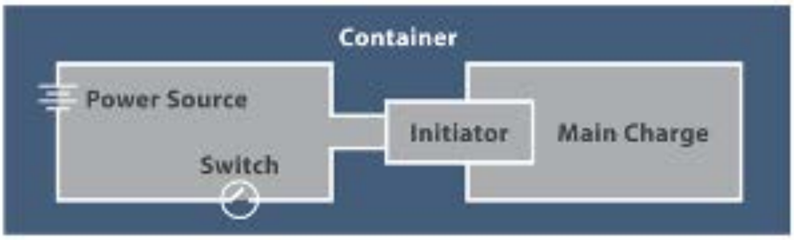

Figure 1: IED components (United Nations 2020)

- Container
- Power Source
- Switch
- Initiator
- Main Charge / Explosive

In the below diagram, some additional components have been added to the IED to increase the number of casualties. Shrapnel, such as ball bearings, nails, screws is an optional component. Another optional component is a booster. A booster is used to trigger the main charge in an explosive where the initiator will not suffice.

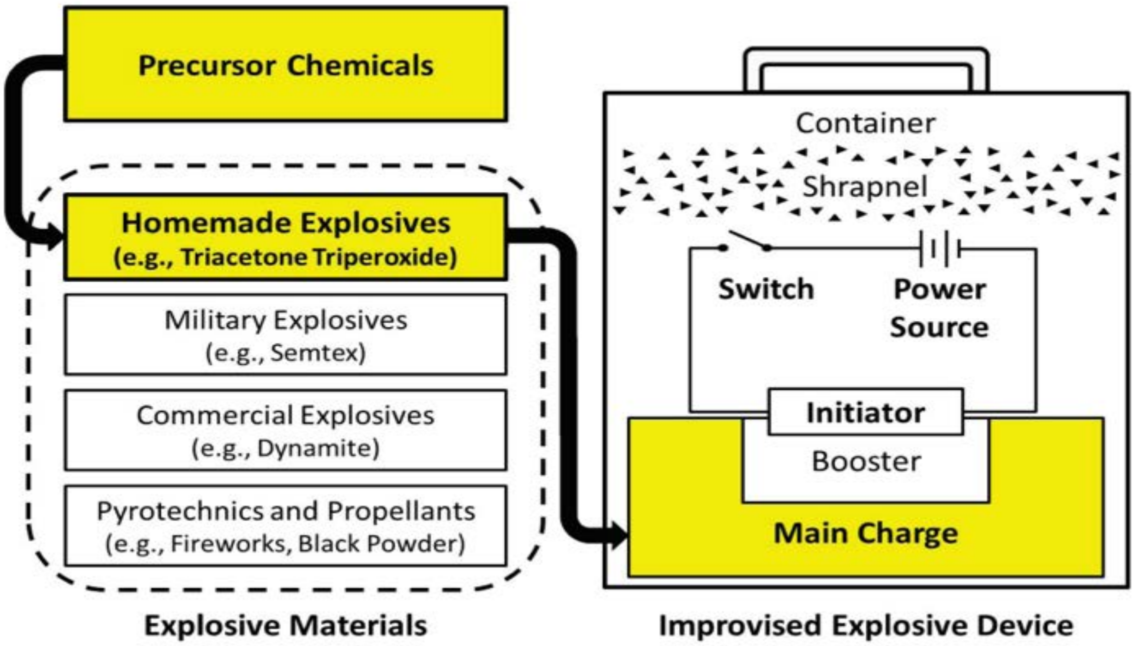

Figure 2: (NATIONAL ACADEMIES OF SCIENCES AND MEDICINE 2018)

Container

The container of the IED can serve multiple roles. It can be used to provide a way of carrying the IED to the target or protecting it when burying it in the dirt to target a convoy or used in other ways.

For example, Ted Kaczynski, the Unabomber who terrorized the U.S with IED's sent in in the mail service or placed in person, used a Cigar box to contain his explosives or, in one case, hidden in a book. This method would be described, as concealment as illustrated below.

The IED used in the Boston Marathon were confined in a pressure cooker. The pressure cooker confined method is used to confine the explosion and amplify the effect with increased pressure.

For example, a steel pipe bomb container would be classified as 'Confinement' and material used 'Metal' and type 'Pipe' in the below example. In this case, the steel pipes could also be used as shrapnel to cause more damage.

A dead cow on the side of the road with a hidden IED inside it as a container is classed as 'Concealment' material 'Organic' and type 'Carcass'. In this example, the sole is conceal and protect the device from detection.

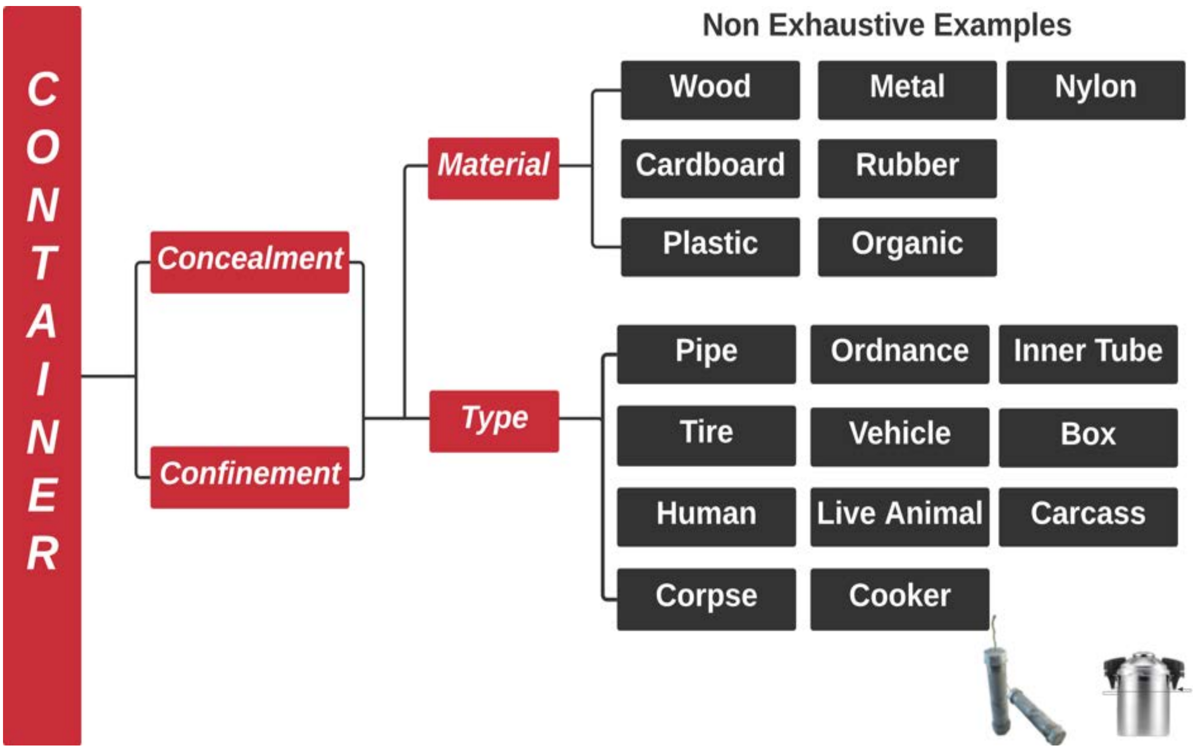

Figure 3: (United Nations 2020 – Adapted by Author)

Power Source

The Power source is a critical component of the IED. Its role is to facilitate the closing of the switch that triggers the initiator. The power source takes on two forms electrical or mechanical. Electrical is simply an AC/DC power supply like a cart battery, cell phone battery, or a capacitor.

The other power supply which does not require batteries is mechanical energy. An example of this would be a spring, coil, rubber band or kinetic energy.

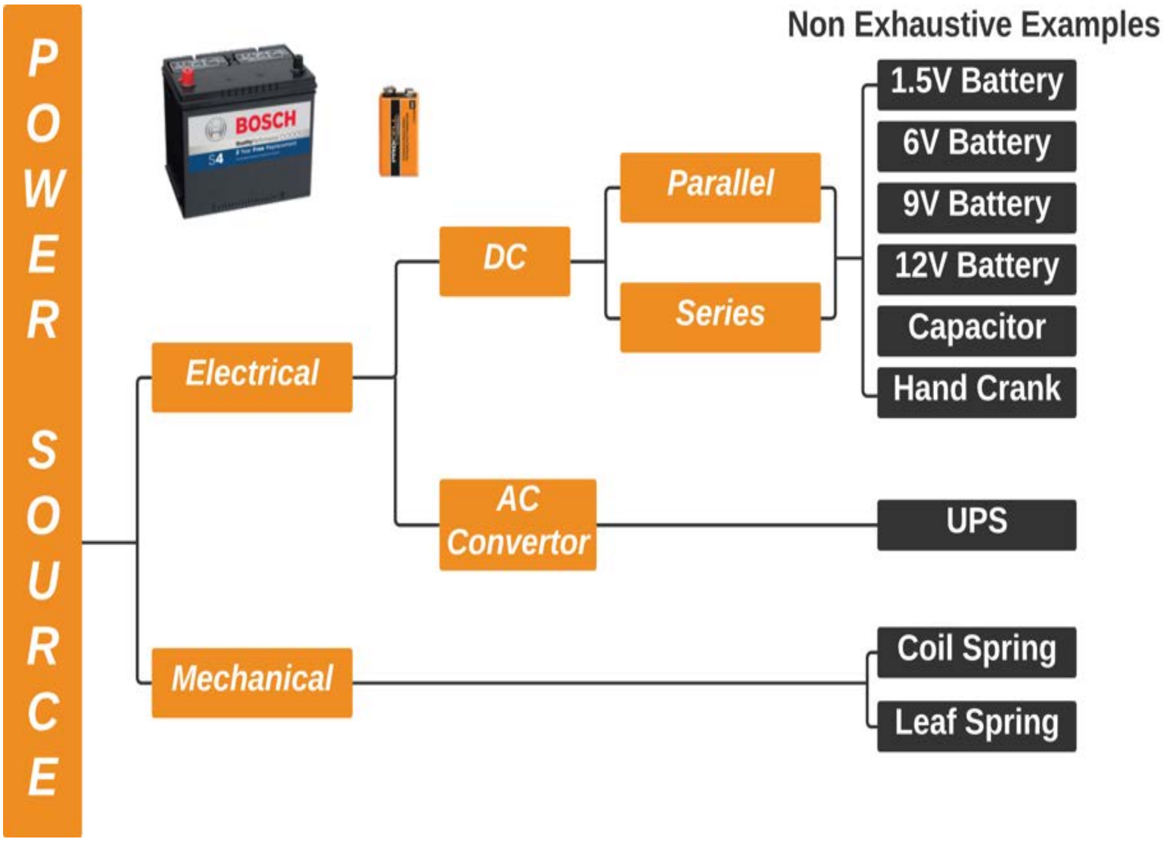

Figure 4: (United Nations 2020 - Adapted by Author)

Switch

The switch in the IED is responsible for changing the IED state to armed or firing and will be the focus of this book. The switch is what triggers the start of the IED process whether it be the victim opening a cigar box that triggers the IED or a cell phone that triggers the explosion when a call is made to it.

A switch can take two roles, firing switch, that triggers the IED, or a two-part process, arming then firing. Arming allows the IED not to be triggered until the IED is safely in place.

The switch then has three categories to begin the explosion.

- Command
- Time
- Victim operated

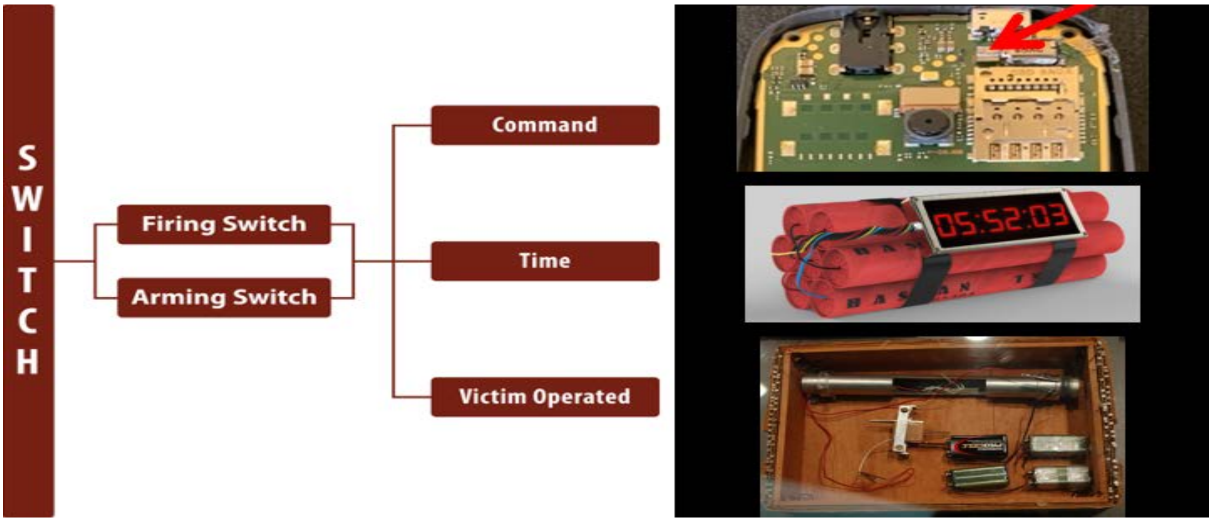

Figure 5: (United Nations, 2020 - Adapted by Author)

Command

Command provides the attacker/terrorist to control the timing of the explosion. An example of command would be a cell phone call to the IED, a garage door remote control, or a doorbell. It is this command method that this paper will focus on. Below is a list of command-based switches.

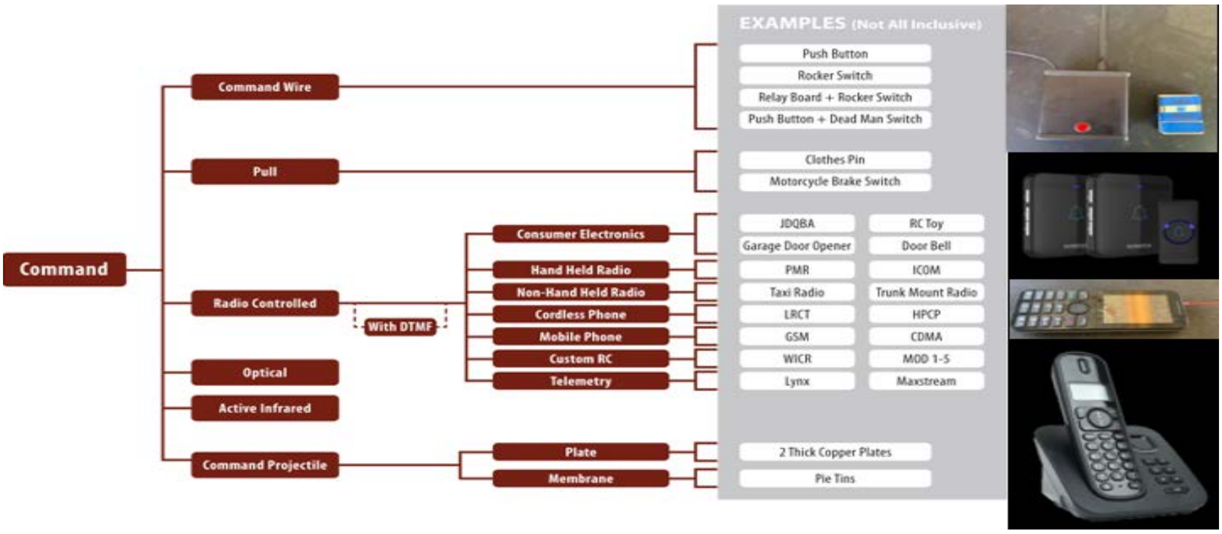

Figure 6: (United Nations, 2020 - Adapted by Author)

Time

Time-based switches on an IED could be a countdown cooking clock, a washing machine cycle switch. Other time-based examples involve chemical reactions. During World War 2, a British chemical-based pencil detonator named the Number Ten delay switch was used (Illustrated below). It was made of brass with a copper end and contained a glass vile with cupric chloride. The attacker would crush the copper section of the pencil, breaking the glass vile and releasing the acid that would slowly burn through a small wire that would trigger a detonator/initiator - (discussed in the Initiator section).

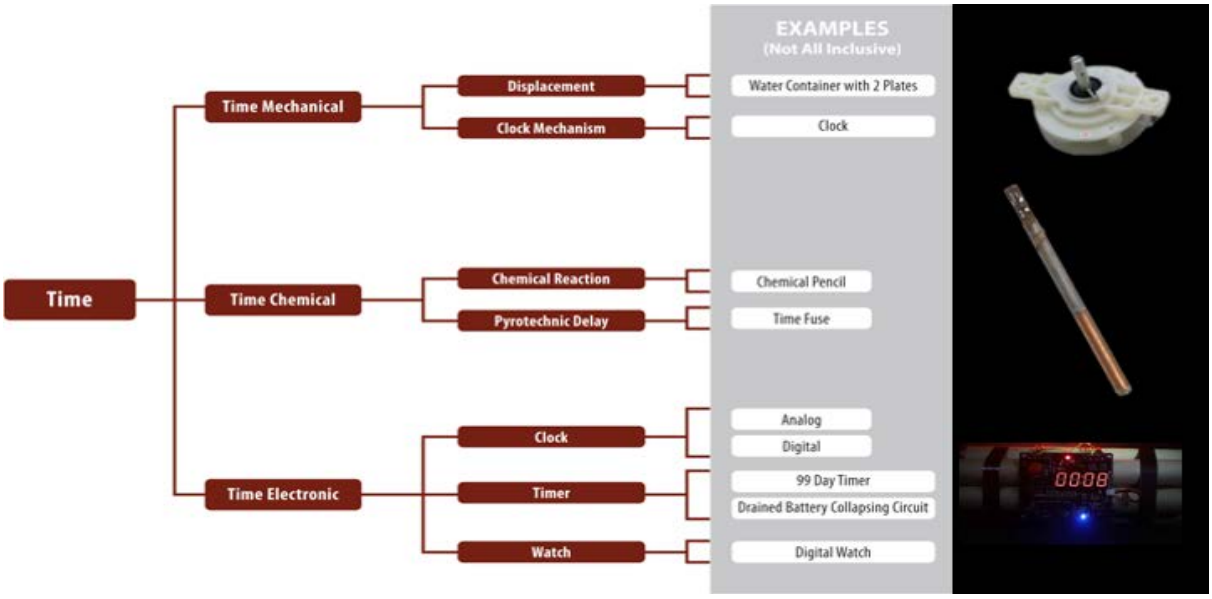

Figure 7: (United Nations 2020 - Adapted by Author)

Victim

The third switch classification is *victim operated*. The victim will trigger the IED based on their response. This could be the victim opening a letterbox to get mail, a cigar box like what the Unabomber used, or breaking an infrared beam across a doorway. It could also be used as a switch that a suicide bomber presses, triggering the IED.

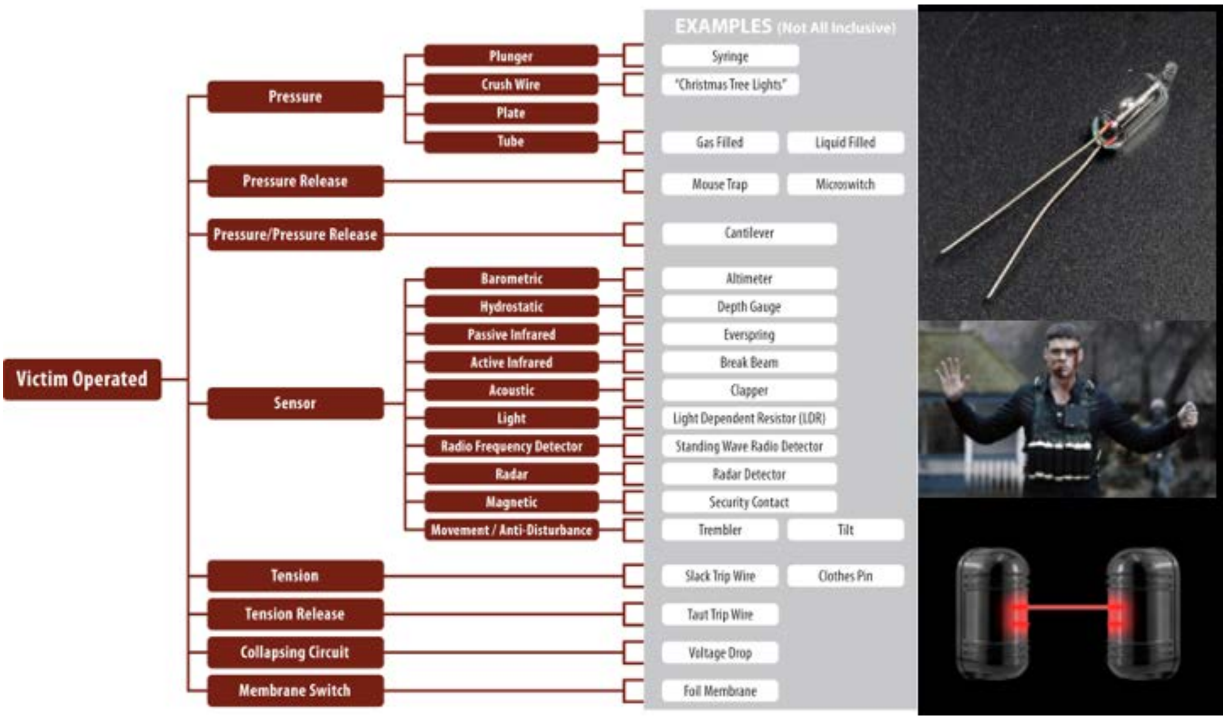

Figure 8: (United Nations 2020 - Adapted by Author)

Initiator - Detonator

The initiator component of the IED is sometimes referred to as the detonator is a small explosion/force that triggers the main explosion. Some examples of the Initiator are Mercury Fulminate, Lead, or Silver Azide. These ignitors are highly volatile and are great ignitors to the primary explosive. Some IED rudimental but effect initiators are fuses, match heads, and black powder.

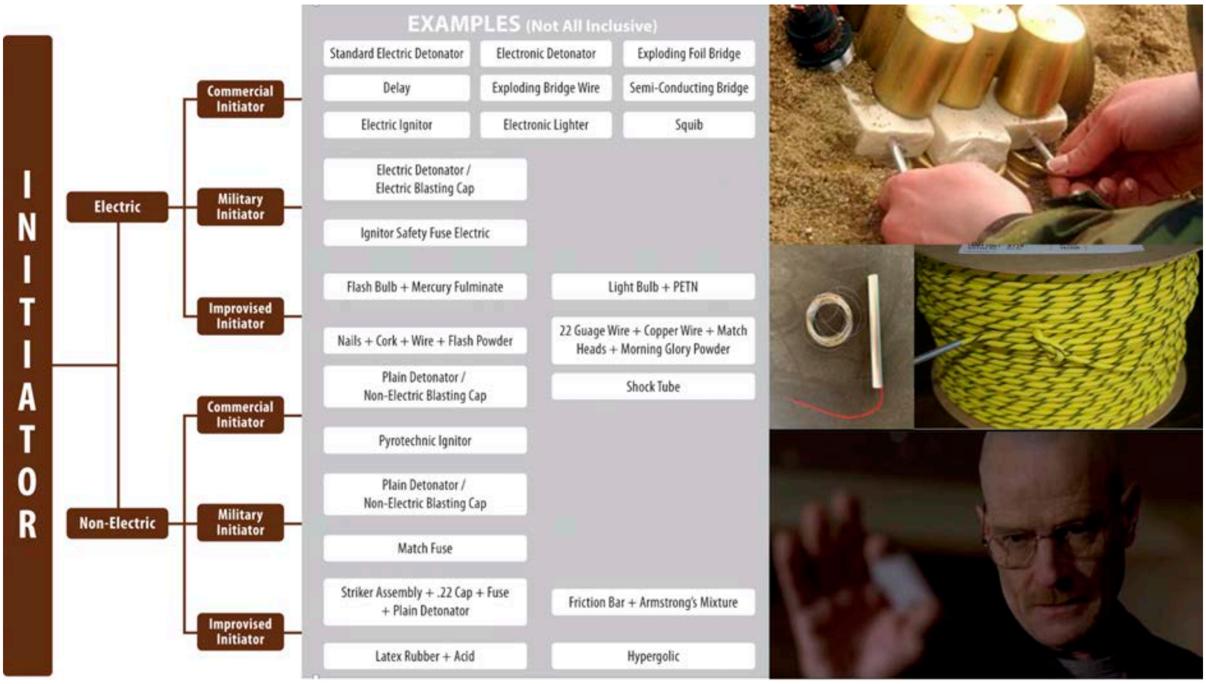

Figure 9: (United Nations 2020 - Adapted by Author)

Why do we need an initiator and not just the primary explosives? Some primary explosives must be triggered first by smaller initiators. For example, C4, a common military explosive, cannot be triggered by fire, bullets, or elemental force. Shockwaves must first initiate it commonly found in military or commercial detonators.

There are three types of imitators.

Non-Electric - This is a shock tube used to initiate the main charge in mining where the mining conditions are risky to non-controlled explosions like gas pockets. A non-electric shock wave prevents premature explosions.

Electric - Used in the mining or rock quarry industry to detonate the main charge

Electronic - Similar to Electric but allows for microsecond explosion accuracy

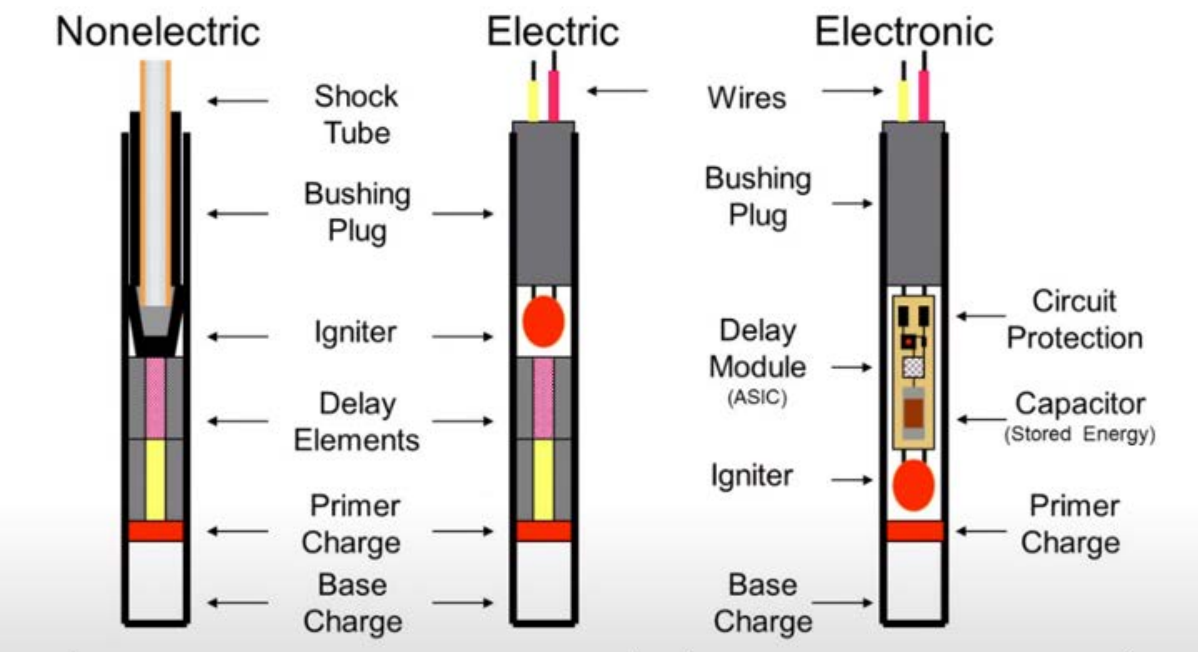

Figure 10: (DynoNobel 2021 - Adapted by Author)

Interesting fact: Swedish chemist, Alfred Nobel, invented the detonator and blasting cap also invented dynamite in the 1880s. In 1888, Alfred's brother Ludvig died, and a French newspaper mistakenly published Alfred Nobel's death notice with the headline "The merchant of death is dead" Alfred Nobel was so shocked that his life works in the explosives industry would be his legacy, setup the Nobel foundation and, in his death, left his fortune to this foundation. The Nobel foundation awards prizes in Chemistry, Physics, Medicine, Literature and Peace in Sweden every year.

Explosives

The main charge or explosives is the force behind the IED. These explosives can come from various sources, including unexploded munitions in a war zone, to fertilizer.

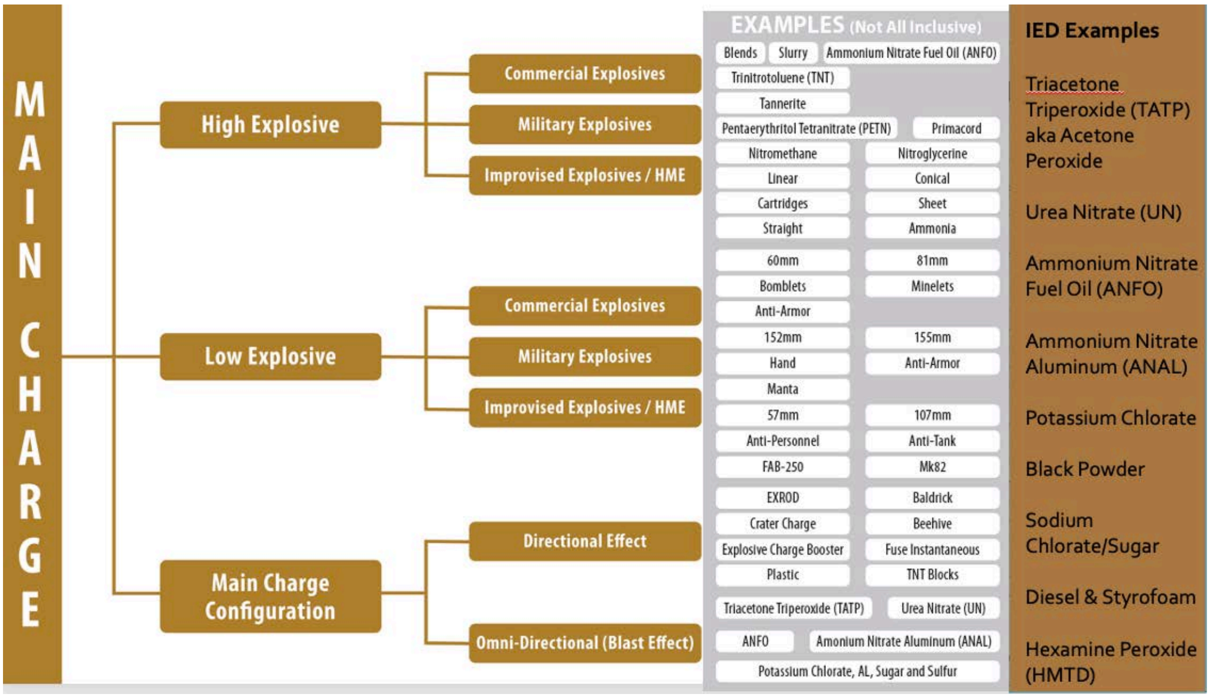

Figure 11: (United Nations 2020 - Adapted by Author)

Radio Frequencies

The first radio transmissions over distance were achieved in the late 19th century by Italian inventor Guglielmo Marconi and Nikola Tesla in separate competing experiments. Their achievements in this field were based on previous work by physicist James Maxwell. Maxwell using earlier work by Albert Einstein, developed a series of equations to formalize the understanding of electricity and magnetism. The reader will see some of the Maxwell equations in this book's VLF/ULF simulation research.

Radio transmission or wireless transmission is based on a transmitter sending electric current periodic waves oscillating to a wired antenna. Think of your home wireless router. The antenna radiates the alternating current as an electromagnetic wave to your phone or laptop's computer aerial. The oscillator determines the wavelength or frequency of what is transmitted. For example, your laptop receives a signal from your router at 2.4-5GHz while your TV via its aerial receives a signal between 54-710 MHz in the United States.

The below diagram shows the different oscillating transmission frequencies for different purposes. What is important to note is the wavelength size for different frequencies. For example, the wavelength size of a TV is between 10cm-10 meters. When you think about the aerial on your roof for TV that is about right.

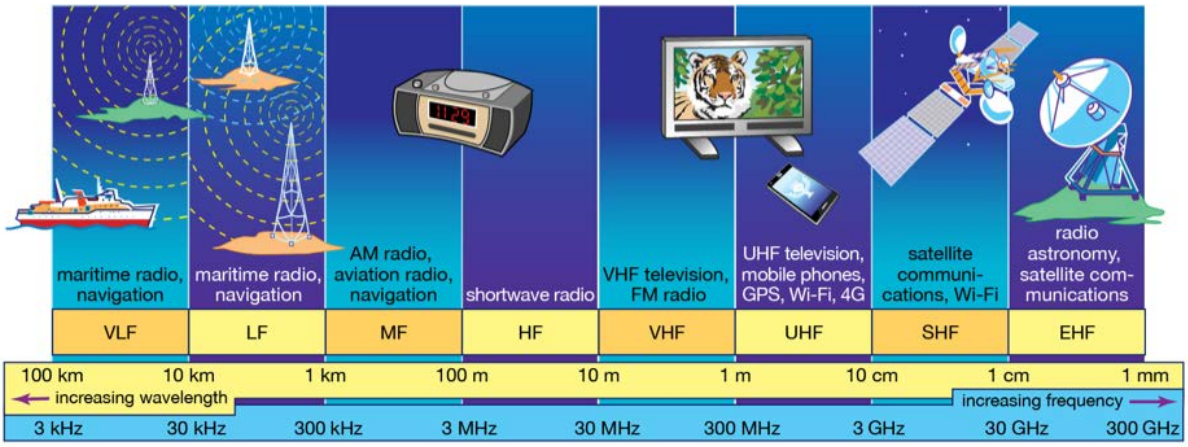

Figure 12: (Britannica 2021)

A rule of thumb for an aerial size is that you need at least 1/10 of the wavelength to receive the signal transmitted That said, the VLF frequency chart above with a wavelength of 10km-100km long would need an antenna 1-10km long and this plays an important part in this paper.

Radio Spectrum

The below diagram is a snapshot of frequency allocation for the United States. This ensures transmission of applications is not sharing the same space. For example, no one wants to have the TV frequency the same as the Mobile phone wavelength frequency.

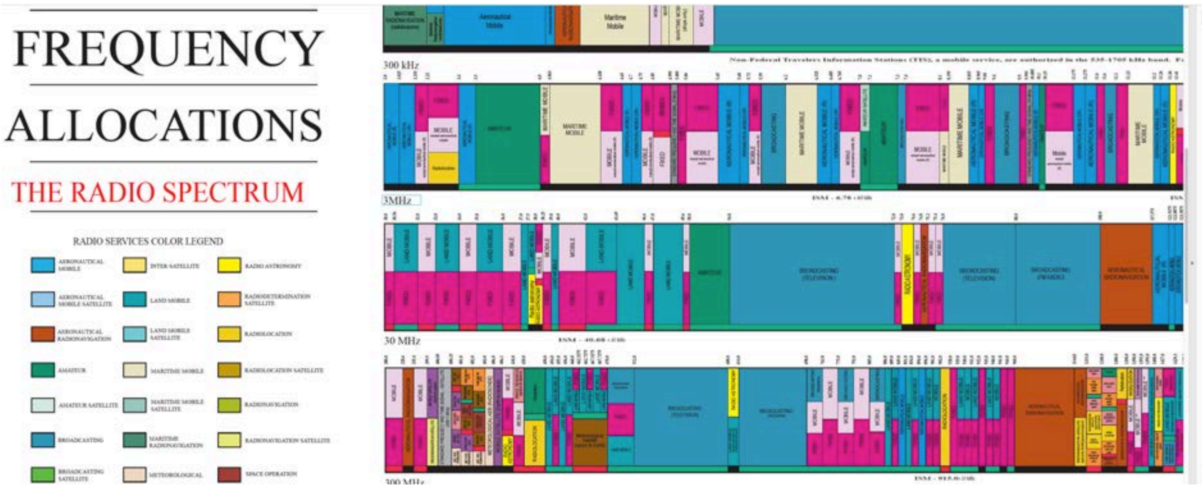

Figure 13: (NITA 2016)

The below diagram shows the size of the wavelength in each application. You can see the radio waves we talked about earlier in the introduction but notice the small wavelengths like X-Ray and Gamma Rays. It is the size of these wavelengths that allow us to see in the human body, for things like broken bones.

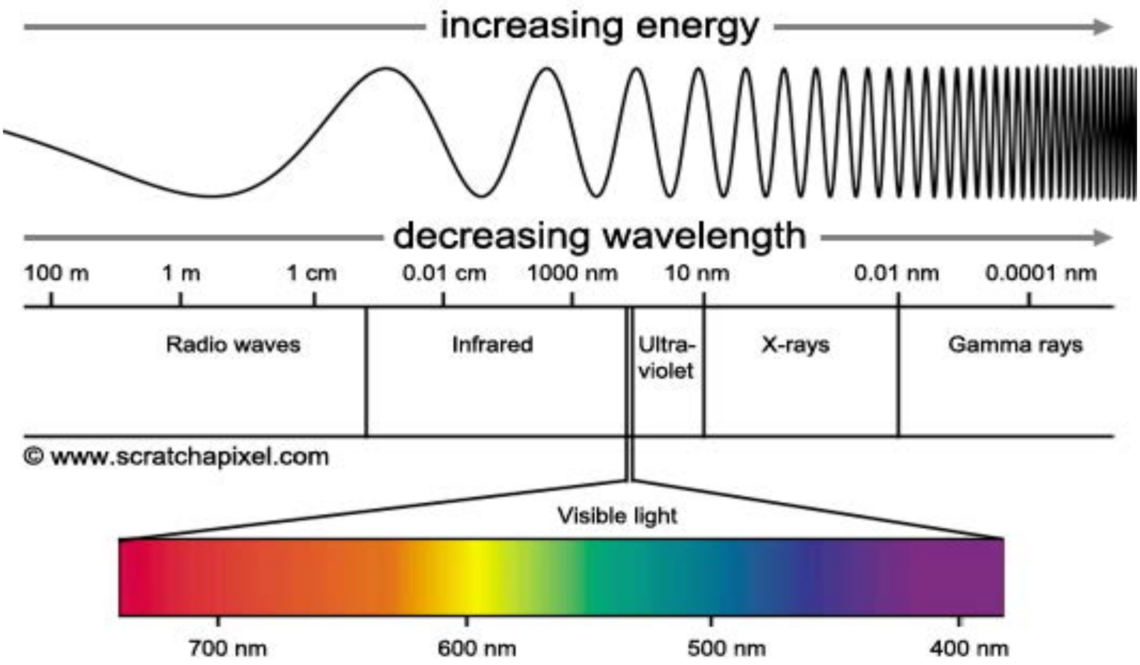

Figure 14: (Scratchapixel 2021)

Wavelengths historically have been placed in categories based on their wavelength size see below. Extremely Low Frequency (ELF) is predominantly used in military applications. It allows land to see communications like communication with a submarine. However, as you can see by the aerial size required to support a 10,000Km wavelength, these arrays are massive. These frequencies can travel around the earth's curve over mountains, through water but bounce off the ionosphere (diagram below for VLF), not penetrating space.

Name	Symbol	Frequency Range	Wavelength
Extremely Low Frequency	ELF	3 Hz - 30 Hz	10,000 km – 100,000 km
Super Low Frequency	SLF	30 Hz - 300 Hz	1,000 km – 10,000 km
Ultra Low Frequency	ULF	300 Hz - 3 kHz	100 km – 1,000 km
Very Low Frequency	VLF	3 kHz - 30 kHz	10 km – 100 km
Low Frequency	LF or LW	30 kHz - 300 kHz	1 km – 10 km
Medium Frequency	MF or MW	300 kHz – 3,000 kHz	100 m – 1 km
High Frequency	HF or SW	3 MHz – 30 MHz	10 m – 100 m
Very High Frequency	VHF	30 MHz – 300 MHz	1 m – 10 m
Ultra High Frequency	UHF	300 MHz – 3,000 MHz	10 cm – 100 cm
Super High Frequency	SHF	3 GHz – 30 GHz	1 cm – 10 cm
Extremely High Frequency	EHF	30 GHz – 300 GHz	1 mm – 10 mm

Figure 15: (BERRY 2018)

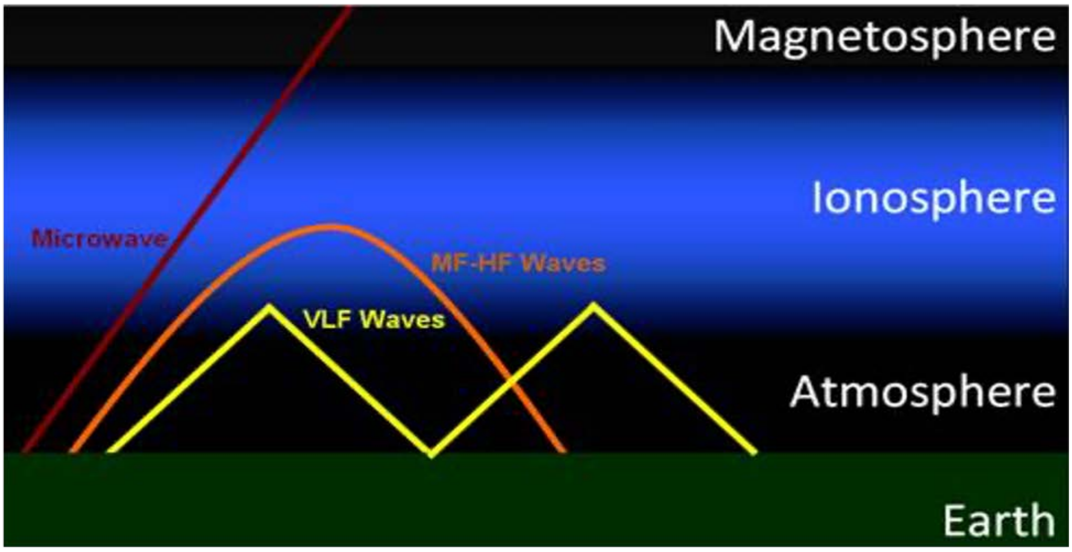

Figure 16: (ESTERS 2021)

The most common bands used today for wireless communications are in the Medium, High, and upwards bands. These bands are sometimes referred to as C-band 20-6000MHz or commercial/consumer bands. These bands are used for things like 3/4/5G Mobile phones, Drones, Wireless Doorbells, Garage door openers and anything that you can think off that use wireless communication. It is also this band that attackers use to set to set off IEDs to target their victims wirelessly, from a same distance.

Figure 17: (United Nations 2020 - Adapted by Author)

VLF/ULF

VLF/ULF Overview

The Very Low Frequency VLF band is between the 3-30-kHz range of the spectrum. The total wavelength for 3 kHz is approximately 100 km long.

The Ultra-Low Frequency ULF band is between 300 Hz and 3 kHz. The wavelength ranges from 1000km to 100km.

"ELF/VLF waves are useful scientifically because they largely reflect at the D region of the Earth's ionosphere (60-90 km altitude) and are thus efficiently guided in the Earth-ionosphere waveguide to global distances. For instance, if you set up a radio receiver just about anywhere on Earth, you can pick up short bits of radiation from lightning strikes halfway around the world. These are called radio atmospherics, or spherics. ELF/VLF waves also penetrate seawater, which has led to their use over the past several decades for communication with submerged submarines at long distances." An introduction to VLF, Stanford University VLF Group.

It is a general guideline that a transmitting antenna should be at least one-tenth the length of the wavelength as discussed earlier for reasonable efficiency and suitable radiation resistance, so the VLF-antenna problem is obvious.

Below is a photo of a large U.S Navy antenna array used to send signals to underwater submarines.

Figure 18: (KEYSER 2007)

In 1968 the military proposed turning 41% of Wisconsin into the largest antenna globally with underground cables with the ability to communicate with submarines all around the world. The project was never approved, but a smaller project, Project ELF was established in 1989 and continued until 2004 to communicate to underwater submarines. Today submarines communicate via VLF via a series of sea buoys as trailing antennas. (COOPER 2019)

TACAMO (Take Charge and Move out) is a U.S military communication system including, VLF and satellite to send information to its nuclear fleet including underwater submarines. A series of 16 Mercury E6-B airplanes based on a Boeing 707 operated by the U.S military. These Mercury planes have trailing ~8km aerials to communicate using VLF to submarines. The pilot performs a sharp pylon turn manoeuvre which turns the trailing antenna into a vertical antenna.

VLF/ULF Earth Mode

Historically texts and studies of earth mode communication use single term reference. According to the NATO Advisory Group for Aerospace Research and Development (AGARD) there are three distinctly different modes that utilize the earth a communication link.

The first approach is "earth current communication" (or up, over and down mode), wherein the electromagnetic (EM) wave travels up to the surface from a buried antenna, thence through the air to another buried antenna. In the second case, a part of the radiated energy from the subsurface radiator will travel towards the interface of earth and air. It will set up secondary waves in reaching the interface. These secondary waves, while propagating as a surface wave, will continuously leak into the earth's surface

The second approach is "deep strata" communication, though stratified rock or under the sea bottom. The EM wave travels along the surface between media with high and low conductivity. Vertical monopole antenna penetrating through media. This method is commonly used in mining where above-ground crew can communicate to their teams underground and detonate explosives underground such as the commercial Blast PED system. Historically they have used leaky feeder systems that are vulnerable to cave-ins.

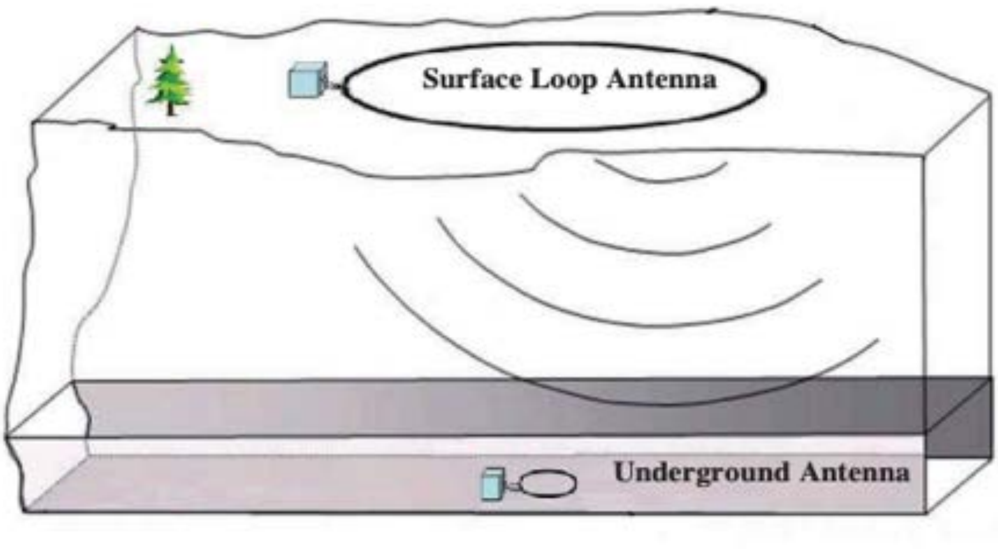

Figure 19: Surface to Underground Antenna

The third approach – "conduction current mode" communication. In this case the current is injected into the earth through a pair of electrodes and the resultant field sampled by the receiver using similar electrodes or loop antenna. The radiation in this case (in the sense of EM wave propagating within inverse square attenuation rate) is extremely low. This fact defines enhanced security of the communication link and quite limited operation range.

Earth current flows are indicated by (I) within the lower hemisphere over the earth's surface. It creates a magnetic field (H). The magnetic field (H) is picked up with a Rx coil (Inductive coupling). The Tx electrodes create the eclectic field, the current flowing within the resistive media defines the voltage drop (V=I*R) between Rx electrodes. Finally, that voltage drop can be measured.

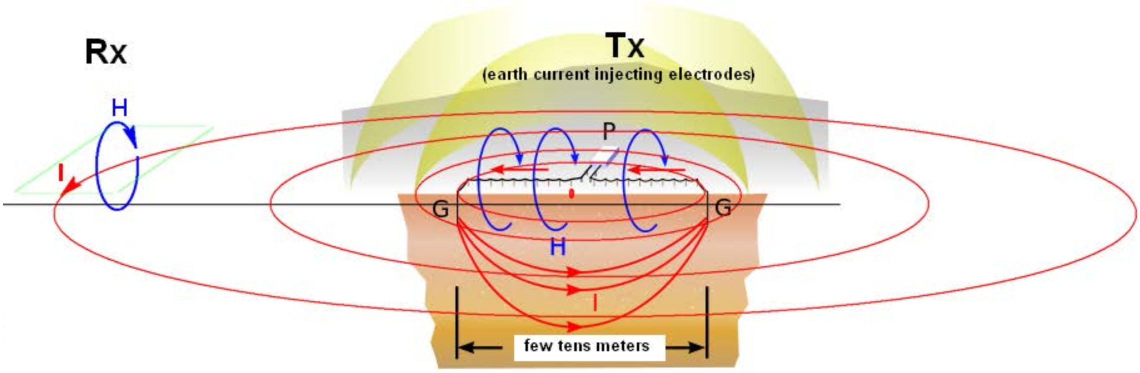

Figure 20: Conduction Current Mode

It is this third approach "Conduction current mode" that this paper focuses on.

Jammers

Overview of Electronic Countermeasures

Communications electronic warfare (EW) is the name applied to activities taken to accomplish the intercept or denial of communications and consists of Electronic Attack (EA), Electronic Support (ES), or Electronic Protect (EP). EA is the EW area that is focused on Electronic Countermeasures (ECM) and will be the primary focus of this paper.

The three principles of EA are jamming, deception, and directed energy designed to disrupt communication on the electronic spectrum. The military use ECM to trick enemy radar, jam signals, or thwart intelligence gathering. With the ever-increasing use of guided missiles, drones and GPS, this research area has never been so crucial on the battlefield ECM has been used. (POISEL 2011)

Historically ECM techniques were used by the British in World War II to thwart the German Airforce and disrupt German radar for the France invasion at D-Day to hide the U.S bombers.

Today the ECM market or Electronic Warfare (EW) for the U.S alone is over 10 billion annually. The counter IED market including Jammers will be worth 2 billion USD by 2022. Australia recently signed a deal worth 250 million dollars for counter IED equipment. (CONGRESSIONAL RESEARCH SERVICE, 2020)

This paper will only provide an overview of jammers' technology as an ECM as there are large numbers of research publicly available and other areas of Electronic Warfare.

Introduction to the Jammer

There are three defined areas used to detonate an IED or bomb device. The three areas we covered off previously were

1. Command
2. Time
3. Victim operated

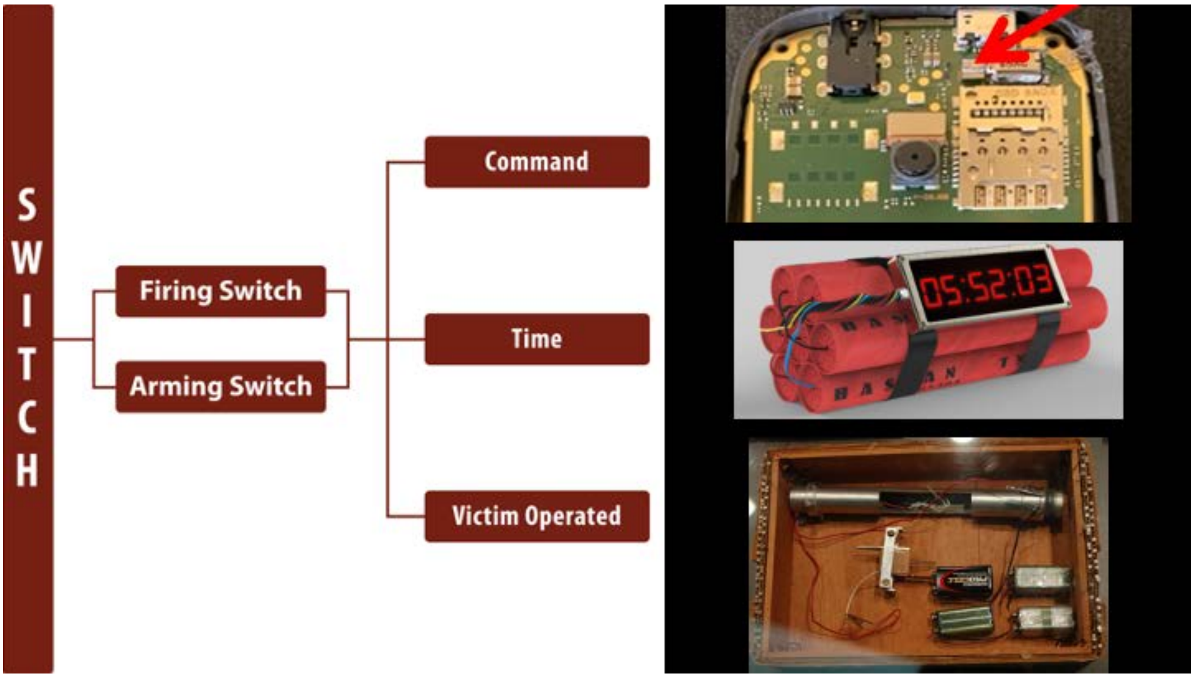

Figure 21: (United Nations 2020 - Adapted by Author)

Time and Victim operated are not covered in detail in this paper. These IED switch mechanisms can be discovered/disarmed using bomb/metal detectors, visual inspection, and disposal robots. The paper is focusses on Command controls, i.e., using the Radio Frequency (RF) spectrum used to trigger IED's remotely such as a Garage Door Opener, Mobile phone etc. Their remote-control switches provide the attacker with precise target and timing of the attack.

For example, a victim operated IED could be triggered by the wrong victim, or a Time attack is not accurate on a moving vehicle or delegate that is late to the podium.

The Jammer, both for civilian and military, is a device that disrupts the attackers signal (Phone, Garage door opener) from reaching the IED device. Police, prisons, and the military use jammers for wide variety of uses. In a prison, Jammers are used to stop inmates with stolen mobile phones to communicate outside the prison. In the private and military sector, jammers are used to stop signals from recording, listening, or setting off an IED.

Jammers come in many shapes and sizes, from small portable jammer blocking 3G/4G network transmissions to Military trucks that block signals in the 20Mhz - 6000Mhz range.

The below diagram is a simple civilian Jammer used to block signals within a small range (20-50 meters).

Figure 22: (PERFECT JAMMER 2021)

Commercial Jammers combine portable, vehicle and stationary application in one system for protection of VIPs against eavesdropping devices that use radio transmitting channels. They are also used to stop RCIED attacks as well as protection personnel during explosive ordnance disposal (EOD) operation. Jammers suppress HF, VHF, UHF, SHF bands, cellular networks, GPS, Wi-Fi etc.

The jammers are designed for single broadband or few narrow bands to suppress digital transmitting standards. They produce a continuous wave signal of a particular wattage to drown out the Tx signal. Customization of operating frequency ranges is available depending on the customer's request and local cellular standards and varies from 20 MHz up to 6500 MHz.

There are specific HF jammers that operate in the 1MHz – 20 MHz range for High frequency radio such as the Purga HF Radio jammer from Belarus or Phantom Technologies HF jammer from Israel. Both jammers operate in the 1.5Mhz – 20 MHz range.

A Commercial product catalogue specifications sample:

PRODUCT SPECIFICATIONS

MODEL NAME		CSU-1000	CSU-3500			
			CSU-3500-M1		CSU-3500-M2	
Operating frequency bands		20-1000 MHz	20-3500 MHz divided by 4 channels:			
			Ch1	20-750	Ch2	750-1000
			Ch3	1000-1700	Ch4	1700-3500
Output power		55W	95W (total)			
Power supply		Build-in battery	Build-in battery			
Continuous operation time on one battery		30 min	30 min			
Power supply voltage		12.6-15V / 220V	12.6-15V / 220V			
Power consumption, less than	Battery unit	300W	650W			
	Power supply	400W	850W			
Dimensions		530x430x220 mm	530x430x220 mm		530x430x220 mm	
Weight, less than		22 kg	23 kg		23 kg	

The device can be customized in accordance with customer request within 20-6000 MHz frequency range with up to 55W output power.

Figure 23: (ELECTRONICS 2020.)

MILITARY JAMMER

Below are the specs for a Thor III System Military Jammer. Note the 3 aerials below for the portable IED jammers on the Military Jammers. Low (20-50MHz), Medium and High Band.

USMC Counter Radio-Controlled Improvised Explosive Device (RCIED) Electronic Warfare (CREW) 3.1 Thor III System

System Characteristics:

TAMCN: A0326
NSN: 5865-01-580-4854
Technology: Digital
Spectrum: Classified
Orientation: Adjustable position for Antennas
Mobility: Man portable / Dismounted CREW
Power: 18 to 32VDC, 2.5A maximum (Low)
18 to 32VDC, 4.5A maximum (Mid)
18 to 32VDC, 5.0A maximum (High)
Distance: Classified
Operational Mode: Standby – System is idle, no scanning or jamming
Operate – System is scanning and jamming as programmed.
Encryption: N/A
Quantity Fielded: 0
AAO: 823 systems + spares (Pending SON)
336 systems (Original AAO)
+ 50 Spares per SONs

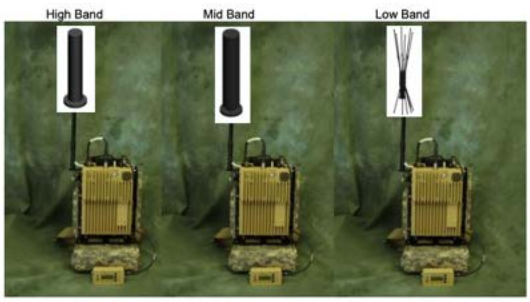

Figure 24: (MILITARY 2010)

The diagram below is the U.S militaries Crew Duke System, that provides protection from remote controlled improvised explosives (RCIED) against a military convoy.

Figure 25: (SRC 2020)

Frequency range

All jammers are based on the effective lower range of 1 MHz and the upper limit of 6500 MHz. however, jammers are manufactured to block out a specific range 1-20MHz or 20-6500Mhz because of power, antenna requirements. Jammers block E-Field or Far field communications not H-Field Near field communications.

The diagram below highlights this effective jamming range but does not cover the lower spectrums because of antenna size and power required to cancel out the VLF wavelengths.

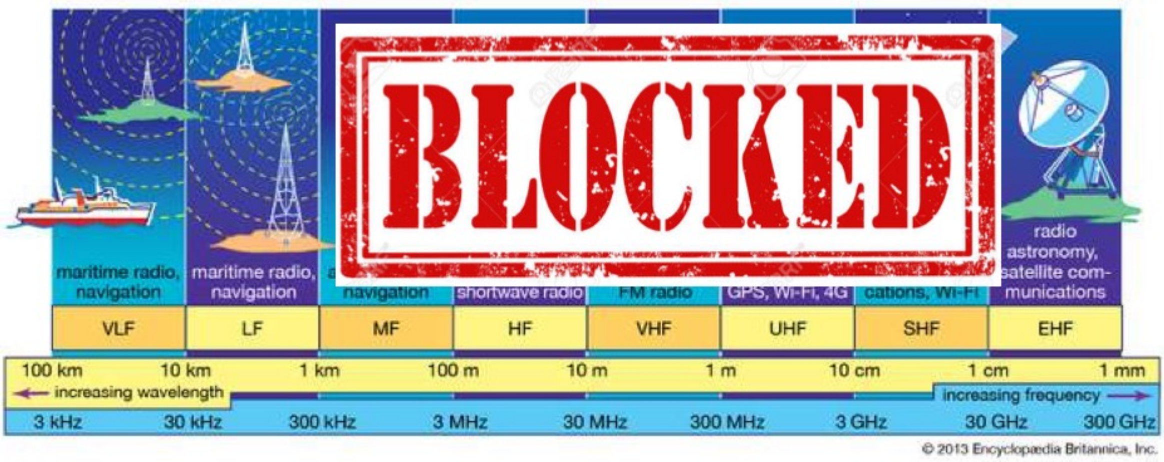

Figure 26: (Britannica 2021)

The cartoon diagram below shows the coyote trying to trigger an RCIED with a remote garage door opener (433 MHz) transmitter to the IED to blow up the 2nd car in convoy. The U.S military Crew jammer on the front vehicle emitted a stronger signal on the 433 MHz spectrum amongst other frequencies to cancel the Coyotes signal stopping the IED from detonating.

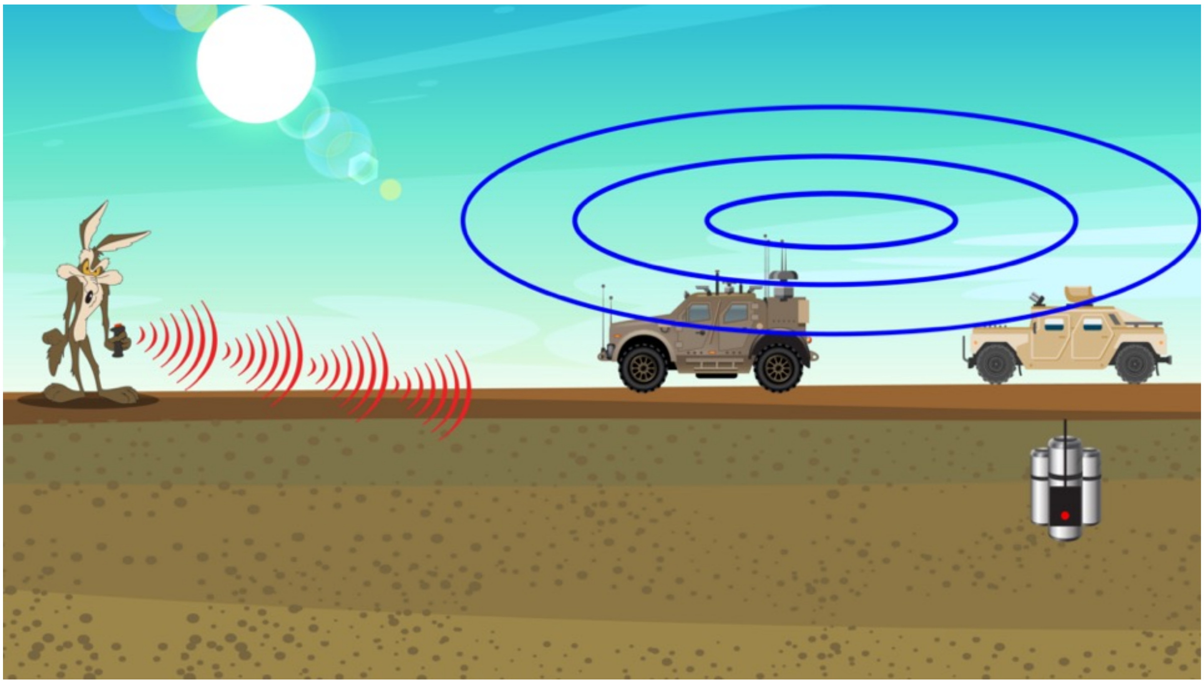

Figure 27: (ROCK 2021)

It should be noted here that Jammers operate in Far-Field E (electric), drowning out RF transmissions. Far-field (E) does not require the Jammer to know where the Receiver (Rx) is located and sends blanket noise wattage to drown out the Rx. The VLF Earth Mode scenario operates in Near-Field. The Electronic Counter Countermeasure (ECCM) hardware developed is designed to effectively operate in the Near Field zone, making current-day jammers ineffective.

Overview of Electronic Counter Countermeasures

Electronic Counter Countermeasures (ECCM) are techniques to thwart or defend against your adversaries' Electronic Countermeasures (ECM).

If the adversary uses Jammers to block the broadcast using Anti Jam (AJ) communications is an example of ECCM. Increasing your broadcast signal wattage power that is higher than the Jammers is a basic ECCM technique. Other techniques against Jammers include low probability of intercept (LPI) when the result is to avoid interception (POISEL, R. 2011). An example of this would be the VLF Earth mode technique in this paper. Hiding under the Jammers ranges and communicating using Near Field H signals vs. Far Field E signals and as using different TX modulation techniques such as Adaptive Noise Cancellation (ANC) and Decision aided feedback (DAFB).

Another example of this is the B2 Stealth bomber developed by Northrop Grumman which uses a variety of technologies to hide from enemy radar using reduced sound and radar signatures in the tail design, embedded engines in the fuselage anti reflective paint.

Other ECCM techniques include Frequency-Hopping Spread-Spectrum (FHSS). "FHSS is a spread-spectrum modulation technique, meaning that the transmitter rapidly switches the frequency of the carrier wave in a random fashion across a wide spectrum. This makes it much more difficult for an enemy force to jam the signal since it is always changing, and it is almost impossible to predict what frequency it will jump to the next. FHSS is used along with encryption for an added layer of radio communication security." (BLILEY TECHNOLOGIES. 2017).

ECCM in Earth Mode is covered in more detail in the Hardware Design chapter under ECCM using various of techniques especially LPI.

VLF/ULF Earth Mode Simulation Research

Simulation Methodology

Multiple simulation tools have been selected for this study. These include full wave 3d simulations such as Ansys HFSS for calculations. Ansys HFSS is a 3D electromagnetic (EM) simulation software for designing and simulating high-frequency electronic products such as antennas, antenna arrays, RF, or microwave components. Other tools include RES2Mod and CST Studio for calculation checking, which is a high-performance 3D EM analysis software package for designing, analyzing, and optimizing electromagnetic (EM) components and systems. (OLNEY, S. 2011.)

Purely analytical analysis is difficult in current conduction-based communications simulation modelling. Therefore, multiple tools were used in the simulation before field work commenced. The difficulty in current conduction mode communications-based approach on “DC resistivity method”, using modelling software RES2DMOD requires multiple tools.

A reference model has been built and analyzed with the above simulation tools.

The main difference between these tools and the RES2DMOD tool is

1. No simplification approaches are used: the task is considered with a full wave 3D approach.

2. Besides current/voltage, the electric and magnetic field distribution can be obtained.

3. AC rather than DC is considered. Different propagation modes (not only the conduction current mode) could be considered.

4. Any additional objects, such as the different configurations of Tx and Rx antenna (including loop), buried pipes etc. could be included in the model, relief of earth surface. The role and the corresponding effects of the above-mentioned factors will be considered later results obtained with the rigorous approach, and RES2DMOD will be compared.

The Earth is represented as a block of the material diagram below with dielectric constant ~10 and Conductivity ~0.01 S/m (typical values for wet soil). It should be noted here that the model is not limited to such monolithic block with homogeneous dielectric properties; in future, any number of different layers or arbitrary distributed dielectric properties could be set. The electrodes at Tx side are represented as metal rods 200x6x6cm^3 that are buried at ~1m depth.

These electrodes are arranged along X-axis (symmetrically respect to coordinates origin) and separated on ~10m.

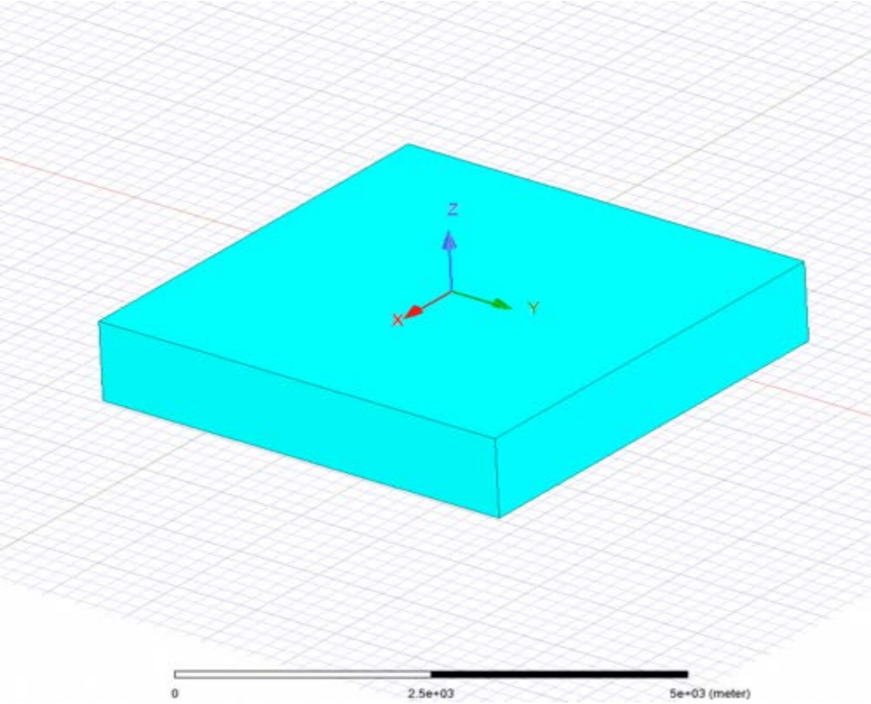

Figure 28: Earth Calculation Domain

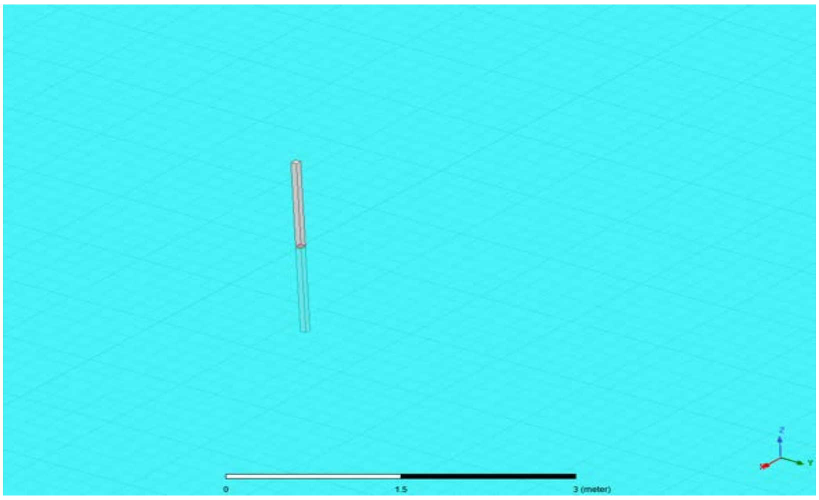
Figure 29: Single Metal electrode buried in the earth.

Two are used with set distances apart in this paper’s simulations.

Initial Simulation Results

The RF amplitude current injected is 1Amp. The EM setup simulation has been performed at three frequencies: 0.1 kHz, 9.0 kHz, and 73 kHz. The results are represented for amplitude of normal component of Magnetic Field amplitude over single quadrant (X, Y are positive) of the reference plane – earth surface at Z=0. Field distribution is symmetric under mirroring respect to X, Y axis. The operation area could be defined by using the expected sensitivity values.

Initial tests are done without amplification power at frequencies 0.1 kHz, 9kHz and 73 kHz. The green zone is where the signal is received within the DB with expected sensitivity. This zone is where communication without natural and made noise is the most effective.

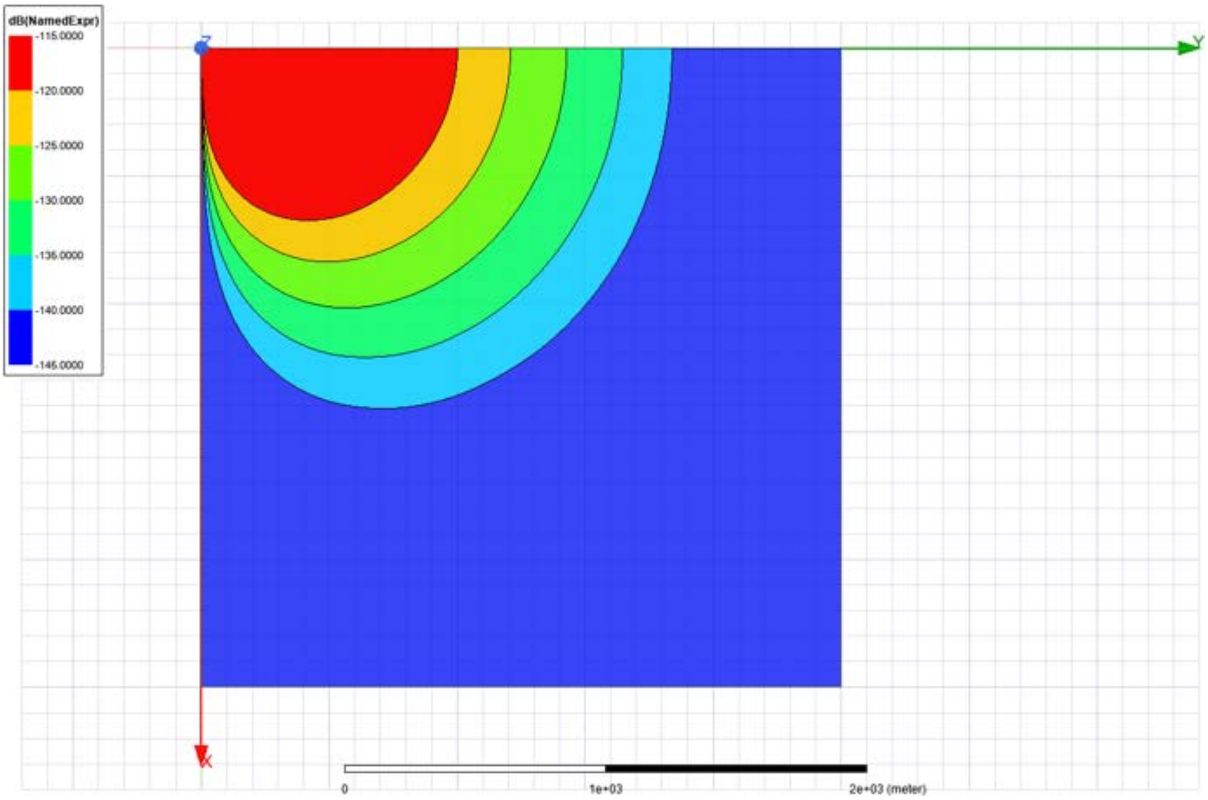

Figure 30: Simulation without large power input at 0.1 kHz

Total magnetic field amplitude (dBA/m) distribution over earth surface, at 0.1 kHz, electrodes separation ~10m. Injected current ~ 1A. Distance scale 100m/div.

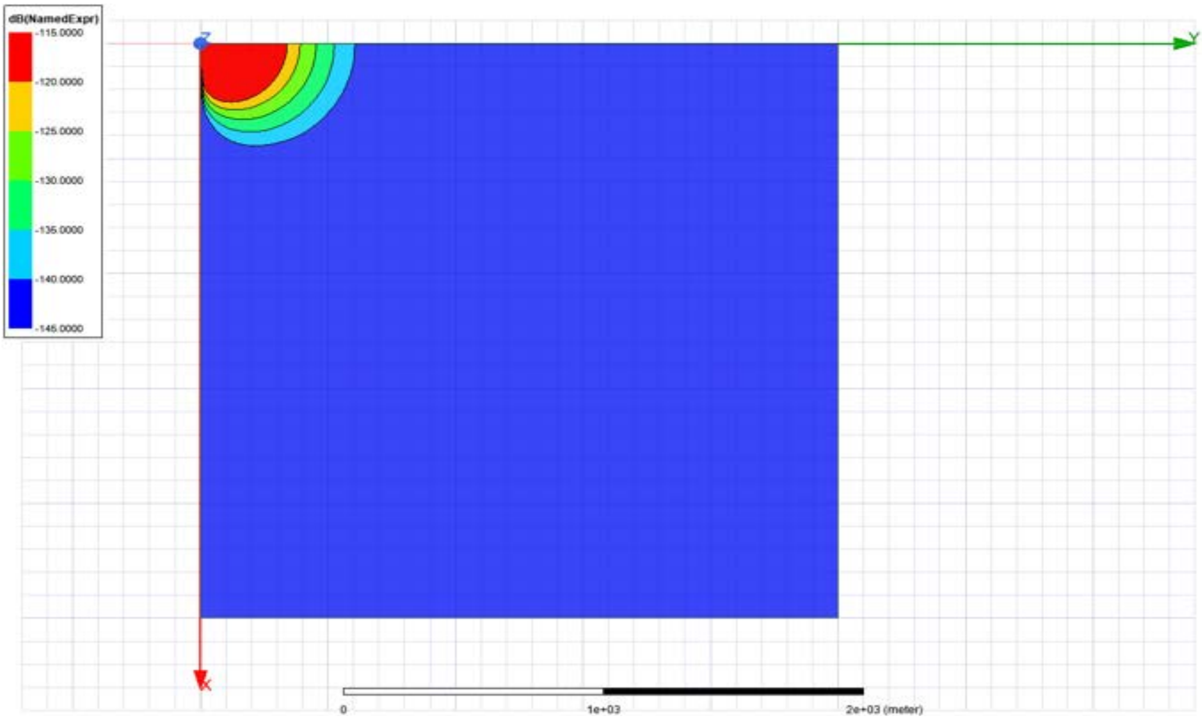

Figure 31: Simulation at 9kHz

Total magnetic field amplitude (dBA/m) distribution over earth surface, at 9 kHz, electrodes separation ~10m. Injected current ~ 1A. Distance scale 100m/div.

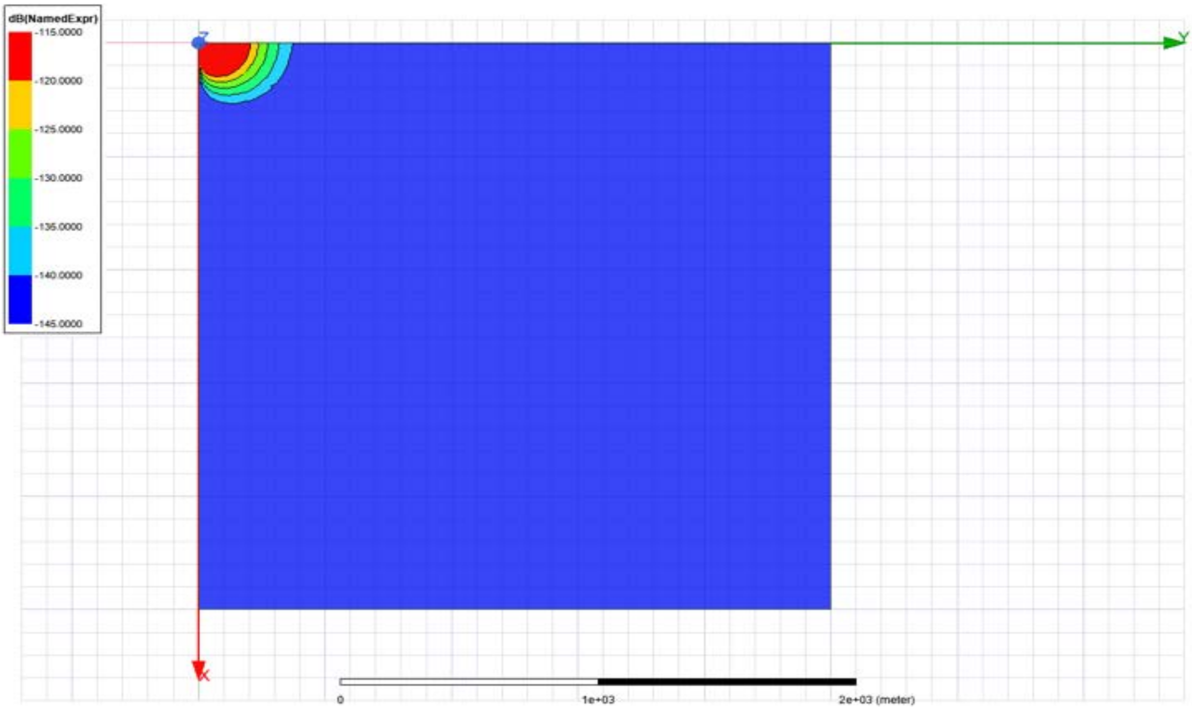

Figure 32: Simulation at 73 kHz

Total magnetic field amplitude (dBA/m) distribution over earth surface, at 73 kHz, electrodes separation ~10m. Injected current ~ 1A. Distance scale 100m/div.

Operational Range

We define the operation range as the situation where the next Condition is satisfied: the signal of interest (Man-Made signal) would have an instantaneous SNR of 0 dB at the antenna with respect to local natural noise (the natural noise will be considered in more details below). An antenna/amplifier that claims high sensitivity for this signal must maintain this SNR with minimal degradation, which requires antenna + electronic noise (associated with device Noise Figure referenced to Rx antenna terminals) at or below the natural noise floor. In other words: if the Condition is satisfied, then receiver sensitivity, which determines the minimum detectable signal (MDS), is limited by antenna thermal noise, and amplifier voltage and current noise. The sensitivity of the antenna alone can be defined as the B-field equivalent of the thermal voltage noise density.

$$B_A = \frac{\sqrt{4 \cdot k \cdot T \cdot R}}{2 \cdot \pi \cdot f \cdot N \cdot A} \qquad [1]$$

where thermal voltage noise density $V_R = \sqrt{4 \cdot k \cdot T \cdot R}$

is associated with coil ohmic resistance R and electromotive force EMF (Volts) induced in coil of area A in response to a harmonic B field with frequency f

$$\mathrm{EMF} = 2 \cdot \pi \cdot f \cdot B \cdot N \cdot A$$

Rx antenna is assumed as wire wound coil comprised of N turns operating immediately over and parallel to earth surface within normal component of uniform magnetic field B.

R could be expressed as $R = \rho \cdot \frac{l_C}{A_C} = \rho \cdot \frac{N \cdot l_{LP}}{A_C}$

ρ - resistivity of winding wire material, l_C - total length of wire, A_C - cross-section area of wire,

l_{LP}

Introducing winding wire material density σ and winding wire mass M_C

the [1] can be represented in more compact and informative form (for square shape coil)

$$B_A = \frac{4\sqrt{k \cdot T \cdot \rho \cdot \sigma}}{\pi \cdot f \cdot \sqrt{M_C \cdot A}}$$

This indicates, in particular

1. The antenna becomes more sensitive with increasing frequency (especially with that fact the expected natural noise spectral density drops significantly with the range 10kHz - 100kHz; to be considered in more details and confirmed in further testing).

2. Only practical way to improve antenna sensitivity is to increase winding mass and/or coil area

It could be estimated for the next set of Rx antenna and receiver parameters:

1. Operation frequency ~ 10kHz
2. Operation BW ~ 1Hz
3. Antenna area ~1 m^2
4. Copper winding mass ~1 Kg

Sensitivity limited by device internal noise is expected to be

B ~ 1 fT

That is below the natural noise floor. Therefore, the expected value of natural noise flow within 1 Hz bandwidth around values of carrier frequency should be chosen as actually reachable theoretical (best case) sensitivity (maybe excluding the carrier frequency raises up to ~100 kHz) **

B > 100 fT at 0.1 kHz

B > 5 fT at 10 kHz

B > 1 fT at 100 kHz

It is estimated for S/N ratio ~0dB at antenna and for 1 Hz bandwidth (reachable lower limit would be defined by reachable Q-factor of antenna and under external and internal detuning factors). Also, it should be noted that natural noise value could show season/time/location variation on the order of 20dB within the band 10kHz – 100kHz.

Also, allowing ~20 dB margin for S/N ratio So, it is reasonable to expect practically reachable sensitivity

B > 1000 fT at 0.1 kHz

B > 500 fT at 10 kHz

B > 100 fT at 100 kHz

Or in dBA/m units

B > -122 dBA/m at 0.1 kHz

B > -128 dBA/m at 10 kHz

B > -142 dBA/m at 100 kHz

Low Power vs no High Power

Below is a side-by-side comparison result, with the same simulation with one difference one is 20W injected from a standard 12 Volt DC and the other is ~3600W. The simulation settings were

Frequency: 9 kHz
Electrodes separation 20m
Distance scale 100m/div.

The diagram on the Left is the simulation with low power ~20W injected
The diagram on the right is with ~3600W injected

The final design's trade-off will be the complexity of a Tx high powered unit achieving greater distance vs the less complex Tx low powered unit. The high-powered unit will require a bulkier design with a high voltage dual-polarity DC supply, good thermal sink, and high-power output transformer.

We will investigate further on power/distance trade-offs; before moving into hardware design.

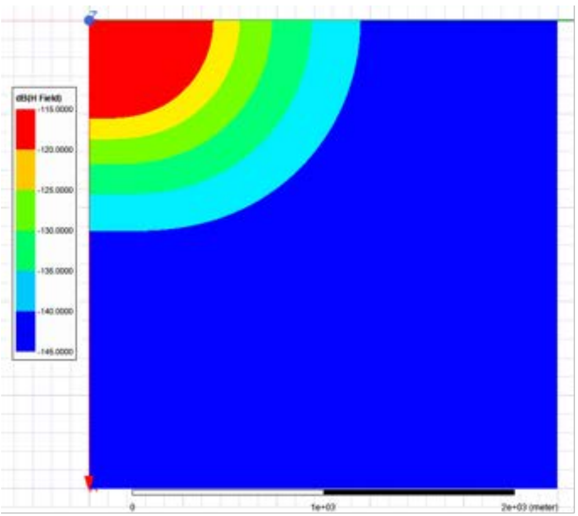

20 W (9kHz, 20-meter Electrodes)
(Distance ~1km)

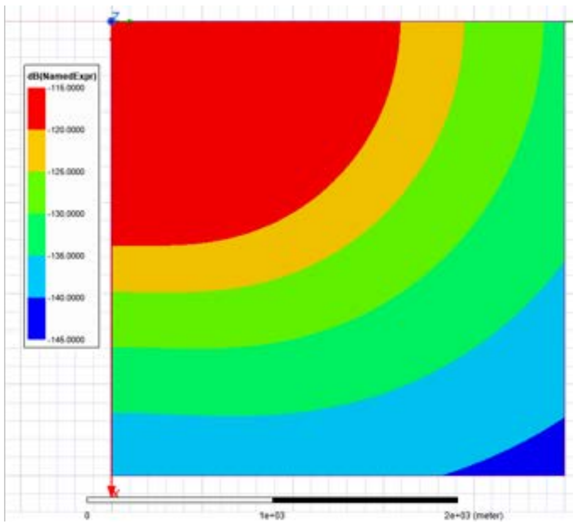

3600 W (9kHz, 20-meter Electrodes)
(Distance ~2.5km)

Figure 33: Injected power distance simulation 20W vs 3600W

Initial Conclusion Summary

The following conclusion and summary can be observed from the simulation results.

1. Relative decay rates for current density and magnetic field vs. distance (relative respect to the reference distance – electrode separation) are extremely high.

2. Distribution of normal component of the magnetic field has “zeros” direction along the direction of the electrode array (X-axis), that is defined by zero curvature (curl) of corresponding current lines.

3. Field distribution over the earth surface is frequency dependent.

Notes:

1. Current results data is normalized on injected current, not power.

2. Data for natural noise level requires to be updated with more modern data. Also, this actual data is related to vertical component of the E-field and horizontal component of H-field, while, in fact, the data for horizontal component of the E-field and vertical component of H-field is required. Currently used data is taken from “E. L. Maxwell and D. L. Stone, “Natural Noise Fields at 1 cps to 100 kc”, IEEE Transactions on Antennas and Propagation, AP-11, No. 3, pp. 339-343, 1963.”

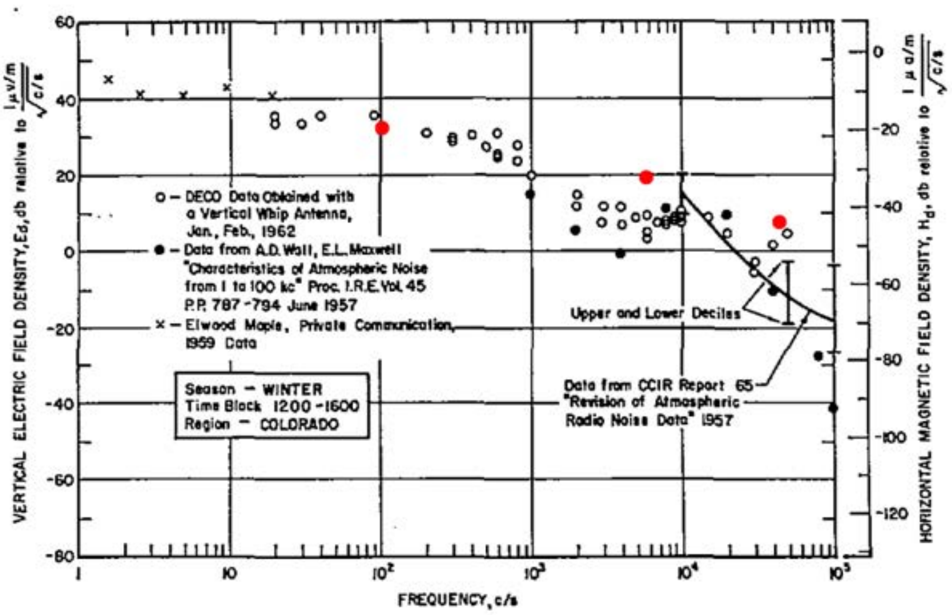

Figure 34: Noise levels with modern data

Data is taken from “E. L. Maxwell and D. L. Stone, “Natural Noise Fields at 1 cps to 100 kc”, IEEE Transactions on Antennas and Propagation, AP-11, No. 3, pp. 339-343, 1963.”

Exploratory Simulations

The simulations' primary goal is to find the best frequency, power input and transmission probe (TX) separation distances to transmit data to the receiver (RX). Man-made noise, like electricity grounding, manufacturing equipment, and natural noise like lighting, magnetic fields can then analyzed to find the ideal settings to communicate on.

The variables in the simulations are

1. Frequency - (VLF Frequencies). The low the frequency the further, the communication distance however the lower the frequency results in higher the noises, as explained above.

2. Power - Different power inputs of 1800W and 3600W were chosen to mimic U.S/European and Asia possible Wattage from a standard home/business point or circuit.

3. TX probe separations of 10, 20, and 50 metes

Magnetic Field amplitude over single quadrant (X, Y are positive) of the reference plane – earth surface at Z=0, injected power ~3600/1800W, accepted power. Field distribution is symmetric under mirroring respect to X, Y-axis. The operation area could be defined by using the expected sensitivity
values

B > -122 dBA/m at 0.1 kHz

B > -128 dBA/m at 10 kHz

B > -142 dBA/m at 100 kHz **

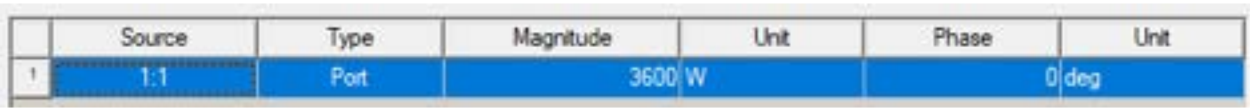

	Source	Type	Magnitude	Unit	Phase	Unit
1	1:1	Port	3600	W	0	deg

Figure 35: Maximum power available from signal source

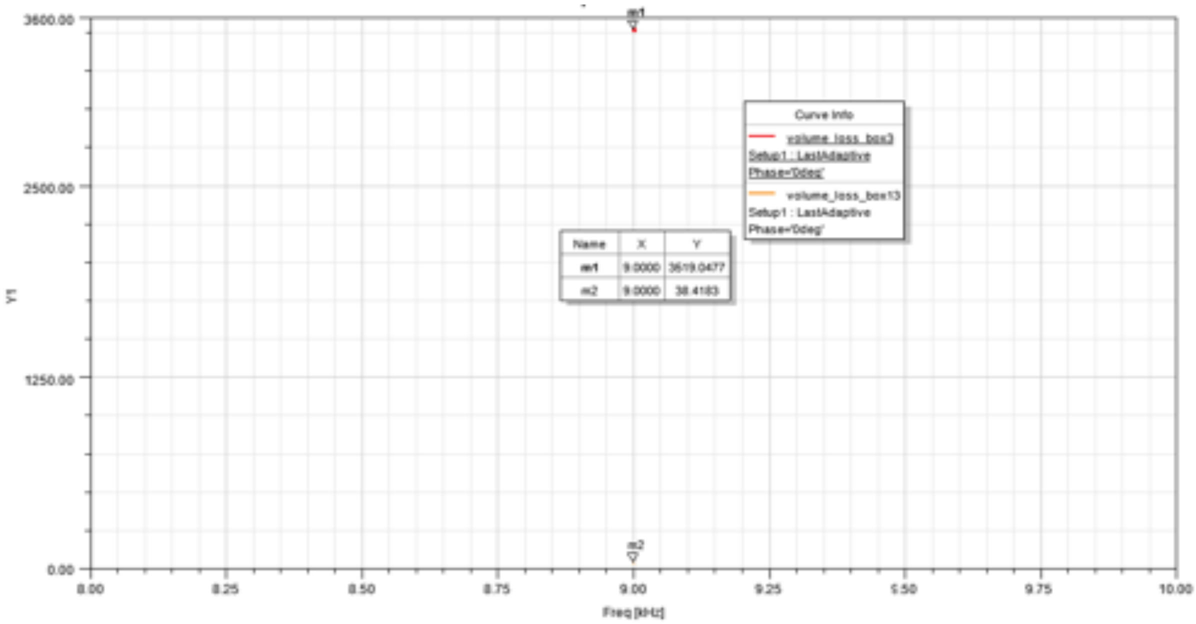

Figure 36: Simulation markers

Actual accepted power: marker 2 (m2) – by earth material block with dimensions 20x20x5 m^3 around origin, Marker 1 (m1) – by rest of volume within computation domain.

Theory

In general, Electric and Magnetic components both surround any "radiator". The space around the "radiator" can be divided into two zones, the Near-Field zone and the Far-Field zone. The specificity of the Far-Field zone, in particular, are:

1. E- (electric) and H- (magnetic) components are mutually orthogonal.
2. The phase shift between oscillations of E- and H-field is zero degrees (i.e., they oscillate "in-phase".

This behaviour is observed from starting from the distances ~< wavelength (Lambda) from the radiator. Let's note, in the VLF case the wavelength, is ~50 -100 km. On the distances much less than the specified above the E- and H- field components are:

1. Non-orthogonal
2. The phase shift between them is 90 degrees. This zone is called the Near-Field zone. So, on the distance for IED triggering 600m-2.5km is in the Near-Field zone.

Concerning H- field vs E- field. There could be a different type of radiators: so-called Electric field radiators (E-field component mainly within Near-Field zone) or Magnetic field radiators (H-filed component is mainly within Near-Field zone) or a combination of the two.

The example of a pure Electric field radiator is a short monopole antenna, the example of a pure Magnetic field radiator is a small loop (coil) antenna. It is my theory that the radiator with two electrodes injecting the RF current into the well-conducting earth medium. The RF current paths inside the earth medium form something like a “winding” that create Magnetic field we are sensing this with either the Rx coil (transformer type coupling between Tx and Rx) or with Rx electrodes (autotransformer type of Tx Rx coupling). So, in this case it would be classified as Near-Field communication via a Magnetic field.

0.1 kHz Frequency Simulations

The following table represents the simulations over 0.1kHz, Normal magnetic field amplitude (dBA/m) distribution over earth surface from Tx to Rx operations distances. The variables changed are Electrode Separation 10-100 metres and Injected Power 1800-3600 watts to see the effects of increasing the operational range. Detailed results are in the Appendix.

Frequency (kilohertz)	Electrode Separation (Metres)	Injected Power (Watts)	Operational Range (Metres)
0.1	~ 10	~ 3600	~ 1900-2400
0.1	~ 10	~ 1800	~ 1800-2200
0.1	~ 20	~ 3600	~ 2600-3200
0.1	~ 20	~ 1800	~ 2600-3000
0.1	~ 50	~ 3600	~ 2800-3500
0.1	~ 50	~ 1800	~ 2800-3500
0.1	~ 100	~ 3600	~ 3000-4000
0.1	~ 100	~ 1800	~ 2800-4000
0.1	~ 1000	~ 3600	~ 3800-4800
0.1	~ 1000	~ 1800	~ 4000-5000

Figure 37: 0.1 kHz Frequency simulations with variable power and electrode separation

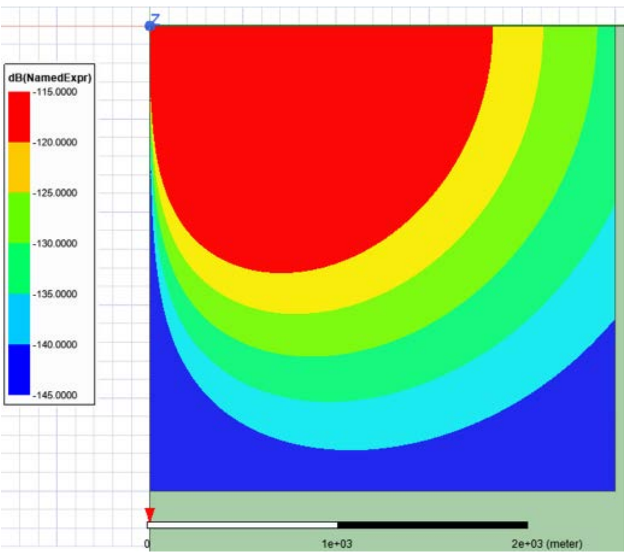

Figure 38: Simulation example 0.1 kHz, 10m Electrode Separation and ~3600W power

9 kHz Frequency Simulations

The following table represents the simulations over 9 kHz, Normal magnetic field amplitude (dBA/m) distribution over earth surface from Tx to Rx operations distances. The variables changed are Electrode Separation 10-100 metres and Injected Power 1800-3600 watts to see the effects of increasing the operational range. Detailed results are in the Appendix.

Frequency (kilohertz)	Electrode Separation (Metres)	Injected Power (Watts)	Operational Range (Metres)
9	~10	~3600	~ 700-1000
9	~10	~1800	~ 600-800
9	~20	~3600	~ 800-1000
9	~20	~1800	~ 700-1000
9	~50	~3600	~ 900-1300
9	~50	~1800	~ 800-1200
9	~100	~3600	~ 1100-1600
9	~100	~1800	~ 1000-1400
9	~1000	~3600	~ 2000-2800
9	~1000	~1800	~ 1800-2600

Figure 39: 9 kHz Frequency simulations with variable power and electrode separation

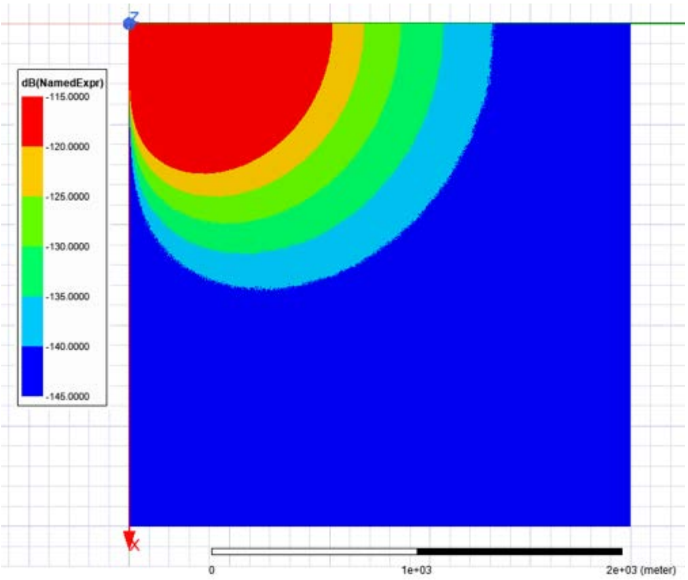

Figure 40: Simulation example 9 kHz, 100m Electrode Separation and ~3600W power

73 kHz Frequency Simulations

The following table represents the simulations over 73 kHz, Normal magnetic field amplitude (dBA/m) distribution over earth surface from Tx to Rx operations distances. The variables changed are Electrode Separation 10-100 metres and Injected Power 1800-3600 watts to see the effects of increasing the operational range. Detailed results are in the Appendix.

Frequency (kilohertz)	Electrode Separation (Metres)	Injected Power (Watts)	Operational Range (Metres)
73	~ 10	~ 3600	~ 400-550
73	~ 10	~ 1800	~ 400-500
73	~ 20	~ 3600	~ 500-650
73	~ 20	~ 1800	~ 400-550
73	~ 50	~ 3600	~ 600-800
73	~ 50	~ 1800	~ 500-700
73	~ 100	~ 3600	~ 700-1000
73	~ 100	~ 1800	~ 600-900
73	~ 1000	~ 3600	~ 1000-1600
73	~ 1000	~ 1800	~ 1000-1400

Figure 41: 73 kHz Frequency simulations with variable power and electrode separation

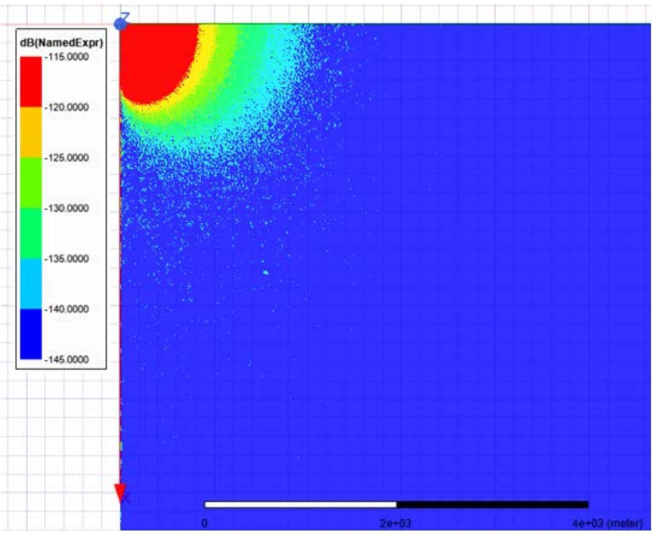

Figure 42: Simulation example 73 kHz, 1000m Electrode Separation and ~3600W (Scale 200/m div)

E-Field considerations

Changing the RX (receiver) to underground electrodes instead of the Loop aerial, identical to the transmitter 10/20 meters apart at 1 meter deep and performing the analysis similar to the one presented and using the natural noise data, it can be concluded that

The expected E-field thermal noise spectral density

$$E_A = \frac{\sqrt{4 \cdot k \cdot T \cdot R}}{d}$$

d – distance between Rx electrodes is much lower than the expected E-field natural noise spectral density

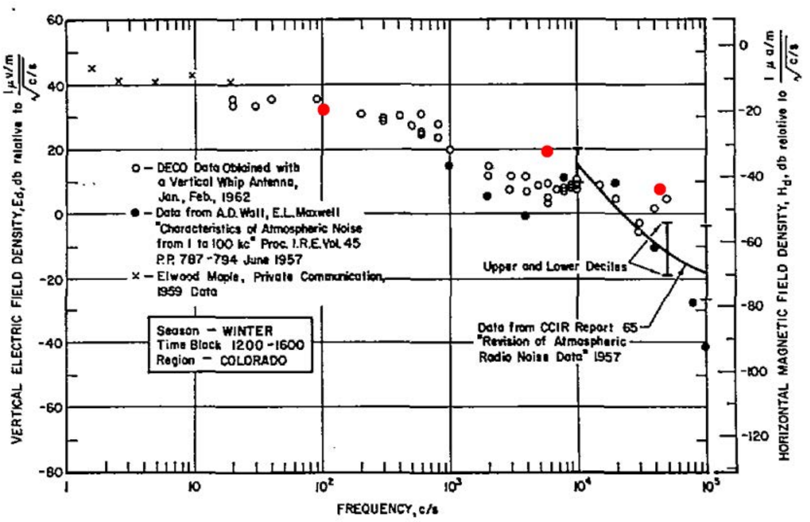

Fig. 1—Natural noise density.

Data is taken from "E. L. Maxwell and D. L. Stone,
"Natural Noise Fields at 1 cps to 100 kc", *IEEE Transactions on Antennas and Propagation*,
AP-11, No. 3, pp. 339-343, 1963."

Figure 43: Natural Noise density

With allowing ~20 dB margin for S/N ratio it is reasonable to expect practically reachable sensitivity

dBV/m

E > -70 dBV/m at 0.1 kHz

E > -76 dBV/m at 10 kHz

E > -90 dBA/m at 100 kHz

The operation area could be defined by using the expected sensitivity values, specified above with E-field (x-component).

Simulation 1: 0.1kHz E-field

Frequency: 0.1 kHz
TX Electrodes separation ~10m
RX Electrodes separation ~10m aligned X-direction
Injected power ~ 3600W. Accepted power ~ 3560W.
Distance scale 100m/div.

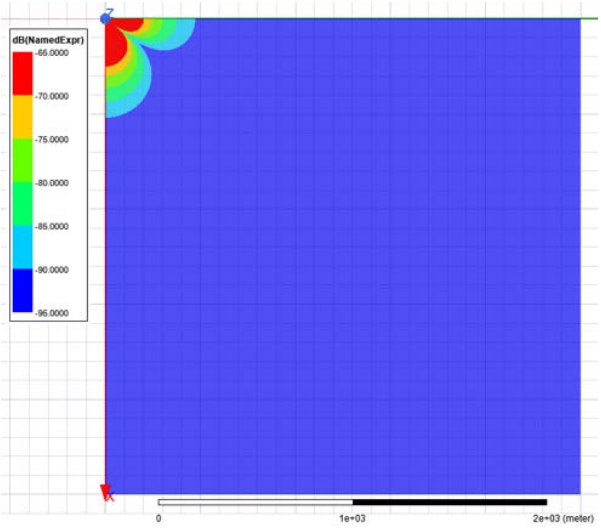

Figure 44: Simulation 1: 0.1kHz E-field results

Simulation 2: 0.1kHz E-field

Frequency: 0.1 kHz
TX Electrodes separation ~10m
RX Electrodes separation ~10m aligned X-direction
Injected power ~ **1800W.**
Distance scale 100m/div.

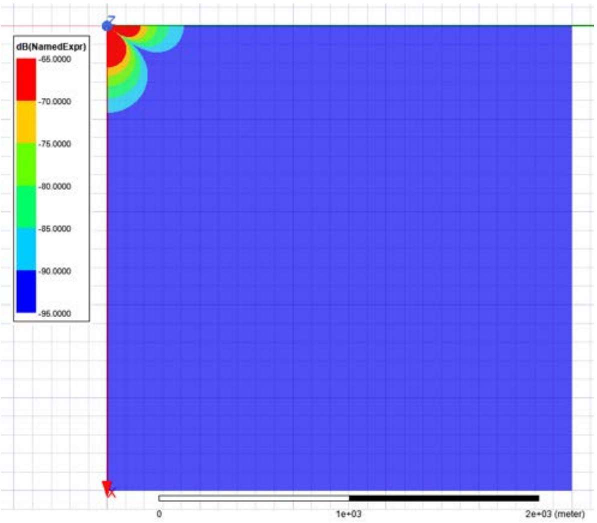

Figure 45: Simulation 2: 0.1kHz E-field results

Simulation 3: 9 kHz E-field

Frequency: 9 kHz
TX Electrodes separation ~10m
RX Electrodes separation ~10m aligned X-direction
Injected power ~ 3600W. Accepted power ~ 3560W.
Distance scale 100m/div.

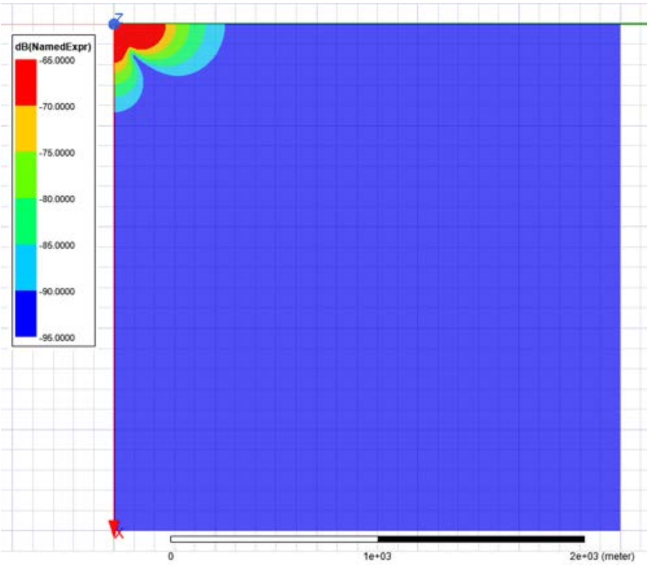

Figure 46: Simulation 3: 9 kHz E-field results

Simulation 4: 9 kHz E-field

Frequency: 9 kHz
TX Electrodes separation ~10m
RX Electrodes separation ~10m aligned X-direction
Injected power ~ **1800W.**
Distance scale 100m/div.

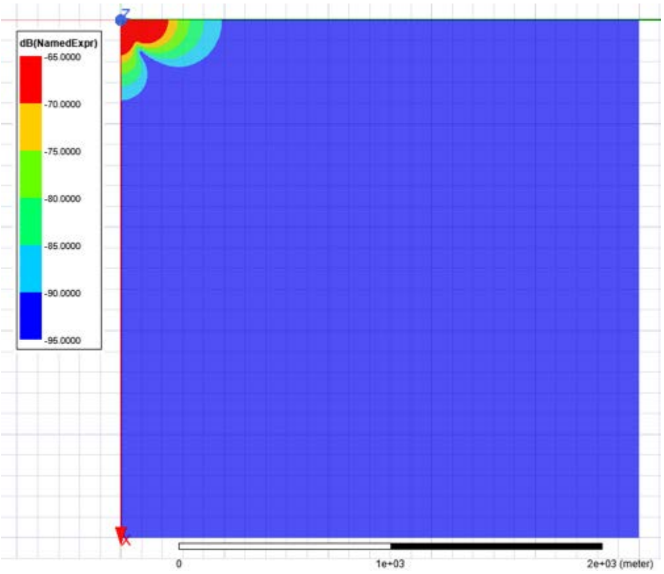

Figure 47: Simulation 4: 9 kHz E-field results

Simulation 5: 73 kHz E-field

Frequency: 73 kHz
TX Electrodes separation ~10m
RX Electrodes separation ~10m aligned X-direction
Injected power ~ 3600W. Accepted power ~ 3560W.
Distance scale 100m/div.

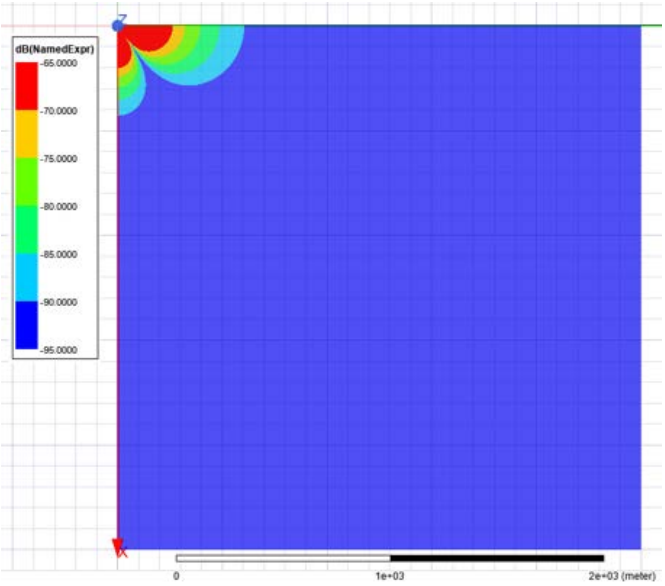

Figure 48: Simulation 5: 73 kHz E-field results

Simulation 6: 73 kHz E-field

Frequency: 73 kHz
TX Electrodes separation ~10m
RX Electrodes separation ~10m aligned X-direction
Injected power ~ **1800W.**
Distance scale 100m/div.

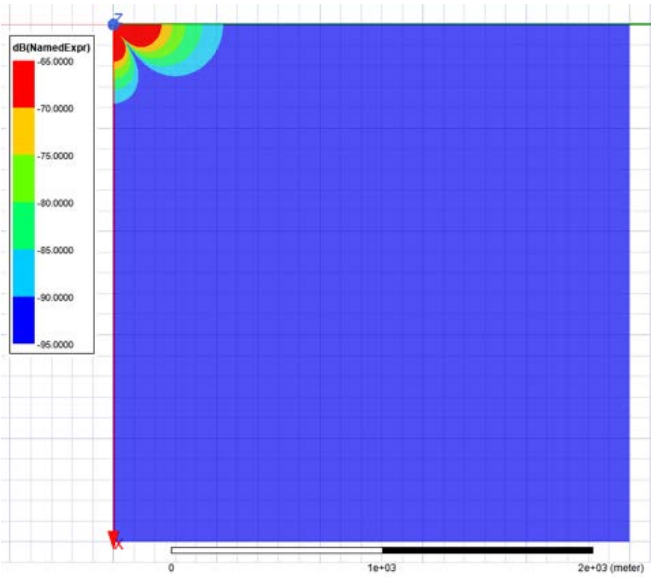

Figure 49: Simulation 6: 73 kHz E-field results

Other considerations

Concerning the selection of the correct frequency band for communication, it is essential to see what other researchers have achieved and compare them against our simulations to take the next step.

In the simulations performed the mentioned effect has been not observed. Possibly, related to more complex dependence of impedance on frequency than it was assumed in simulation setup. It is reasonable to check how that effect is significant. “The impedance value decreases with frequency;” (Munoz. 2011)

“…however, the electrical field generated suffers from an exponential attenuation due to skin effect, increasing this value with frequency. Thus, a trade-off is established in the frequency selection.” (Munoz. 2011). The mentioned effect of increasing of attenuation vs frequency was observed, and so, confirmed. The effect is relatively significant.

“Although a larger current generates more electric field intensity, the range of communication is not very large due to the strong signal attenuation. Therefore, the SNR is the main parameter to consider in receiver design. So electrical noise/interferences captured by the receiver electrodes must be studied and measured.” (Munoz. 2011) This state confirms the great importance of drawing attention to acquiring noise data. Unfortunately, in this article electrical field noise is considered, but in any case, that could help to cross-verify the available data.

“In the TTE communication with electrodes only the human-generated noise is studied because the other sources of noise are negligible in comparison with this contribution.” (Munoz. 2011) This statement coincides with the conclusion presented in the Initial Simulation Results section: the device internal (thermal) noise could be ignored for well build receiver; human–generated (in our terms – natural noise) dominates.

“As it has been commented before, not only is the frequency location of the interferences important but also its temporal distribution” (Munoz. 2011) It confirms the info provided in the source mentioned below. Some quantitative data is provided in the considering article it can be concluded for now that the noise expectation (E-field noise) seems to be coincided with that one specified in Figure 2 below, but it is different with one specified in Figure 1 that confirms the conclusion about great dependence of natural noise on location.

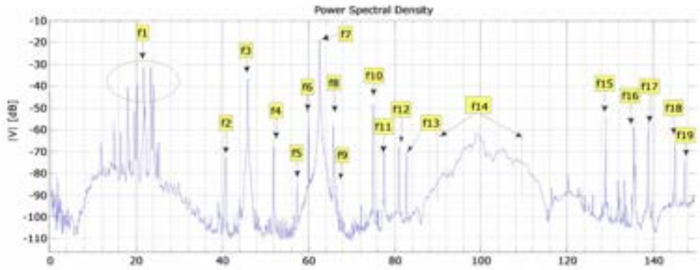

Code	Freq (kHz)	Origin	Country
f1	18-25	Navy	-
f3	45.9	US. Navy	I
f7	63.75	Unknown	-
f10	75	HBG TS	STZ
f14	90-110	LORAN-C	-

Figure 1: PSD of noise measurement in Belsué with most powerful interferences.

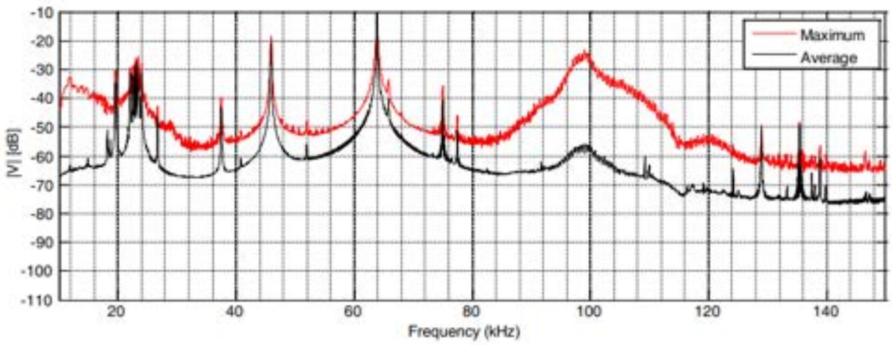

Figure 2: Noise amplitude spectrum measurement in Esteban Felipe cave (Huesca).

Figure 50: Noise measurements at low frequencies

“As a result of the measurements analyzed, it can be concluded that it is very important to measure and characterize the noise with electrodes at the time to choose a communication frequency.” (Munoz. 2011). This conclusion is finally made in the considered article, but it would be possible to find more or less optimal stationary frequency niches for testing purposes, especially if natural noise data would be available for certain location.

1. “It is advised to use the carrier frequency within the band 70kHz – 90kHz. For lower frequencies the equipment (at the Rx side) becomes bulky; for higher frequencies the losses on radiation become increasing.” (PETROVICH, 2021) We observe the main effect of increased attenuation on higher frequencies is the skin-effect discussed earlier.

2. “It is advised to orient the Rx loop (in the case of communication via magnetic field) vertically (i.e., adjust for acquiring tangential component of magnetic field).” (PETROVICH, 2021) The normal component of magnetic field is defined with curl of current vector field, and it is expected as relatively small. Tangential component of magnetic field is expected as much stronger, but it should be noted that vertical loop should be oriented properly to take advantages of such approach: the optimal receiving will we achieved when the current direction is parallel to plane of loop. It requires, in generally, knowing of direction to Tx and orientation of Tx electrodes array. Also, the natural noise level could be different for normal and tangential components of natural noise magnetic field and it will affect the overall S/N ration for both cases.

3. “Magnetic field decreases according to the "inverse cubes" law: each time the distance between the Tx and Rx is doubled, the signal strength decreases by 18 db.” (PETROVICH, 2021) This statement is mentioned in most known sources. It is observed with more or less satisfactory accuracy in the results simulations represented in the Power vs No Power simulations.

4. “It is advised to use single sideband suppressed carrier (SSBSC).” (PETROVICH, 2021) It is true that SSBSC modulation allows to decrease required bandwidth and do not waste power into transmission the carrier. But it should be noted that, in the case when bandwidth is not so critical, it could be more reasonably to use reduced carrier modulated transmission. But, even with this simpler approach, the conventional AM detector demodulation on Rx will not be sufficient; more sophisticated demodulator will be required.

EM signal visualization

Someone asked during my simulations what does the magnetic fields look above/below the ground. The diagrams below show distribution of tangential (respect to XY plane; to be picked with orientation matched vertical loop) component of magnetic field for Tx electrodes 20 m apart, 3600W power, at 0.1, 9 and 73 kHz. The orthogonal references planes (within the sub domain X>0, Y>0) are shown. The triad on the bottom right would help to imagine the sub domain orientation (point of view).

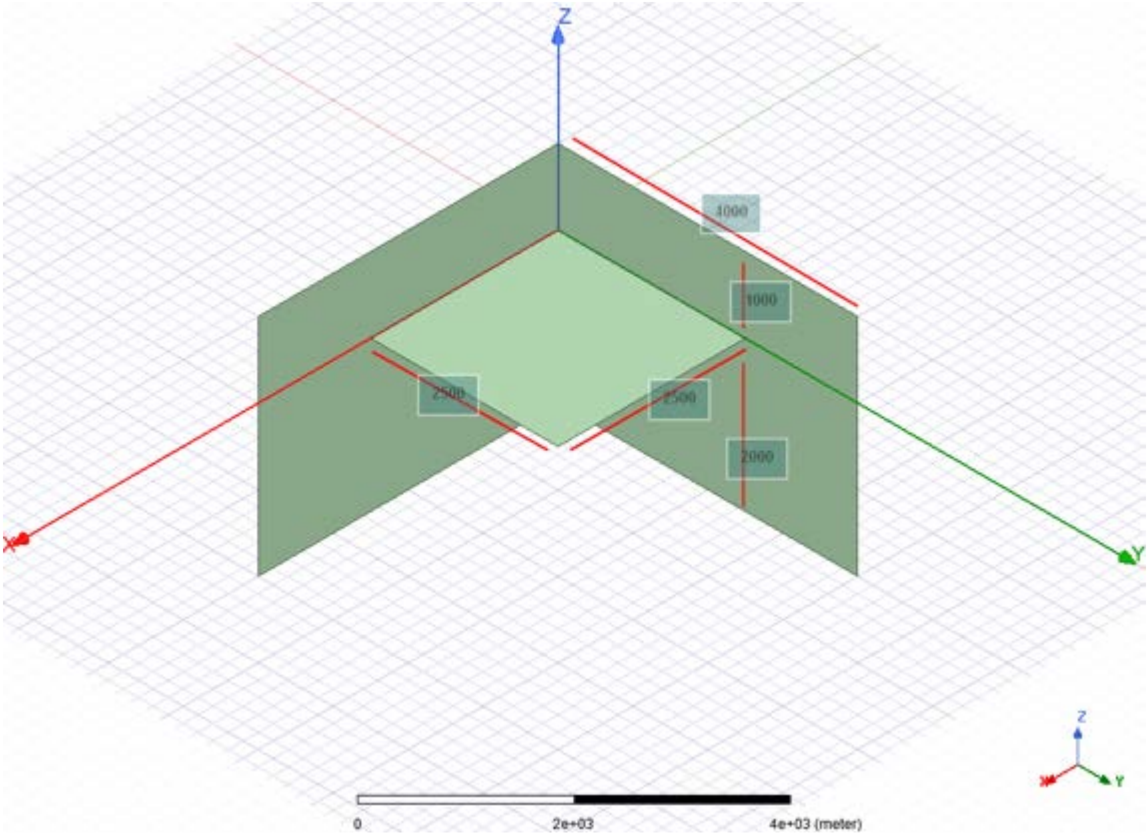

Figure 51: EM signal visualization

Signal Visualization: 0.1 kHz

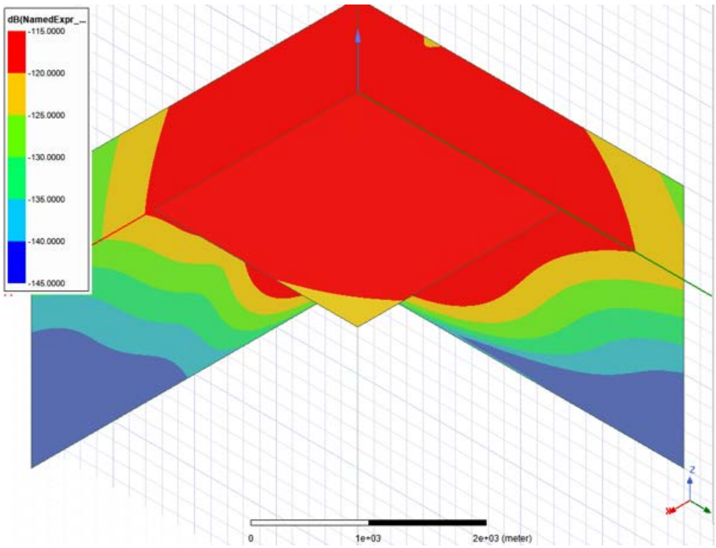

Figure 52: Signal Visualization simulation at 0,1 kHz

Signal Visualization: 0.1 kHz

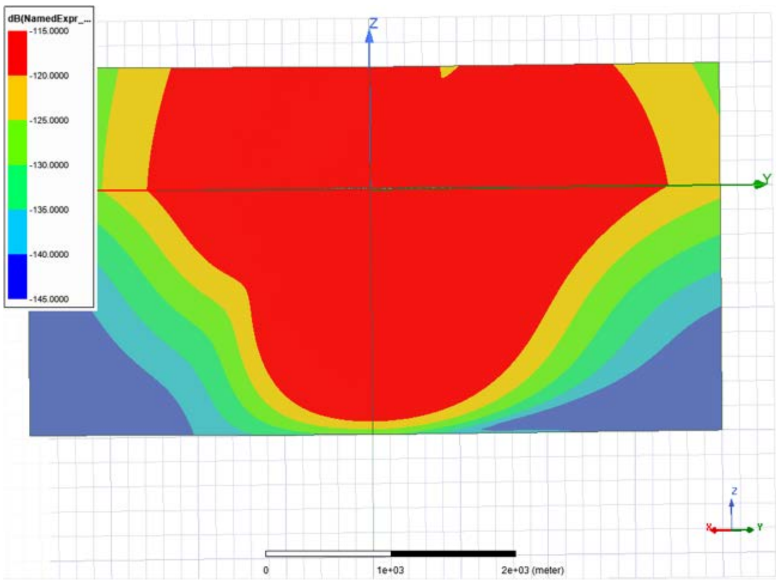

Figure 53: Multi axis visualization

Signal Visualization: 9 kHz

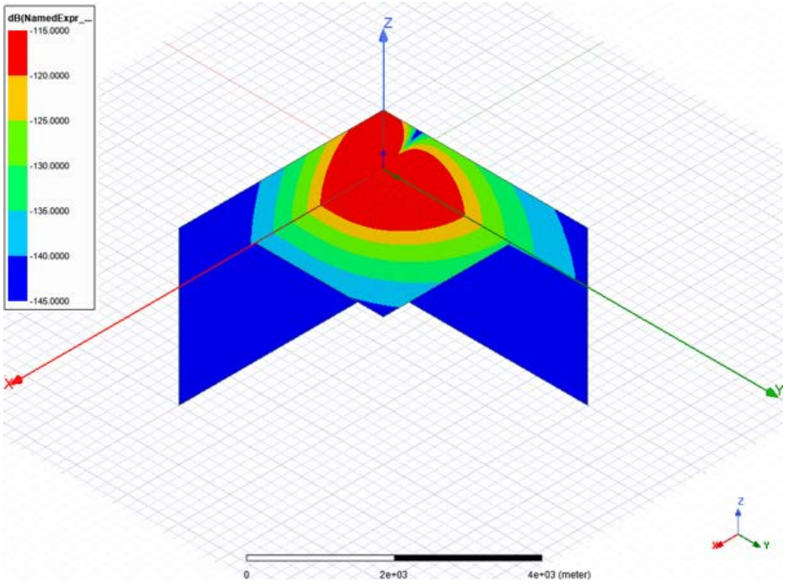

Figure 54: Signal Visualization at 9kHz

Signal Visualization: 9 kHz

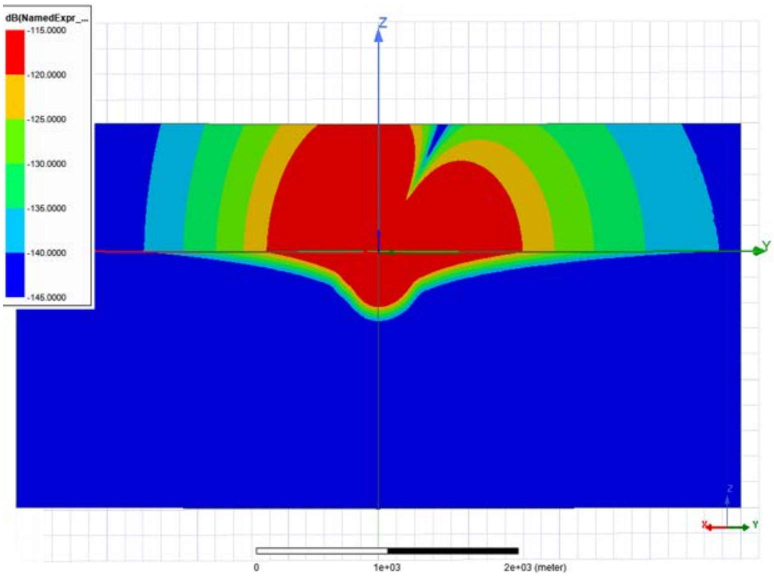

Figure 55: Signal Visualization cross axis

Signal Visualization: 73 kHz

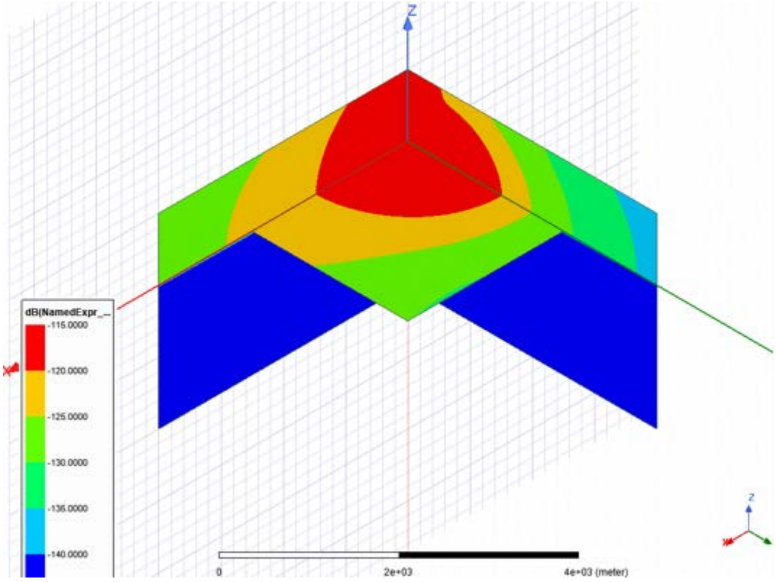

Figure 56: Signal Visualization at 73kHz

Signal Visualization: 73 kHz

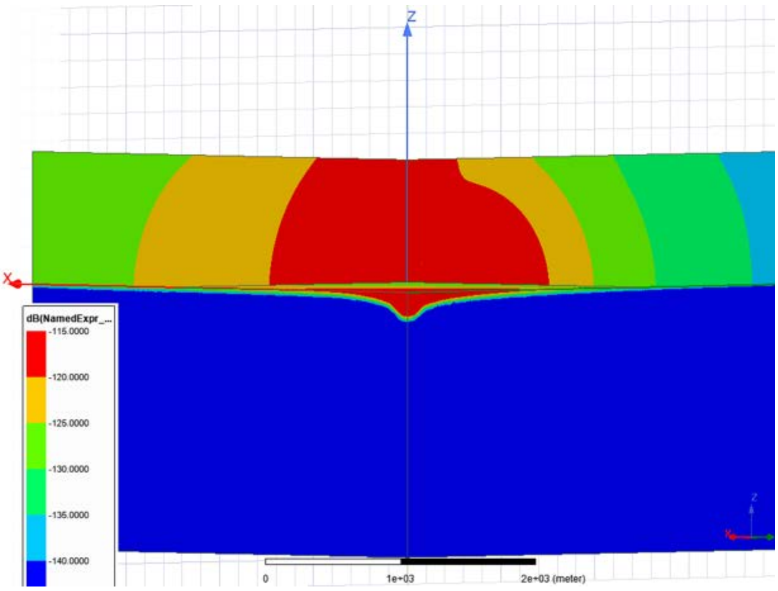

Figure 57: Signal Visualization Cross section

Signal Speed (or signal delay)

An important part of the research is how fast the transmission speed (or signal delay) to determine whether pushing the button to trigger the IED is fast enough to detonate on a moving target like an armoured or VIP vehicle. To determine this, the following setup has been analyzed.

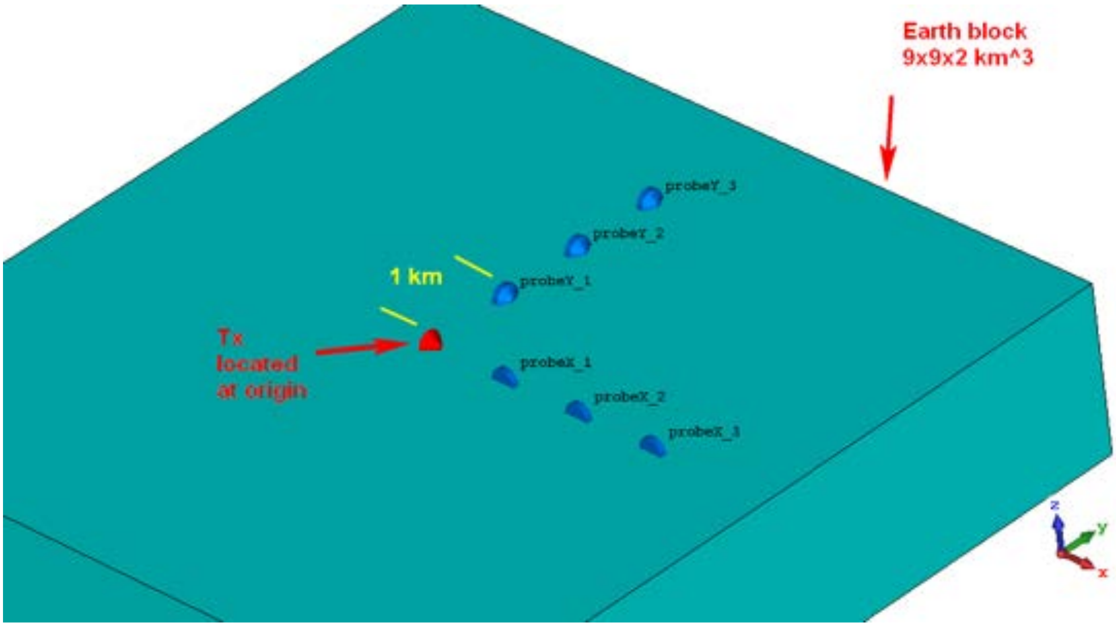

Figure 58: Earth block simulation probe separation

Tx signal source is located on coordinates origin. Rx signal probes are located along the X- and Y directions and separated with 1 km distance.

Sine step excitation signal form is chosen to emulate the modulated transmitting signal: carrier frequency ~ 5 kHz, Trise ~ 0.4 ms (corresponds to BW~0.8 kHz), total duration ~ 1ms. Trise being the maximum amplitude on a sine step.

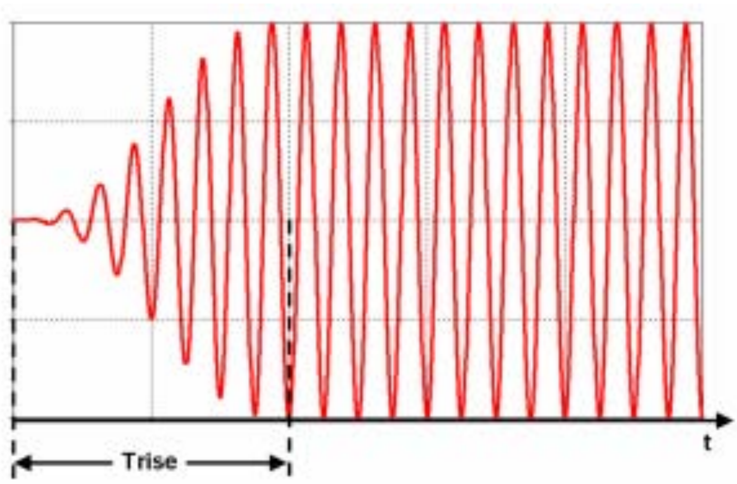

Figure 59: Trise frequency transmission speed

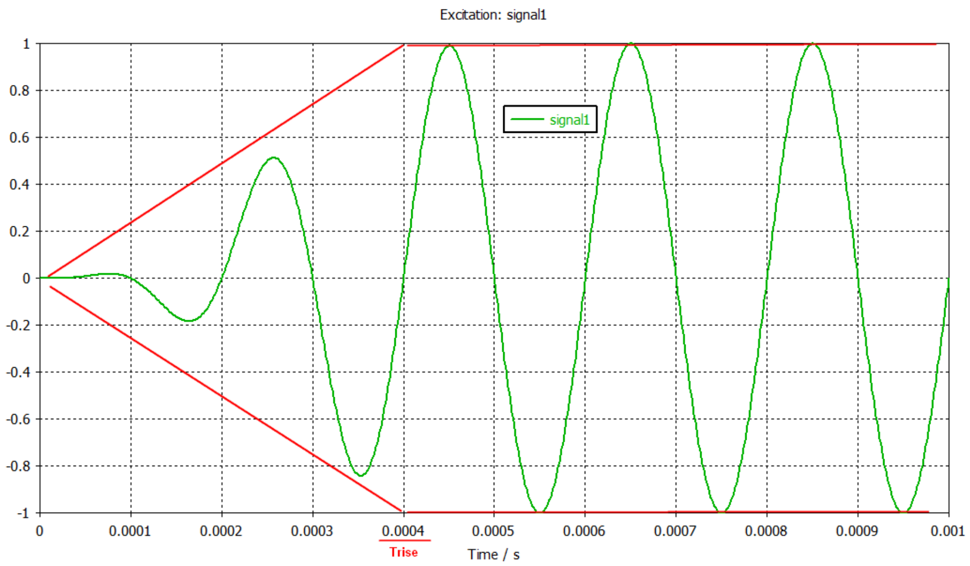

Figure 60: Trise signal time/s

But actually, for this purpose it is important the turn-on step at zero time, see image below:

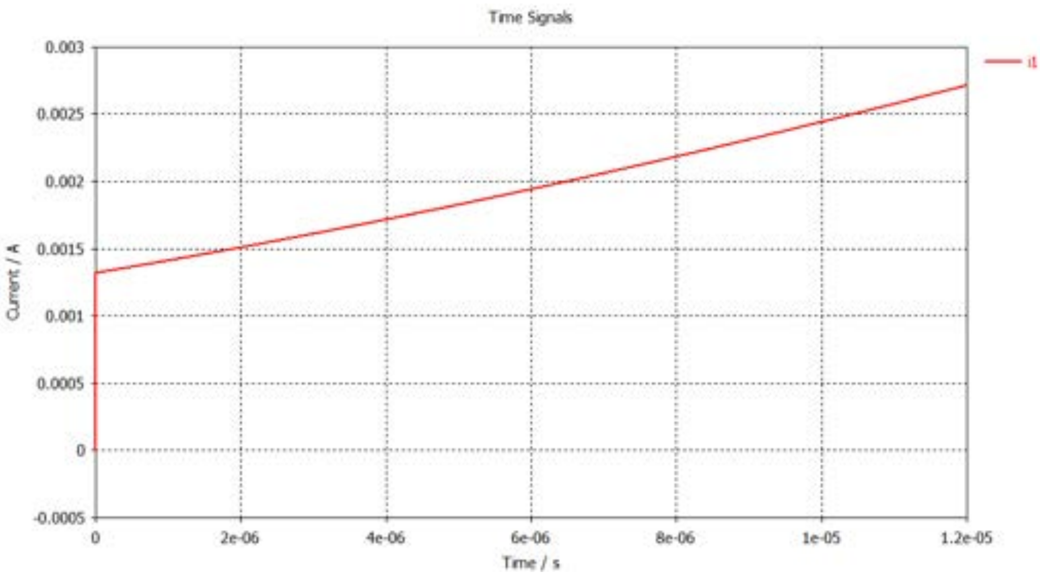

Figure 61: Zero-time graph

The correspondent probe picked Rx signal are represented on figures below.

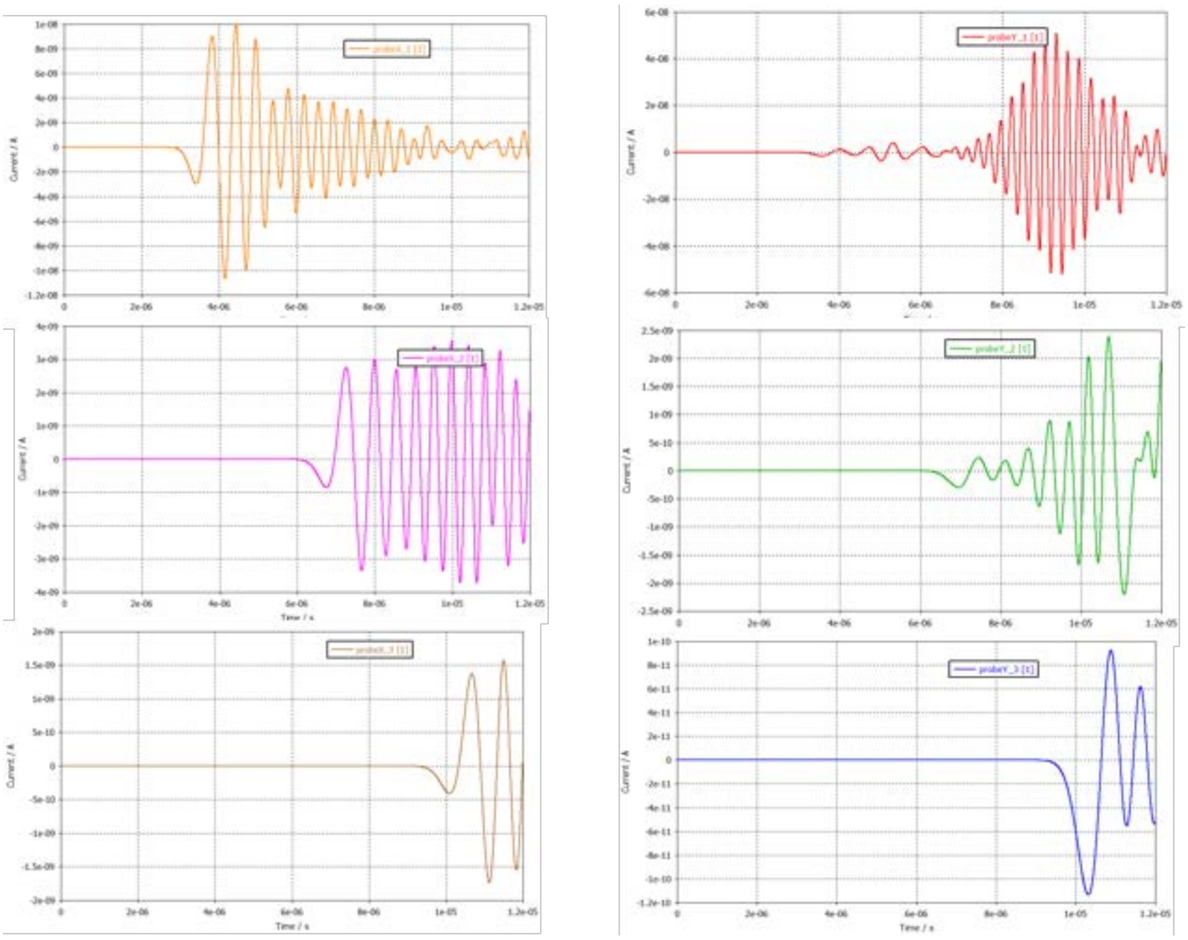

Figure 62: Signal speed

Based on the time delay data represented on the diagram above, it could be concluded that the signal velocity in near field zone (we are operating within) would still be close to light velocity in a vacuum. In other words, when you press the switch, the IED will receive the signal instantly.

Normal Magnetic vs Tangential

The magnetic field direction is arbitrary with respect to the earth's surface. It is reasonable to consider the normal (respect to earth surface) and tangential components separately. It should be noted that the components are mutually independent i.e., particularly the signal pickup from the Rx coil. The normal component can be acquired with horizontally oriented (in plane with earth surface) Tangential component can be acquired with vertically oriented coil. Also, it should be noted these components have important specificity that could be important for optimal receiving. In particular:

3. Generated by our Tx source magnitude of Tangential component much stronger than magnitude of Normal component. As it was mentioned in the reports, it is because of the Normal component is proportional to Curl (actually, curvature) of the conduction current within the earth while the Tangential component is proportional to current. Curvature of current path is small, especially along the X-axis.

4. On the other hand, the natural noise is much stronger for the Tangential component, because of, as a rule, the natural noise is associated with signal originated by external sources such as atmospheric phenomena, man-made RF power sources etc; they are expected to be in far-field zone, so arriving to our Rx as transversal EM wave with magnetic field oriented along the earth i.e., as Tangential. Taking account, the factor mentioned under point a. above the figure of merit for Rx i.e., Signal-to-Noise ratio (SNR) will be finally defined how strong useful signal and how strong arriving natural noise signal. As it is mentioned in some sources it is expected that better SNR would be for receiving Tangential magnetic field. But, again, that conclusion should not be considered as absolute because of the expected great instability of natural noise level, its dependence on the season/time/location etc.

5. Additionally, some other factors could be important when making choice between the Normal and Tangential component , for example, such as: convenience of Rx coil installation (certainly, the horizontal installation i.e. in plane with earth is expected as more convenient) and, what is more important, the optimal vertical installation (for picking Tangential magnetic field) will require the knowing of the direction toward the Tx source - axis of vertically oriented Rx could should be pointed along the direction to Tx. There is drawback of the approach for Tangential magnetic field pick up. Of course, there are potentially thinkable "universal" approaches such as with using 3 mutually orthogonal Rx coils when the signal is combined (obviously that will complicate Rx H/W). And in addition, one thin more: if we could think about advanced possible approaches for further optimization of receiving. natural noise signal arriving from far-field zone and our useful signal originated by our Tx source being in near field zone have intrinsically different phase shifts between H and E field (zero degree for far-field source and 90 degrees for near-field source). Potentially they could be distinguished with proper H/W and S/W and, for example, near-field useful signal could be "cleaned" from the external far-field noise (far field jammer suppressing).

2 kHz Frequency Magnetic Field Simulations

Based on what we have learnt from the simulation, EM signal and speed we can now narrow down the best frequency for data transmission whilst avoiding noise to disrupt that signal.

The simulations below are based on magnetic field distribution is represented for parameters sets Power, (20, 1800, 3600W) Tx Probe Distance (10, 20, 50 meters), Frequency (2 kHz) and Magnetic field (Normal, Tangential)

Frequency (kilohertz)	Magnetic Field (Normal/Tangential)	Electrode Separation (Metres)	Injected Power (Watts)	Operational Range (Metres)
2	Normal	~ 50	~ 20	~ 600-800
2	Tangential	~ 50	~ 20	~ 700-900
2	Normal	~ 20	~ 20	~ 500-600
2	Tangential	~ 20	~ 20	~ 500-700
2	Normal	~ 10	~ 20	~ 400-500
2	Tangential	~ 10	~ 20	~ 500-600
2	Normal	~ 50	~ 1800	~ 900-1300
2	Tangential	~ 50	~ 1800	~ 1600-1900
2	Normal	~ 50	~ 3600	~ 1000-1400
2	Tangential	~ 50	~ 3600	~ 1600-2000
2	Normal	~ 20	~1800	~ 800-1000
2	Tangential	~ 20	~1800	~ 1000-1300
2	Normal	~ 20	~3600	~ 800-1100
2	Tangential	~ 20	~3600	~ 1200-1500
2	Normal	~ 10	~1800	~ 600-900
2	Tangential	~ 10	~1800	~900-1100
2	Normal	~ 10	~3600	~ 700-1000
2	Tangential	~ 10	~3600	~ 1000-1200

Figure 63: 2 kHz Frequency simulations with variable Antenna position, power, electrode separation

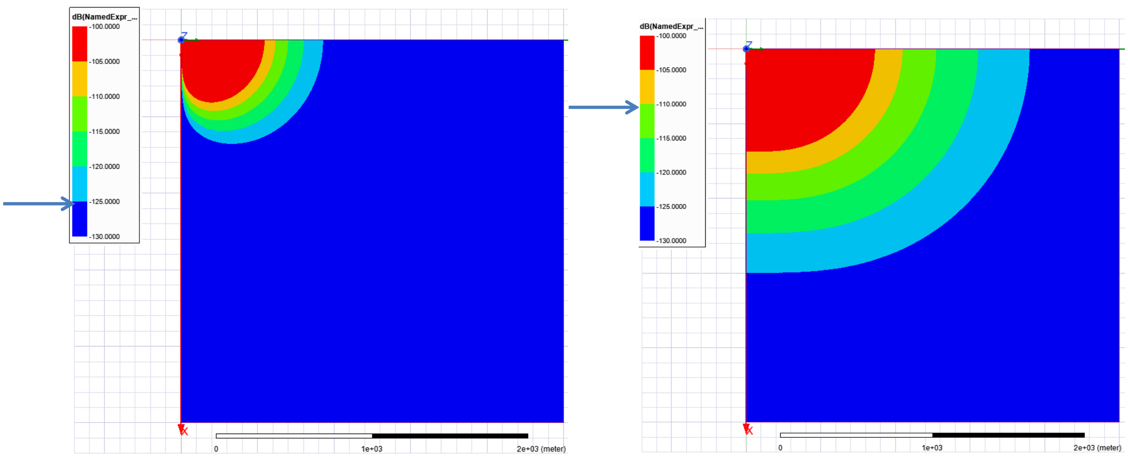

Figure 64: Normal vs Tangential Antenna Simulation dB

3 kHz Frequency Magnetic Field Simulations

Based on what we have learnt from the simulation, EM signal and speed we can now narrow down the best frequency for data transmission whilst avoiding noise to disrupt that signal.

The simulations below are based on magnetic field distribution is represented for parameters sets Power, (20, 1800, 3600W) Tx Probe Distance (10, 20, 50 meters), Frequency (3 kHz) and Magnetic field (Normal, Tangential)

Frequency (kilohertz)	Magnetic Field (Normal/Tangential)	Electrode Separation (Metres)	Injected Power (Watts)	Operational Range (Metres)
3	Normal	~ 50	~ 20	~ 500-800
3	Tangential	~ 50	~ 20	~ 700-800
3	Normal	~ 20	~ 20	~ 400-600
3	Tangential	~ 20	~ 20	~ 600-700
3	Normal	~ 10	~ 20	~ 300-400
3	Tangential	~ 10	~ 20	~ 400-500
3	Normal	~ 50	~ 1800	~ 1000-1200
3	Tangential	~ 50	~ 1800	~ 1400-1500
3	Normal	~ 50	~ 3600	~ 1000-1400
3	Tangential	~ 50	~ 3600	~ 1500-2000
3	Normal	~ 20	~1800	~ 700-900
3	Tangential	~ 20	~1800	~ 1000-1200
3	Normal	~ 20	~3600	~ 700-800
3	Tangential	~ 20	~3600	~ 1000-1500
3	Normal	~ 10	~1800	~ 600-800
3	Tangential	~ 10	~1800	~ 800-1000
3	Normal	~ 10	~3600	~ 600-800
3	Tangential	~ 10	~3600	~ 800-1200

Figure 65: 3 kHz Frequency simulations with variable Antenna position, power, electrode separation

4 kHz Frequency Magnetic Field Simulations

Based on what we have learnt from the simulation, EM signal and speed we can now narrow down the best frequency for data transmission whilst avoiding noise to disrupt that signal.

The simulations below are based on magnetic field distribution is represented for parameters sets Power, (20, 1800, 3600W) Tx Probe Distance (10, 20, 50 meters), Frequency (4 kHz) and Magnetic field (Normal, Tangential)

Frequency (kilohertz)	Magnetic Field (Normal/Tangential)	Electrode Separation (Metres)	Injected Power (Watts)	Operational Range (Metres)
4	Normal	~ 50	~ 20	~ 500-700
4	Tangential	~ 50	~ 20	~ 600-800
4	Normal	~ 20	~ 20	~ 400-600
4	Tangential	~ 20	~ 20	~ 400-600
4	Normal	~ 10	~ 20	~ 400-500
4	Tangential	~ 10	~ 20	~ 500-600
4	Normal	~ 50	~ 1800	~ 900-1200
4	Tangential	~ 50	~ 1800	~ 1300-1500
4	Normal	~ 50	~ 3600	~ 900-1300
4	Tangential	~ 50	~ 3600	~ 1400-2000
4	Normal	~ 20	~1800	~ 700-800
4	Tangential	~ 20	~1800	~ 1200-1400
4	Normal	~ 20	~3600	~ 700-1000
4	Tangential	~ 20	~3600	~ 1100-1400
4	Normal	~ 10	~1800	~ 600-800
4	Tangential	~ 10	~1800	~ 800-1000
4	Normal	~ 10	~3600	~ 700-1000
4	Tangential	~ 10	~3600	~ 900-1100

Figure 66: 4 kHz Frequency simulations with variable Antenna position, power, electrode separation

Modulation

To proceed with the choice of modulation/demodulation type, it is reasonable to define an appropriate figure of the merit of cost vs. signal distance. For this project, the operation distance vs. the certain modulation type implementation associated costs is key. Using specific modulation techniques, we can increase the signal distance 400% from our previous simulations in this project, i.e., from 2.5km to 10km in distance signal received. However, doing so will increase the hardware costs from ~$100 to ~$3,000+, which is defensible for high-value target assassinations but not so much for the improvised explosive guerrilla fighter.

Combined with increased power from the original (20W,1800W, 3600W) increased out to 20,000W we could increase the previous simulations signal distance even further.

However, the costs and design requirements are unfeasible in this RC-IED scenario.

These parameters should be considered under the given set of the rest of the parameters. They will be considered as the fixed:

- Bitrate,
- Acceptable bit error rate (BER)
- Tx antenna configuration,
- Tx output power (average),
- Soil conditions,
- Natural noise level,
- Rx antenna(s) configuration,
- Rx receiver RF-front-end configuration,
- baseband signal processing.

A common scenario of estimating the figure of merit could be described as follow:

- The given set of the fixed parameters and chosen modulation defines the required minimum signal to noise ratio (SNR).

- The required minimum SNR the defining the operation distance.

- Estimating the relative expected cost (H/W and S/W) required for implementing the chosen modulation type. For reference, for example, Amplitude Key Shifting (ASK) modulation could be chosen as the simplest one.

Based on the reported data from known sources, the integrated combination of advanced modulation schemes, adaptive noise cancellation (ANC), maximum-likelihood detection (MLD), nonlinear processing (NLP), and decision-aided feedback (DAFB) can provide 10-to-24 dB improvement in SNR. (RAAB 1995)

The expected operation distance is doubled when the SNR is improved by 18dB (25% increasing for 6dB improvement in SNR).

The expected cost of implementing certain modulation/demodulation type depends on factors related to H/W design (for example, necessity for coherent demodulation, clocks synchronization etc.) and factors related to S/W design (matched filtering, advanced signal processing etc.).

The expected difference in costs between the most straightforward modulation/demodulation schemes and advanced ones is significant. For example, ASK-based models are sub $50, and Single sideband modulation (SSB) would start at $2000 combined with the cooling and power requirements of more significant 3600W injected. These costs are a negligible for commercial or military application. For an RC-IED based project with maximum line of sight or spotter for triggering an IED do not need to be greater than 2km then the simpler ASK vs ANC/DAFB will be considered as a modulation technique.

Electrode Size and Depth

Simulations were performed using various depths of the electrodes at 1-3meters and varying the thickness of the electrodes from 60-200mm to see if signal distance increased in both normal and tangential antenna placement. The results are shown below for both normal and tangential. There was no significant net gain on the signal distance using these variables. There was approximately 10% gain on the thicker, deeper electrodes.

Frequency: 3 kHz
Magnetic Field: **Tangential**
Electrodes separation **~50m**
Injected power ~ **20W**
Distance scale 100m/div.

The diagram on the left is a **60** mm X **60** mm at **1**-meter depth into the earth.
The diagram on the right is a **200** mm X **200** mm at **3**-meter depth into the earth.

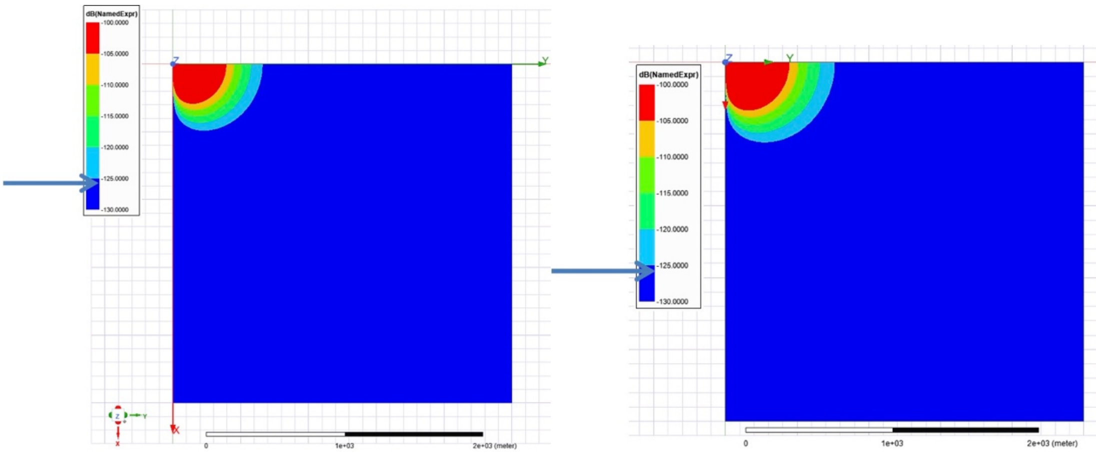

Figure 67: Electrode size and depth variable for tx distance increase with Tangential Antenna

Frequency: 3 kHz
Magnetic Field: **Normal**
Electrodes separation ~**50m**
Injected power ~ **20W**
Distance scale 100m/div.

The diagram on the left is a **60** mm X **60** mm at **1**-meter depth into the earth.
The diagram on the right is a **200** mm X **200** mm at **3**-meter depth into the earth.

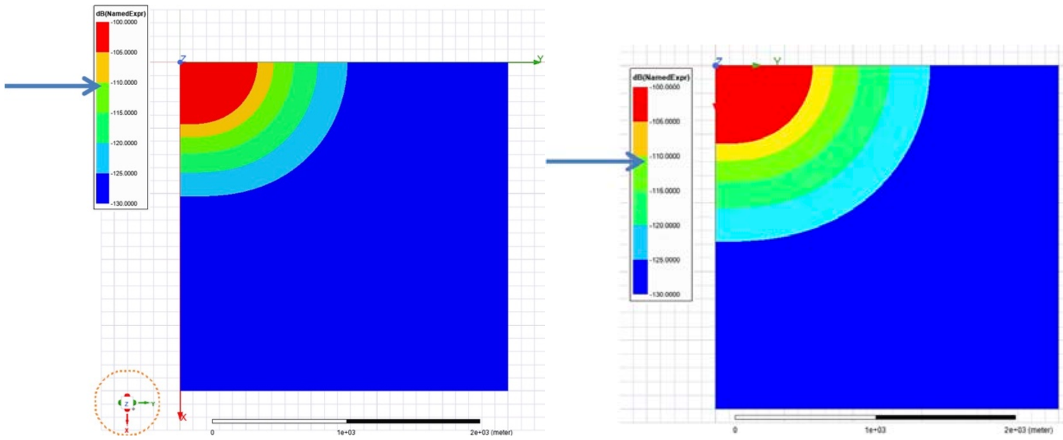

Figure 68: Electrode size and depth variable for tx distance increase with Normal antenna.

Soil Condition, Impedance, and operational distance

Soil and ground conditions will result in varying operational range due to differing earth conductivity and Tx source to earth impedance matching condition. The original reference case performed in the simulations of this paper was standard soil was a conductivity of 0.01 S/m. However, using different earth conductivity in both simulation and real world will alter the operational range. The below table shows the Electrical Resistivity and Conductivity of different soil types. Topsoil was used in the reference case simulations. We can see from the table that sand soil and loose sand have a lower conductivity. These conditions should yield longer operational distances.

Material	Soils and Clays	Electrical Resistivity (Ωm)	Electrical Conductivity (mS/m)
Soil Types	Clay (general term)	1 - 100	10 - 1000
	Loam	4 - 40	25 - 250
	Top Soil	40 - 200	5 - 25
	Clay-rich Soil	100 - 400	2.5 - 10
	Sandy Soil	400 - 4000	0.25 - 2.5
	Loose Sands	$1000 - 10^5$	0.01 - 1
Clay Type	Kaolinite	50 - 5000	0.2 - 20
	Montmorilonite	4 - 15	67 - 250

Figure 69: Soil condition resistivity/conductivity (Katsube, 2003)

The soil simulations have been performed for 2KHz, 50 metres spaced Tx electrodes, 3600W available Tx power for 4 different values of soil conductivity:

1. 0.0001S/m – Dry
2. 0.001S/m – Sand
3. 0.01 S/m – Soil, the reference case
4. 0.1 S/m - Clay

Since the operation range depends on the earth conductivity and Tx source-to-earth impedance matching conditions (depends on the earth conductivity) the data is organized in rows and columns: 4 columns for different values of the earth conductivity and 2 rows for different impedance matching conditions. The “matched” means that the Tx source output impedance is assuming as matched to the earth input impedance on the electrode terminals regardless of if the matching can be realized with thinkable H/W configuration or not. The “non-matched” means the simulation has been performed with Tx output impedance settings available with the recent H/W configuration (few ohms, few tens ohm, few hundreds ohm).

Earth Conductivity S/n	**0.0001 (Dry)**	**0.001 (Sand)**	**0.01 (Soil)** **Reference Case**	**0.1 (Clay)**
Matched Impedance	**Normal: 2km** **Tangent: 1.5km** Source impedance: ~6000 ohm	**Normal: 1.9 km** **Tangent: 1.85 km** Source impedance: ~600 ohm	**Normal: 1.4 km** **Tangent: 1.85km** Source impedance: ~100 ohm	**Normal: 1.05 km** **Tangent: 1.9 km** Source impedance: ~7 ohm
Non matched Impedance	**Normal: 1.45 km** **Tangent: 0.7 km** Source impedance: ~100 ohm	**Normal: 1.75 km** **Tangent: 1.65 km** Source impedance: ~100 ohm		

Figure 70: Earth Conductivity signal in various soil conditions

Clay Soil Simulation Results: 0.1 S/n

Frequency: 2 kHz
Magnetic Field: **Normal**
Electrodes separation **~50m**
Injected power ~ **3600W**
Distance scale 100m/div.

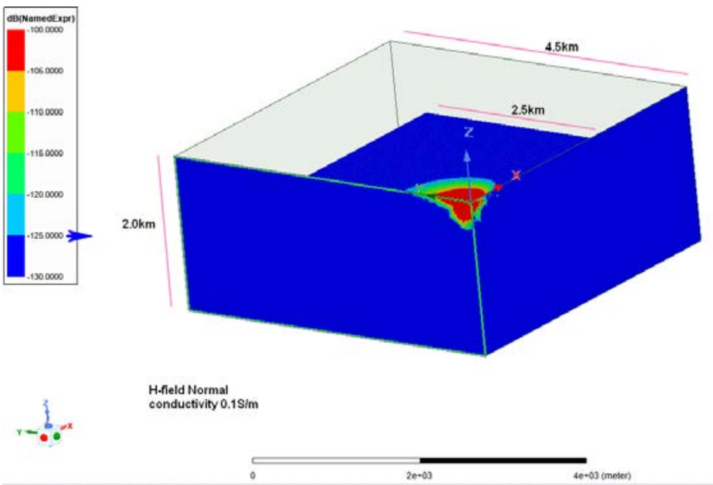

Figure 71: Clay Soil 2kHz Normal 3600W at 50m results

Clay Soil Simulation Results: 0.1 S/n

Frequency: 2 kHz
Magnetic Field: **Tangential**
Electrodes separation **~50m**
Injected power ~ **3600W**
Distance scale 100m/div.

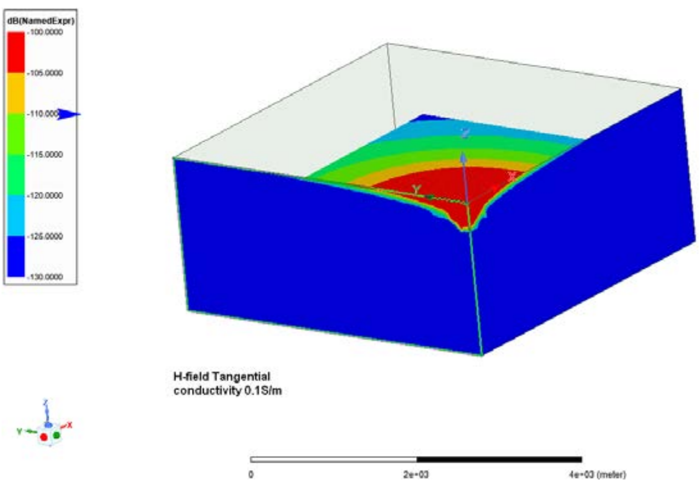

Figure 72: Clay Soil 2kHz Tangential 3600W at 50m results

Dry Earth Simulation Results: 0.0001 S/n

Frequency: 2 kHz
Magnetic Field: **Normal**
Electrodes separation **~50m**
Injected power ~ **3600W**
Distance scale 100m/div.

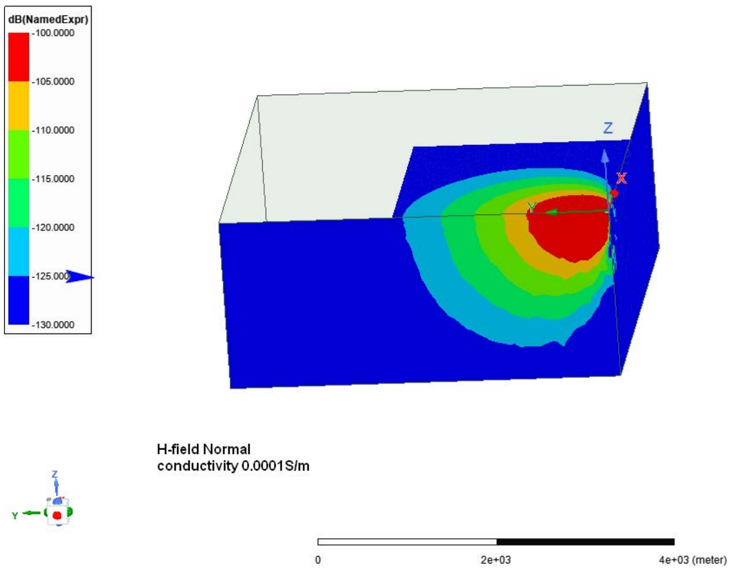

Figure 73: Dry Soil 2kHz Normal 3600W at 50m results

Dry Earth Simulation Results: 0.0001 S/n

Frequency: 2 kHz
Magnetic Field: **Tangential**
Electrodes separation **~50m**
Injected power ~ **3600W**
Distance scale 100m/div.

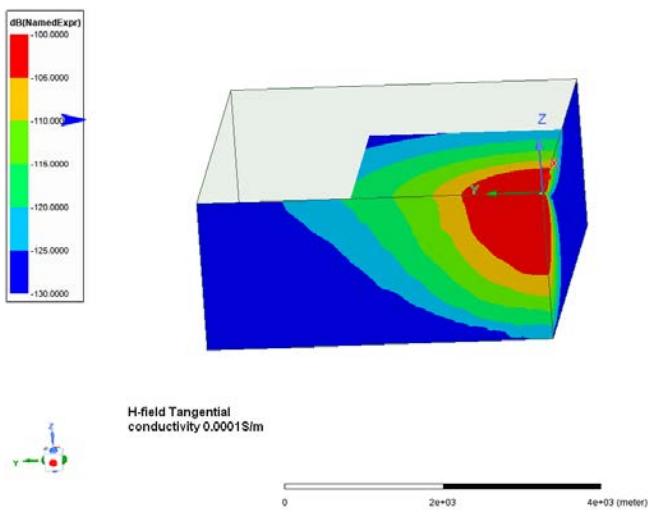

Figure 74: Dry Soil 2kHz Tangential 3600W at 50m results

Input Impedance

Input impedance of the Tx electrodes can vary within wide range depend on conductivity of the earth medium. In particularly, for the conductivity 0.0001 S/m – 0.1 S/m the corresponding impedance range for the electrodes separated on 50 mm would be 7 ohm – 6000 ohms. To provide the optimal power transfer conditions the output impedance of Tx source should correspondingly adjusted. While the lower limit of the mentioned impedance value is easily realizable with the conventional solid-state amplifiers, the realization of higher values of the output impedance could be difficult even with implementation impedance step up output transformer. In this case it could be reasonable to consider dual stage impedance step up circuitry: Tx source (output impedance – few ohms) - > transformer -> (output impedance few hundreds of ohms) -> impedance matching circuit (output impedance – few thousands ohm).

As a rule, the last stage has intrinsic relatively lower bandwidth, but for this specific application that is not an issue, if the carrier frequency if fixed. The below diagrams LC matching circuit is designed for source impedance 200 ohm (transformer output) and load impedance 6000ohm (earth dry).

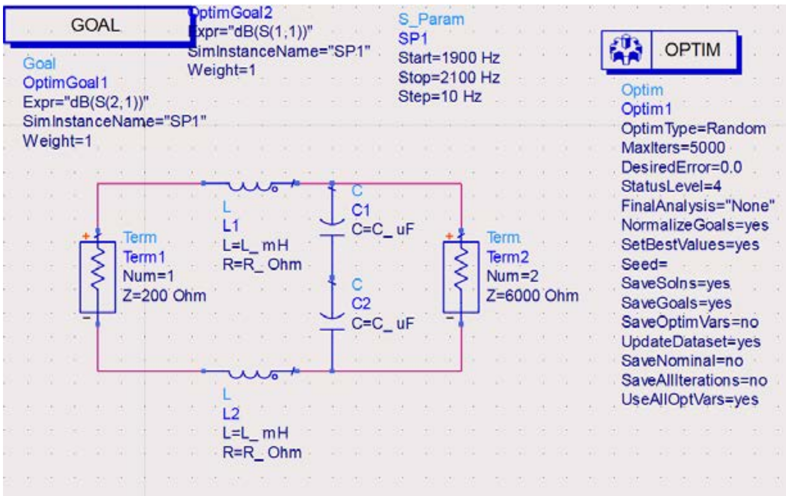

Figure 75: High Level Circuit design to for input impedance variables

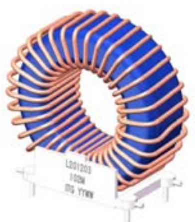

Figure 76: L1/L2 = Unshielded Toroidal Inductor 3.48Ohm Max Radial, Vertical (Open)

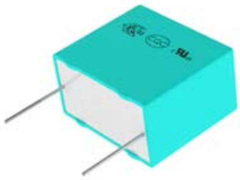

Figure 77: C1/C2 = Film Capacitor 310V 630V Polypropylene (PP), Metallized Radial

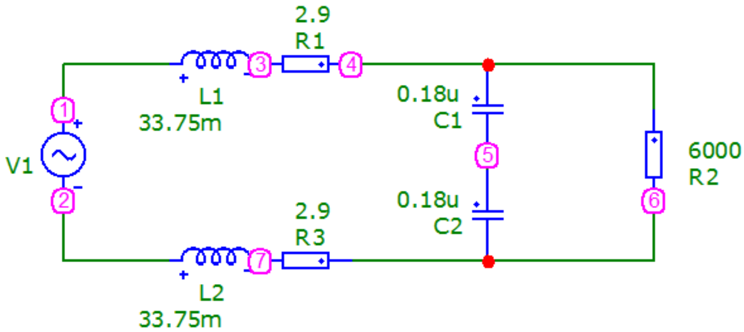

Figure 78: Circuit design

The performance is simulated in frequency (FD) and time (TD) domains both and the results are presented below.

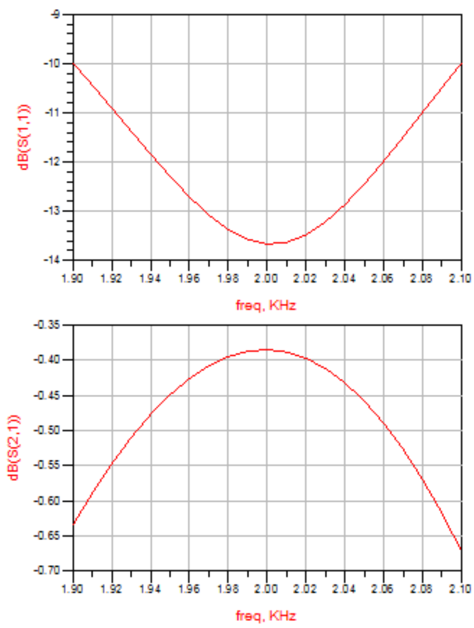

Figure 79: Frequency and time domains

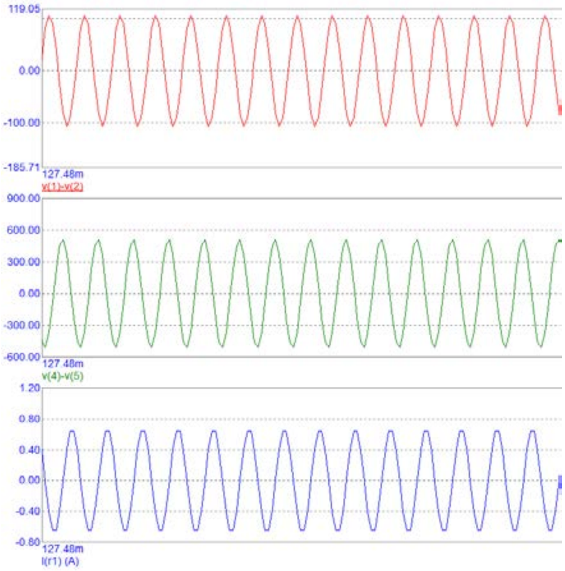

Figure 80: Return loss

As it can be seen the matching circuit provides acceptable low Return Loss, S11<~-10dB, low Insertion loss S21>-1dB within relatively wide frequency band 1.9 -2.1 kHz. The corresponding components that could withstand the voltage/current.

Wireless Power Transfer

The Near Field region is defined over 1 wavelength whereas the Far Field Region is from 2 wavelengths onwards. Within the Near Field region there are two areas, reactive and radiative. This reactive zone can transfer power of the air, like a payment card tapping close to a payment terminal. The illustration below shows this zone close to the Tx transmission source. Because we are using NFC in the reactive zone, I created some simulations on how far we can transmit power over this medium to power a remote device like an underground USB RX IOT temperature/moisture sensor for agriculture.

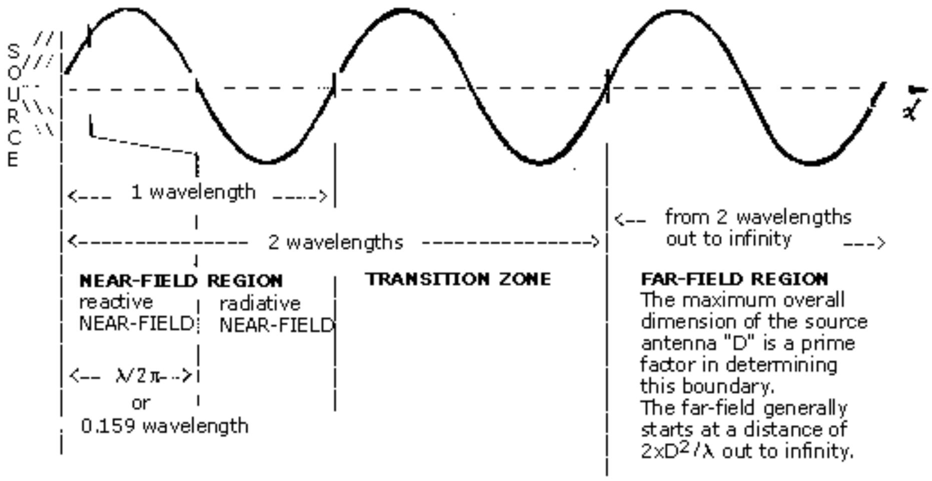

Figure 81: Near Field vs Far Field wavelength (OSHA 1990)

The estimation of the USB DC power supply capability by means of Wireless Power Transfer (resonant NFC coupling) is explained below with simulations. To provide power ***P*** at a perfectly matched load (USB powered device, for example) the required strength of magnetic field ***H*** is:

$$H = \frac{4 \cdot \sqrt{\rho}}{f \cdot \pi^{3/2}} \cdot \frac{\sqrt{P}}{\sqrt{S_w} \cdot D^{3/2} \cdot \sqrt{N}}$$

Where:

D – diameter of Rx coil (assumed 1m)
N – number of turns of coil winding (assumed 100 turns)
Sw – cross-section area of wire (0.312 mm^2)
f – frequency of wireless power transfer (2 kHz)
p - resistivity of wire conductor (1.72 x 10^{-8} Ωm)

The estimated required strength of magnetic field ***H is*** -62 dBA/m

The threshold level is shown on the screenshots bellow for horizontally and vertically aligned coils, correspondingly. The maximum powered distance using these variables is 50 meters.

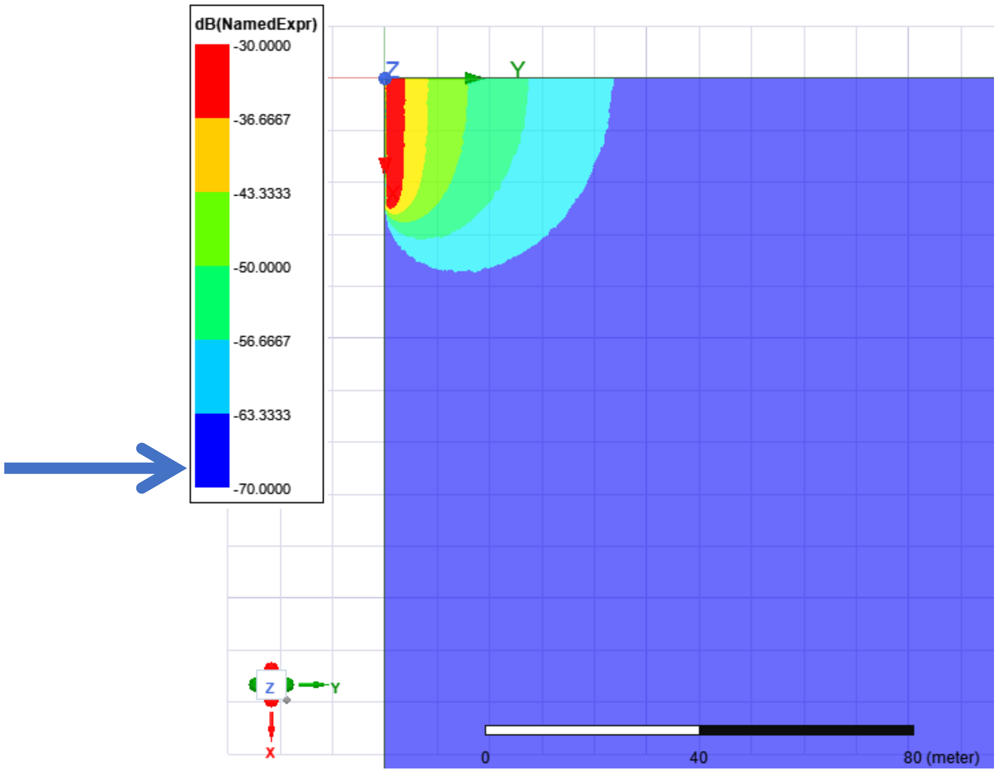

Figure 82: Horizontally aligned coil (in plane with earth's surface)

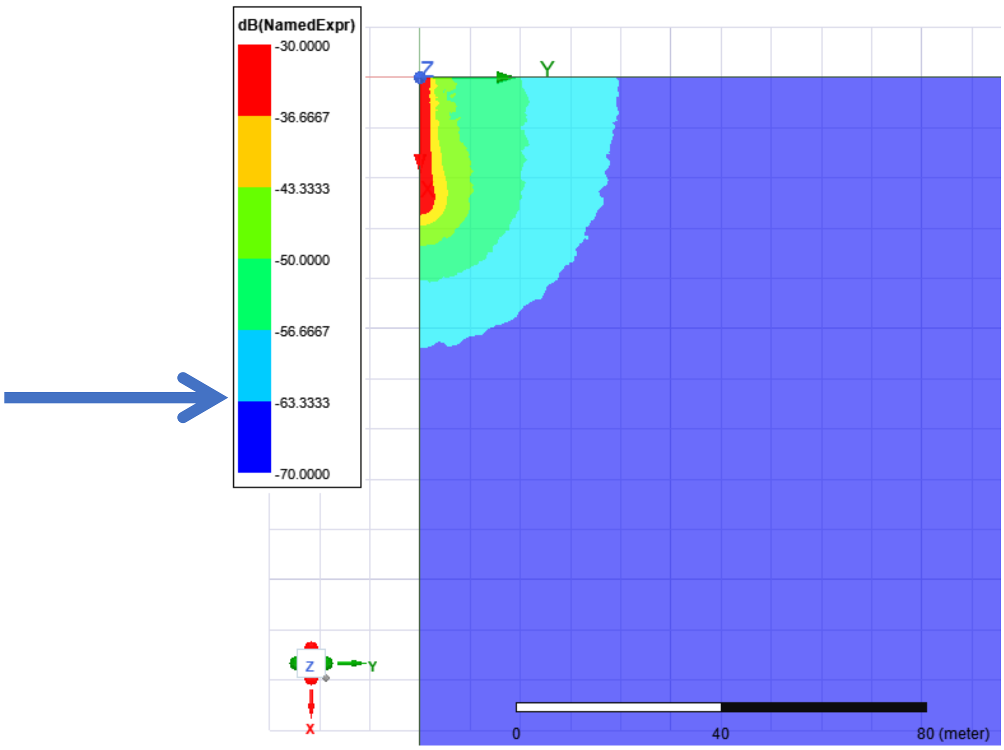

Figure 83: Vertically aligned coil (normal to earth surface oriented in proper direction)

Summary before TX/RX design

Concerning the choice of operation frequency: the factors to be taken into account

a. For lower frequencies, the equipment (particularly at Rx side) becomes bulky.

b. For higher frequencies, the losses on radiation become increasing (to be verified),

c. Decay rate is increasing because of skin-effect.

d. Earth impedance is lower (that is more convenient) at higher frequencies (to be verified)

e. According to the FCC: frequency below 9 kHz are not regulated.

f. Natural noise (including man-made noise): to be considered in more details basing on the sources (JACOBSEN, 2021)

g. Soil conditions will alter the operation performance

Concerning the required Tx power:

a. Operation range increases much slower than Tx power increases: to double the operation distance Tx power should be increased at ~18dB (to be verified)

b. Design complexity and manufacturing cost increases much quickly than Tx power increases

Concerning other possible options

a. Discrimination between the transmitting (useful) signal and a jamming signal: the transmitting signal is assumed to be a Near-Field signal. If the jamming signal is Far-Field, then the difference between two signals (E- and H-field is out-of-phase for near-field sign and in-phase for far-field signal) could be used.

b. An electrode depth of 3 meters such as a light pole or road sign in the real world with a 200mm X 200mm thickness over the simulated 100mm X 100mm will gains a 10% increase in signal distance.

Below is a summary at this time in the context of proceeding with Tx/Rx design and testing from our simulations, basing on info presented in (Durkin 1983)

The performance of through-the-earth (TTE) communication systems is limited by natural noise (rather than "instrumentation" noise in contrast with the situation for the conventional RF communication; probably, that is one of the main reasons for not widely using the TTE-like approaches). The natural noise (atmospheric and man-made) may vary considerably with time and frequency.

Man-made noise is a continuous-wave (CW) interference that generally occurs at 60(50) Hz and various harmonics of 60(50) Hz extending to several kilohertz. Also, some high-power artificial sources mentioned in (JACOBSEN, 2021) should be considered under operation frequency choice.

There are three main factors to consider in relation to man-made noise

- Man-made could be minimized with proper choice of operation frequency (somewhere below 9kHz, between 2-4 kHz, excluding the harmonics of 60(50) Hz) the atmospheric noise.
- Powerful artificial sources associated with military/NAVY/submarine communications
- Possible deliberate jamming of our signal.

In some cases, the discrimination between the transmitting (useful) signal and the noise signals could be made based on the difference in polarization (easier approach) or E/H phase shift (much complex approach) characteristics of the noise signals or a combination of the two. It should be noted the approaches are applicable for the case only when the noise sources, are within the Far-Field zone. For far-field noise sources the expected polarization is vertical (magnetic field component is tangential with respect to earth surface) while the Rx polarization can be set to horizontal where the Rx coil is parallel to earth surface. The phase shift between E and H is zero while that is 90 degrees for near-field sources.

Concerning the Rx polarization setting vertical (Rx coil is normal to earth surface) vs. horizontal (Rx coil is parallel to earth surface): the vertical component of magnetic noise field tended to be 10 to 15 dB below the horizontal component while, according to the simulated results, the vertical component of the magnetic field of useful signal is, at least, 25 dB below the horizontal component of the magnetic field of useful signal. So, in this sense it is expected as an optimal Rx coil orientation as vertical (acquiring the horizontal component of magnetic or vertically polarized EM wave in terms of EM wave polarization), as it is recommended in (PETROVICH, 2021) It should be noted here once more such orientation would require knowing (or pelengation) on proper direction of arrival (in contrast to the case when the Rx coil is normal to earth surface).

Concerning the Tx, Rx hardware, in particular Tx driven amplifier and Rx low noise pre-amplifier: it would be reasonable to use on the test stage as standalone units within the signal flow chain to make the challenging tasks at the test stage as easier. The assumed full chain is expected as follow:

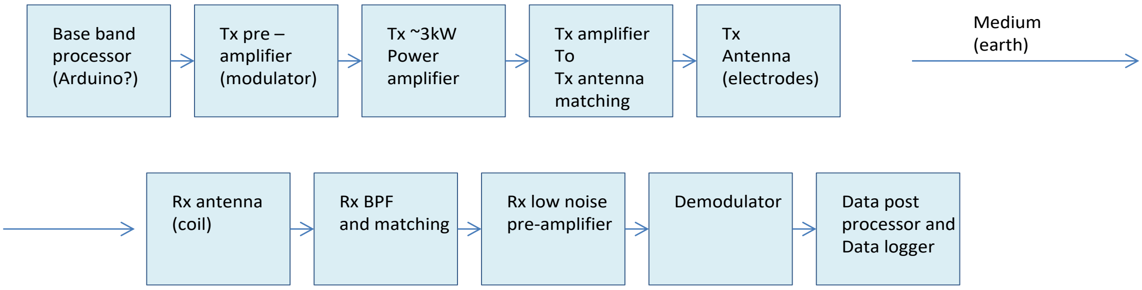

Figure 84: Theoretical hardware modules required from end to end

Concerning the possible approaches with enhanced data transmission security: to keep the transmitting data as secure as possible, the RF link should stay underground. In other words, the useful signal associated field should not leave earth medium (for such mode, correspondingly, the Rx will be less affected by aerial noise due to the reciprocity principle). It is expected that such mode is potentially available with completely buried vertically polarized antennas (either vertical monopoles or horizontal loops).

As indicated in the VLF overview, the earth current flows indicated by (I) within the lower hemisphere over the earth’s surface. It creases a magnetic field (H). The magnetic field (H) can be picked up with an Rx coil (Inductive coupling). The Electric field is created by the Tx electrodes. The current flowing within the resistive media defines the voltage drop (V=I * R) between Rx electrodes. Finally, that voltage drop can be measured.

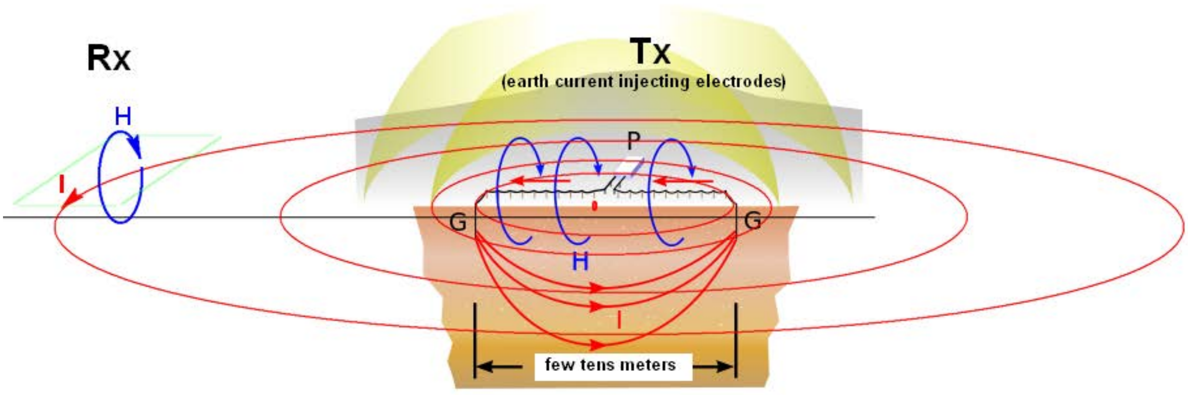

Figure 85: Theoretical signal transmission between Tx electrodes and RX loop over NFC

It can be shown that the magnetic field H has a non-zero tangential and zero normal component if the current path is a straight line. (normal to the plane of this projection image with zero curvature). As the distance between the Tx and the Rx increases, the curvature decreases, and the normal component becomes weaker, rapidly.

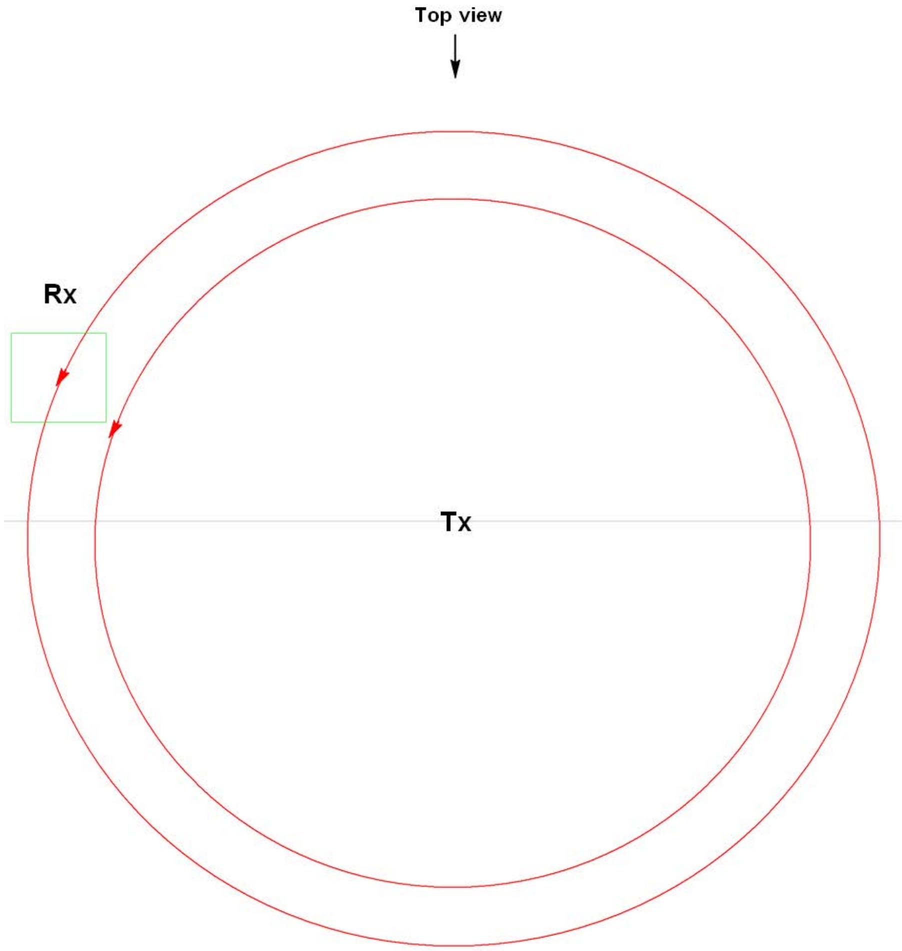

Figure 86: Top view shows weak signal to avoid for RX placement

It should also be noted that there are areas with near to zero curvature at small distances, for example, below in the green rectangle simulation in a single quadrant. Correspondingly induced normal component of the magnetic field is weak.

Frequency: 3 kHz
Magnetic Field: **Normal**
Electrodes separation **~50m**
Injected power ~ **3600W**
Distance scale 100m/div.

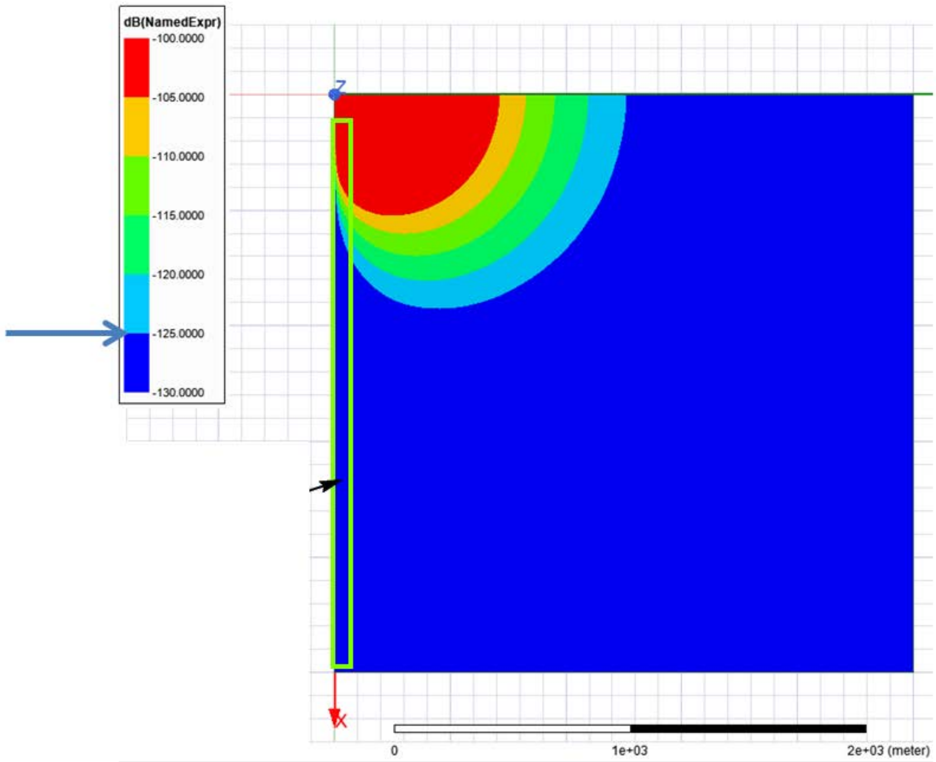

Figure 87: Green rectangle reveals weak signal zone to avoid for rx placement.

In all four quadrants, aerial view in a grass field, for example, would look like the below with the corresponding TX electrodes. The area at 12 o'clock and 6 o'clock (north/south) would be the worst places to put the RX coil as the magnetic field is weak with small to zero curvature.

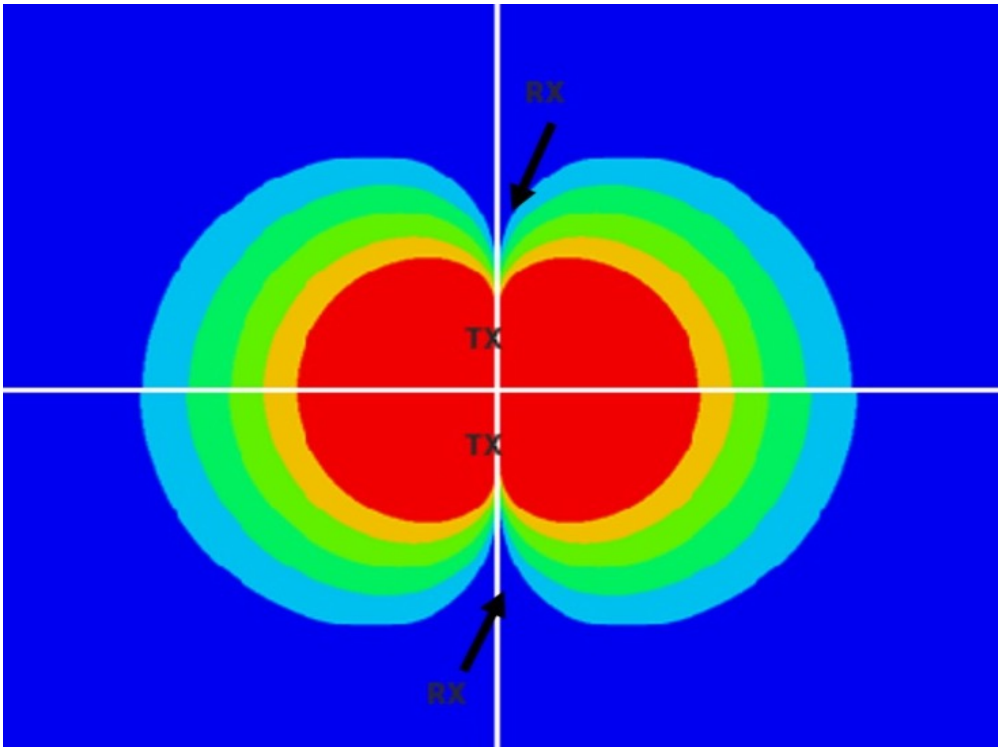

Figure 88: Aerial view weak signal for Rx

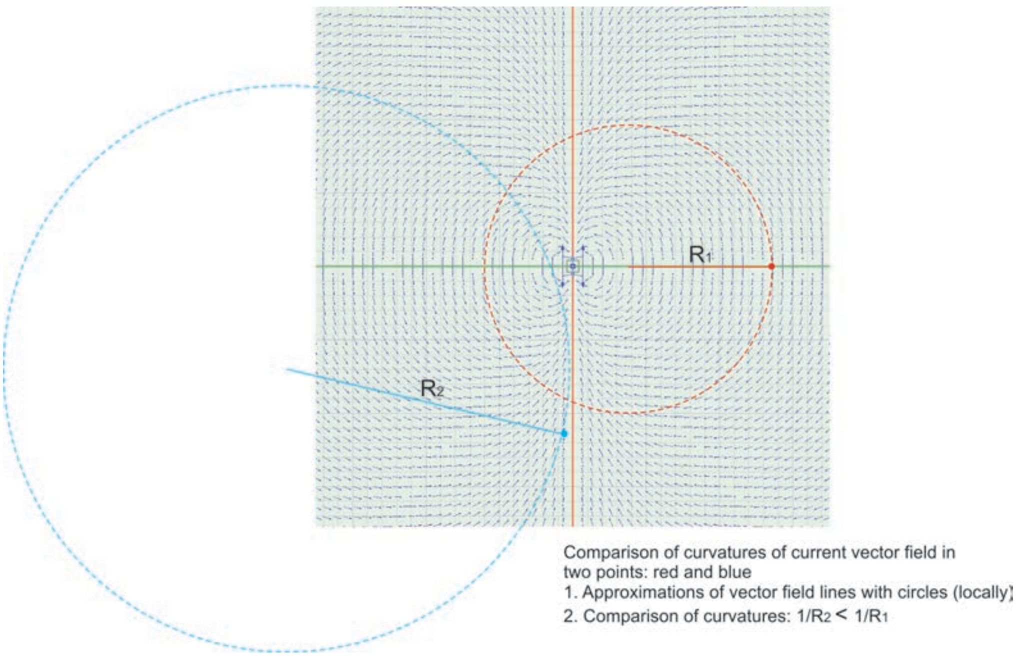

Figure 89: Curvature field Rx weak spot

Hardware Design

Tx

The transmitter operates on 24 volts, at an adjustable frequency of 1-14khz depending on noise and seasonal conditions at an operation bandwidth of 60 Hz. Based on the simulation work, the best general frequency is between 1-4 kHz. This is connected to the earth probes, or in an IED setting. These probes could be power, light poles, stop signs, fence posts. The adversary will simply press a button to send a signal to the Rx for initiation. The Tx weighs less than 1kg.

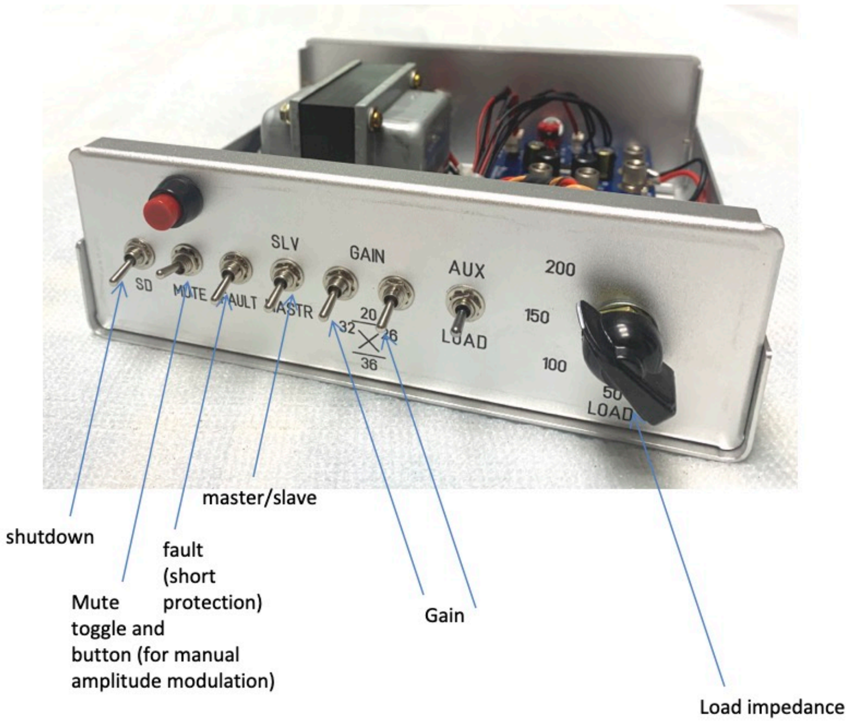

Figure 90: Variable Tx Hardware with adjustable impedance

Choosing the optimal operating frequency is defined as trade-offs between the next main factors:

1. Sub 9-kHz frequency band. No licensing is required.

2. The lower frequency, the weaker skin-effect for earth medium. Negative dependence vs Frequency.

3. The higher frequency, the lower natural noise level (including harmonics of utility frequency). Positive dependence vs. frequency.

If in certain environmental conditions the factor of utility frequency harmonics becomes dominant than the factor of harmonics of utility frequency should be considered, and it is reasonable to choose the operation band between two sequent harmonics of utility frequency. In the case of utility frequency, 60 Hz, the operation band can be chosen, for example, between 2.82kHz and 2.88kHz. Correspondingly, the center frequency will be 2.85kHz and operation bandwidth ~< 60 Hz.

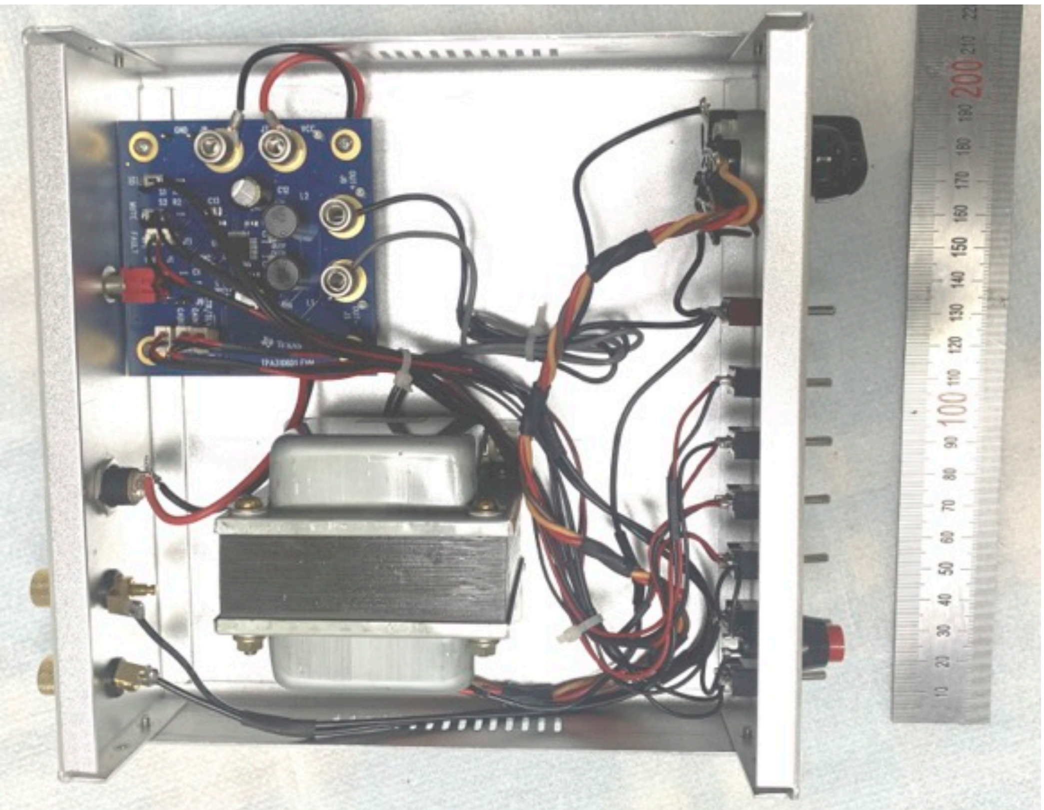

Figure 91: Top View of the Tx

Figure 92: Rear View of the Tx

Commercial Tx design

Figure 93: Commercial Tx design

Tx Base Band

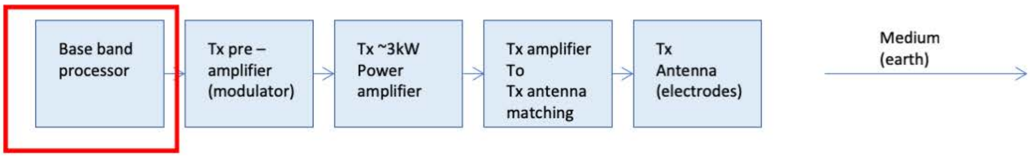

Figure 94: Base band

The Arduino or Raspberry PI device provide the ideal base band processor base. Both come with encryption/decryption libraries and are cheap and require a low footprint for the Tx.

Tx Pre Amplifier

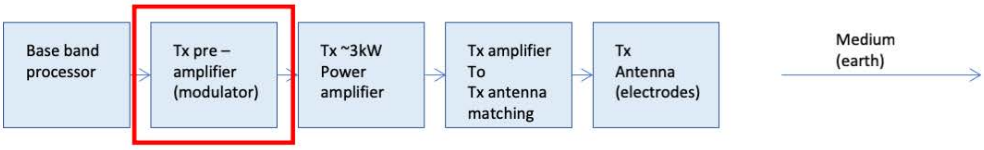

Figure 95: Tx Pre Amp

The Tx amplifier output power level depends on the gain settings on the power amplifier and the input signal (from waveform generator or, in general case, form the baseband signal processor).

Under min. gain setting 20dB the input signal level ~< 5 V p-p (typical output signal from such source as Arduino); under max. gain setting 36 dB the input signal level ~0.8 V p-p (typical output signal from such source as PC sound card line out). Exceeding input signal levels leads to output signal clamping. Using an Arduino as a based band processor if the TX signal is fully synthesized then the preamp is not required in this design and can be omitted.

The current Tx power amplifier circuitry can be used as drive amplifier for the next amplification stage, so the output power could be increased up to ~ 500W.

Front and rear view of the waveform generator to power amplifier chain to be connected to Tx antenna /electrodes.

Figure 96: Custom Field-testing equipment

Tx Base Power

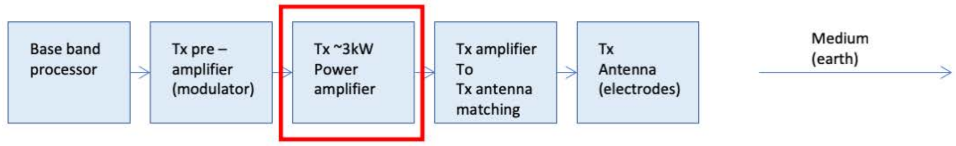

Figure 97: TX Power design

In the current design, the Tx power amplifier is chosen as class D, 24V DC powered, with controlled output power up to 40W (margin to compensate the expected mismatching loss because of lack of data for the actual earth impedance, varying it vs. the electrodes separation distance). It is assumed the power amplifier will be directly driven with relatively lower power audio output such as for example, analogue audio output of PC. The wideband output is designing to be a wideband impedance matching output audio transformer.

Operation frequency: 4kHz
Bandwidth: 1kHz - 8kHz
Power: up to 40 Watt
Source impedance: few ohms (connected to primary)
Load impedance: 100 Ohm, 150 Ohm, 200 Ohm (connected to secondary) to be switched to certain value under fine tuning to specific earth conductivity conditions.
Efficiency: >~0.92

Tx Amp to Antenna Matching

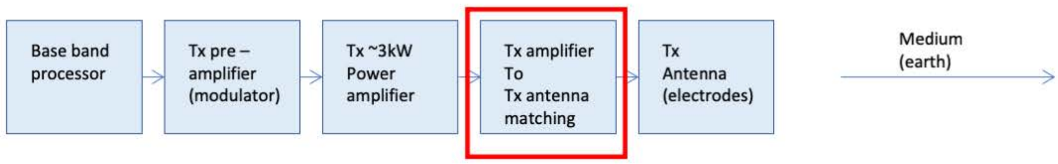

Figure 98: TX Amp to Antenna

Wide band output transformer to provide optimal impedance matching conditions the knowing of the actual impedance of earth is required. Earth impedance is not measured for now. The values used in the simulations is acquired from available sources. The actual value will depend on soil type, electrode configuration.

Tx Electrodes

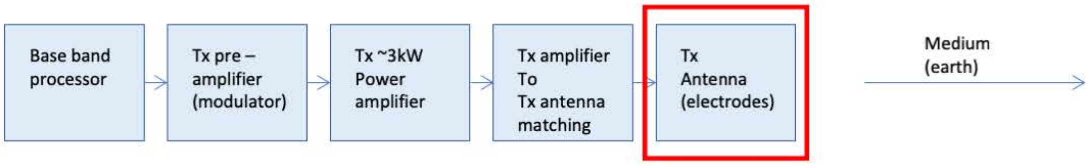

Figure 99: Electrode design module

The electrodes at the Tx side are represented as metal rods 200x6x6cm^3 that are buried at ~1m depth**.** The common rule is that the larger electrode surface area underground (defined with electrode thickness/diameter and burial depth), the lower impedance and, so, the larger injected current. When using AC application (where no polarization effects in the soil are expected), specificity of metal is not so important. The injected current (depends on earth impedance between the rods) would depend on the buried depth and earth conductivity. So, for testing purposes, any metal pipe could be used, for example, a steel pipe. For a real-world application, something like earth helix anchor or ground screw made of steel with any protective paint removed. Well, conducting media can be buried around the earth probes such as copper sulphate, ionic conductivity salts to lower the impedance.

Sample view of Tx electrodes as a set of ground anchor screws with wrench with Outside Diameter (OD) ~50 mm at 1 meter length.

Figure 100: Screw in Tx electrodes

Common view of two Tx electrodes with Tx feeding cables (25 m length of each) with with contact clamps. 60cm ruler is for scale.

Figure 101: Field test TX Electrodes

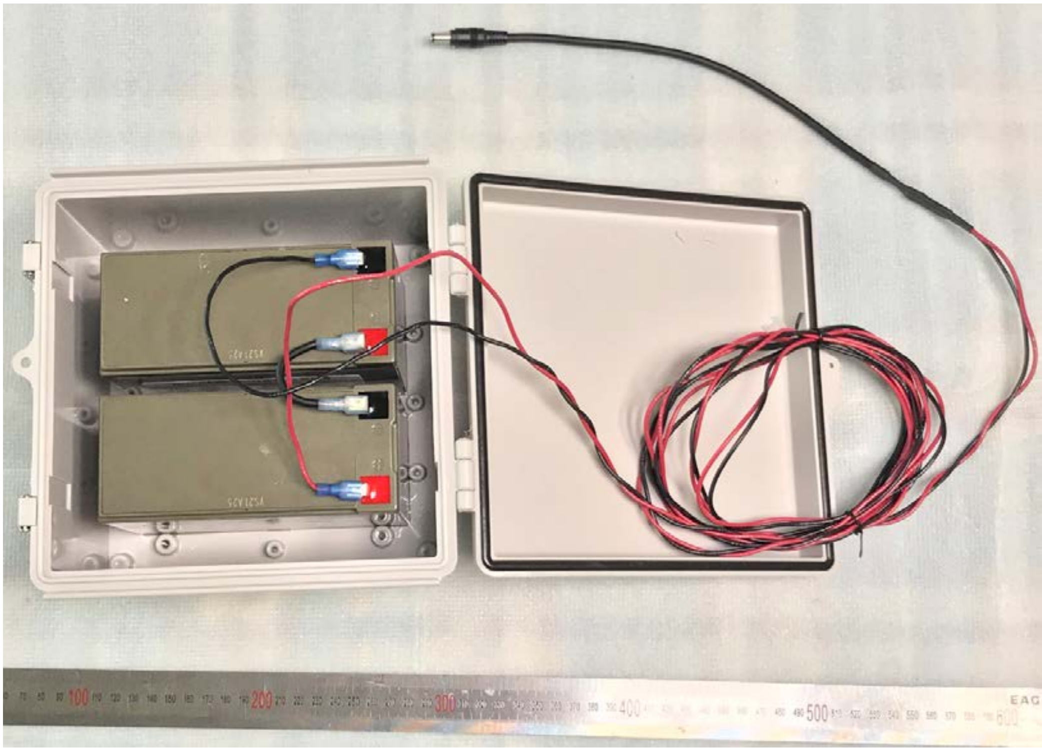

Figure 102: Field Test Portable battery unit 24V 7Amp hour

Rx

The diagram below shows three different IEDs. The one on the left and right are the traditional cell phone detonation triggers wired to a thermos of explosives. This would be defeated in a jammed environment. The IED in the middle with the black Rx with the red button is using the VLF method for initiation with the tangential aerial underneath. The device is powered by a series of 9V batteries. This device will detonate in a jammed environment using the earth as a medium in the 2-9 kHz range.

Figure 103: IED with RX loop and receiver between two Cell phone IED's

RX Antenna

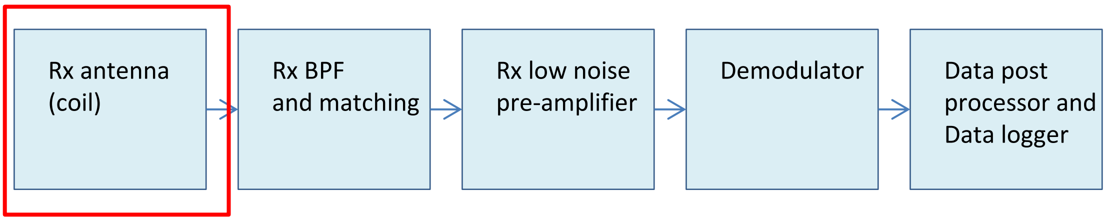

Figure 104: RX antenna module

Rx antenna coil: to be customized completely basing on the requirements to be defined with the rest parts of the signal flow chain. Fortunately, the antenna could be designed and manufactured as "universal", i.e., suitable for the testing purpose as well as for your actual application case. Let's note, in brief here, that under testing is assumed, first, the testing on the actual environment conditions (natural noise level per polarization, location, time, etc.) with the final goal the defining the optimal operating frequency and bandwidth.

An antenna with an area ~1m^2 and copper winding mass of ~ 1kg will provide antenna associated thermal noise spectral density ~1 fT/sqrt(Hz) that is much lower than the expected value of natural noise spectral density within the band of interest. So, such an antenna would be guaranteed fit for the application.

The antenna has been manufactured as dielectric material former wound circular coil. The winding parameters and the expected electromagnetic parameters are specified below. It should be noted here that the real part of the impedance of the antenna itself is within 10 – 20 Ohm and should be transformed, i.e., stepped up to ~ 1 Mohm to be optimally matched with high input impedance of pre-amplifier. On the stage of testing of the system that will be done with low noise input transformer (that provides wideband matching); while under actual application, the impedance step up would be naturally reached with relatively narrow bandwidth Rx BPF (to be realized with an additional RC circuit and implemented into antenna circuitry.

Figure 105: Antenna Cad drawing

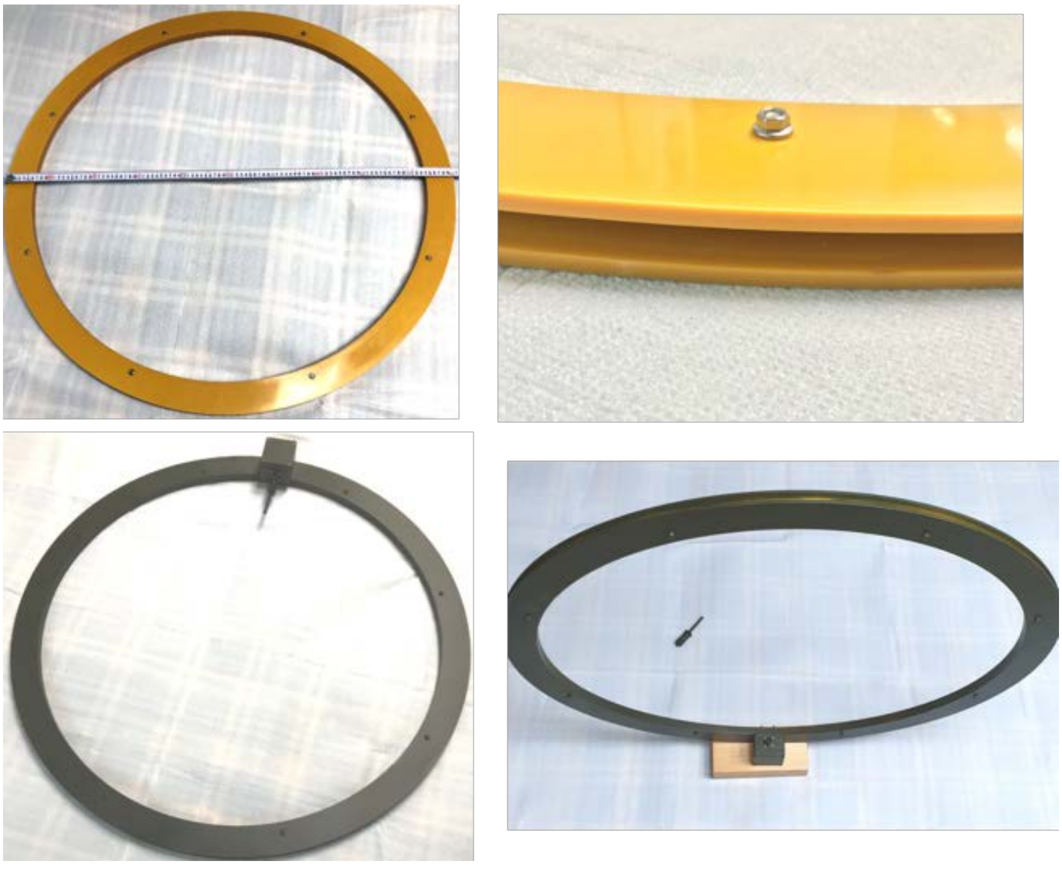

Figure 106: RX coil input balanced to dual unbalanced adapter testing for optimum signal.

RX BPF and matching

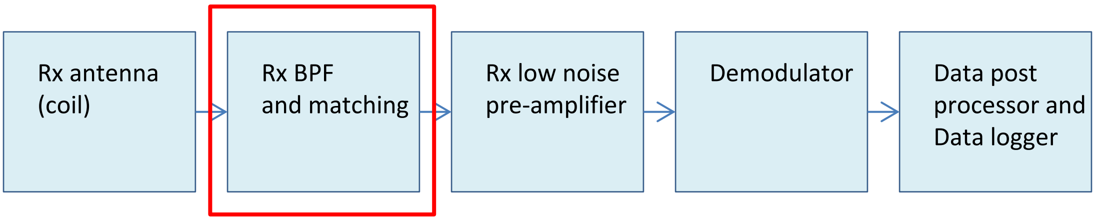

Figure 107: RX impedance matching

Concerning the Rx BPF, impedance matching, and low noise pre-amplifier in more detail. It is assumed two configurations for the Rx BPF, impedance matching, and low noise pre-amplifier:

1. For using under testing
2. For use in real world applications

Common requirements and description of the Rx BPF and the impedance matching stage for testing: The Rx low noise pre-amplifier should be flexible, i.e. tunable within the frequency band center, bandwidth, gain, and should possess very low noise within wideband.

These requirements define the relatively large complexity of the pre-amplifier as well as the impedance matching transformer to be used for testing. To provide wideband signal input, the Rx BPF should be omitted at the testing stage; all settings for center frequency, bandwidth (LF roll-off and HF roll-off) will be performed via a low-noise pre-amplifier. Assuming the Rx antenna coil of maximum bandwidth, i.e., from DC to self-resonance frequency, 10000:1 impedance matching transformer, low noise pre-amplifier. High transformation ratio is required to match Rx antenna coil with a relatively low real part of impedance (~ 17 Ohm) with high impedance input (~ 1 Mohm) of low noise pre-amp and provide low equivalent noise at its input (the expected noise figure for this matching condition is expected ~ 0.05dB).

After defining and confirming with the testing the operation band, bandwidth, noise level those parts could be replaced with relatively lower complexity, relatively lower cost, low noise, fixed frequency, fixed narrow bandwidth parts: Rx BPF, Rx antenna to Rx amp impedance matching facilities and Rx amplifier.

Under real-world application, the Rx antenna (coil) to low noise pre-amp matching would be naturally reached with relatively narrow bandwidth Rx BPF (to be realized with an additional RC circuit and implemented into antenna circuitry).

To fit the requirements for impedance/noise, the antenna will be reconfigured (not rebuilt) for a specific band, bandwidth impedance by means of adding setting capacitor and resistor (optional). See images below.

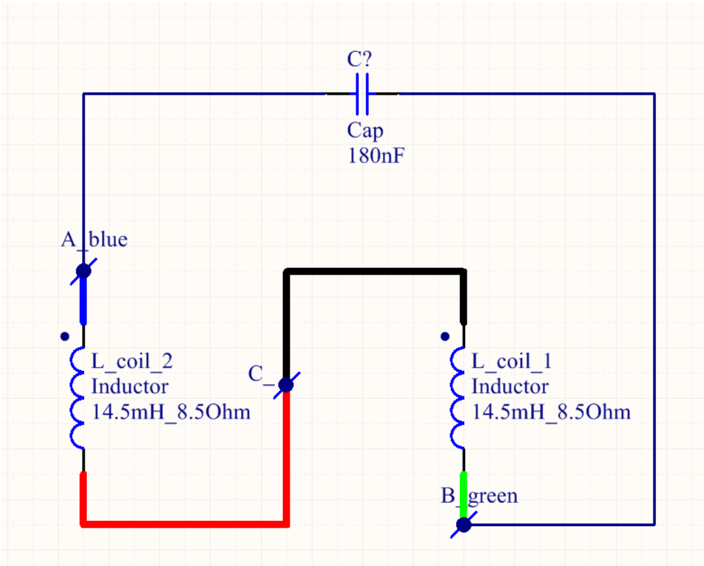

Figure 108: RX circuit design

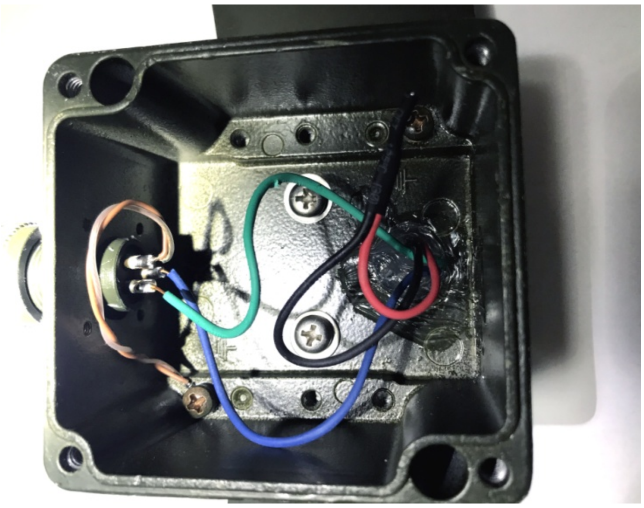

Figure 109: Common view RX design

Some quantitative estimations are presented below

Value of capacitance *C* required to make the Rx antenna (coil) with inductance *L* as resonant of frequency *f* ~ 2850 Hz:

$$C = \frac{1}{(2 \cdot \pi \cdot f)^2 \cdot L} \qquad \sim 108\text{nF}$$

Obtained parallel LCR circuit (tank) with resistance ~17 Ohm (resistance of the coil) has quality factor *Q*:

$$Q = \frac{2 \cdot \pi \cdot f \cdot L}{R} \qquad \sim 31$$

That defines peak resistance of the tank at resonance

$$R_{res} = Q^2 \cdot R \qquad \sim 16.3 \text{ kOhm}$$

With such impedance of the signal source, the noise figure of typical high impedance input low-noise pre-amplifier is expected as about 1dB, that acceptably low value.

The relative bandwidth associated with the above estimated Q-factor:

$BW = {}^{1}/_{Q}$ ~ 0.03

The absolute value of bandwidth at the frequency *f:* ~2850Hz * 0.03 ~ 85 Hz is satisfactory narrow for natural noise-suppressing, excluding maybe the case when the utility frequency harmonics are dominant. In such case, the additional filtering could be performed with H/W based filters in particular, with active filters or with software filters.

RX low noise pre-amplifier

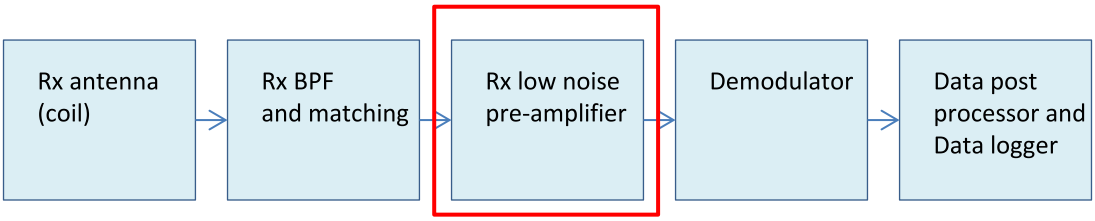

Figure 110: Rx Low noise preamp module

The Rx low noise pre-amplifier should be flexible, i.e., tuneable within the frequency band centre, bandwidth, gain, and should possess very low noise within wideband. These requirements define the large complexity of the pre-amplifier as well as the impedance matching part (transformer). After defining the operation band, bandwidth, acceptable noise figure of this stage, those parts will be replaced with single one relatively lower complexity, relatively lower cost, low noise, fixed frequency, narrow bandwidth amplifier.

To fit the requirements for impedance/noise matching, the antenna will be reconfigured (not rebuilt) for a specific band, bandwidth impedance by means of adding a setting capacitor and resistor.

Universal lab pre-amplifier (see images below) is chosen for the highest flexibility under test and as the base for further modification and adjusting for the application-specific requirements.

Figure 111: Preamp for RX

The main functions and characteristics of the preamplifier:

- AC 110/220 Volts, powered, ~6 Watt. But, for better lower noise performance, it is adjusted to operate with an internal rechargeable battery pack that is doing as a type of voltage regulator. Operation time in autonomous mode > 40 hours.

- Input: switchable between DC, AC, single-ended, differential. Input impedance - ~10 Megohm

- Output: single-ended, output impedance ~ 600 Ohm *

- Gain: variable, up to 10^4 (80dB)

- Frequency band: variable 0.05 Hz – 250 kHz

- Common mode rejection 40 -120 dB depending on gain and frequency band.

- Noise figure: <0.5dB for high impedance source (> 1 Megaohm). In the case when the Rx coil impedance much lower (as is expected), the higher impedance could be provided either with a step-up transformer (if operation bandwidth 1 -10 kHz is required) or with making the coil as resonant (when narrow bandwidth is satisfied).

- Concerning the output following stage H/W: an available off-the-shelf SDR tuner (relatively low cost) and PC (notebook) could be considered that will act as Demodulator, Data post-processor, and Datalogger.

- Smaller pre-amplifiers can be used for RC-IED or smaller projects include

    - Oscilloscope Preamplifier LNA10
    - Single chip low noise amplifier that could be customized with Analog Devices LT1567 chip
    - INA217 Tiny Microphone Preamp

Circuitry of the Pre-Amp

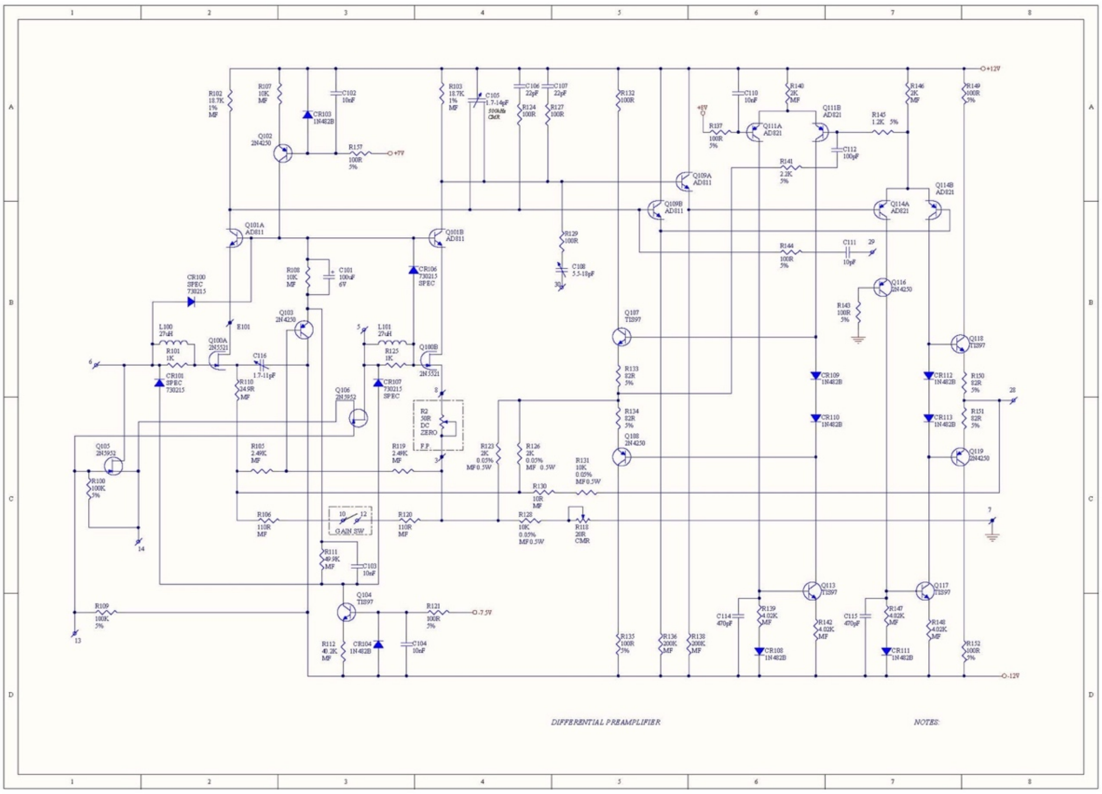

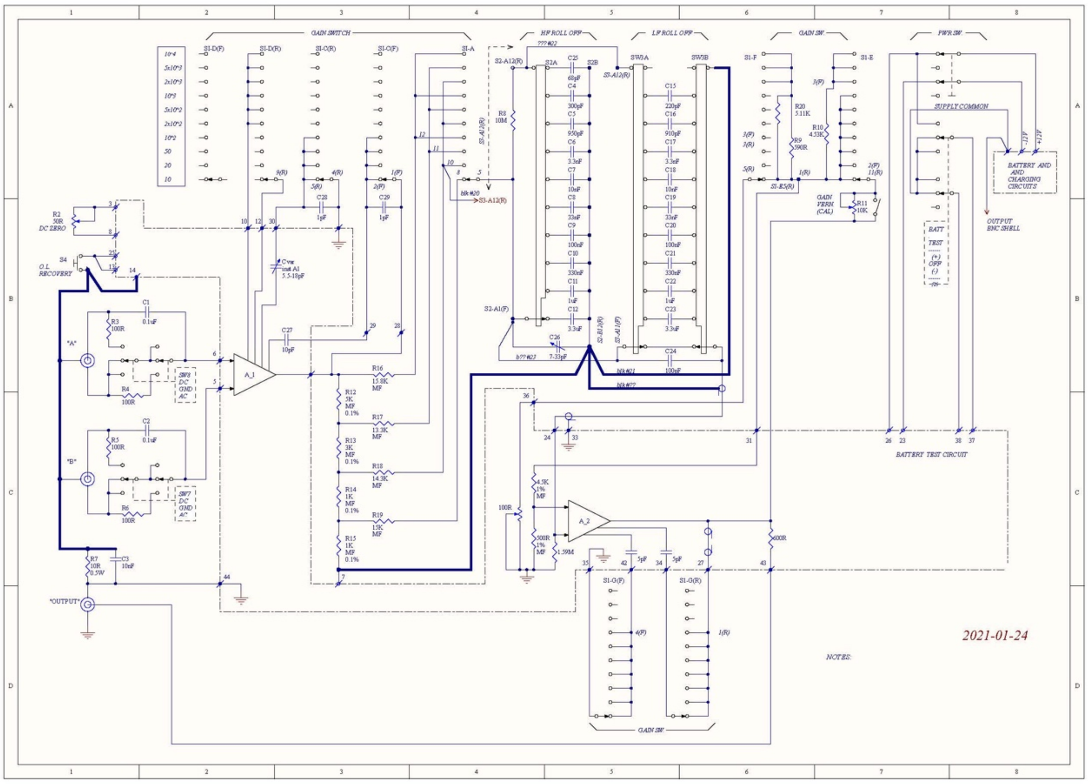

Figure 112: Rx Amp design specs

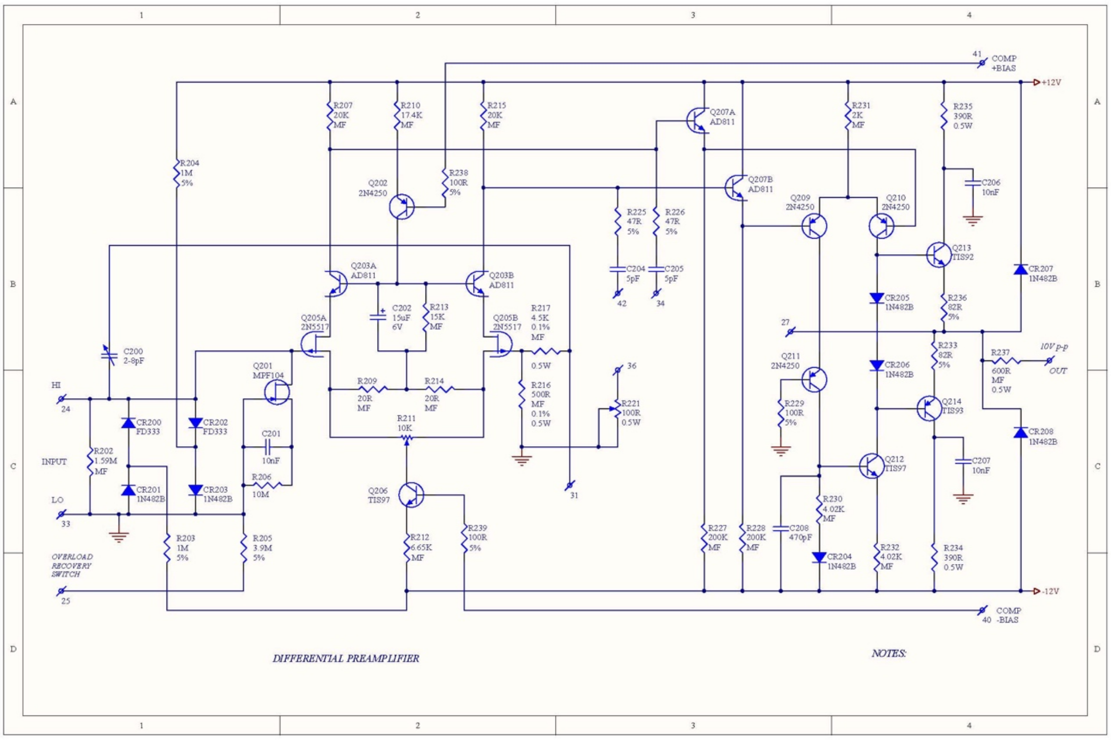

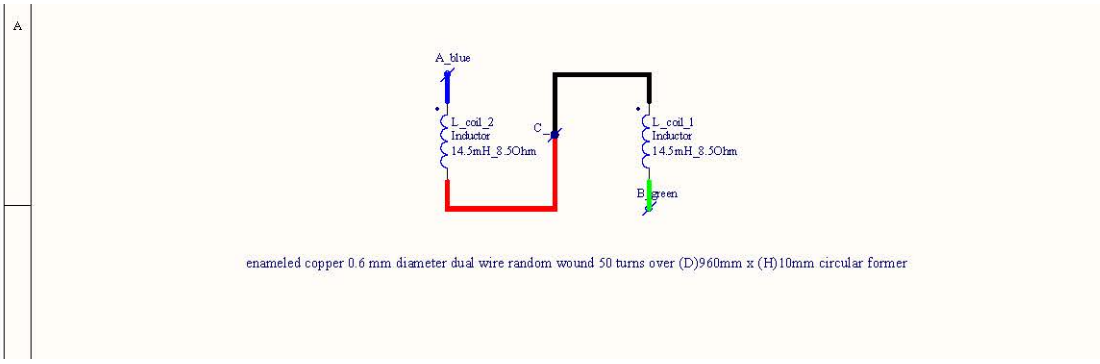

Figure 113: RX design specs continued

Off the shelf smaller pre-amps

Oscilloscope Preamplifier LNA10 is a smaller pro amp that can be used for the project,

Figure 114: LNA 10 Low Noise Amplifier

Or even smaller INA217 chip based low distortion amplifier is an option.

Figure 115: Tiny Professional Microphone preamp

Demodulator & Data Post Processor

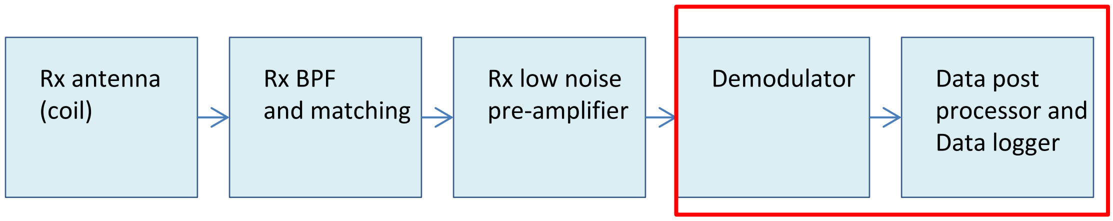

Figure 116: RX logger

Demodulator -> Data post-processor and Datalogger: it would be reasonable to use a single, off-the-shelf available single unit that is easily assessable and cheap, with slight modifications to optimize that for the defined fixed frequency band such as the RTL-SDR with RTL 2832U chipset. The data post-processor logger can be a PC/Arduino/Raspberry Pi device to view the sent messages from the TX device for underground communications, including encrypt/decryption libraries.

Billing of Materials Homebrew

The biggest expense of this project is in the Rx BPF/Rx pre-amp and impedance matching transformer with stock both overpriced and rare. To overcome this, we have replaced this with a custom transformer with a narrower bandwidth which is fit for purpose. Below is a Billing of Materials Table for the exercise.

Stage	Materials	Costs	Comments
Base band processor (Arduino)	Arduino Board	\$20	Message encoded for Arduino
Tx pre-amplifier (modulator)	Wire, jumpers, switches, modulated with TX ~20W Amp. **Can be removed** if Arduino is used and signal is fully synthesized.	\$300 / \$0	An off the shelf Tx ~20W PA design kit
Tx ~20W Power Amplifier	Enclosure, DC 24V 7A*h rechargeable battery pack	\$100	Cutting, drilling, PCB Assembly, and soldering.
Tx amp-to Tx antenna matching	Copper wire, transformer core and coil former	\$50	Transformer winding and soldering
Tx Antenna (electrodes)	~55mm ID Steel Pipe 2m ~50mm OD Steel pipe 2m 200x800x3 mm^3 steel plate Bolts and welding clamps	\$115	Cutting, griding, bending, welding, and soldering.
Rx antenna (coil)	3 pcs of 1000X1000X10mm ^3 Foam PVC sheet. Copper wire, enclosure, connector, PVC bond	\$170	Cutting, bonding, winding, soldering.
Rx BPF and impedance matching	Low noise input impedance matching transformer or 2nd Preamp below either or	\$2500 new or \$100 custom	Rare stock and overpriced new, Replaced with a custom narrow band transformer for \$100
Rx low noise pre-amplifier	Differential input low noise preamplifier	\$1000 new or \$100 custom	Rare stock and overpriced can be replaced with a custom Dual Amp building block chip.
BPF amplifier and signal conditioner	PCB, components	\$50	PCB Assembly
Data post processor and data logger	Arduino Board	\$20	Message encoded for Arduino

Figure 117: BOM costs

Further home brew kit details

INA849: Ultra-low noise (1 nV/√Hz), high-speed (28 MHz, 35 V/µ), precision (35 µV) instrumentation amplifier, to be used as input stage price $9.25

OPA192: Rail-to-Rail Input/Output, 5µV, 0.2µV/˚C, Precision Operational Amplifier, to be used as output stage $3.13

INAEVM-ALT-SO8: Universal instrumentation amplifier evaluation module with alternate pin-out $25 Additional SMD discrete components (R, C, headers etc.).

EPCOS TDK Electronics: Ferrite core P 8.4UH N48 Low noise input transformer

Oscilloscope Preamplifier LNA10 Preamp kit as a preamplifier.

Dual Amp building block based on a LT1567 operation amplifier
https://www.analog.com/ru/technical-articles/lt1567-dual-amplifier-building-block.html

Field Testing

The first field test was done with the prototype equipment in Korea. In Korea permission was sought from the Central Radio Management Service and limited approval with certain domestic conditions implemented, i.e., small scale area (150m) low power (20W). Secondary testing done in Central Victoria, Australia with no limitations on area size.

Test area location: 33, Bongan-gil, Anseong-si, Gyeonggi-do, Korea; coordinates 37.06504, 127.26057

Test date: June 13, 2020, afternoon local time

Frequency: Operation carrier frequency 2.01 kHz (between the 33-th and 34th harmonics of 60 Hz fundamental), Max. bandwidth up to few hundred Hertz with a maximum power at Tx 20W

Tx side: The earth electrodes have been buried to a depth of 1 meter ~<50 meters and connected to the Tx source. Tx power amplifier output impedance has been set to 200 Ohm. The signal has been modulated with an external modulation signal source with low frequency ASK modulation.

Rx side: Rx setup contains the 1-meter diameter Rx coil antenna, impedance matching input transformer, low noise preamplifier, USB adapter with ADC converter, notebook with the installed free SDR utility “sdrsharp” for signal demodulation and spectrum observation.

Low noise preamplifier has been set to provide optimal receiving in the actual operation conditions: coupling – AC, LF roll-off – 1kHz, HF roll-off – 1kHz, Gain – 200 (linear). The test results have been post-processed.

The Rx signal setup that has been used under the field test has been calibrated (description of the calibration procedure to be provided later) and the observed level of the signal has been represented in absolute units: the observed level ~-65dB corresponds the magnetic field strength ~3.3*10^(-5) A/m. The corresponding field strength at 150m distance, obtained with the simulation is ~4*10^(-5) A/m.

The actual strength of magnetic field is specified (by the way that is with respect to Ampere/meter, so -125dB means actually -125dBA/m) in the previous simulations. "Actual" mean here that the value would be observed with a setup with ZERO gain (i.e., without any amplification/attenuation). But under field tests we observe the signal that after acquiring by coil passes through cables, transformer, low noise preamplifier, analogue-to-digital converter, laptop, and digitally proceed in the software. The characteristics of some stages are conditionally known (for example Gain of low noise preamplifier has been set to 200 i.e., 40dB), but characteristics of the rest is unknown.

Figure 118: Initial Testing Area Gyeonggi-do, Korea

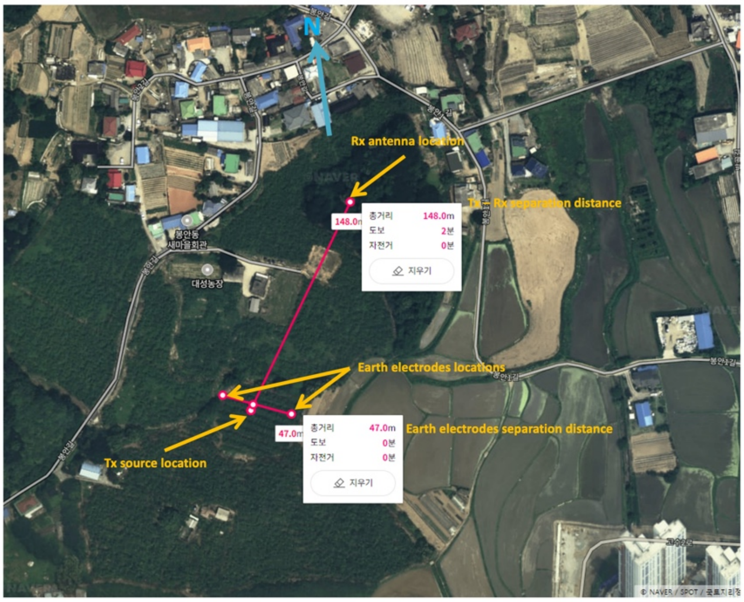

Figure 119: Tx and Rx Antenna placement topical view of the prototype testing

Figure 120: Tx Ground probe 1m into the earth's crust

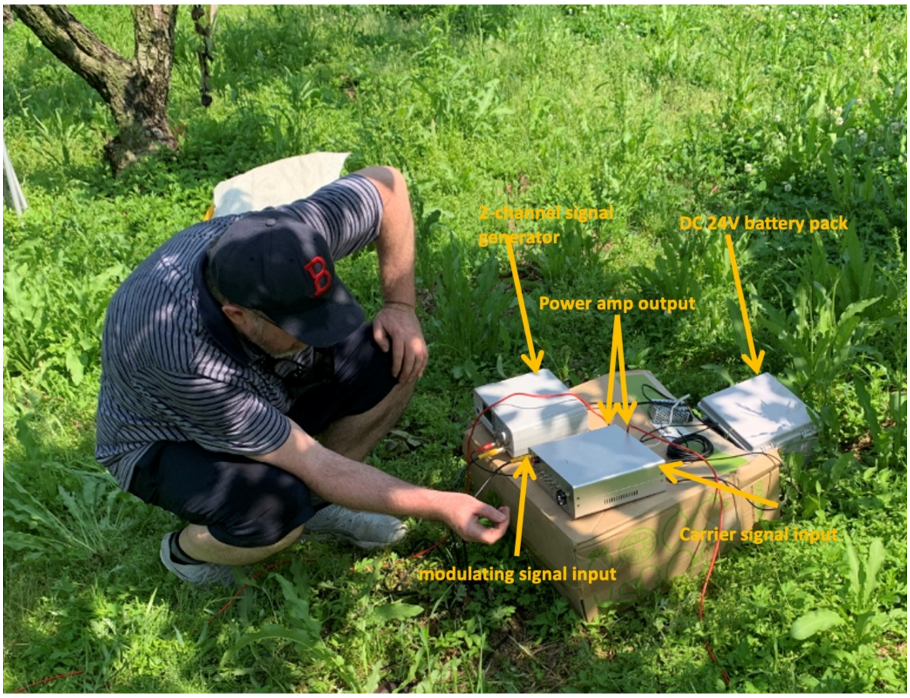

Figure 121: Field Testing Equipment for prototype Tx

Figure 122: View of TX Electrode to Electrode 47m apart path

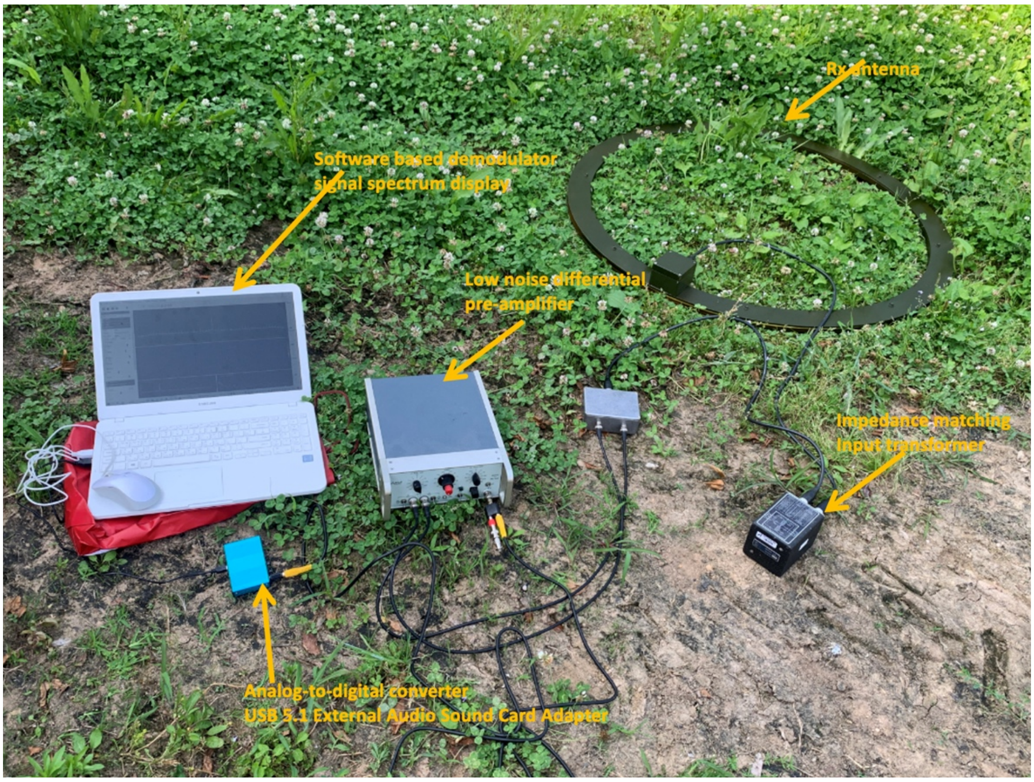

Figure 123: Rx equipment include Antenna, Impedance kit, SDR based demodulator

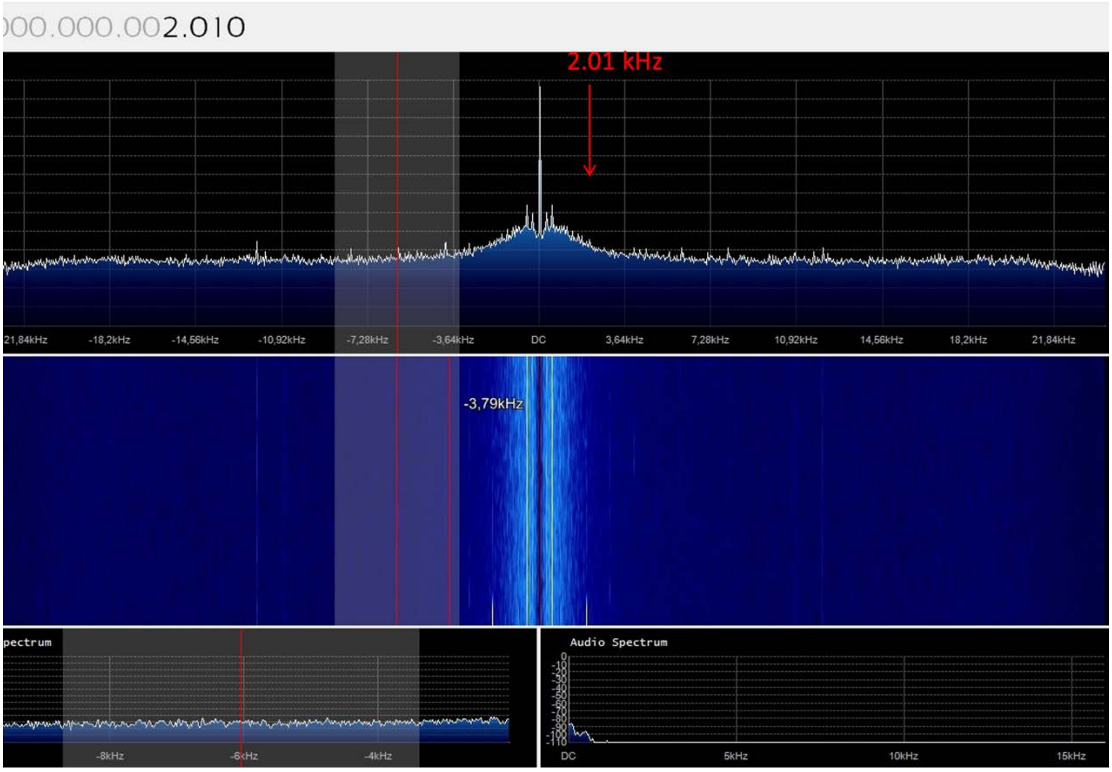

Figure 124: Rx equipment with Tx equipment turned off, no signal at 2.01 kHz

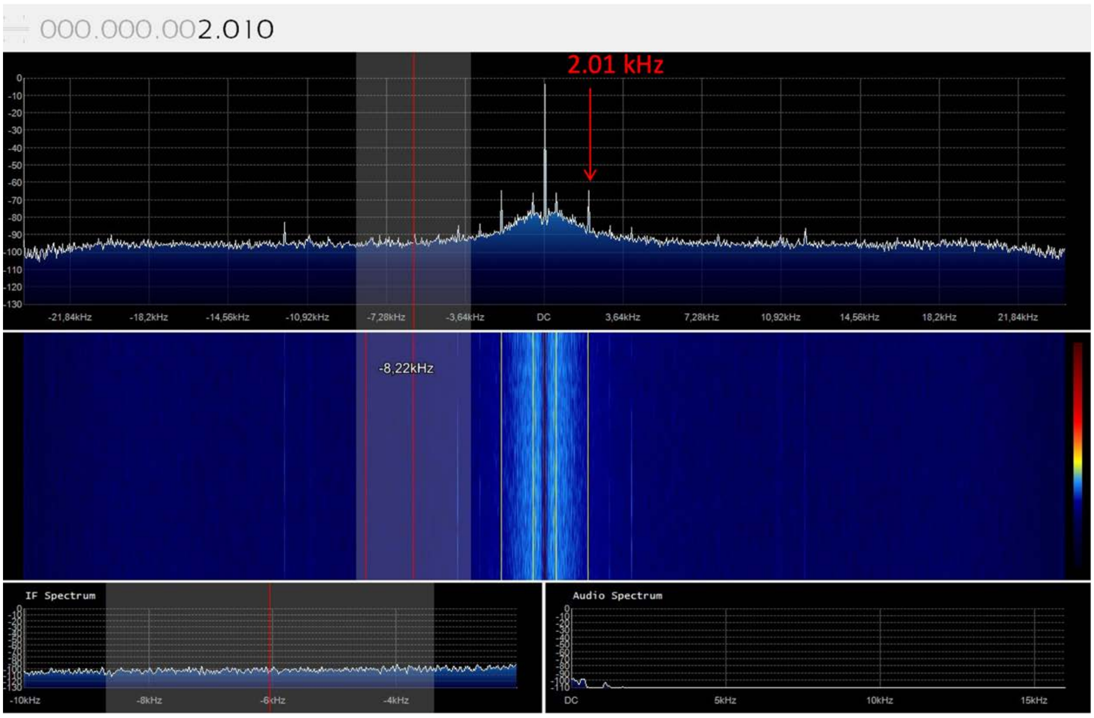

Figure 125: Rx equipment with Tx turned on, signal received at 2.01 kHz

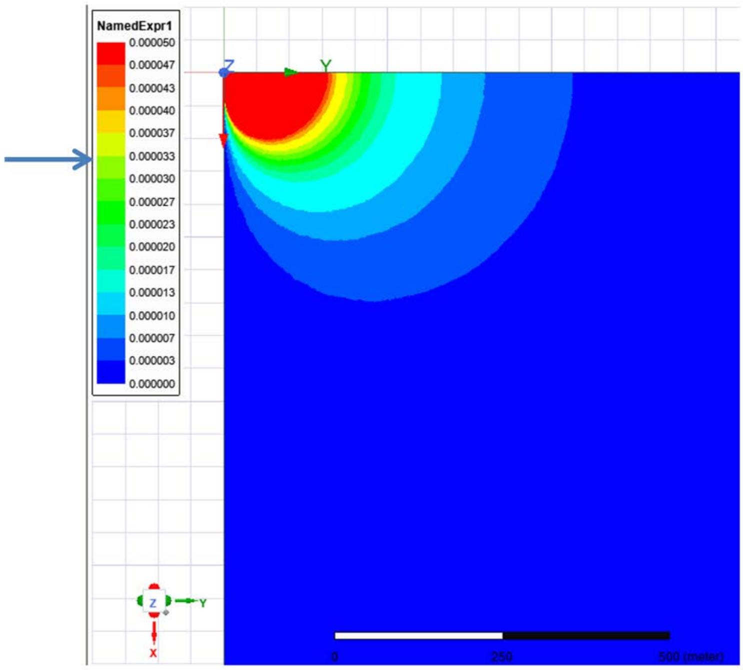

Figure 126: Rx signal visible

During the first field test in the orchard, unusual results were first observed below. A partially buried disconnected irrigation pipe was discovered that had a disruptive effect. It is expected the pipe effect would be constructive if it was in a radial direction. This is referred to as utility assisted mode, where signals can travel many km further using the metal underground water, power pipes, or even railway tracks to propagate the signal further. The buried pipe was removed for the field test.

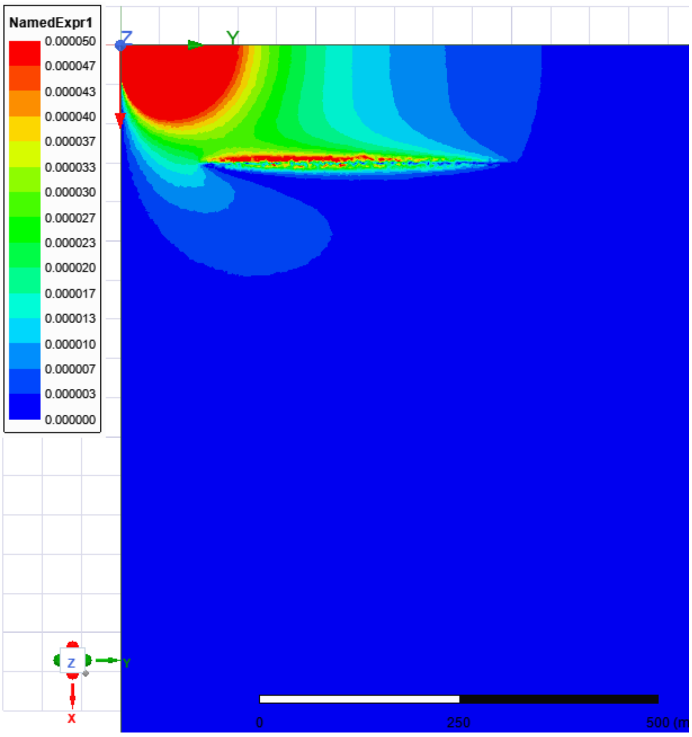

Figure 127: Buried pipe with disruptive effects on the signal

Australia Field Testing

Secondary testing was performed in Central Victoria, Australia with no limitations on area size.

Test area location: Private property 168 Porcupine Ridge Rd Vaughan Springs, Victoria Australia coordinates 37.3223466,144.175688. Soil type dry sandy

Test date: Jan 9th, 2020, mid-morning local time

Frequency: Operation carrier frequency 2.01 kHz (between the 33-th and 34th harmonics of 60 Hz fundamental), Max. bandwidth up to few hundred Hertz with a maximum power at Tx 20W

Tx side: The earth electrodes have been buried to a depth of 1 meter, 50 meters and connected to the Tx source. Tx power amplifier output impedance has been set to 100 Ohm. The signal has been modulated with an external modulation signal source with low frequency ASK modulation.

Rx side: Rx setup contains the 1-meter diameter Rx coil antenna, impedance matching input transformer, low noise preamplifier, USB adapter with ADC converter, notebook with the installed free SDR utility "sdrsharp" for signal demodulation and spectrum observation.

Low noise preamplifier has been set to provide optimal receiving in the actual operation conditions: coupling – AC, LF roll-off – 1kHz, HF roll-off – 1kHz, Gain – 200 (linear).

The Rx signal setup that has been used under the field test has been calibrated and the observed level of the signal has been represented in absolute units: the observed level ~-65dB corresponds the magnetic field strength ~3.3*10^ (-5) A/m at ~923m distance.

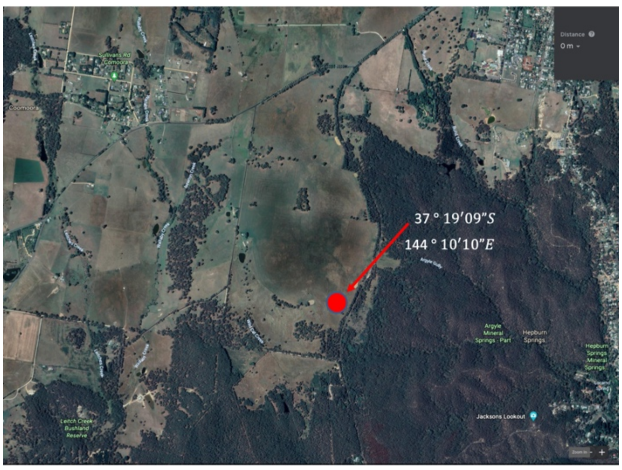

Figure 128: Location in Central Victoria Australia for commercial testing

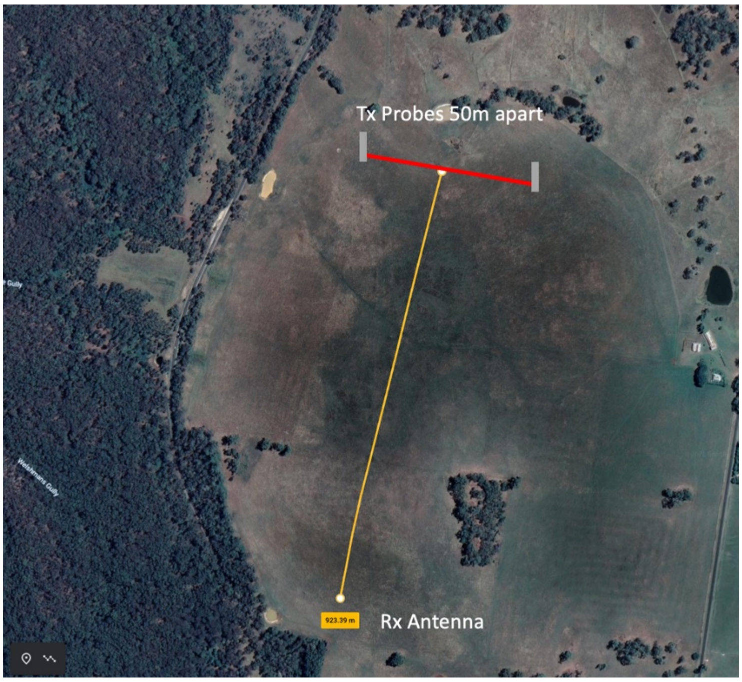

Figure 129: Aerial view of Antenna ~923 metres from Tx probes 50m apart at 2kHz

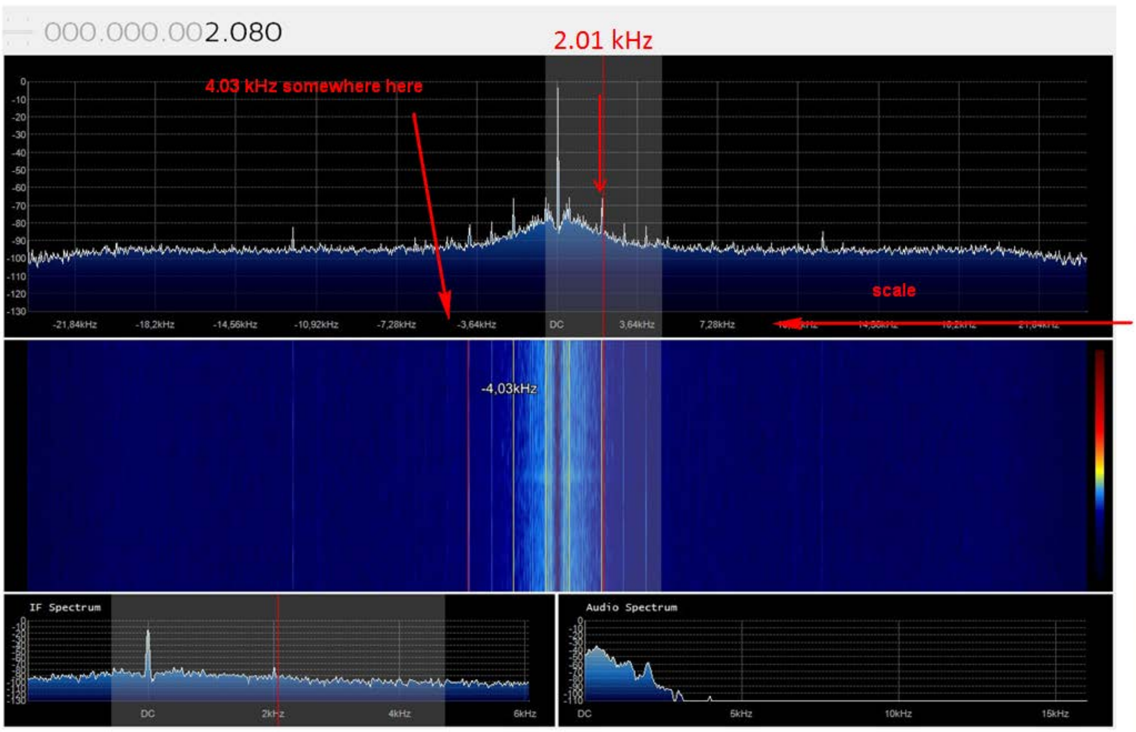

Figure 130: Rx signal received at ~923m successfully at ~20W, 50 Meter separated electrodes

Antenna Calibration

The Rx coil has been wound with a 1 turn secondary (0.5mm diameter copper wire) The secondary has been powered from 2 kHz signal source with 1k resistor on series and the received signal has been measuring within a shielded room environment.

The calibrating current value I_{cal} providing ~-65dB level signal registering with the SDR utility "sdrsharp" is considered as generating the same value magnetic flux as it was Φ_{cal} generated by Tx electrodes under the outdoor field test i.e. Φ_{test}

$$\Phi_{cal} = \Phi_{test}$$

Considering that $$\Phi_{test} = B_{test} \cdot S$$

and $$\Phi_{cal} = B_{cal} \cdot S \cdot k$$

where B_{cal} the magnetic induction value on CENTER of the coil generated by I_{cal}, S – area of the coil and k – the coefficient of magnetic coupling between the primary and the secondary under calibration , then $$B_{test} = B_{cal} \cdot k$$

the magnetic induction value on CENTER of the coil B_{cal} generated by I_{cal} :

$$B_{cal} = \frac{\mu_0 \cdot I_{cal}}{2 \cdot R}$$

where μ_0 is vacuum permeability, R radius of Rx coil. The coefficient of magnetic coupling between the primary and the secondary k has been found with the simulation. The actual value of the magnetic field strength corresponding to the observed value of signal under the outdoor test is:

$$B_{test} = \frac{\mu_0 \cdot I_{cal} \cdot k}{2 \cdot R}$$

Initial Field-Testing Conclusion

Domestic specific constraints in the first field in Korea, tests performed on Tx-Rx distances much smaller (~ 150 m) than the original simulations. The field tests were repeated in Australia with no space limitations at 20 Watts and ~923 meters.

It was observed natural noise background short-period variations up to 20dB possibly, caused local environment condition in proximity (~ 100m) such as electric power communication lines, electric devices etc. and, lightings etc in the Korea field test. It was found that the earth impedance observed at earth electrodes was higher than ~100 Ohm as specified in most earth sources in Korea and more than ~200 Ohm was confirmed with consequent switching the Tx power amplifier output impedance from 100 Ohm – 200 Ohm range. Since 200 Ohm output impedance is the max. value available in the current variant of power amplifier the test has been conducted with this setting was increased to a 100 – 500 range for commercial applications.

Earth impedance of ~100 Ohm was seen in the second field test in Australia with no 20dB background bursts due to the remoteness of the area with farming and natural forest zones.

The Korea and the Australia field test confirmed that a TX signal could be received at both 150m and ~923 with the prototype equipment that did not have high power or advanced modulation techniques. The initial protype test for both Korea and Australia results were within +/-15% of the previous simulations.

Commercial Tx / Rx

Moving from the Tx/Rx protype which had power, size, and impedance limitations we can proceed into the commercial application. This would allow for increased power 3600W, reduce the size of the equipment on Tx/Rx and increase impedance levels from 0-200 Ohms to 0-500 Ohms to allow for different soil scenarios. We can now add in modulation methods discussed earlier to increase the signal range.

Power amplifier is DC powered with dual-polarity +180V/-180V, +12V/-12V and single-polarity power supplies. The carrier and modulation signals are provided with an external signal Arduino source. High impedance load is matched with high-efficiency and high voltage output transformer (approach with LC circuit matching is possible as well). The performance characteristics

- Load voltage (peak) ~0.9 kV
- Output Power at 200 Ohm load~ 3.7kW
- DC power efficiency ~ 0.95

Figure 131: Commercially produced prototype Tx equipment

Figure 132: Commercial Rx with optional E-field or H-field antenna option with internal, compute, power

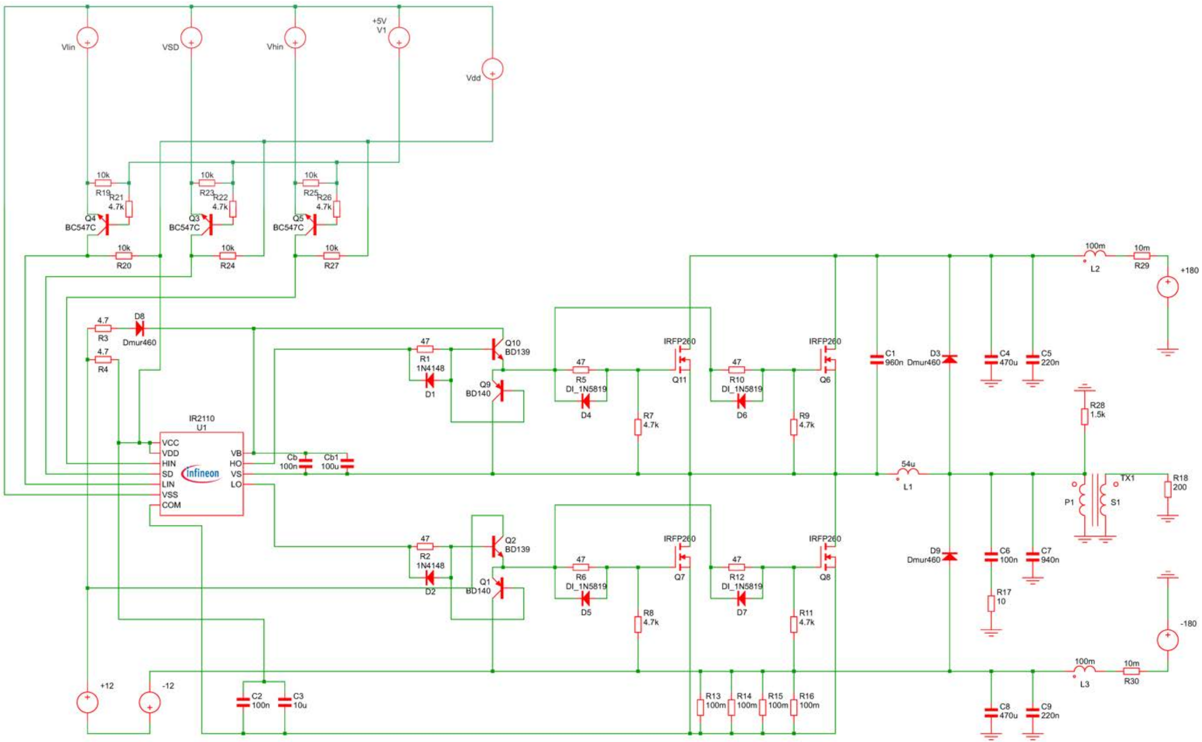

Figure 133: Commercial Schematics Tx Model 1

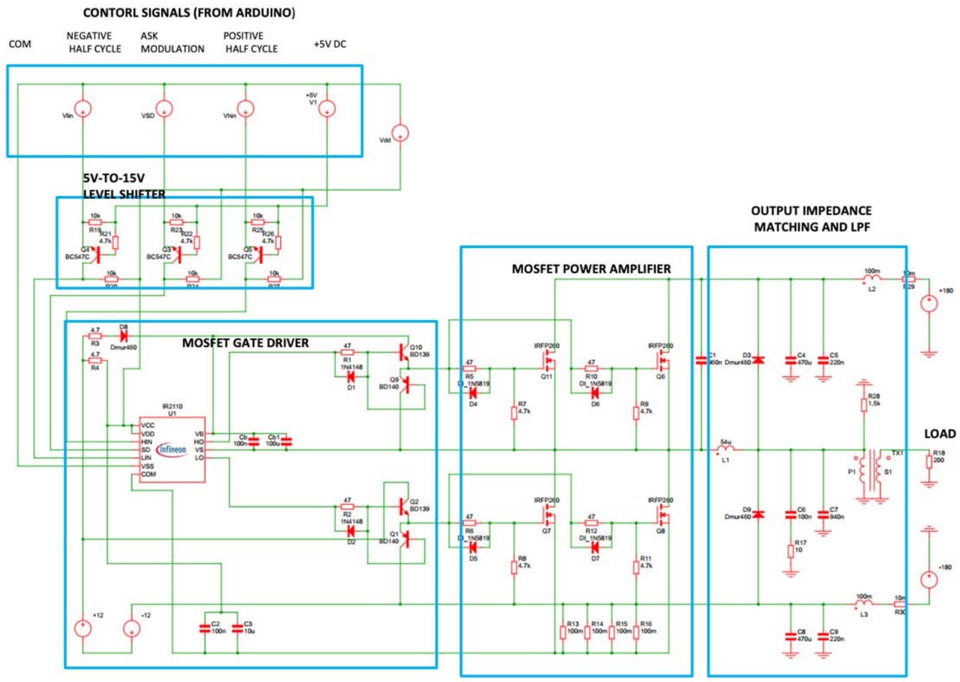

Figure 134: Commercial Tx Model 1 with varying impedance overview

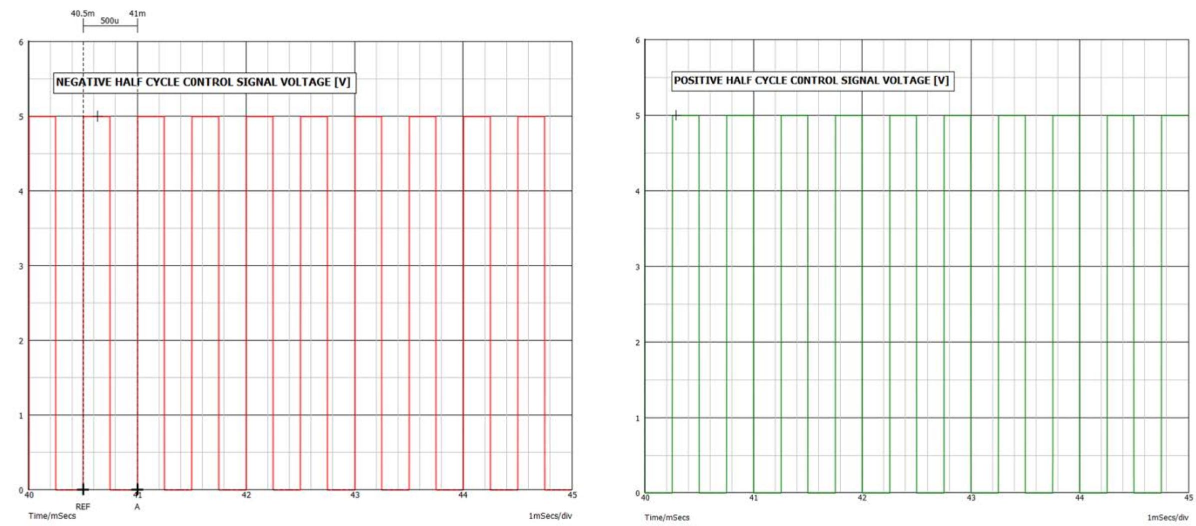

Figure 135: Tx Model 1 Voltage Control

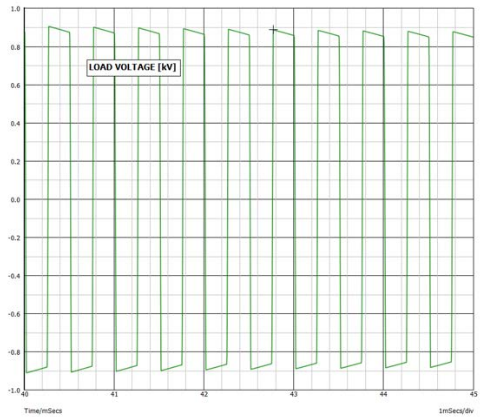

Figure 136: Tx Model 1 Load Voltage

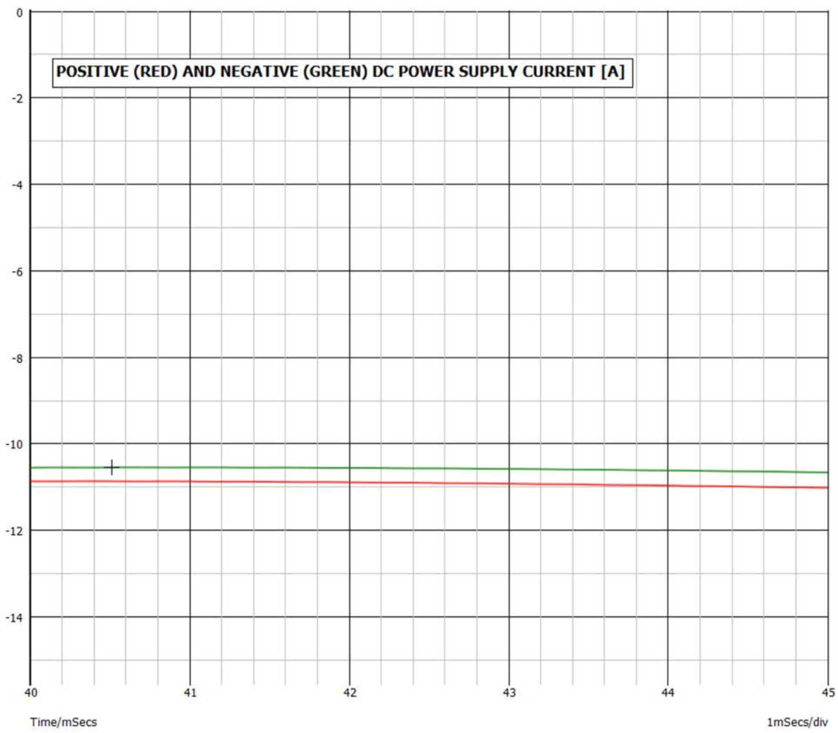

Figure 137: Tx Model 1 DC Power - Amps

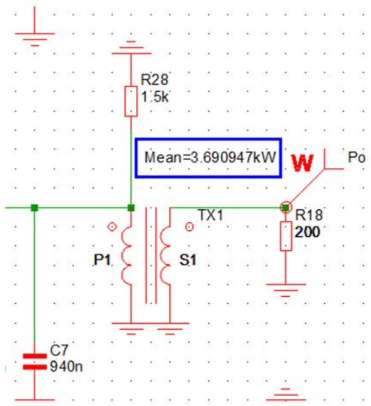

Calculated DC power efficiency: Eff ~ 3.7kW/(2*177V*11A) = 0.95

Figure 138: TX Model 1 DC power schematics

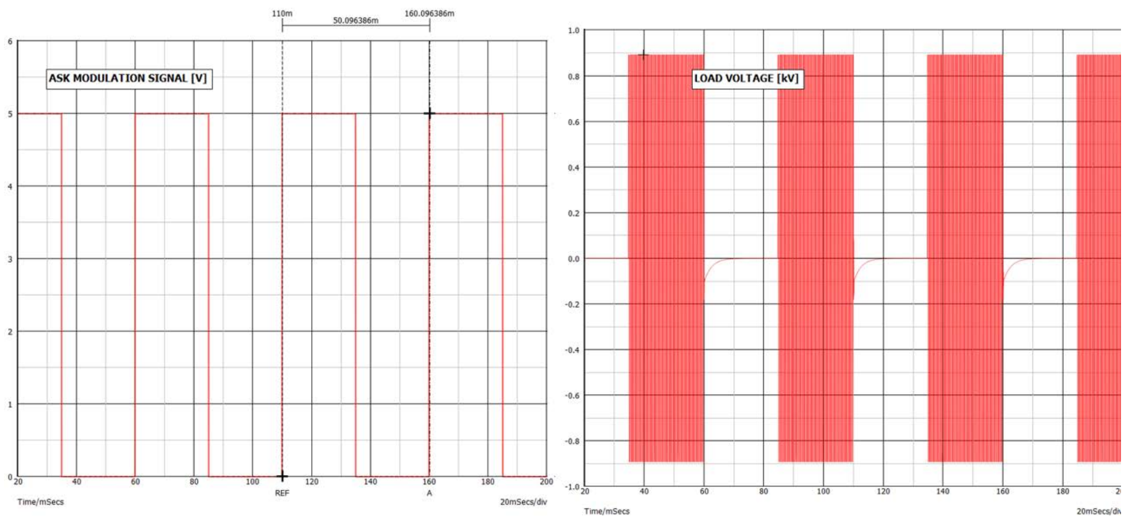

Figure 139: ASK Modulation and Load Voltage

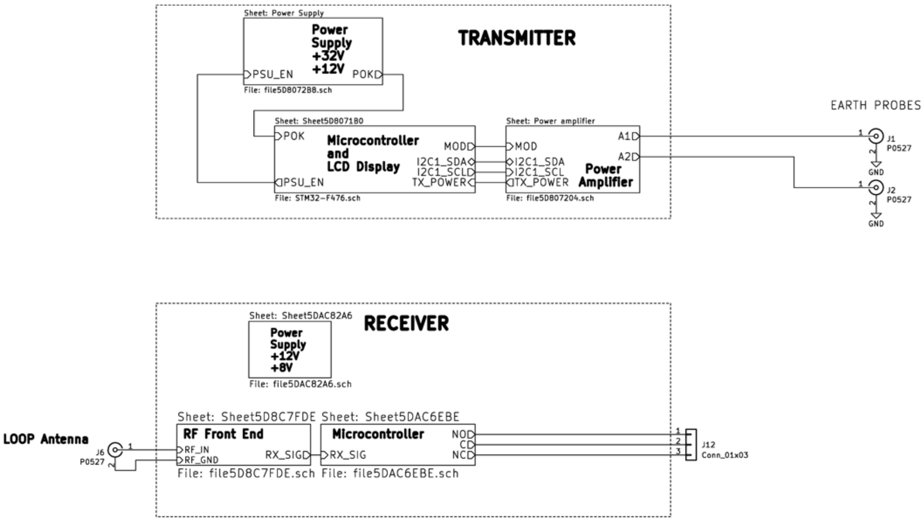

Figure 140: TX Commercial Model 2 TX/Rx Overview

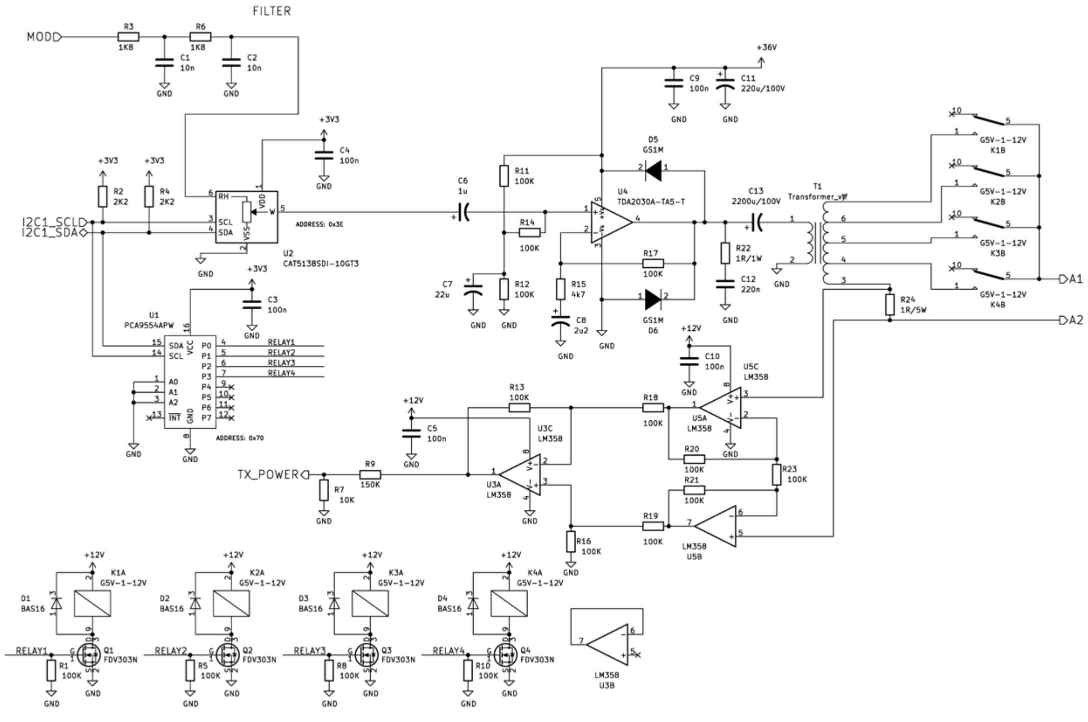

Figure 141: TX Commercial Model 2 TX Design

FSK Modulation Variant

A variant of schematics design for two-tone Frequency Shift Keying (FSK) of 3600W power amplifier is represented below. The two tones carriers f1=2 kHz, f2=1 kHz and modulation signal f_mod=20 Hz are provided with an external signal source, for example Arduino.

The performance characteristics estimated with simulation are close to the ones obtained for the variant with ASK modulation:

- Load voltage (peak) ~0.9 kV
- Output Power at 200 Ohm load~ 3.7kW
- DC power efficiency ~ 0.95

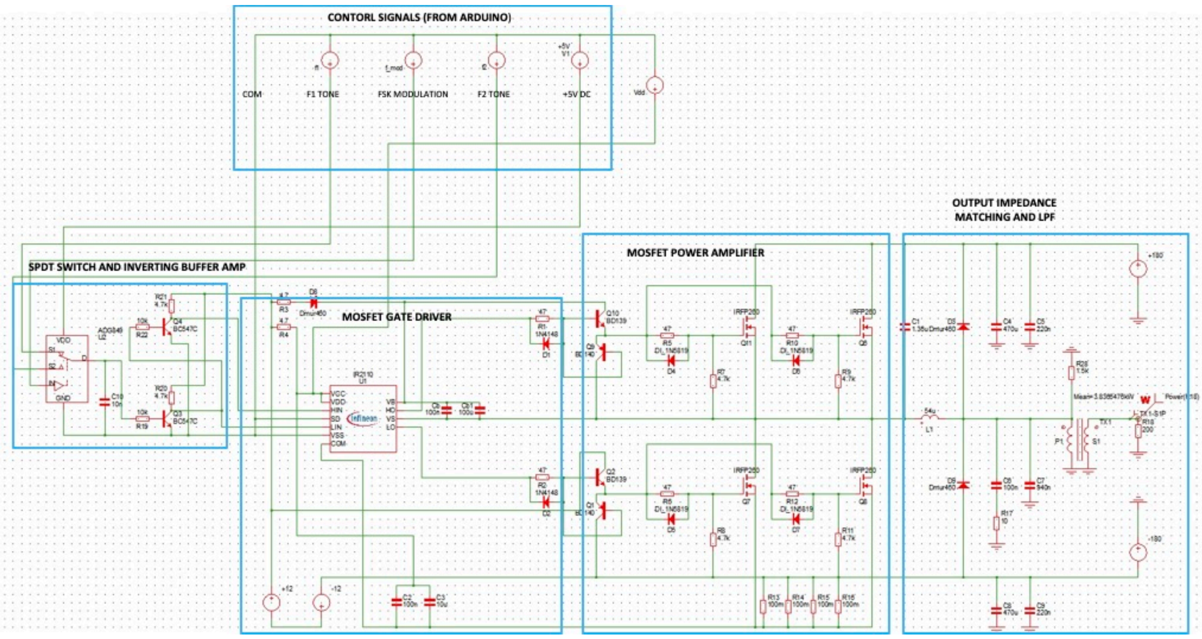

Figure 142: FSK schematics

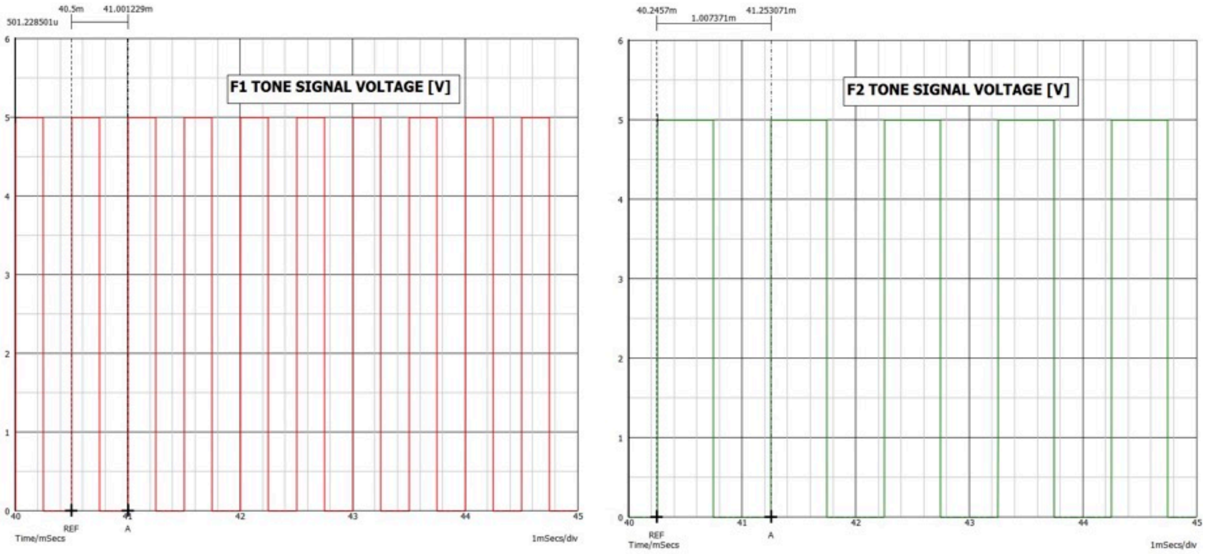

Figure 143: FI/F2 Voltage results

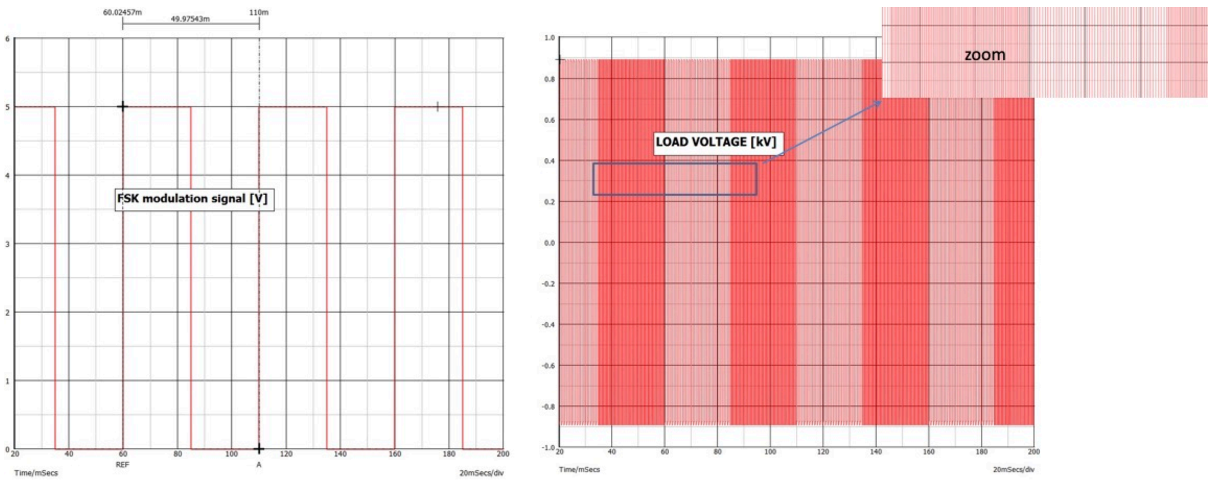

Figure 144: FSK modulation results

Frequency Modulation power amplifier

A variant of schematics design for Frequency Modulation (arbitrary waveform, as it is expected; to be confirmed) of 3600W power amplifier is represented. As an example, the input signal is chosen as sine swept (up-chirp, from few tens of Hz up to 5kHz).

The performance characteristics estimated with simulation are close to the ones obtained for the variant with ASK modulation:

- Load voltage (peak) ~0.9 kV
- Output Power at 200 Ohm load~ 3.7kW
- DC power efficiency ~ 0.95

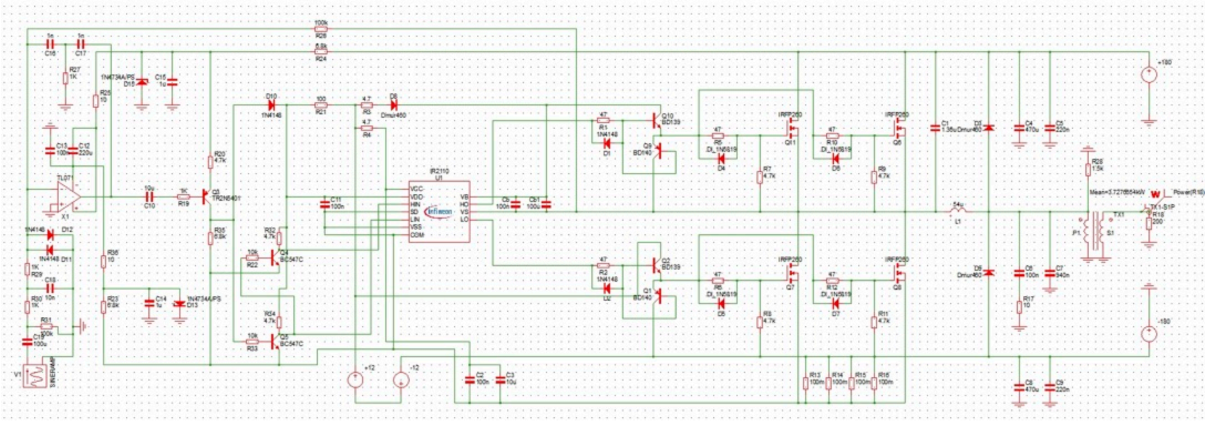

Figure 145: Frequency Modulation

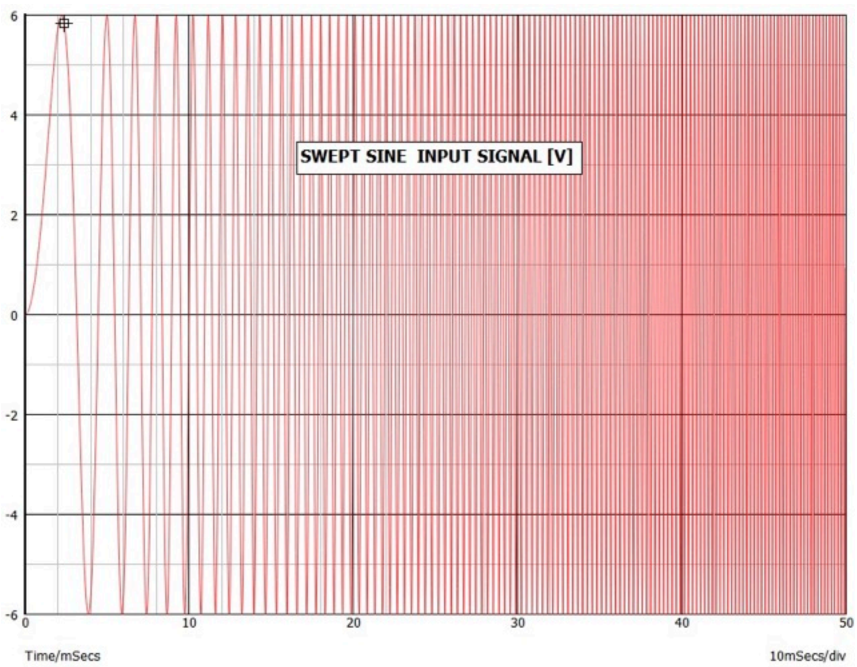

Figure 146: Sine input signal

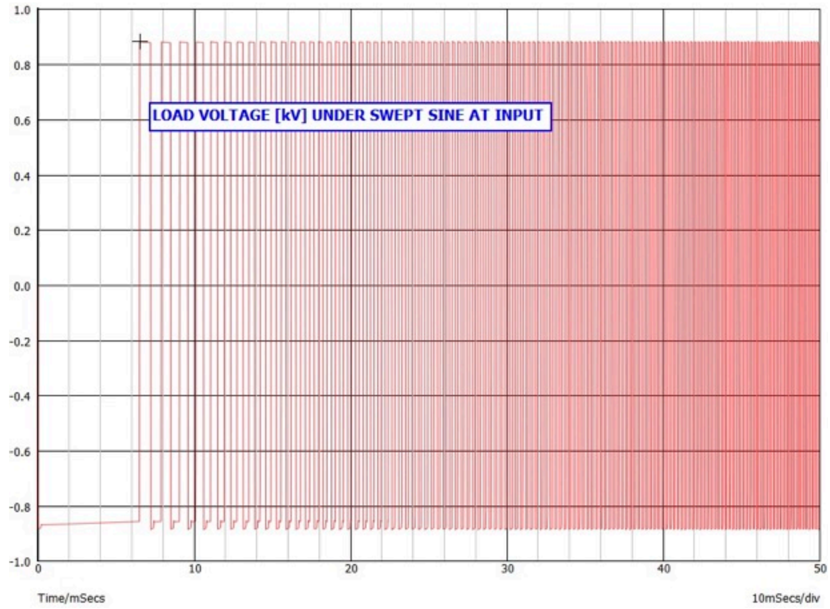

Figure 147: Load Voltage Sine Input

Data Transmission

MSK Encoding

It is assumed here that text-to-binary data conversion is proceeded for Minimum Shift Keying (MSK) encoding for data transfer. The steps to achieve this are as follows.

1. Division of binary data bits into even and odd bits groups with replication into 2 (or 3 for first even bit and last odd bits only).

2. Define the highest frequency of operation f2 and signal s2(t)=inv(t)*sin(2*Pi*f2*t).

3. The lowest frequency of operation then f1=f2/2 and signal s1(t)=inv(t)*(-1)*sin(2*Pi*f1*t) =inv*(-1)*sin(Pi*f2*t)

4. Period of bit duration T=1/f2.

5. Frequency generating table

even	**0**	**0**	**1**	**1**
odd	0	1	0	1
freq	f2(1**)	f1(0)	f1(0)	f2(1)
inversion*	Yes(1)	No(0)	Yes(1)	No(0)

* Inversion means here the signal phase inversion.
** Numbers inside round bracket represent levels of signals for control frequency and inversion choice.

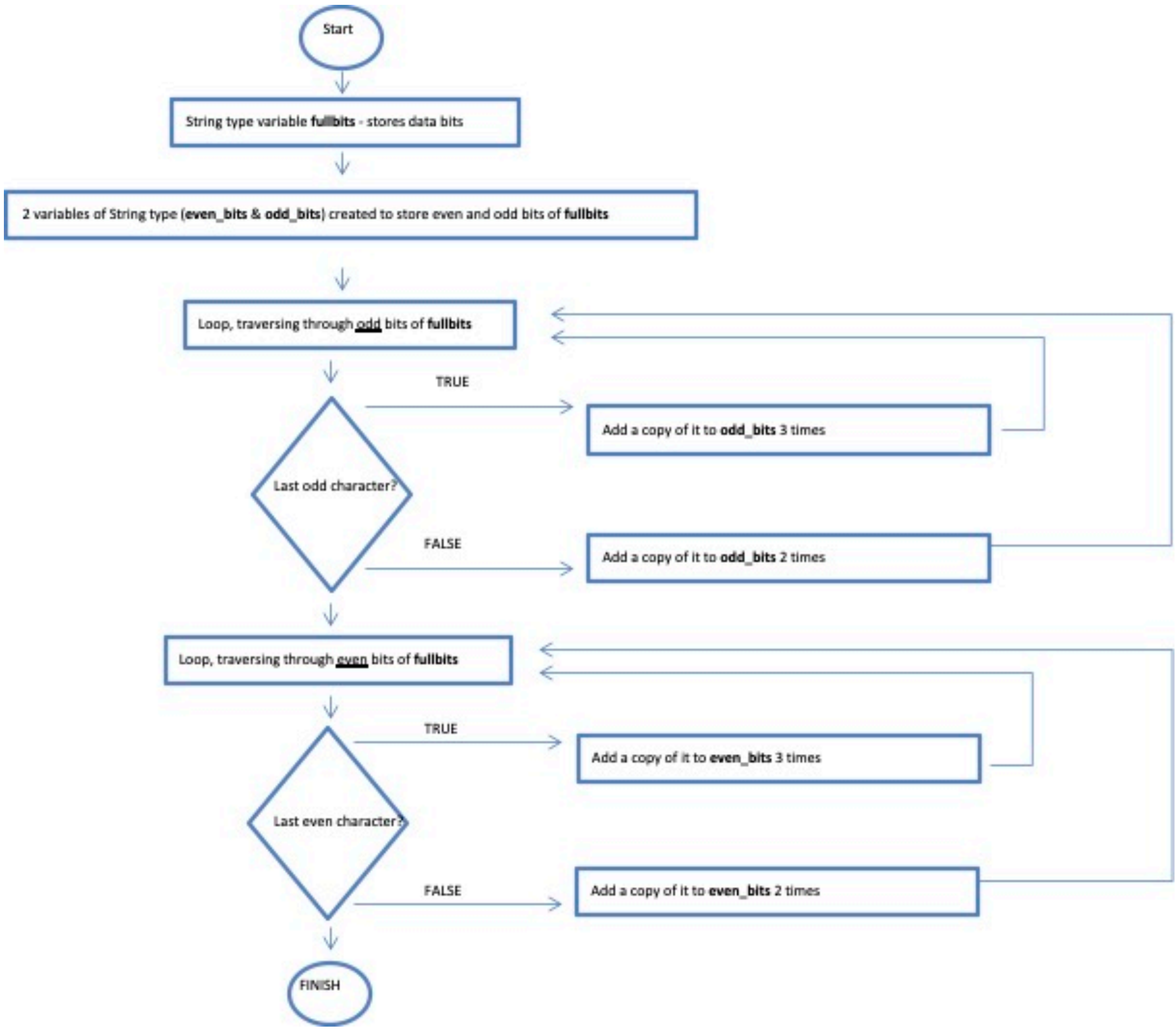

Figure 148: Key Shift flow chart

Data Logic Structure

Before starting the division of binary data into groups, we must first store Binary ASCII bits in a variable **fullbits** of String data type. We create two other variables (**even_bits** & **odd_bits**).

After this “preparation”, we can now start the division process. It is carried through “for loops”, one of which traverses through odd bits of **fullbits**, and second - through even bits. With each iteration of the loop, we access a single character of **fullbits** using the temporary variable of “for loop”.

We then “analyze” each character using the “if-then” conditional statement. In the case of the odd bits traversing “for loop”, the “if” statement compares the current value of the temporary variable with the value of the last odd index of **fullbits.** If the value matches, we proceed to access the character at that index, and add it 3 times to the variable **odd_bits**. Otherwise, the “else” statement gets triggered, and we add a particular character to the **odd_bits** 2 times.

Similarly, in the case of even bits traversing “for loop”, the “if” statement matches the value of the temporary variable to the value of the first even index of **fullbits.** If the values match, we add the character at the index of this value to **even_bits** 3 times. Otherwise, the “else” statement adds the character at other indices to **even_bits** 2 times. After these 2 for loops run, we get separated and replicated even and odd bits, which we can then use for the frequency generating table.

```
E FOR DIVISION OF BINARY BITS INTO EVEN AND ODD BITS GROUPS WITH REPLICATION
t java.util.*;
c class Main{
ublic static void main(String[] args) {
   Scanner scan = new Scanner(System.in);
   //asks for initial input bits (Binary ASCII), and saves it in fullbits
   String fullbits = scan.nextLine();
   //variable which will save the even bits
   String even_output = "";
   //variable which will save the odd bits
   String odd_output = "";
   //for loop traversing through odd indices of "fullbits"
   for(int i = 0; i<fullbits.length(); i+=2){
       if (i == fullbits.length()-2){
           odd_output += fullbits.charAt(i);
           odd_output += fullbits.charAt(i);
           odd_output += fullbits.charAt(i);
       }
       else{
           odd_output += fullbits.charAt(i);
           odd_output += fullbits.charAt(i);
       }
   }
   //for loop traversing through even indices of "fullbits"
   for(int i = 1; i<fullbits.length(); i+=2){
       if(i==1){
           even_output += fullbits.charAt(i);
           even_output += fullbits.charAt(i);
           even_output += fullbits.charAt(i);
       }
       else{
           even_output += fullbits.charAt(i);
           even_output += fullbits.charAt(i);
       }
   }

   //printing out even and odd parts of initial binary ascii bits (for visibility)
   System.out.println("Even: " + even_output);
   System.out.println("Odd: " + odd_output);
```

Figure 149: Sample Frequency Generator Code

```
//FREQUENCY GENERATING TABLE
import java.util.*;
public class Main{
    public static void main(String[] args) {
        //variable freq to save frequency control code
        String freq = "";
        //variable inv to save inversion control code
        String inv = "";
        //for loop traversing through each index of even group (the length of which is same to the odd group)
        for (int i = 0; i<even_output.length(); i++){
            //series of conditional statements, which determine the value of each frequency and inversion control bit
            //based on the character at a particular index
            if (even_output.charAt(i) == '0' && odd_output.charAt(i) == '0'){
                freq += "1";
                inv += "1";
            }
            else if (even_output.charAt(i) == '0' && odd_output.charAt(i) == '1'){
                freq += "0";
                inv += "0";
            }
            else if (even_output.charAt(i) == '1' && odd_output.charAt(i) == '0'){
                freq += "0";
                inv += "1";
            }
            else{
                freq += "1";
                inv += "0";
            }
        }
        //printing out the results (for visibility)
        System.out.println();
        System.out.println("----------------------------------------------");
        System.out.println();
        System.out.println("Frequency: " + freq);
        System.out.println("Inversion: " + inv);

    }
}
```

Figure 150: Sample Frequency Generating Table Code continued

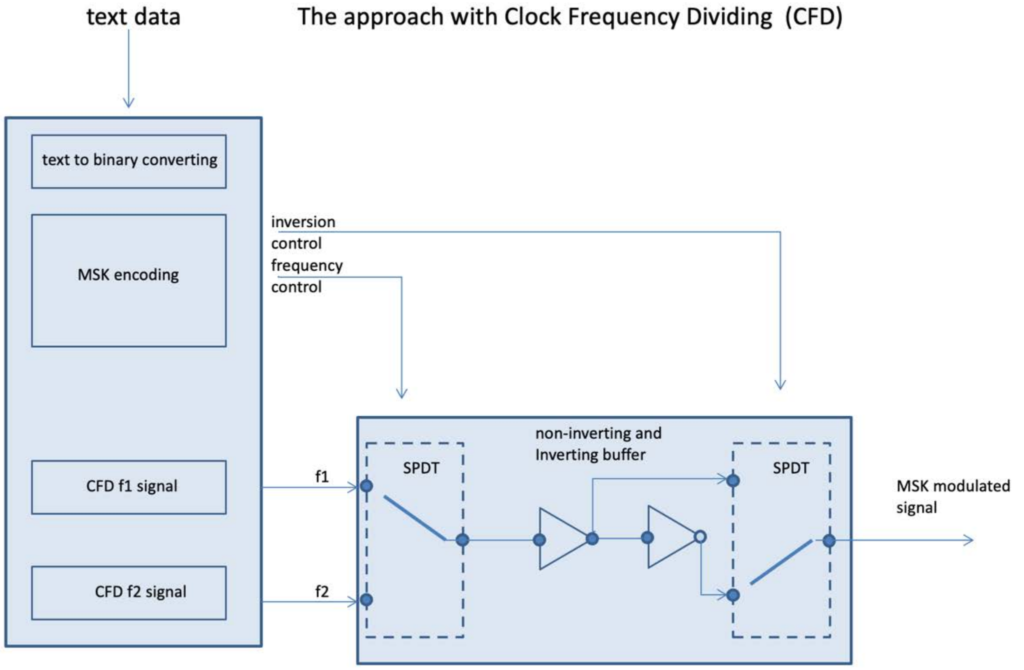

Figure 151: Clock Frequency Dividing

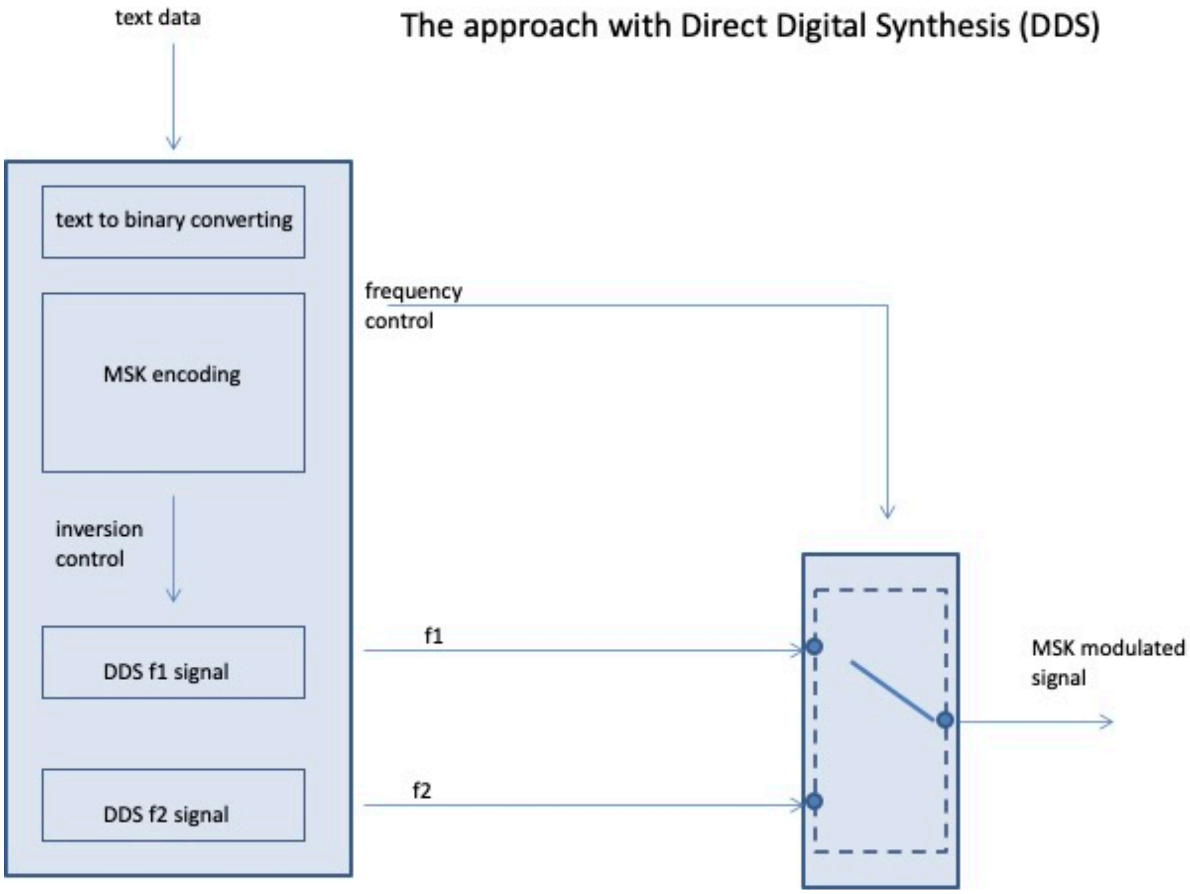

Figure 152: Direct Signal Synthesis

Text data *Hello, World!*

↓

Decimal ASCII
72 101 108 108 111 44 32 119 111 114 108 100 33

Binary ASCII
01001000 01100101 01101100 01101100 01101111 00101100 00100000
01010111 01101111 01110010 01101100 01100100 00100001

↓

Frequency control code: 0001001110101000001001011010010110100111010001011100111111000001100100111001101001010010110101001110011100

Inversion control code: 11110011110011111100001111000011110000000110000111100111111111110011000000110011001100001111001111110011111

Figure 153: Text to Inversion Control Code

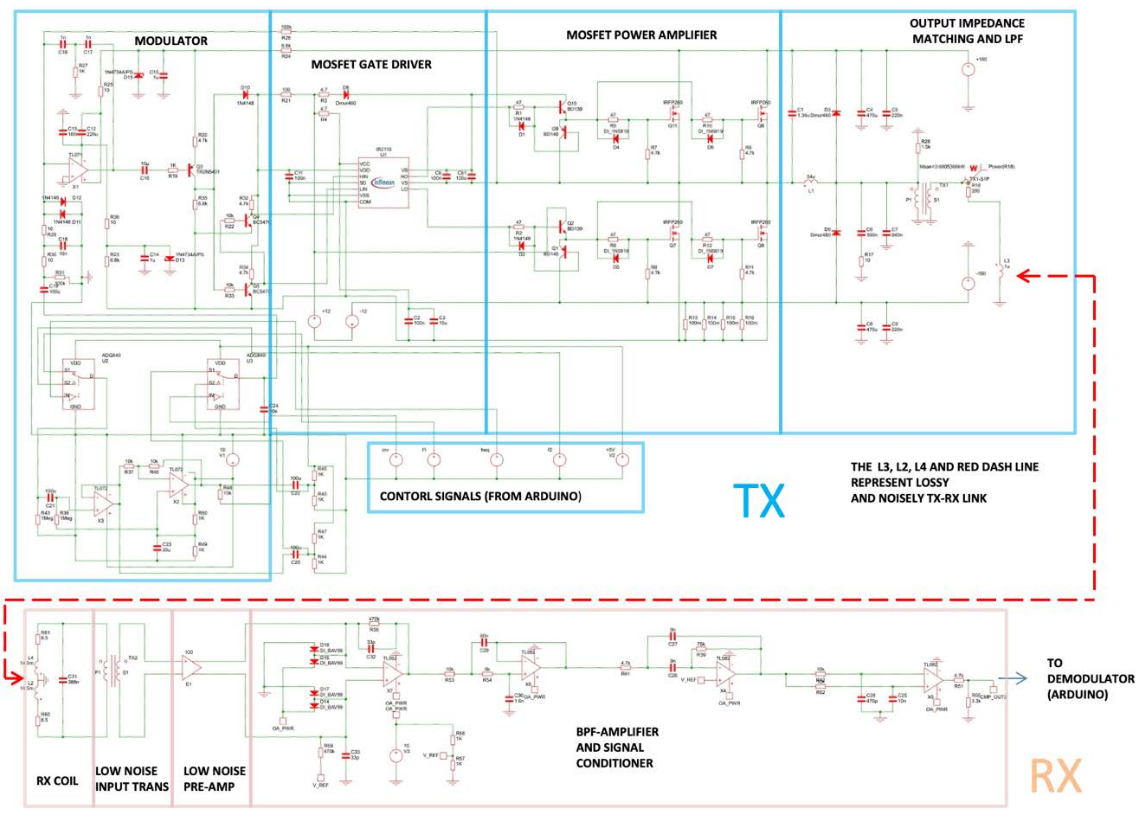

Figure 154: Schematics of 3600W amplifier with MSK Modulator

Schematics design of 3600W power amplifier with MSK modulator and schematics of the receiver consisting of the RX antenna (coil), input low noise impedance transformer, differential low noise pre-amplifier, band-pass active filter and amplifier and signal conditioner.

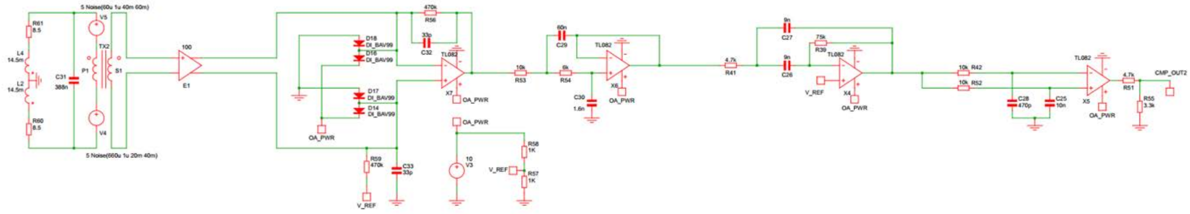

Figure 155: Isolated view of the Receiver schematics

Examples of waveforms for signals f1 (on the top left), f2 (on the top right), also for frequency control (on the bottom left) and inversion control (on the bottom right) for “Hello, World!” encoding.

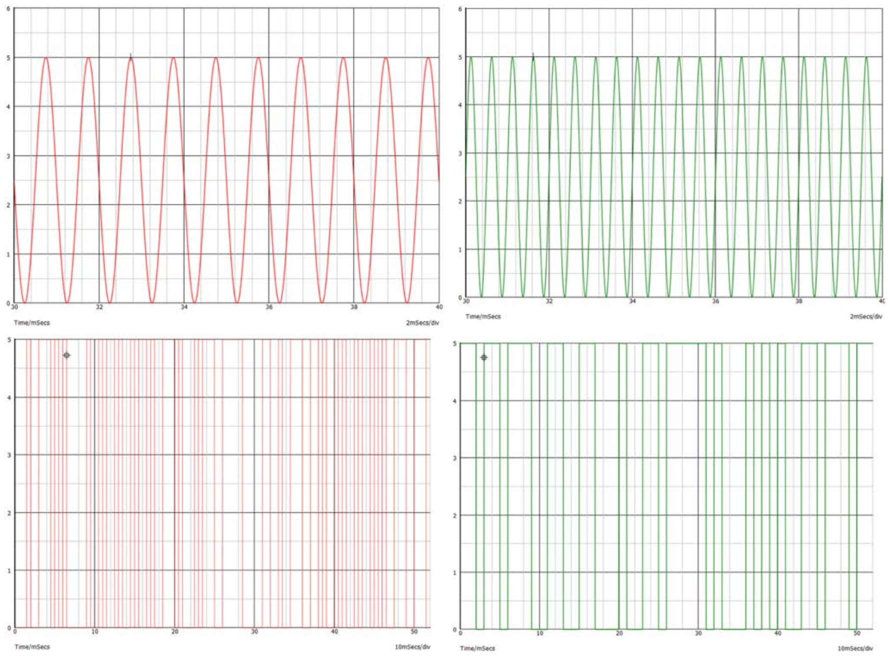

Figure 156: Waveforms

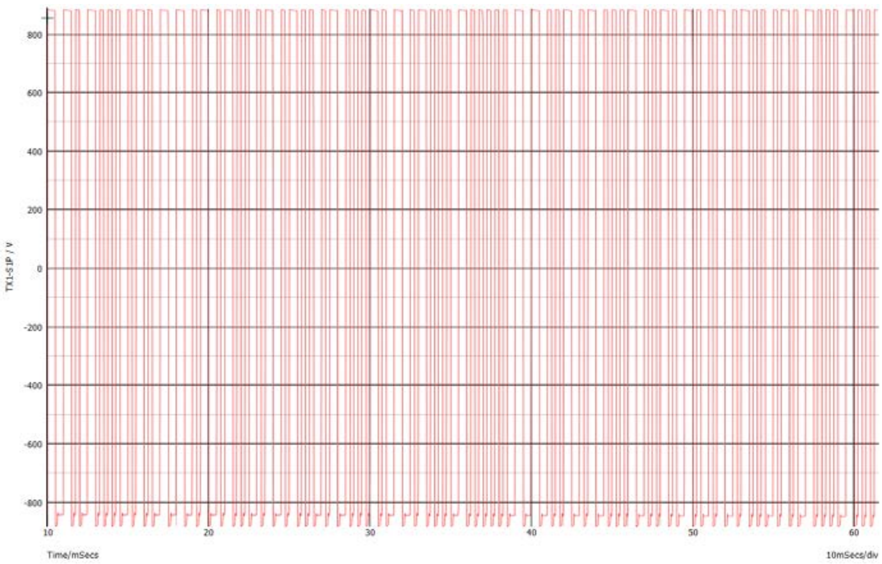

Figure 157: Full length encoded message waveform for “Hello, World!” at Tx amplifier

Full length waveform for encoded message “Hello, World!” at Rx antenna (coil). Communication channel associated noise is added at time intervals 20ms – 40 ms (center frequency of noise spectrum is at 1.5 kHz) and at time intervals 40ms – 60 ms (center frequency of noise spectrum is at 15 kHz).

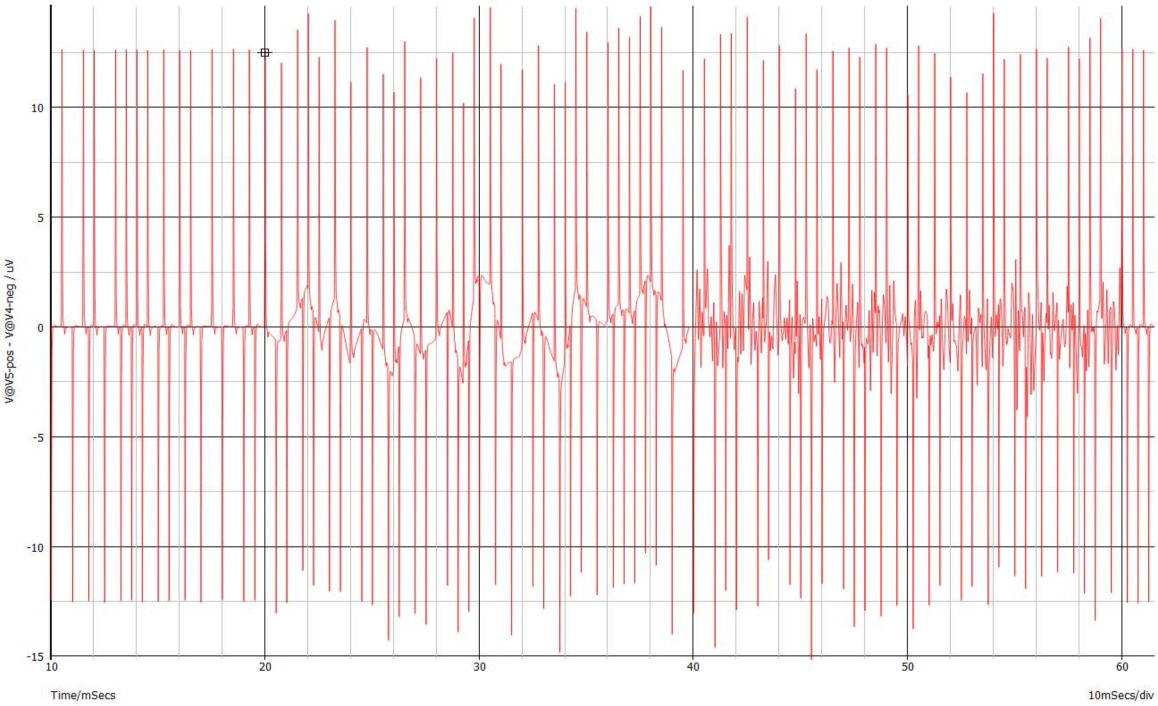

Figure 158: Full Length message at Rx antenna (coil)

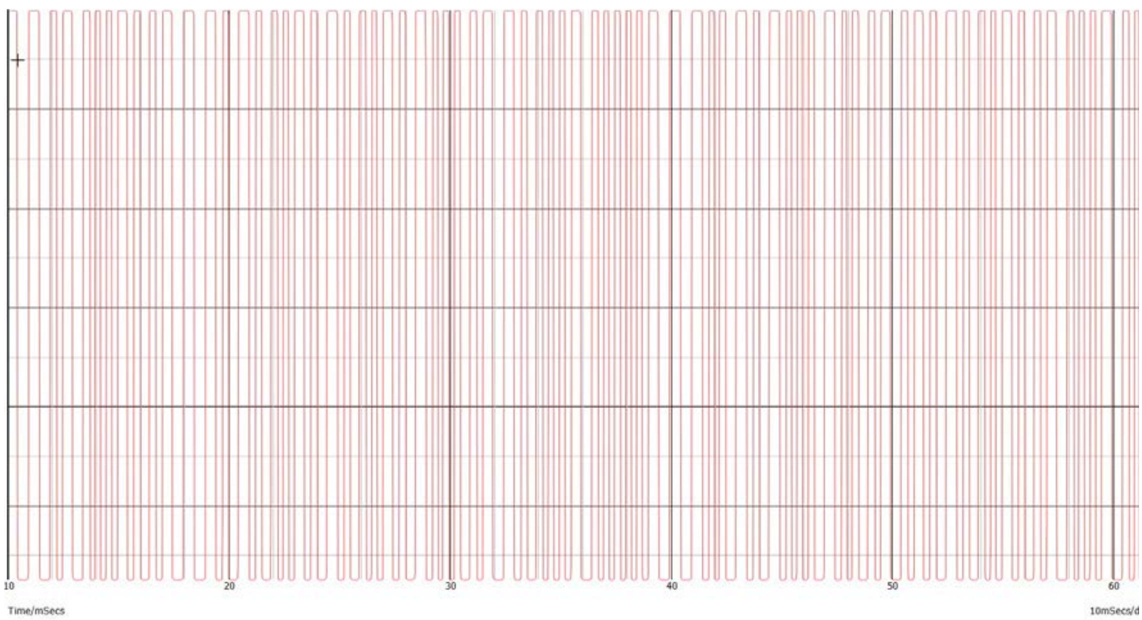

Figure 159: Full length waveform for encoded message at Receiver output after signal filtering

MSK Signal Demodulation

The reason I have chosen the MSK demodulation approach is making the demodulator H/W circuitry as simple as possible while keeping maximum noise robustness. The suggested approach consists in using frequency demodulation circuitry only, with a skipping phase demodulation stage at H/W level with completely dedicating phase demodulation for extensive but simple computations.

Common description of constants and variables used in the next diagrams are explained in detail below

1. **clock_phase** at certain N-th frame - the evaluated phase of the **CFD f1** or **CFD f1** signal on this N-th frame. The **clock phase** at certain N-th frame is calculating as the initial phase of clock + phase shift of clock. The initial phase of clock is constant, and it is equal to zero for f2 and equal to Pi for f1.

2. **phase_signal** at certain N-th frame - the expected phase of actually captured signal on this N-th frame. The **phase_signal** at certain N-th frame is calculating as assumed initial phase of signal + phase shift of signal. The assumption of initial phase of signal depends on frequency on initial frame and inversion on initial frame and could be equal either to zero or Pi. The phase shift of signal depends on number of frames with frequency f1 in the captured signal.

3. The inversion **inv** at (N+1)-th frame should be set either to 0 or 1 depending on whether the values **clock_phase** and **phase_signal** coincide or not at N-th frame. Common description of the suggested MSK demodulating program is represented in the following figures.

Firt, we get frequency control code bits acquired on Rx stage and save it in the **freq** variable. We then initialize **inv1** and **inv2** with values "1" and "0" respectively. Then create a "for loop", which traverses through each bit of **freq**. We then create a conditional statement, which initializes the value of integer variable **clock_phase** depending on the value of **freq** on the next frame.

Then, other conditional statements, which initialize integer variables **initial_phase1** and **initial_phase2** depending on the first bit of **freq.** After that, we create a "for loop" traversing through bits of **freq** up to the current element of **freq** of the outer loop. A conditional inside that loop counts the number of bits that are equal to "0" by incrementing the integer variable **f1_count**.

After the loop, we initialize the variable **phase_shift** the value of which depends upon even or odd count of **f1_count**. Then, we evaluate the value of variables **phase_signal1** and **phase_signal2** depending upon the values of **phase_shift**, **initial_phase1**(in case of **phase_signal1**) and **initial_phase2** (in case of **phase_signal2** respectively). Finally, the conditional statements evaluate the values of **inv1** and **inv2** depending on whether the value of **clock_phase** equals to **phase_signal1** (in case of **inv1**) and **phase_signal2** (in case of **inv2** respectively). The outer loop, then, moves to the next bit of **freq,** and we repeat the process.

Since the input data for inversion for the first frame is probabilistic, we address it through the introduction of 2 variables (**inv1** and **inv2)**, each with either “1” or “0”. Consequently, we get 2 results, where 1 of them will be the correct one (how we find out will be defined later). Such algorithm used by us can be defined as the type of probabilistic algorithm. Its use allows us to substitute complicated hardware and advanced digital signal processing with extensive but still basic computations.

Flowchart representing data processing, java code, frequency control code and inversion examples are explained in more details in the MSK Encoding section for the data “Hello, World!”

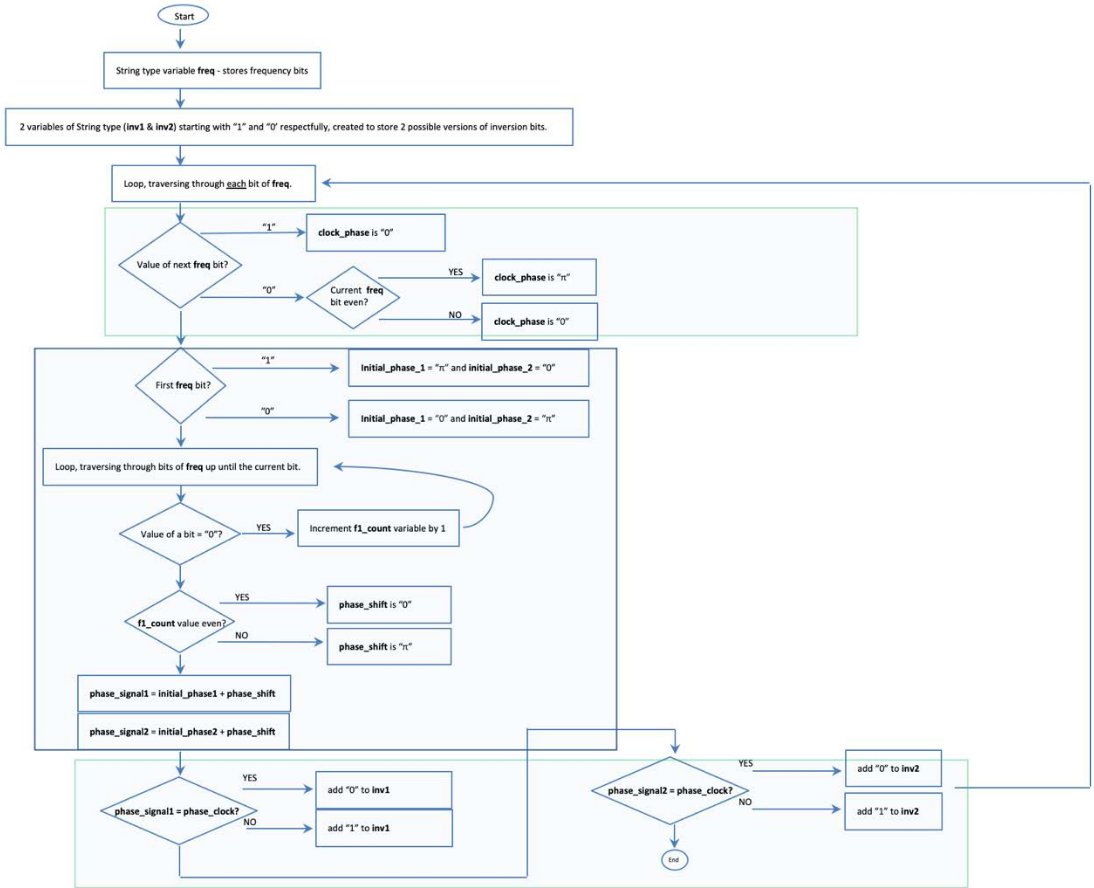

Figure 160: MSK Demodulation Flowchart

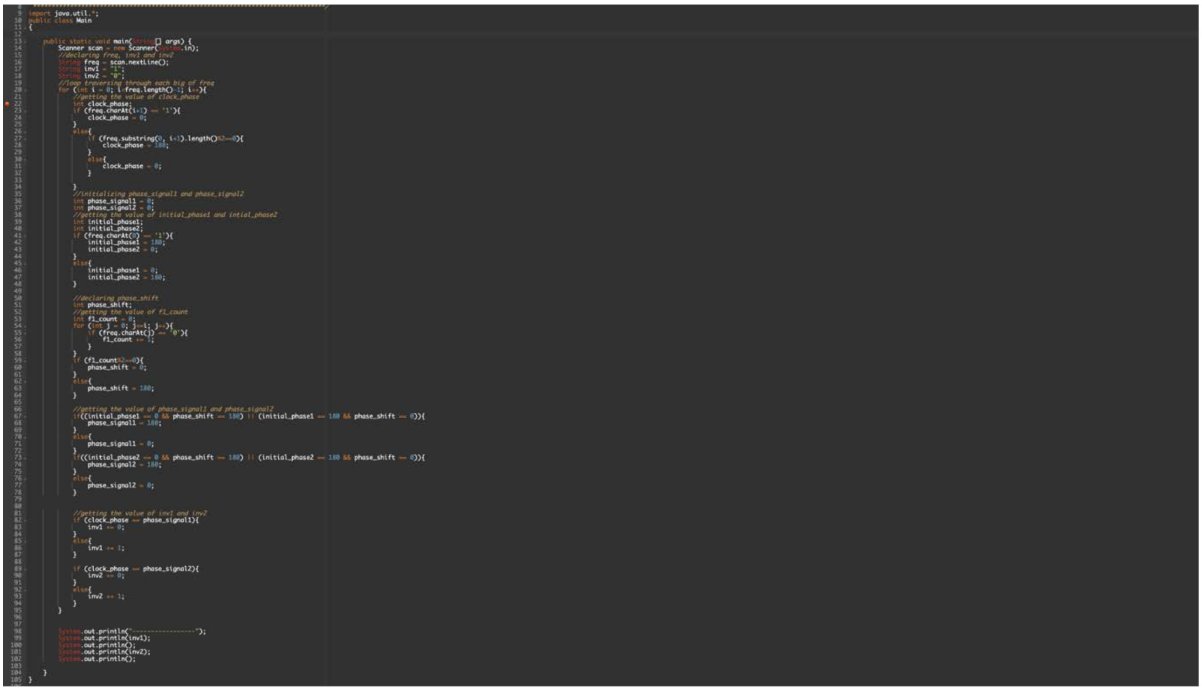

Figure 161: Demodulation Coding example

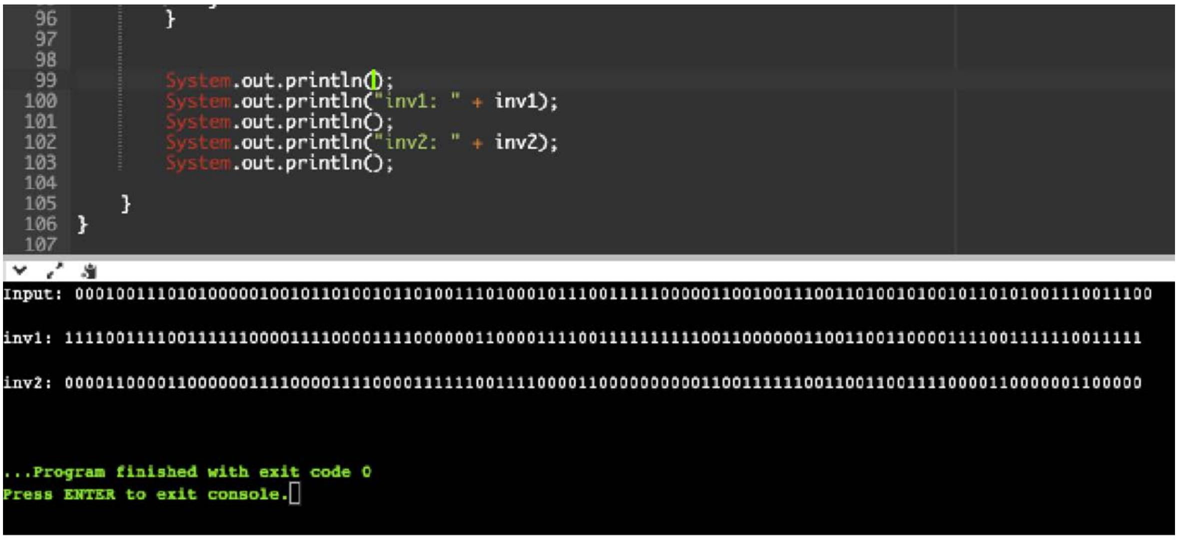

Figure 162: Demodulation data output string

Demodulation program output data strings for inversion **inv**. Only one of them is correct namely inv1 in this case, compare with the inversion control code used under modulation process

Electronic Counter Countermeasure (ECCM) Design

Although external noise source (ENS) (aka jammers) is ineffective in the VLF/ULF signals in Near field due to the antenna size required, it is important to allow for noise cancellation in the design. The design includes combining signal magnitude amplification/attenuation, signals phases shifting, and basing on some inherent differences in our Tx signal, we can cancel out any ENS signal.

In the current design, the Rx is within the Near-Field zone of our Tx source and within the Far-Field zone of ENS source. In other words, our Tx is relatively close to our Rx (less than 11 km), and the ENS is relatively far from our Rx (at least a few tens of kilometres). If the ENS source is placed within the Near-Field zone, the Tx and the ENS signals become indistinguishable. The role of the ENS is to degrade our Signal to Noise ratio, and this chapter includes this design to counter this.

It should be noted that the ENS source antenna is assumed as vertical (monopole). In general, that type of antenna only provides long-range operation (out of Near-Field zone). In this sense to jam this underground signal in the first place, i.e., massive aerials, the jammer operator underground probes would mean that ENS source should operate within Near-Field zone with all the ensuing consequences.

A single ENS source only, can be cancelled with the below approach. Placing several ENS sources operating from different directions of arrival will make cancellation of the signal impossible.

Also, the Tx signal could be effectively jammed in the above-mentioned constraints (ENS is within the Far-Field zone and vertically polarized) if the orientation of the Rx coil is vertical. If the Rx is oriented horizontally (for acquiring normal component of magnetic field), that will be affected for jamming signal much less, although available signal strength from Tx will be much less as well.

It should also be noted that under the external noise source (ENS) (aka jammer), it is understood the EM radiation source that satisfies certain requirements (to be potentially cancelled with the considering approaches).

The source should be within the Far-Field zone from the Rx. That means the radiation of the source is vertically polarized, a phase shift between E- and H-components of EM wave is 90-degree. Regarding the strongly vertical polarization of the noise source radiation, it could be noted that the horizontally oriented Rx coil (acquiring the normal component of magnetic field) will not be affected by such noise types. So, the approach considering below is actual for the case when the Rx antenna is oriented vertically.

It should be certain, a single direction of arrival (it means, in particular, single source only can be cancelled with this approach).

Approach A: requires

1. Using pair of identical mutually orthogonal vertically oriented Rx coils (let's call XZ and YZ coils)

2. Single electric field probe antenna (a kind of electrically short whip antenna).

As it will be seen from the description, this approach will not require the direction of arrival from Tx but does require knowing the direction of arrival from the noise source. A possible procedure of defining of the direction of arrival from noise source will be suggested below.

So, the RX approach 3-antenna arrangement and can be represented as:

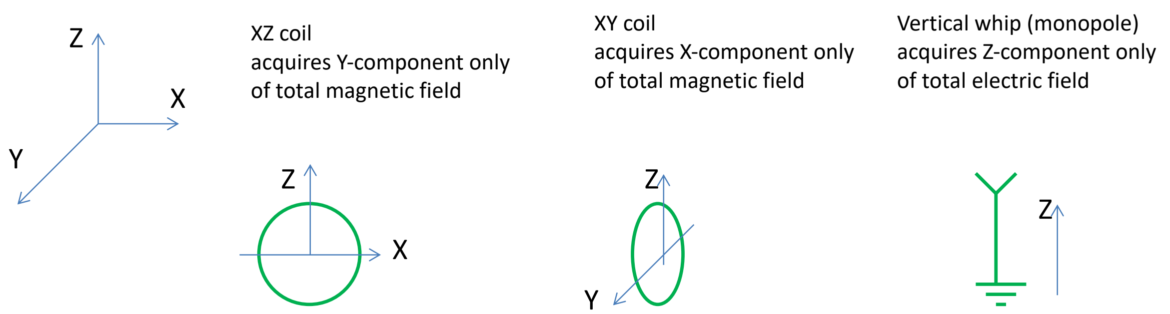

Orthogonal reference system with dashed lines in XY plane that represent directions of arrival of incoming signals of Tx (data) and ENS (jammer).

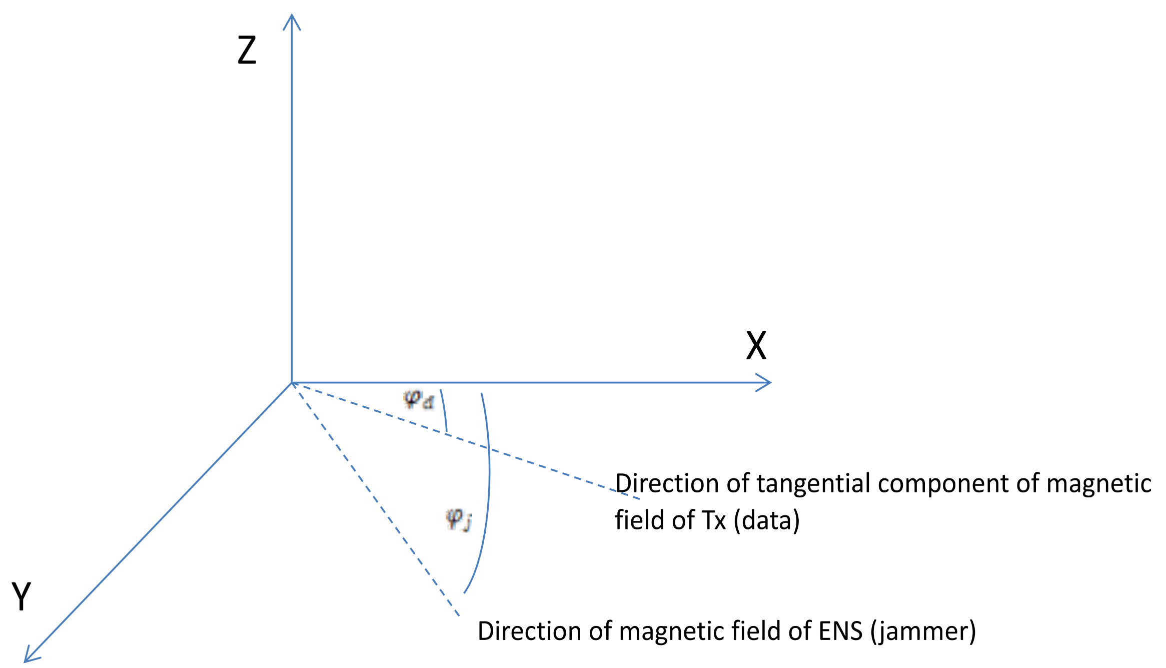

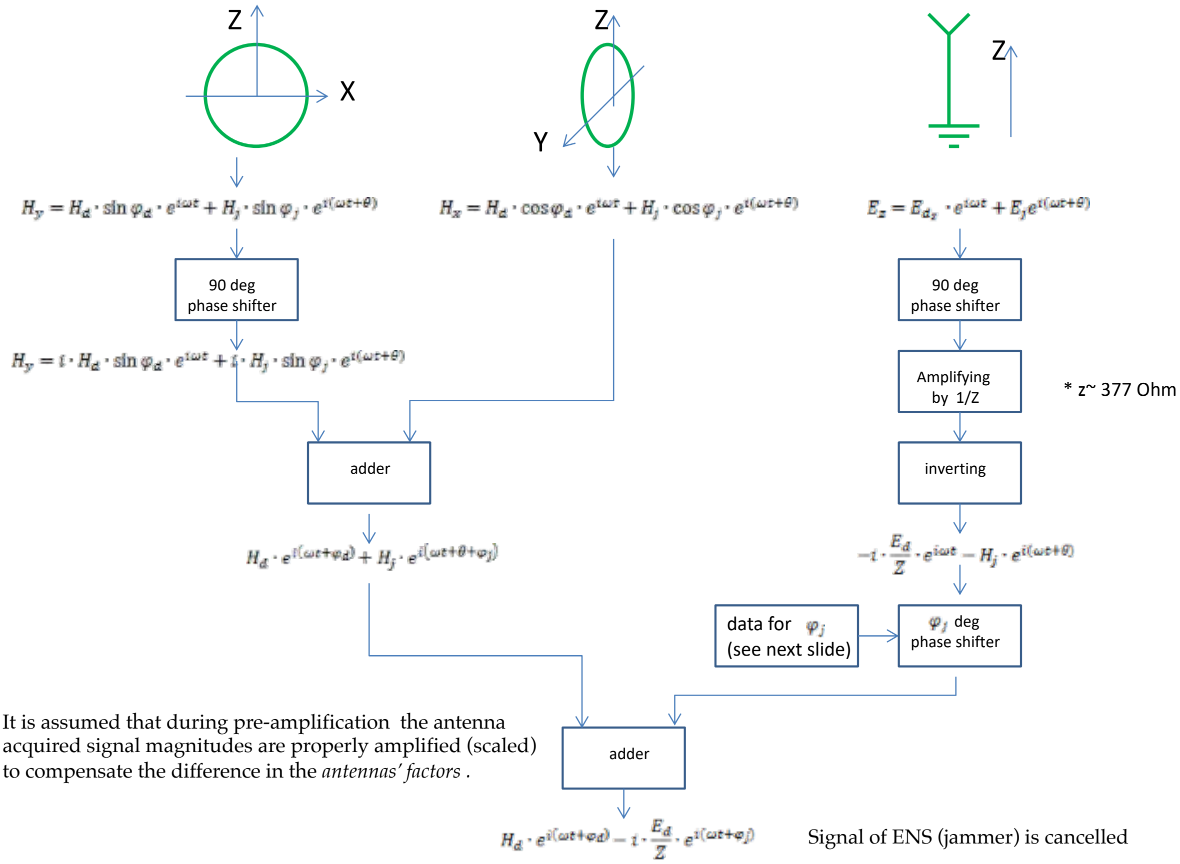
Z
X
Z
Y
Z
$H_y = H_d \cdot \sin\varphi_d \cdot e^{i\omega t} + H_j \cdot \sin\varphi_j \cdot e^{i(\omega t+\theta)}$
$H_x = H_d \cdot \cos\varphi_d \cdot e^{i\omega t} + H_j \cdot \cos\varphi_j \cdot e^{i(\omega t+\theta)}$
$E_z = E_{d_z} \cdot e^{i\omega t} + E_j e^{i(\omega t+\theta)}$
90 deg phase shifter
90 deg phase shifter
$H_y = i \cdot H_d \cdot \sin\varphi_d \cdot e^{i\omega t} + i \cdot H_j \cdot \sin\varphi_j \cdot e^{i(\omega t+\theta)}$
Amplifying by 1/Z
* z~ 377 Ohm
adder
inverting
$H_d \cdot e^{i(\omega t+\varphi_d)} + H_j \cdot e^{i(\omega t+\theta+\varphi_j)}$
$-i \cdot \frac{E_d}{Z} \cdot e^{i\omega t} - H_j \cdot e^{i(\omega t+\theta)}$
data for φ_j (see next slide)
φ_j deg phase shifter
It is assumed that during pre-amplification the antenna acquired signal magnitudes are properly amplified (scaled) to compensate the difference in the *antennas' factors* .
adder
$H_d \cdot e^{i(\omega t+\varphi_d)} - i \cdot \frac{E_d}{Z} \cdot e^{i(\omega t+\varphi_j)}$
Signal of ENS (jammer) is cancelled

Defining the direction of arrival for the signal of the ENS (jammer), it should be processed prior to the ENS (jammer) signal cancellation setup and under conditions when either Tx is OFF or with frequency offset.

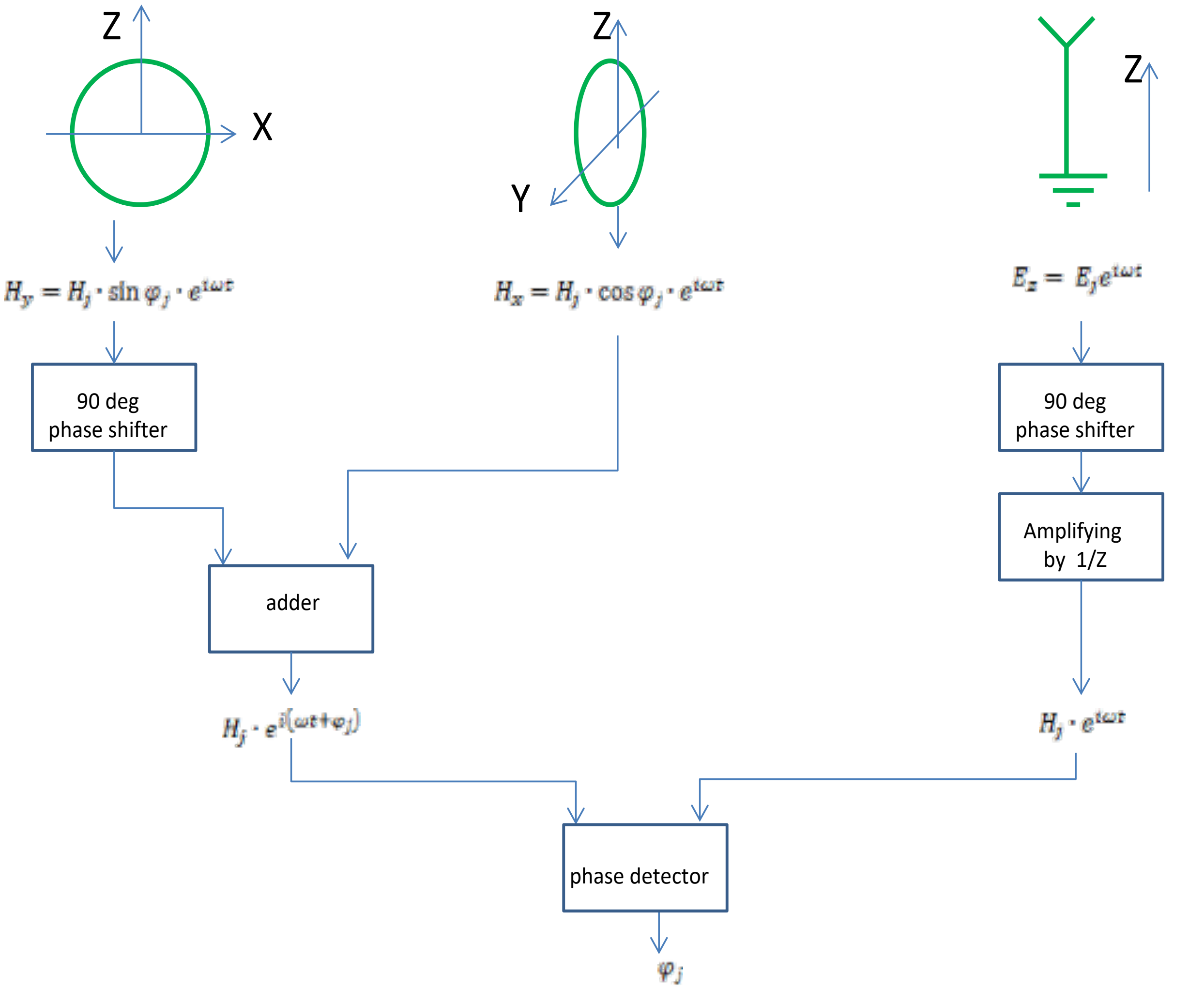

Possible approaches for the external noise cancellation when single vertical coil and whip (monopole) antenna are used only.

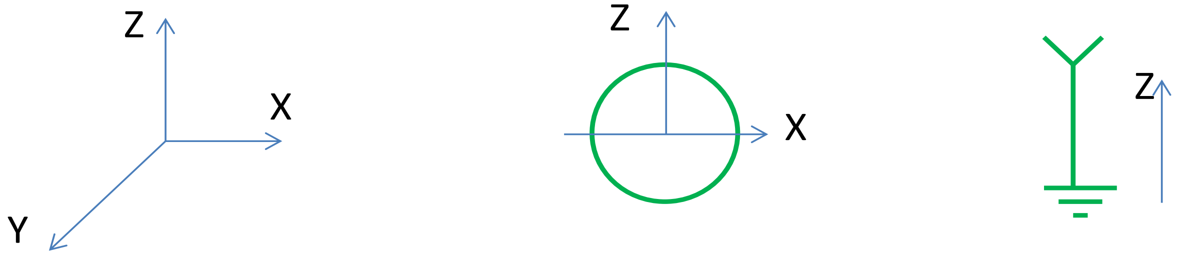

In this case, the quadrature diversity combining is not possible. The direction of the arrival of the ENS (jammer), and Tx signals should be defined in manual mode by means of rotating of Rx coil around the Z-axis until the signal is strongest. The situation when the Tx signal is strongest, and any ENS (jammer) signal is nulled is rarely expected because it assumes a special case of the Tx array – Rx coil – ENS (jammer) mutual location and orientation.

For a better understanding of the expected distribution of the tangential component of magnetic fields with respect to Tx array location/orientation and ENS (jammer) location, the sketch below illustrates the expected direction of magnetic field tangential component generated by Tx (blue arrows) and ENS (jammer) source (red lines), arrow size or color intensity are not mapped to the expected field strength value. Possible approaches for external noise cancellation when a single vertical coil and whip (monopole) antenna are used.

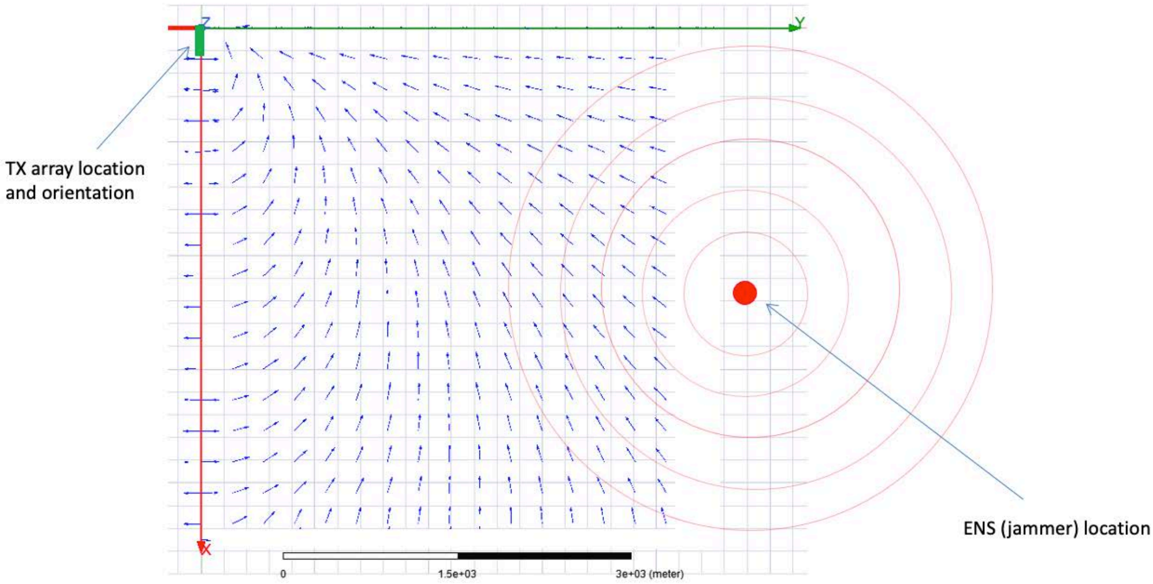

Possible approaches for external noise cancellation when single vertical coil and whip (monopole) antenna are used only.

The direction of the arrival of ENS (jammer) should be defined in manual mode by means of rotating the Rx coil around the Z-axis until the signal is strongest. The direction of arrival is defined with respect to the optimal direction for Tx signal (see blue arrows vector field on the diagram above. The X-axis on the next illustrations is associated with the optimal direction for the Tx signal. Should be processed prior to the ENS (jammer) signal cancellation setup and under conditions when either Tx is OFF or with frequency offset.

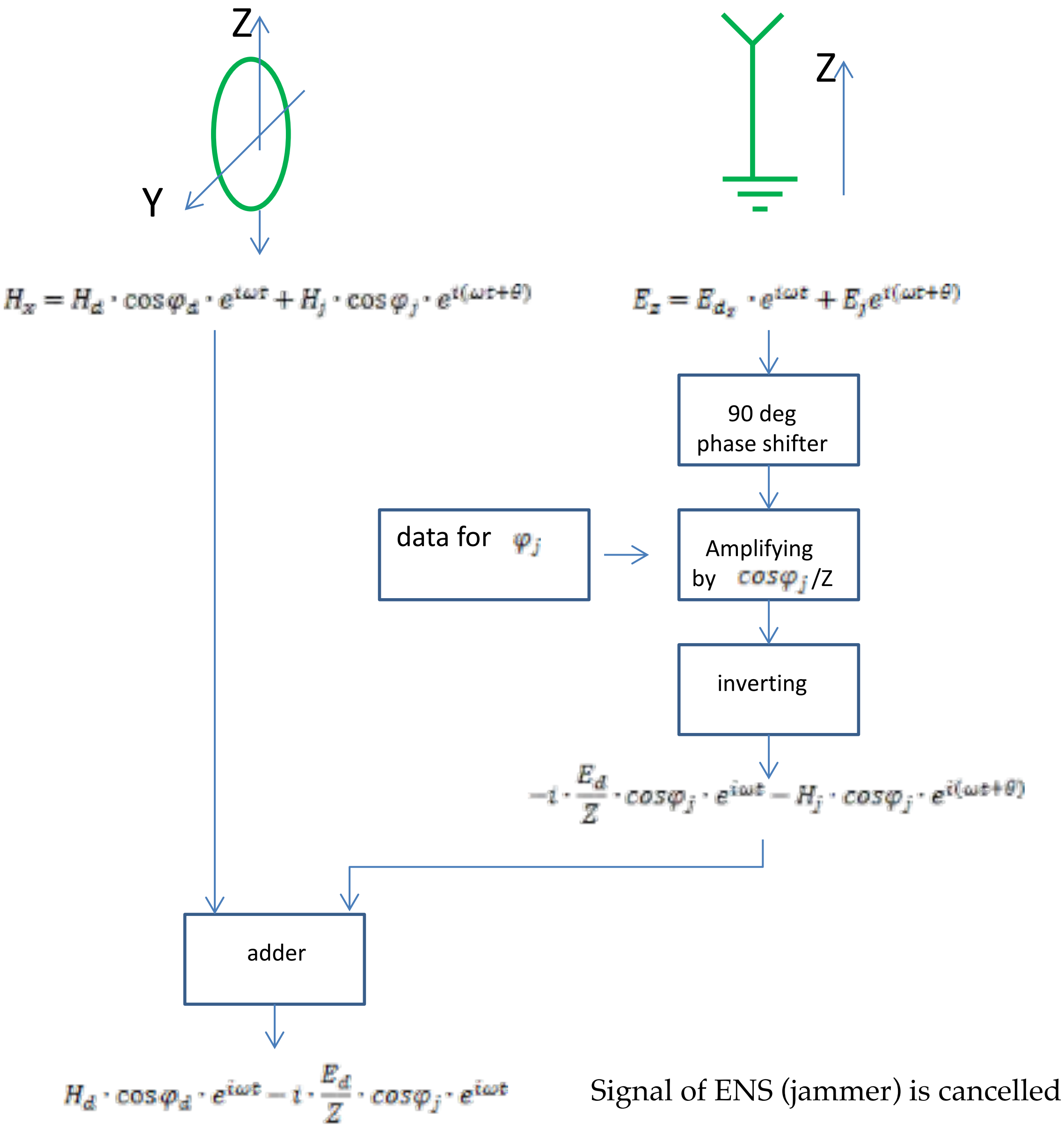

Some possible approaches for external noise cancellation when single vertical coil is used only are explained below. The direction that is orthogonal to the direction of arrival of ENS (jammer) should be defined in manual mode by means of rotating the Rx coil around the Z-axis until the signal is weakest. Should be processed under conditions when either Tx is OFF or with frequency offset.

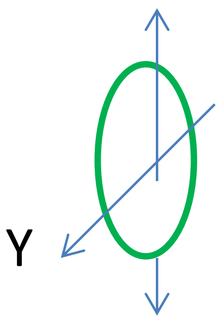

$$H_x = H_d \cdot \cos\varphi_d \cdot e^{i\omega t} + H_j \cdot \cos\varphi_j \cdot e^{i(\omega t+\theta)}$$

rotating of Rx coil around Z-axis until the signal is weakest

$$H_x = H_d \cdot \cos\varphi_d' \cdot e^{i\omega t}$$

Signal of ENS (jammer) is cancelled with the simple approach, but an obvious disadvantage is: the φ_d' is not controlled more, so, if the $\cos\varphi_d'$ occasionally ~0 , than Tx signal will be cancelled as well.

Conclusion

It is more feasible to proceed that with Digital Signal Processing (DSP) rather than with analog hardware. Also, preliminary signals should be amplified before digitizing, so, for example, the approach with three independent Rx antennas will require three independent low noise amp channels.

Conclusion

Building on the initial research in the late 19th century by Marconi, Tesla and further developed by Preece (1900), Kendall (1921), and Bradley (1964), I have investigated conductive current earth mode as communications medium using long range near field zones at low frequencies. The communications method is classified as Near-Field zones via a Magnetic field instead of far field electromagnetic wave communication. zones.

I have designed and built custom Tx/Rx equipment to successfully use ULF conductive current earth mode communications as an underground H-field communications / Near Field Communication (NFC) with an operation range of 400m-11km at 2-4KHz. In this specific case 2kHz has a theoretical near field zone of 75Km. This has been achieved by using modern electronic equipment, techniques into noise cancellation, signal amplification and modulation techniques. The communication channel is effective from 400 meters-11km depending on the power input, soil type and modulation selected.

This covert channel is immune to modern-day military and commercial jamming equipment by operating at 1-4 kHz within Near field zones and using H-field not in the Far field zone used by modern jammers.

By using different modulation methods, ANC, MLD, NLP, and DAFB, we can gain a further 10-24 dB improvement on the Signal to Noise Ratio from our initial simulations and field work operationally. Combined with increasing the power on the Tx from 20W, 1800W, and 3600W, we can further extend the signal distance and bandwidth, but the trade-off is hardware costs, equipment size and complexity goes up significantly.

The author does not believe this technology will be widely used by extremist groups for IED detonation when there are other methods such as Time or Victim operated. However, high-value target (HVT) assassinations, underground communications channels for communications mediums are where this technology could be used in a jammed/noisy or underground environment such as agriculture sensors, especially using power over air methods for the receiver.

BIBLIOGRAPHY

ANTONI MUNOZ, V. B., N AYSO 2011. Noise Characterization in Through-The-Earth Communications with Electrodes.

BATALLER, V. 2010. Earth impedance model for through-the-earth communication applications with electrodes.

BERRY, S. 2018. Radio Frequency Explained. https://itm-components.co.uk/blogs/news/radio-frequency-explained.

BLILEY TECHNOLOGIES. 2017. *How ECCM Techniques Take Electronic Warfare to the Next Level* [Online]. Available: https://blog.bliley.com/eccm-techniques-electronic-warfare [Accessed March 1st, 2021].

BOLAND, R. 2011. *Dialling up the Bandwidth Battle against IEDs* [Online]. Signal Magazine: AFCEA. Available: https://www.afcea.org/content/dialing-bandwidth-battle-against-ieds [Accessed February 28th, 2021 2021].

BRITANNICA. 2021. *Radio Frequency Spectrum* [Online]. Available: https://www.britannica.com/science/radio-frequency-spectrum [Accessed February 28th, 2021].

CONGRESSIONAL RESEARCH SERVICE, 2020. U.S. Military Electronic Warfare Program Funding: Background and Issues for Congress.

COOPER, G. 2019. *Project Sanguine* [Online]. Available: https://ss.sites.mtu.edu/mhugl/2019/10/30/project-sanguine-gecooper/#:~:text=Project%20Sanguine%20was%20officially%20proposed,of%20the%20state%20of%20Wisconsin. [Accessed March 1st 2021].

DEFENSE SECURITY COOPERATION AGENCY, 2020. *–AUSTRALIA SURFACE COMBATANT (ASC) PROGRAM* [Online]. Available: https://www.dsca.mil/press-media/major-arms-sales/australia-australia-surface-combatant-asc-program [Accessed February 28th, 2021].

DURKIN, J. 1983. *Vertical magnetic noise in the voice frequency band within and above coal mines,* Washington, D.C., U.S. Dept. of the Interior, Bureau of Mines.

DYNO NOBEL. 2021. *Electric, Non-Electric and Electronic Detonators* [Online]. Available: https://www.dynonobel.com/ [Accessed February 28th, 2021].

ELECTRONICS, S. 2020. Electronics Warfare Systems Jamming Solutions. *2020.* https://www.narcon.co.id/assets/filesupload/Jamming%20Solutions.pdf.

ESTERS. 2021. *International Workshop "Ionosphere at low frequency"* [Online]. http://esters.obspm.fr/spip.php?article84: Earth's Space Environment: Research & Surveillance. Available: http://esters.obspm.fr/spip.php?article84 [Accessed March 1st, 2021].

GEOSPATIAL WORLD. 2014. *Counter RCIED Systems* [Online]. Geospatial World. Available: https://www.geospatialworld.net/article/counter-rcied-systems/ [Accessed Feb 28th, 2021].

JACOBSEN, T. 2021. *THE OPEN LAB's – ELF and VLF frequency Guide* [Online]. Available: http://www.vlf.it/trond2/list.html [Accessed February 28th, 2021].

JAMMER, T. S. 2021. *The Signal Jammer* [Online]. Available: https://www.thesignaljammer.com/products/TSJ-VIP-6066.html [Accessed February 28th 2021 2021].

KATSUBE, T. J., KLASSEN, R., DAS, Y., ERNST, R., CALVERT, T., CROSS, G., HUNTER, J., BEST, M., DILABIO, R. & CONNELL, S. 2003. *Prediction and validation of soil electromagnetic characteristics for application in landmine detection*, SPIE 2003 Vol. 5089

KEYSER, N. 2007. Cutler VLF. https://commons.wikimedia.org/wiki/File:Cutlervlf2.jpg.

KIRINTEC. 2021. *Kirin Tec C-IED Mercury Jamming system* [Online]. Available: https://www.kirintec.com/mercury/ [Accessed February 28th, 2021].

KLEIN, M. E. 2009. *Autonomous Ultra- Low Power ELD / VLF Receiver Systems.* Doctor of Philosophy, Stanford University.

LAPTHORN, R. 2011. *Earth Mode sub (kHz* [Online]. Available: https://sites.google.com/site/sub9kHz/earthmode [Accessed February 28th, 2021]

MARK A. KEMP, M. F., ANDY HAASE, ERIK JONGEWAARD, MATTHEW T. WHITTAKER, MICHAEL KIRKPATRICK, ROBERT SPARR 2019. A high Q piezoelectric resonator as a portable VLF transmitter.

MAXWELL, E. 1963. Natural Noise Fields at 1 cps to 100 kc.

MCDERMOTT, R. N. 2017. Russia's Electronic Warfare Capabilities to 2025. INTERNATIONAL CENTRE FOR DEFENCE AND SECURITY.

MILITARY 2010. USMC Counter Radio Controlled Improvised Explosive Device (RCIED) Electronic Warfare (CEW) 3.1 THOR III System. *In:* DEFENCE (ed.).

MURTALA ZUNGERU ADAMU, M. M., JOSEPH CHUMA 2017. Optimal node placement in wireless underground sensor networks. *ResearchGate*.

MUSTAFA ALPER AKKAŞ, R. S. 2015. Wireless Underground Sensor Networks: Channel Modelling and Operation Analysis in the Terahertz Band. *ResearchGate*.

NASIR SAEED, M.-S. A., FELLOW, TAREQ Y. AL-NAFFOURI 2019. Towards the Internet of Underground Things: A Systematic Survey. *EESS*.

NATIONAL ACADEMIES OF SCIENCES, E., AND MEDICINE 2018. Reducing the Threat of Improvised Explosive Device Attacks by Restricting Access to Explosive Precursor Chemicals. Washington, DC.

NTIA 2016. United States Frequency Allocations - The Radio Spectrum. National Telecommunications and Information Administration.

OFFICE OF NAVAL RESEARCH 2010. Joint Counter Radio Controlled Improvised Explosive Device Electronic Warfare JCREW 3.3 Technologies RFP - Department of Navy and Science Technology. *In:* RESEARCH, O. O. N. (ed.). Office of Naval Research.

OLNEY, S. 2011. *Earth Mode Antenna* [Online]. Available: http://joataman.net/earth_mode/default.html [Accessed February 21st, 2021].

OSHA 1990. Electromagnetic Radiation: Field Memo. Available https://www.osha.gov/radiofrequency-and-microwave-radiation/electromagnetic-field-memo#:~:text=The%20electric%20(E)%20field%20is,I)%20of%20an%20electric%20circuit. [Accessed March 26th, 2022].

PERFECTJAMMER. 2021. *Cell Phone GPS WiFi Lojack 433/315/868MHz Jammer* [Online]. Available: https://www.perfectjammer.com/ [Accessed March 1st, 2021].

POISEL, R. 2011. Modern communications jamming principles and techniques, Boston, Artech House.

POLLARD, J. June 2020, 2020. RE: CEO of Jefi Electronic Services Pty Ltd.

RAAB, E 1995 "Signal processing for through-the-Earth radio communication," in *IEEE Transactions on Communications*, vol. 43, no. 12

RALCHENKO, M. 2017. Modelling and optimizing through-the-Earth radio *transmissions.* Doctor of Philosophy, Carleton University.

ROCK, C. 2021. Jammer cartoon.

SALAM, A. 2019. An Underground Radio Wave Propagation Prediction Model for Digital Agriculture. *ResearchGate*.

S. A. VAKIN, L. N. S. 1969. Principles of Jamming and Electronic Reconnaissance. I.

SCHWEBER, B. 2019. *Piezo-Based Approach Dramatically Shrinks VLF Antennas* [Online]. Electronic Design. Available: https://www.electronicdesign.com/technologies/analog/article/21808539/piezobased-approach-dramatically-shrinks-vlf-antennas [Accessed February 28th, 2021].

Scratchapixel. 2021. *Electromagnetic frequency and energy difference on wavelength chemistry visual* [Online]. Available: https://scratchapixel.com [Accessed Feb 28th, 2021].

SECOR, H. W. 1919. *America's Greatest War Invention* [Online]. Electrical Experimenter. Available: http://www.rexresearch.com/rogers/1rogers.htm#wx319 [Accessed February 28th, 2021].

SRC. 2020. Electronic Warfare AN/VLQ-12 CREW DUKE. *SRC.*
TECHNOLOGIES, P. 2022. *HF Jamming Relevant More Than Ever* [Online]. https://phantom-technologies.com/hf-jammers/: Phantom Technologies. Available: https://phantom-technologies.com/hf-jammers/ [Accessed March 26th 2022].

United Nations. 2014. *Improvised Explosive Devices (IEDs) Publication* [Online]. Available: https://www.un.org/disarmament/convarms/ieds2/ [Accessed February 28th, 2021].

UNITED NATIONS. 2020. Improvised Nations Mine Action Service - Improvised Explosive Device Lexicon.

URSANO RJ, K. R., NAIFEH JA, MASH HH, FULLERTON CS, BLIESE PD, WYNN GH, ALIAGA PA, WRYTER C, SAMPSON NA, KAO TC, COLPE LJ, SCHOENBAUM M, COX KL, HEERINGA SG, STEIN MB 2018. Frequency of Improvised Explosive Devices and Suicide Attempts in the U.S. Army.

XIAO, L. 2015. Anti-Jamming Transmissions in Cognitive Radio Networks. *Springer Briefs in Electrical and Computer Engineering,* 1st ed. Cham: Springer International Publishing: Imprint: Springer.

APPENDIX A – 0.1 kHz Simulations

0.1 kHz Frequency Simulations

Normal magnetic field amplitude (dBA/m) distribution over earth surface. The Green zone is the ideal DB receive distance.

Simulation 1:

Frequency: 0.1 kHz
Electrodes separation ~10m
Injected power ~ 3600W. Accepted power ~ 3560W.
Distance scale 100m/div.

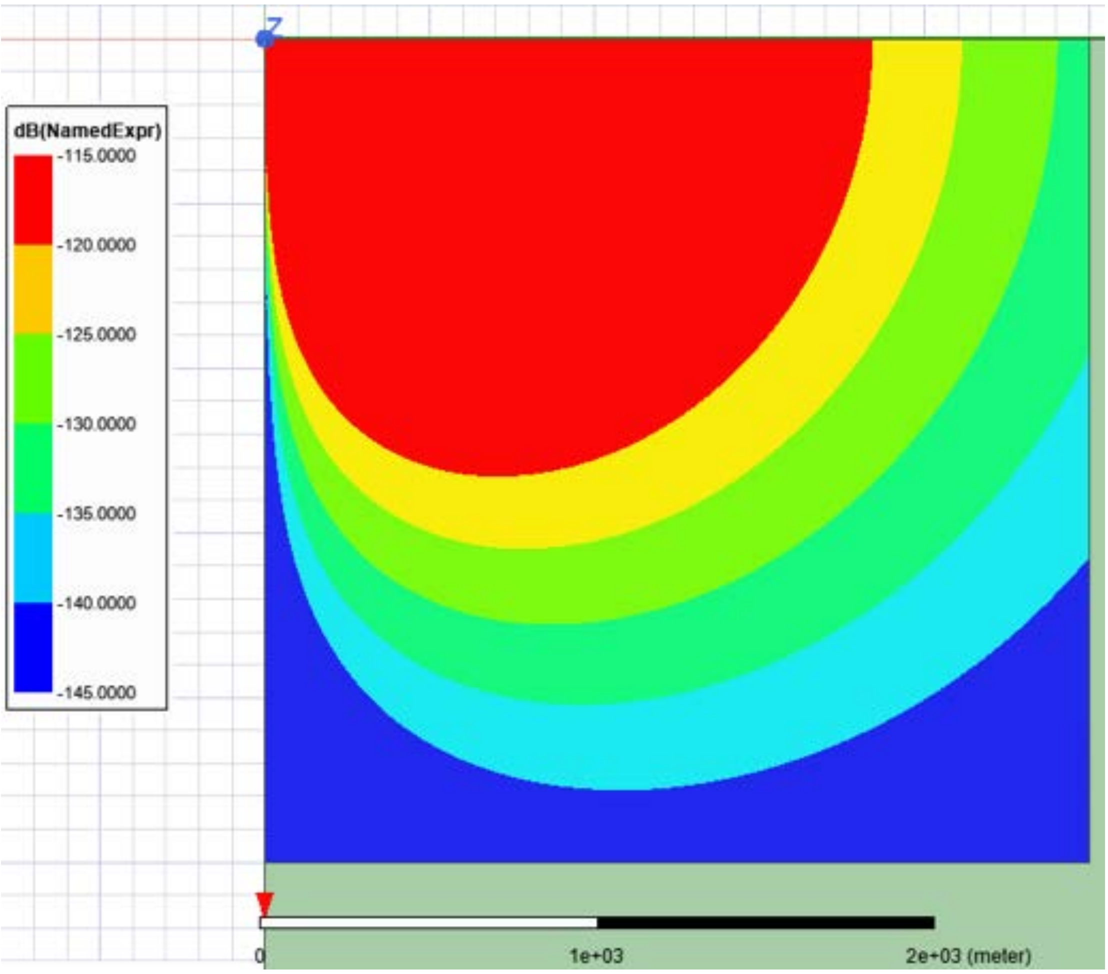

Figure 163: Simulation 1 Results

Simulation 2:

This time 1800W was chosen instead of 3600W

Frequency: 0.1 kHz
Electrodes separation ~10m
Injected power ~ **1800W.**
Distance scale 100m/div.

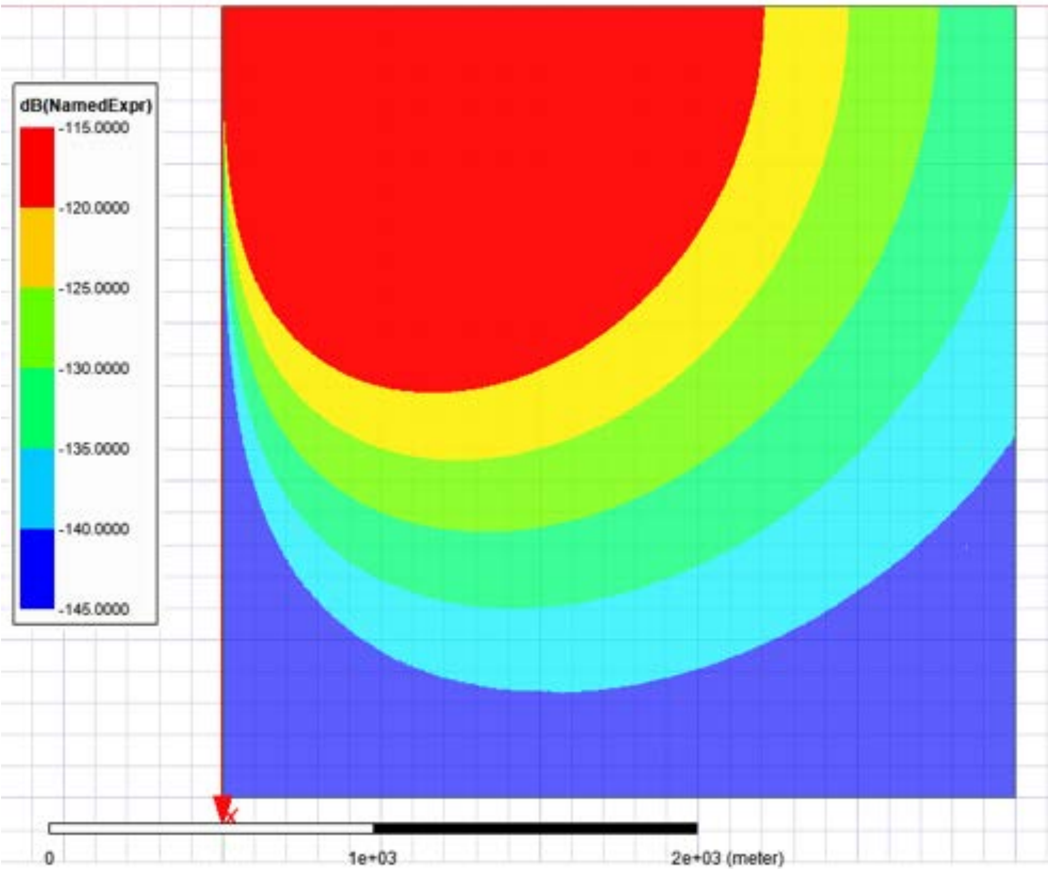

Figure 164:Simulation 2 Results

Simulation 3:

In the next simulation the TX electrodes were moved from 10 meters apart to 20 meters apart.

Frequency: 0.1 kHz
Electrodes separation **~20m**
Injected power ~ 3600W. Accepted power ~ 3560W.
Distance scale 100m/div.

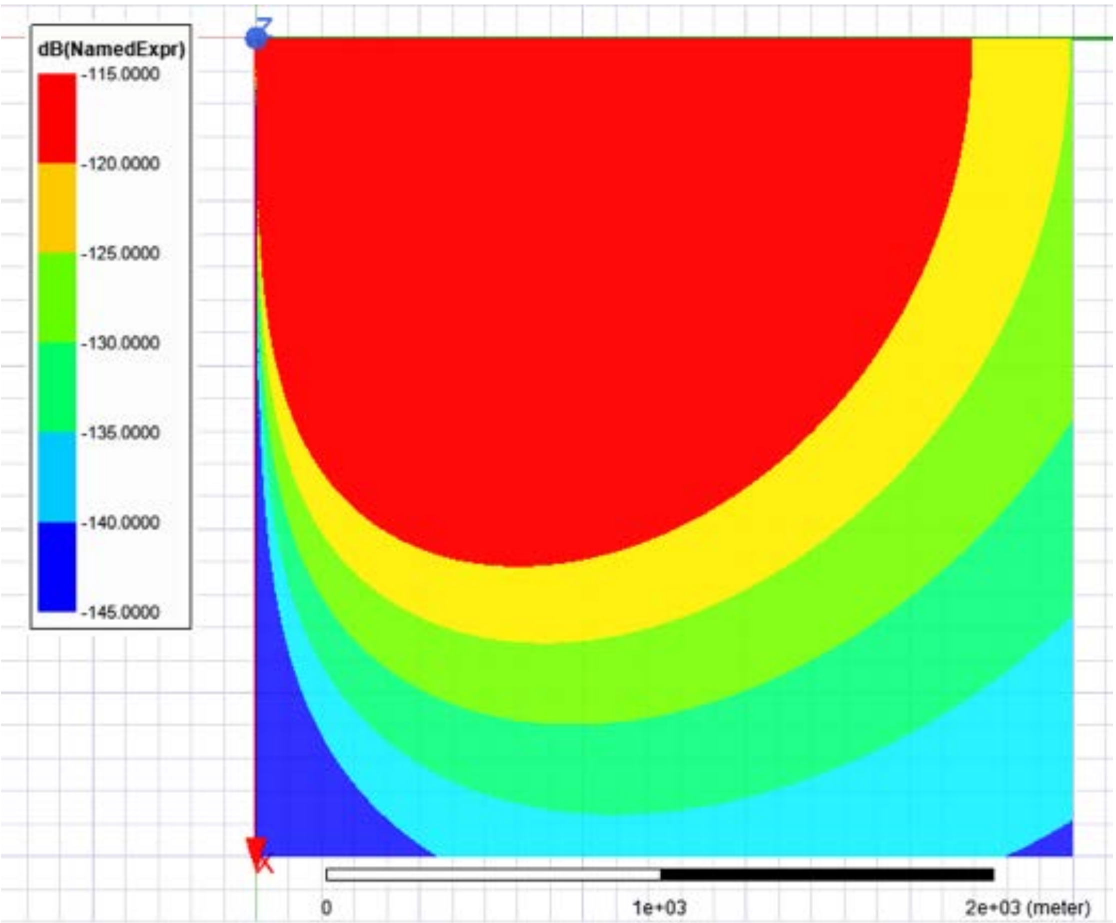

Figure 165: Simulation 3 Results

Simulation 4:

This time 1800W was chosen instead of 3600W

Frequency: 0.1 kHz
Electrodes separation ~20m
Injected power **~ 1800W**.
Distance scale 100m/div.

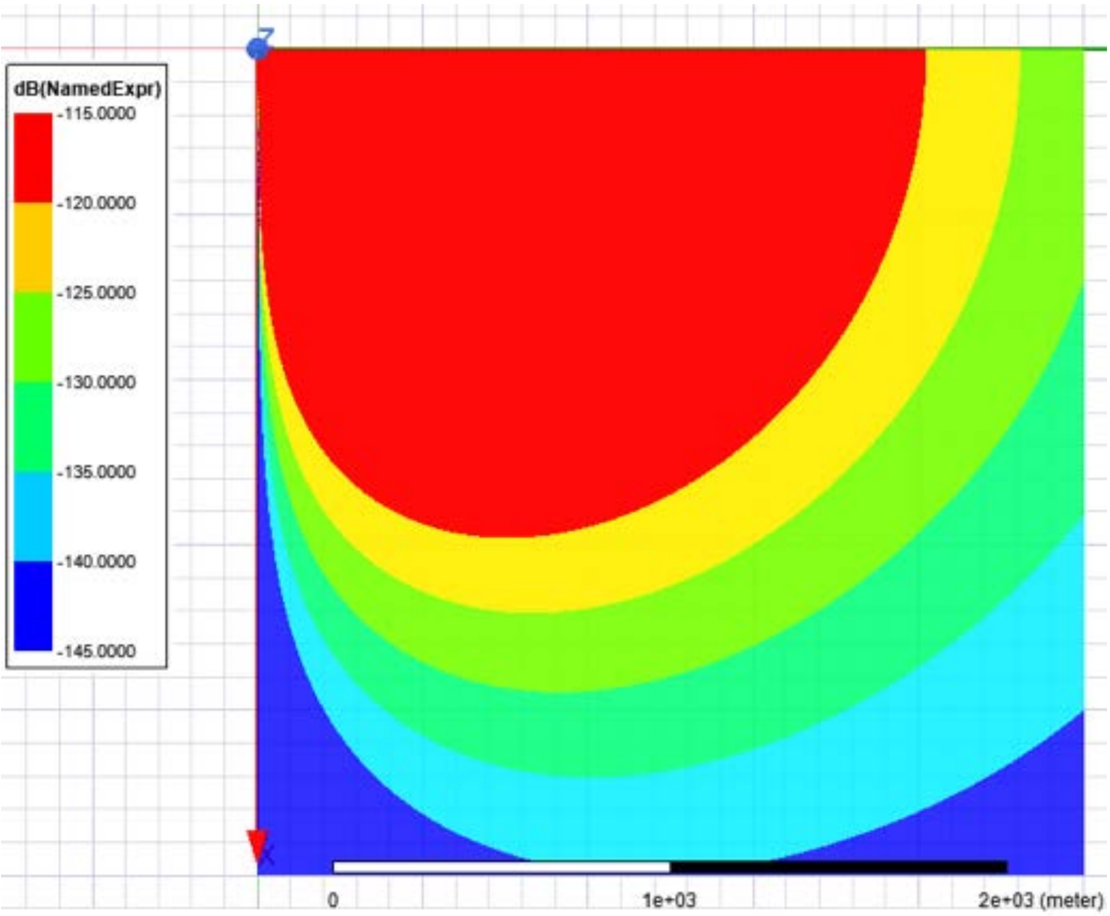

Figure 166: Simulation 4 Results

Simulation 5:

The next simulation the TX probes were increased to 50 meters apart

Frequency: 0.1 kHz
Electrodes separation **~50m**
Injected power ~ 3600W. Accepted power ~ 3560W.
Distance scale 100m/div.

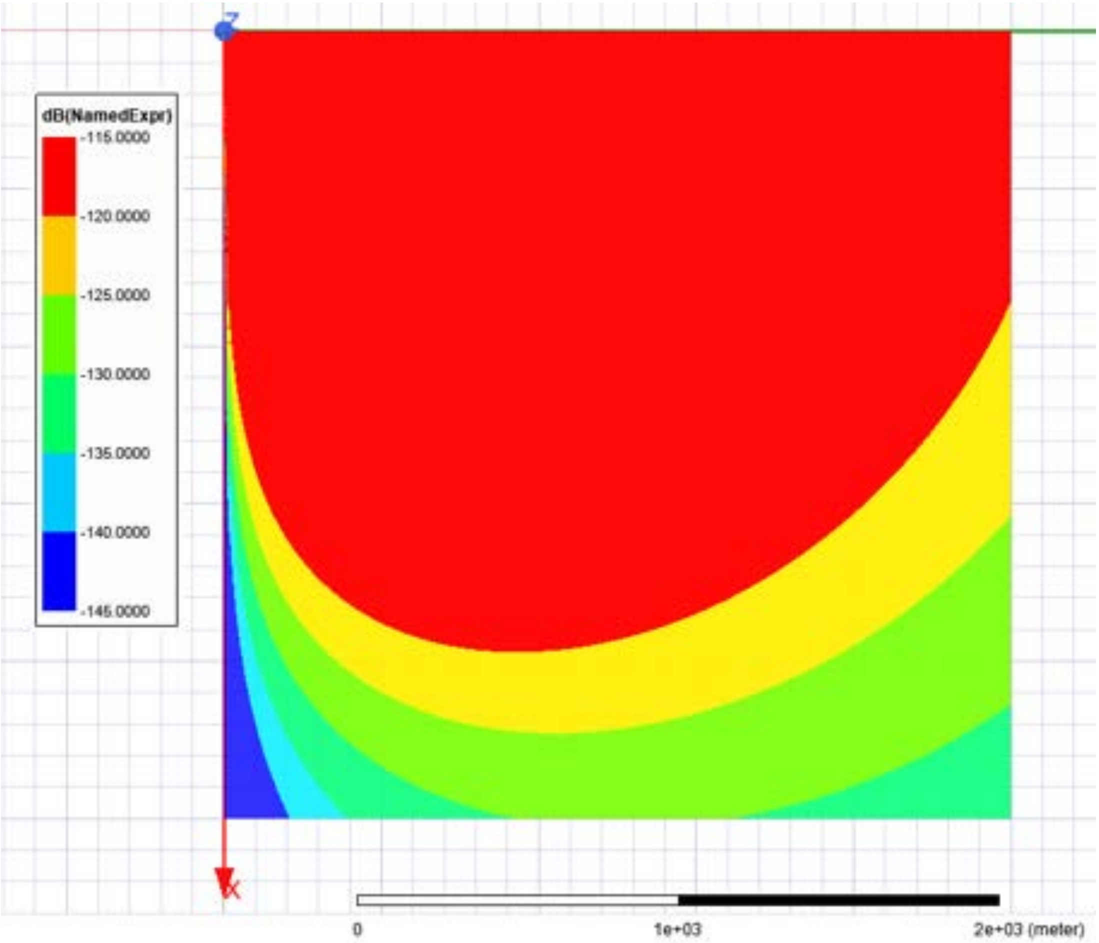

Figure 167: Simulation 5 Results

Simulation 6:

The next simulation the Watts were reduced to 1800W

Frequency: 0.1 kHz
Electrodes separation ~50m
Injected power **~ 1800W**.
Distance scale 100m/div.

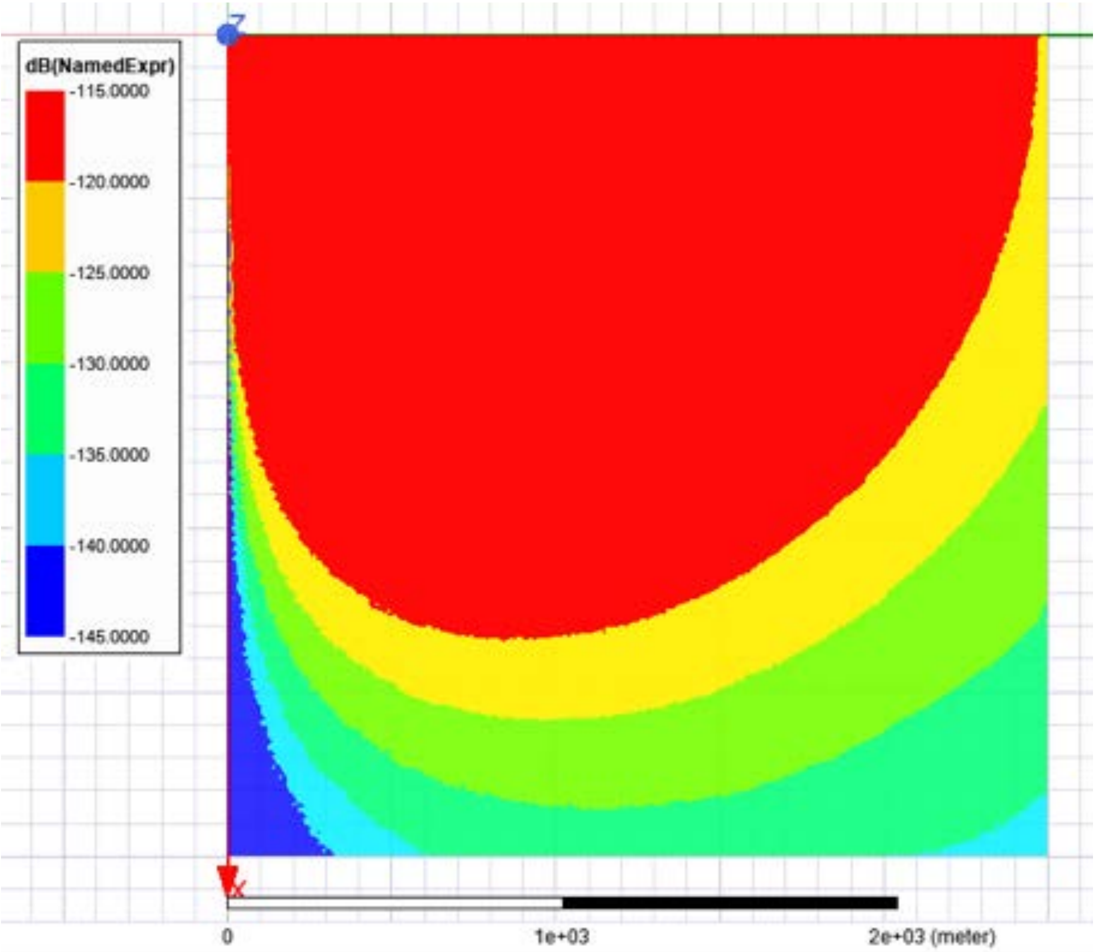

Figure 168: Simulation 6 Results

Simulation 7:

The next simulation the TX probes were increased to 100 meters apart

Frequency: 0.1 kHz
Electrodes separation **~100m**
Injected power ~ 3600W. Accepted power ~ 3560W.
Distance scale 100m/div.

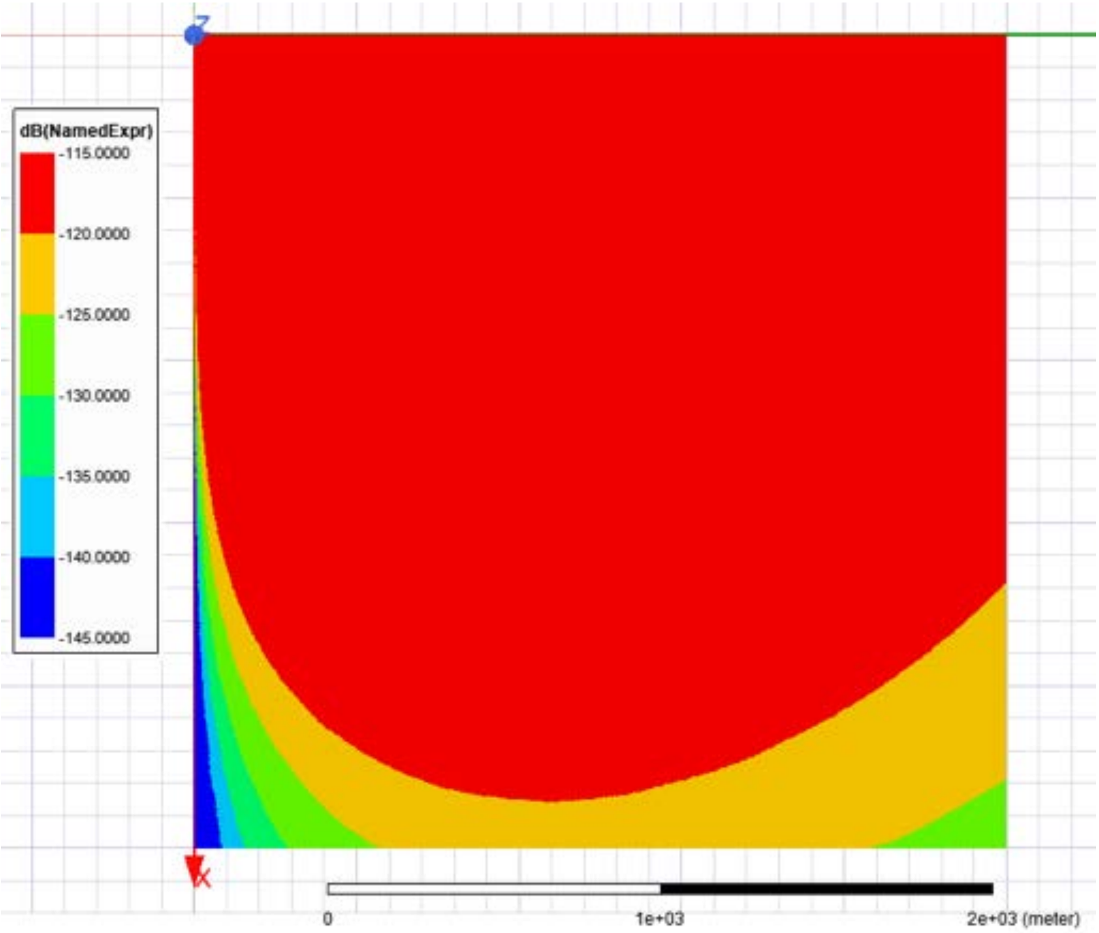

Figure 169:Simulation 7 Results

Simulation 8:

The next simulation the Watts were reduced to 1800W

Frequency: 0.1 kHz
Electrodes separation ~100m
Injected power **~ 1800W**.
Distance scale 100m/div.

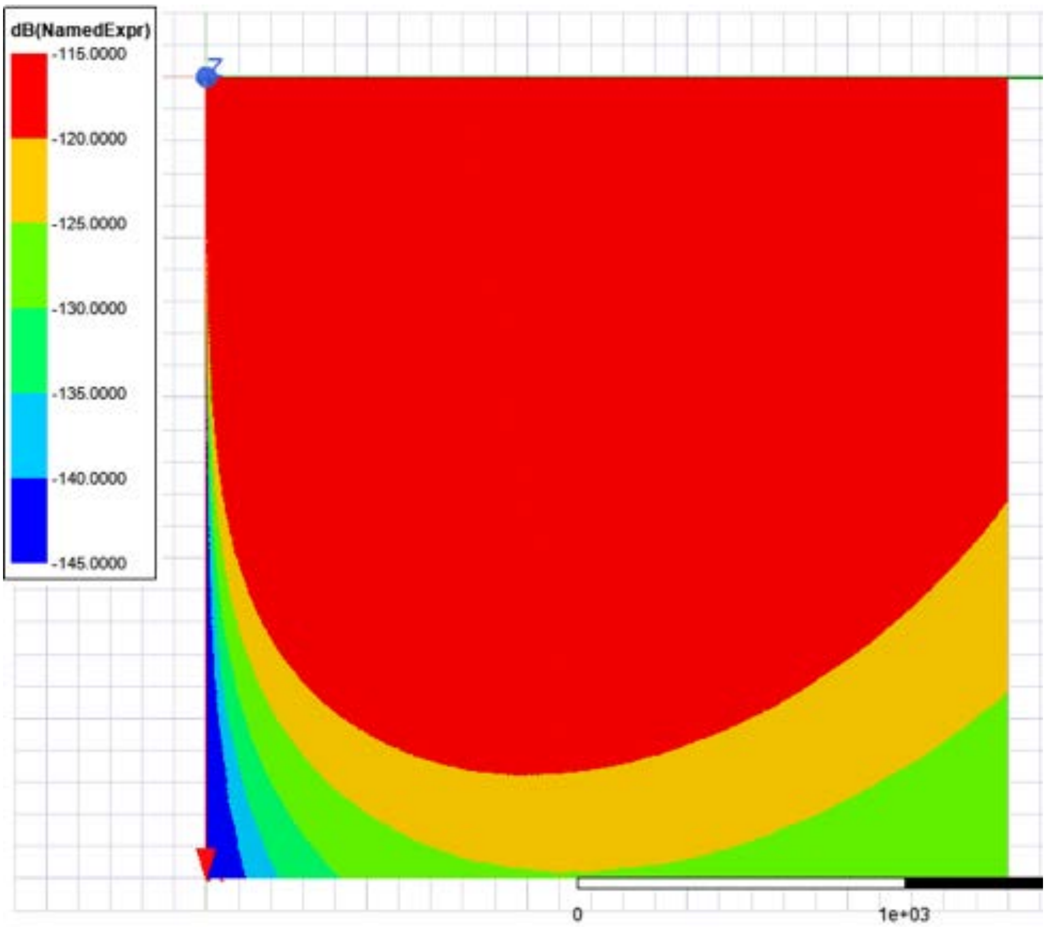

Figure 170: Simulation 8 Results:

Simulation 9:

The next simulation the TX probes were increased to 1000 meters apart. Notice distance scale increase to 200m/div.

Frequency: 0.1 kHz
Electrodes separation **~1000m**
Injected power ~ 3600W. Accepted power ~ 3560W.
Distance scale **200m/div.**

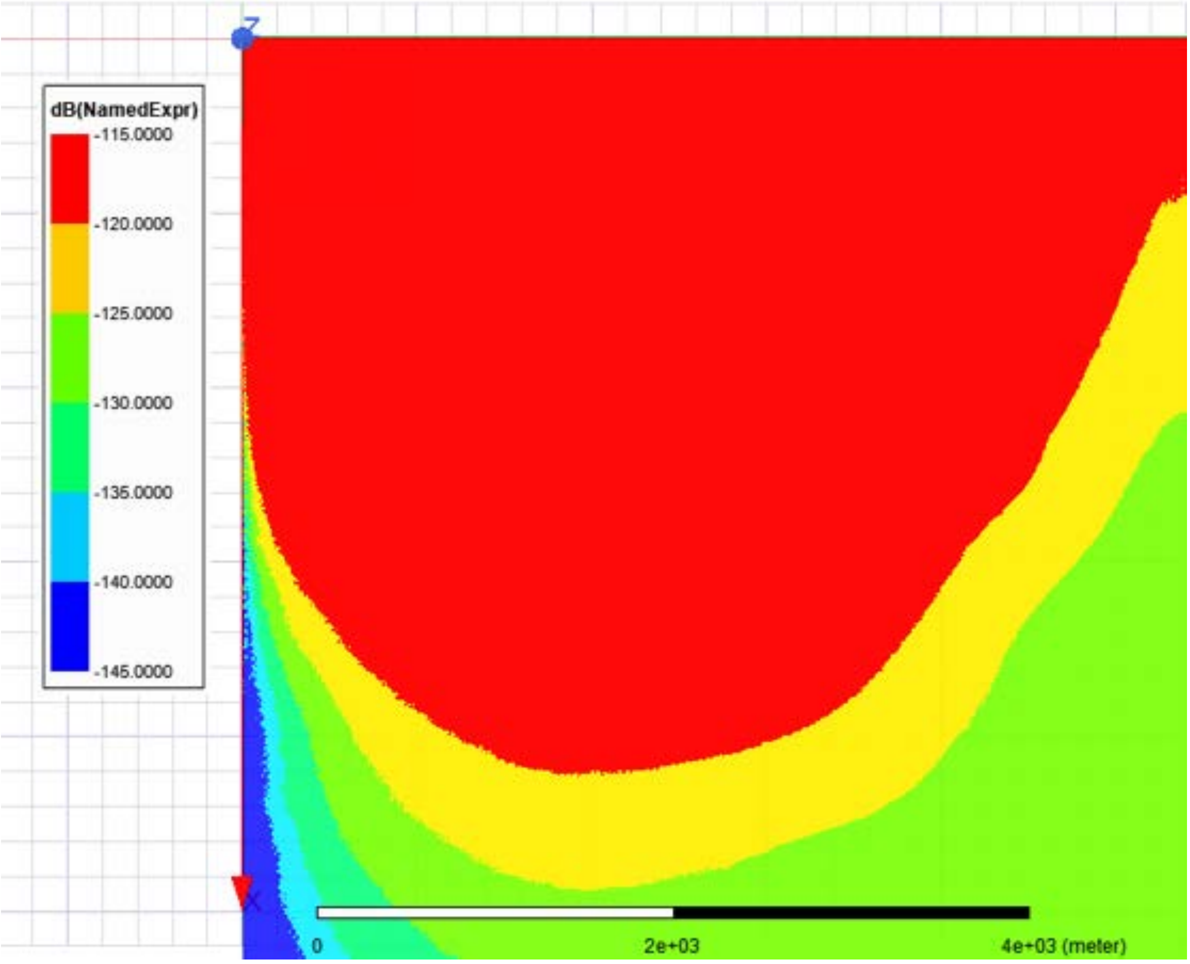

Figure 171: Simulation 9 Results

Simulation 10:

The next simulation the Watts were reduced to 1800W. <u>Notice distance scale increase to 200m div.</u>

Frequency: 0.1 kHz
Electrodes separation ~**1000m**
Injected power ~ **1800W**.
Distance scale **200m/div.**

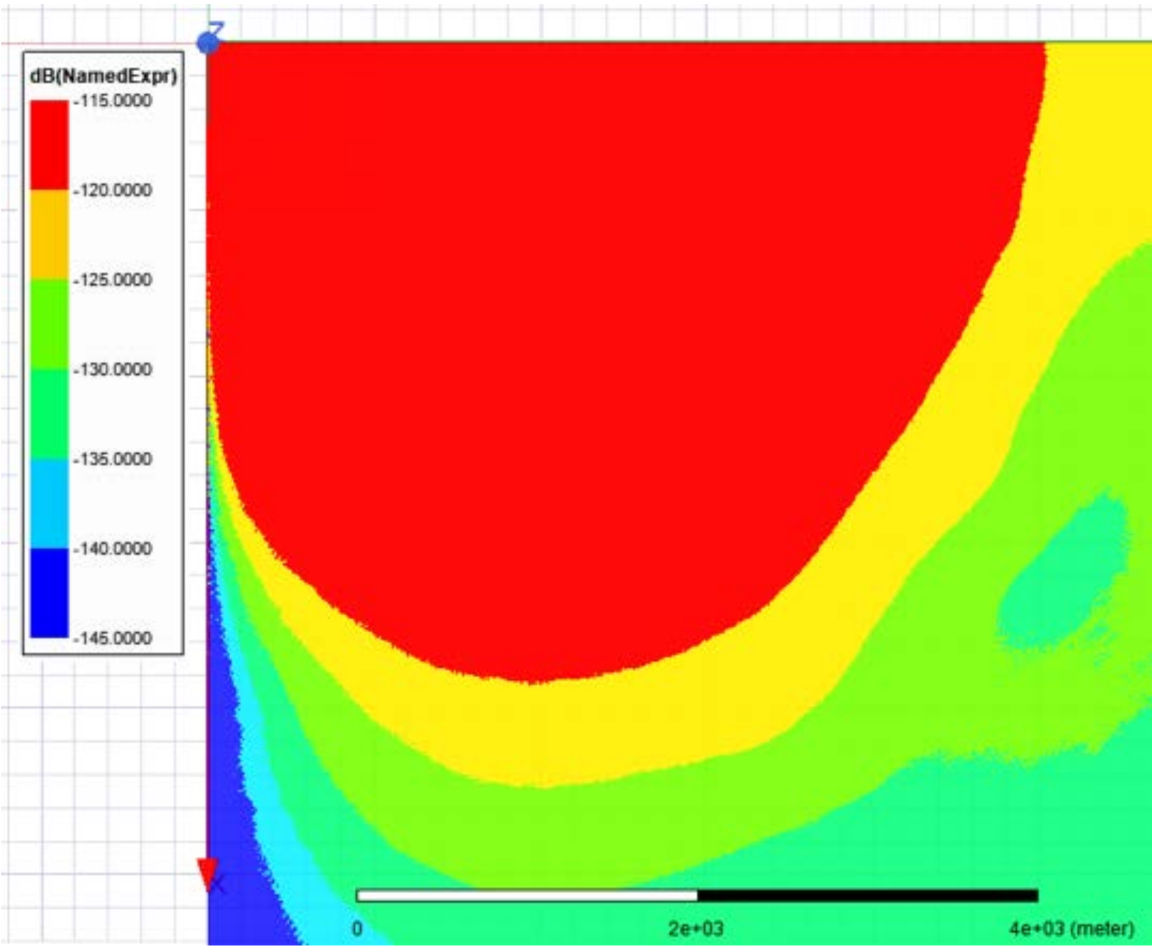

Figure 172: Simulation 10 Results

APPENDIX B – 9 kHz Simulations

9 kHz Frequency Simulations

Normal magnetic field amplitude (dBA/m) distribution over earth surface. The Green zone is the ideal DB receive distance.

Simulation 1:

Frequency: 9 kHz
Electrodes separation ~10m
Injected power ~ 3600W. Accepted power ~ 3560W.
Distance scale 100m/div.

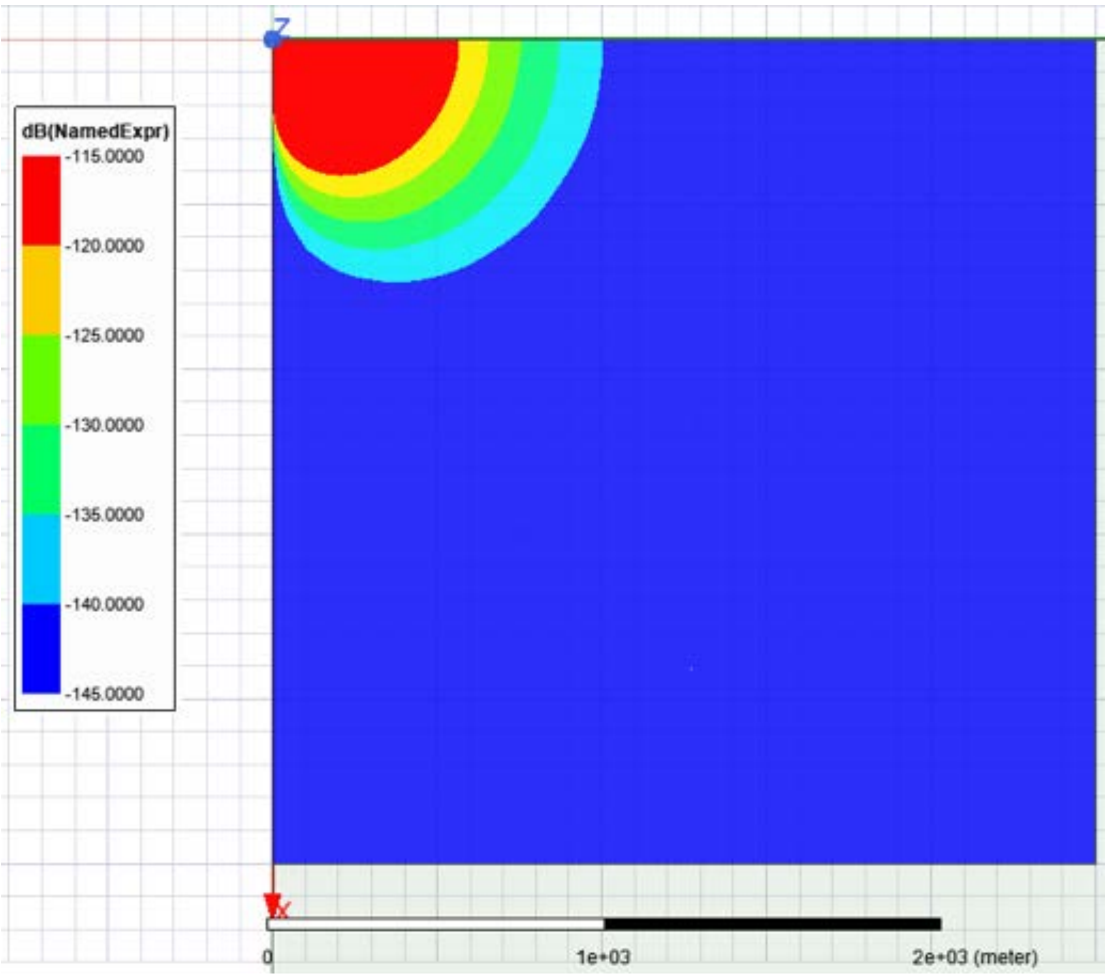

Figure 173 :Simulation 1: 9kHz results

Simulation 2:

This time 1800W was chosen instead of 3600W

Frequency: 9 kHz
Electrodes separation ~10m
Injected power ~ **1800W.**
Distance scale 100m/div.

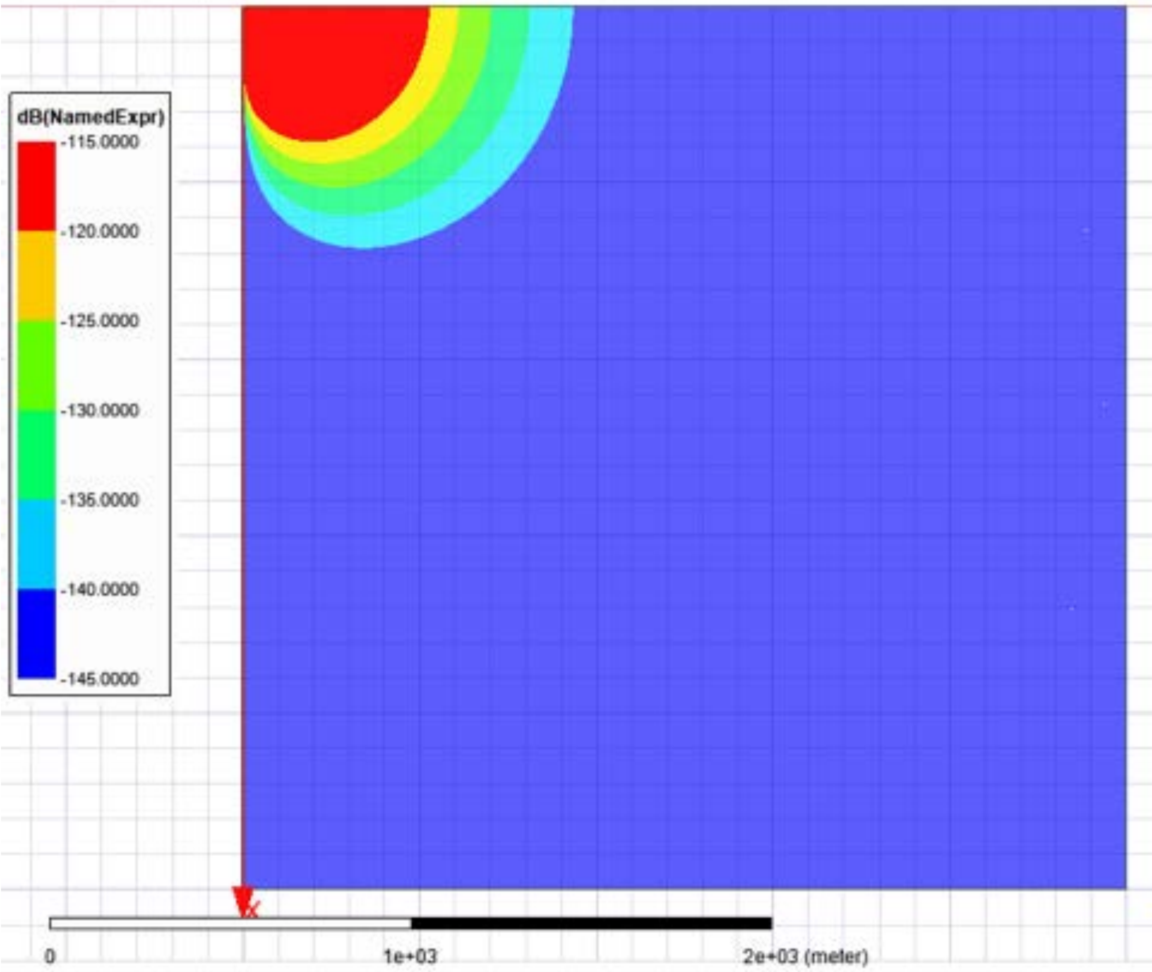

Figure 174: Simulation 2: 9kHz results

Simulation 3:

In the next simulation the TX electrodes were moved from 10 meters apart to 20 meters apart.

Frequency: 9 kHz
Electrodes separation **~20m**
Injected power ~ 3600W. Accepted power ~ 3560W.
Distance scale 100m/div.

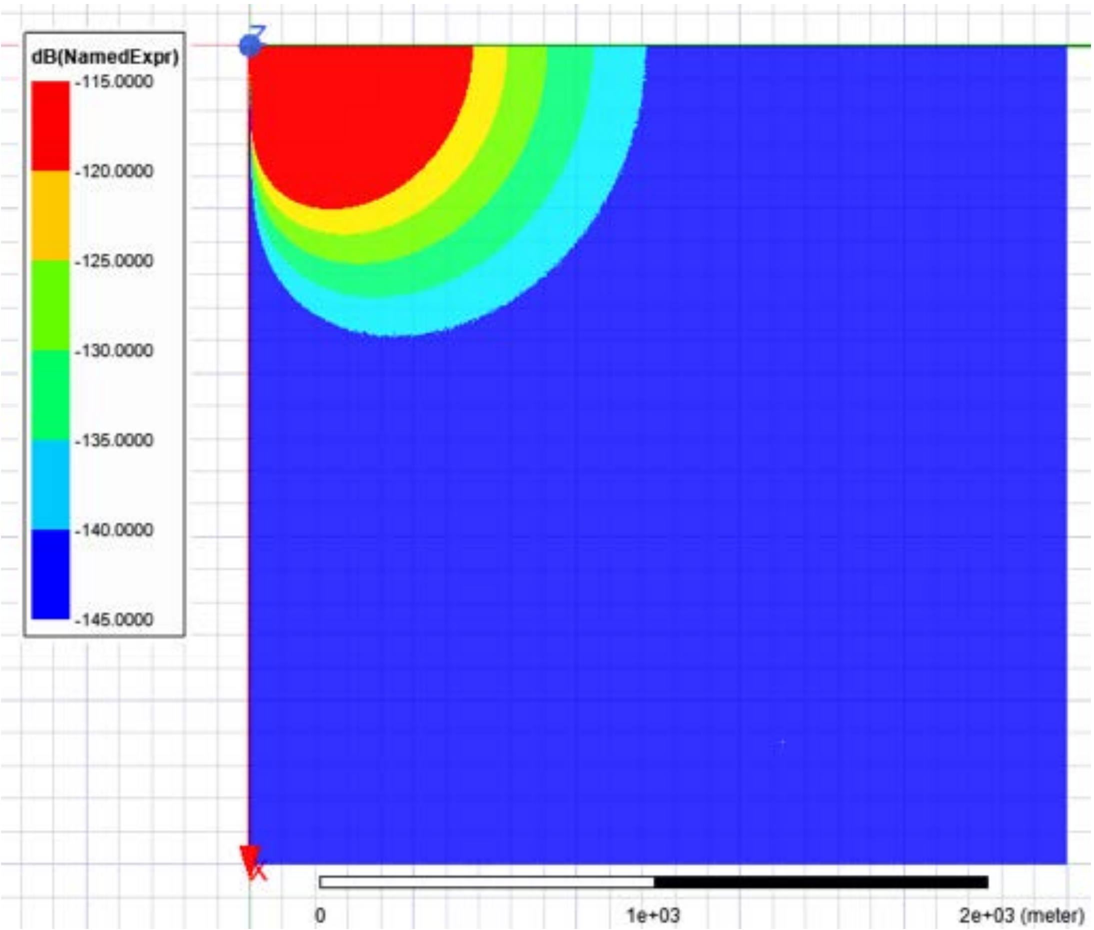

Figure 175: Simulation 3: 9kHz results

Simulation 4:

This time 1800W was chosen instead of 3600W

Frequency: 9 kHz
Electrodes separation ~20m
Injected power **~ 1800W**.
Distance scale 100m/div.

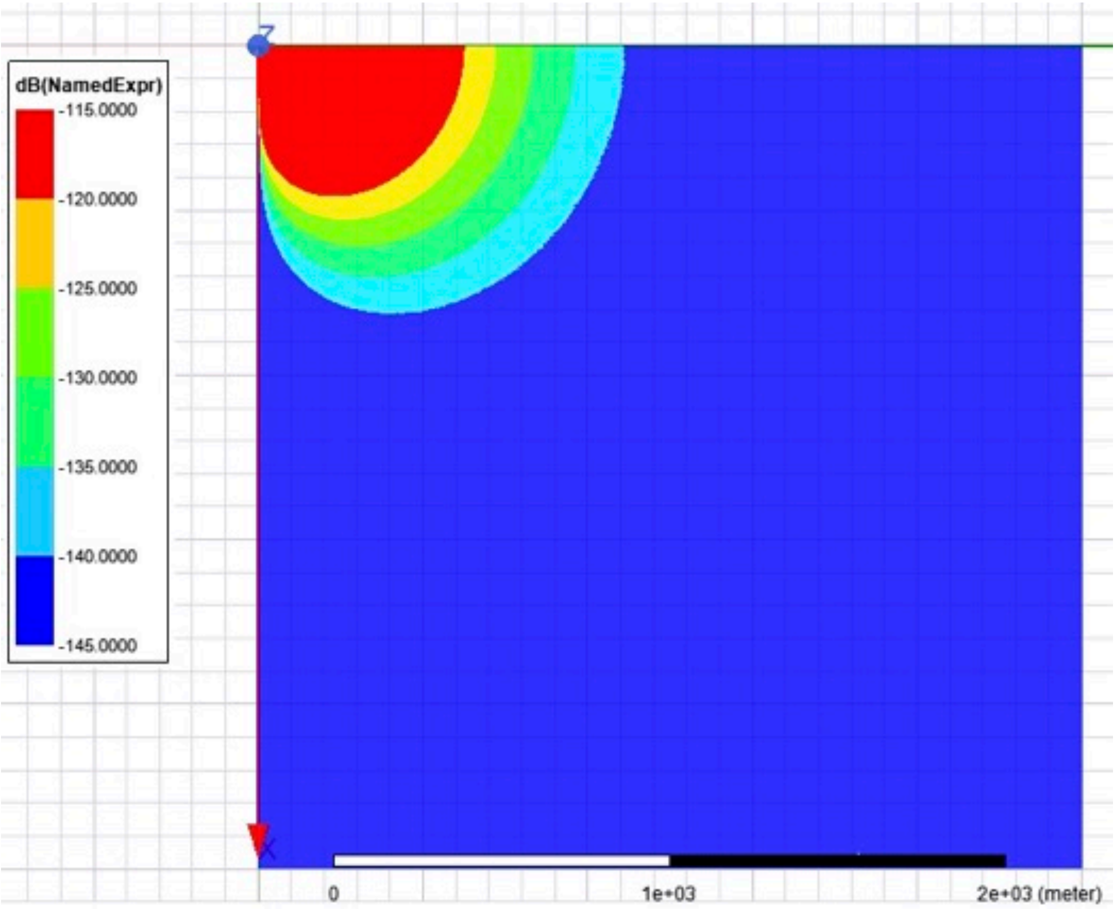

Figure 176: Simulation 4: 9kHz results

Simulation 5:

The next simulation the TX probes were increased to 50 meters apart

Frequency: 9 kHz
Electrodes separation **~50m**
Injected power ~ 3600W. Accepted power ~ 3560W.
Distance scale 100m/div.

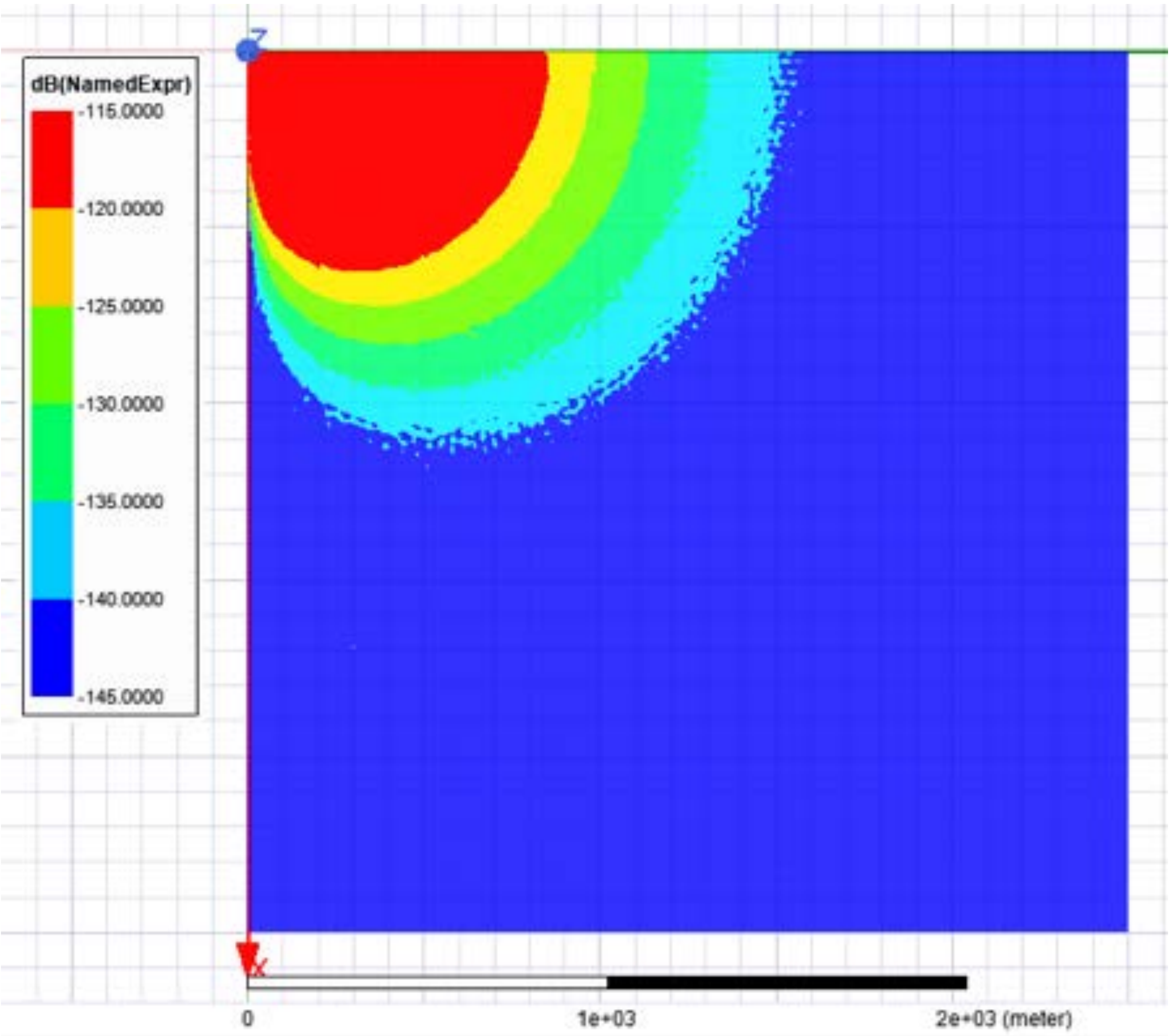

Figure 177: Simulation 5: 9kHz results

Simulation 6:

The next simulation the Watts were reduced to 1800W

Frequency: 9 kHz
Electrodes separation ~50m
Injected power ~ **1800W**.
Distance scale 100m/div.

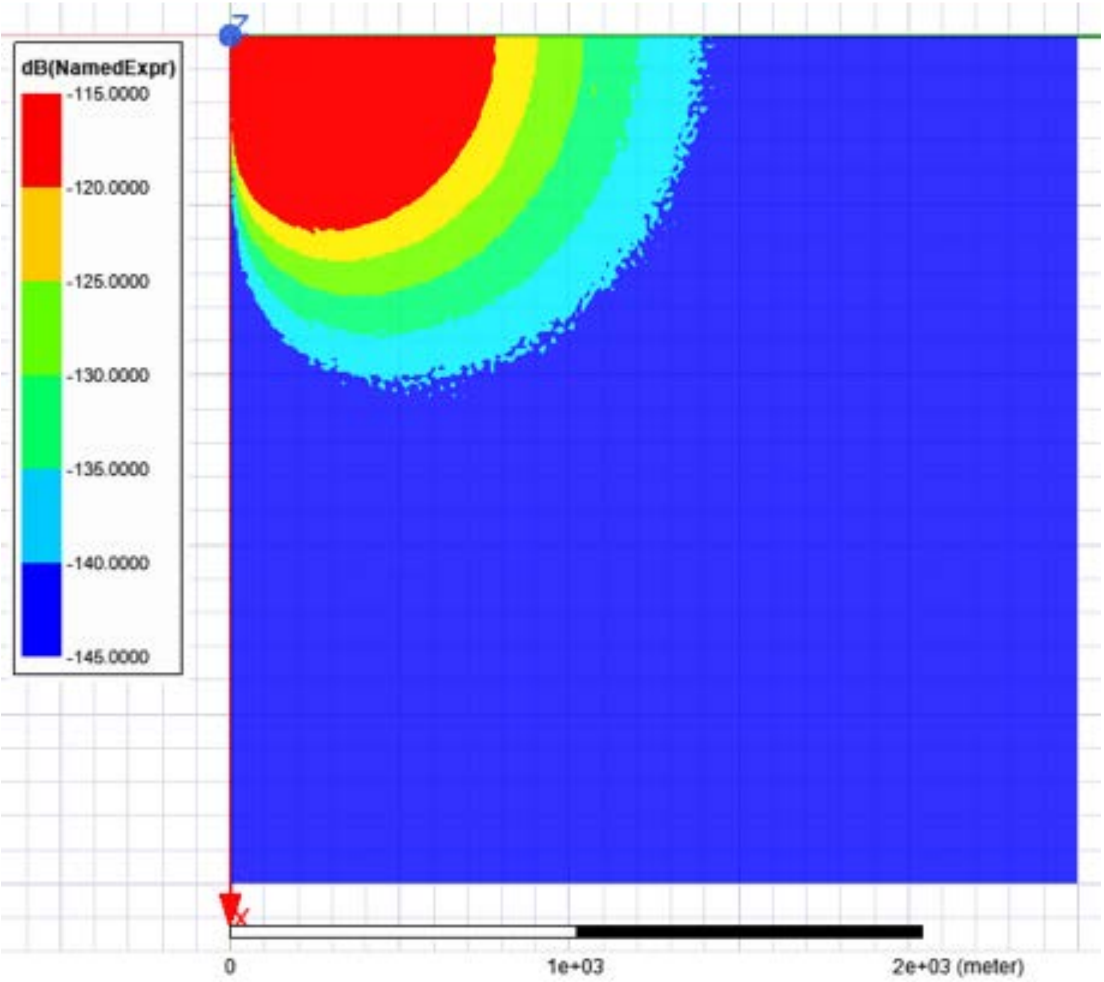

Figure 178: Simulation 6: 9kHz results

Simulation 7:

The next simulation the TX probes were increased to 100 meters apart

Frequency: 9 kHz
Electrodes separation **~100m**
Injected power ~ 3600W. Accepted power ~ 3560W.
Distance scale 100m/div.

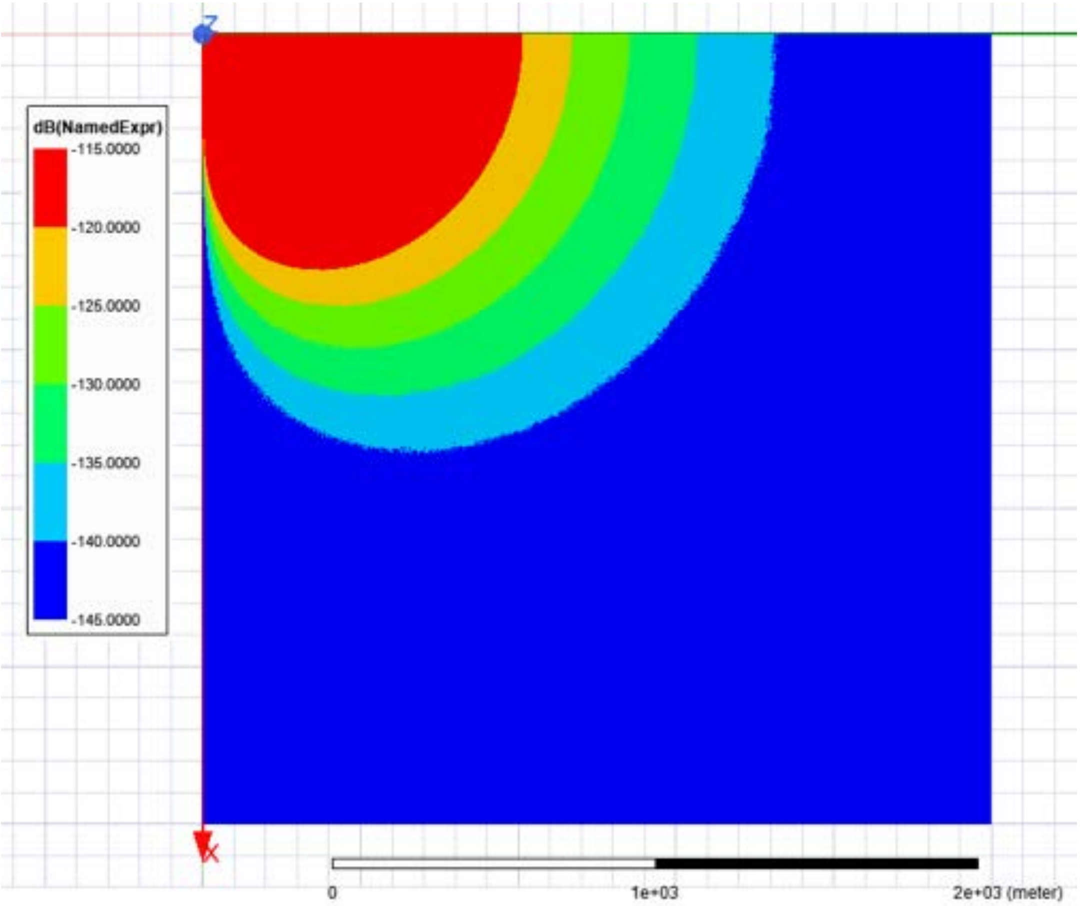

Figure 179: Simulation 7: 9kHz results

Simulation 8:

The next simulation the Watts were reduced to 1800W

Frequency: 9 kHz
Electrodes separation ~100m
Injected power **~ 1800W**.
Distance scale 100m/div.

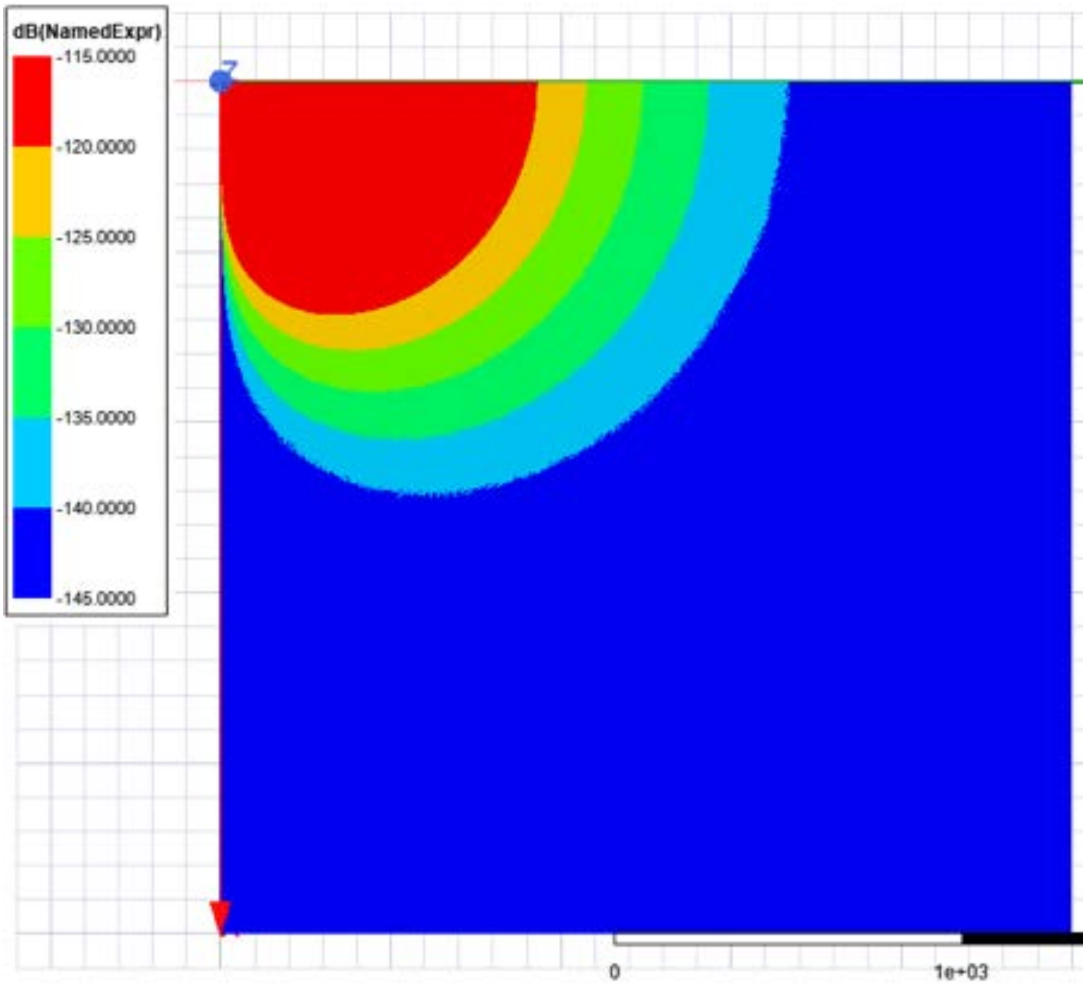

Figure 180: Simulation 8: 9kHz results

Simulation 9:

The next simulation the TX probes were increased to 1000 meters apart. <u>Notice distance scale increase to 200m/div.</u>

Frequency: 9 kHz
Electrodes separation **~1000m**
Injected power ~ 3600W. Accepted power ~ 3560W.
Distance scale **200m/div.**

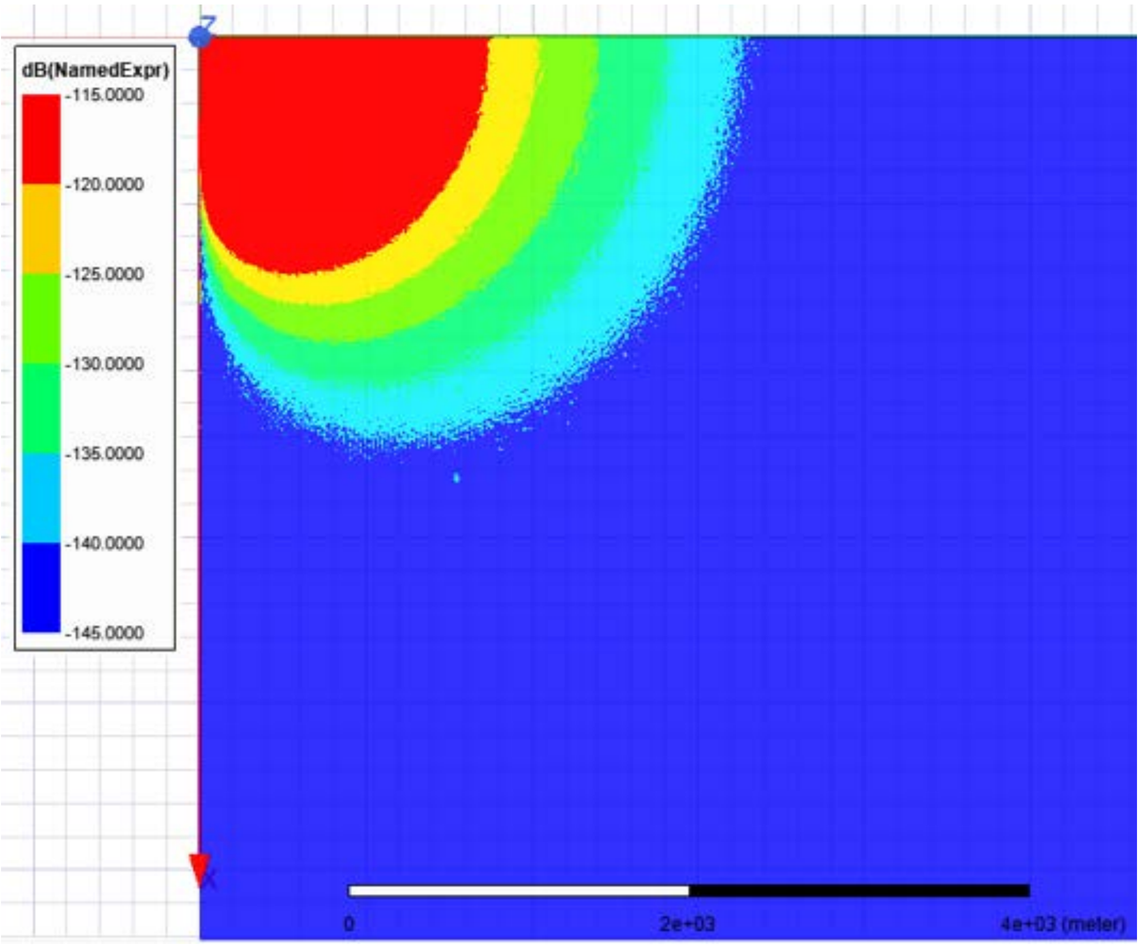

Figure 181: Simulation 9: 9kHz results

Simulation 10:

The next simulation the Watts were reduced to 1800W. Notice distance scale increase to 200m div.

Frequency: 9 kHz
Electrodes separation ~**1000m**
Injected power ~ **1800W**.
Distance scale **200m/div.**

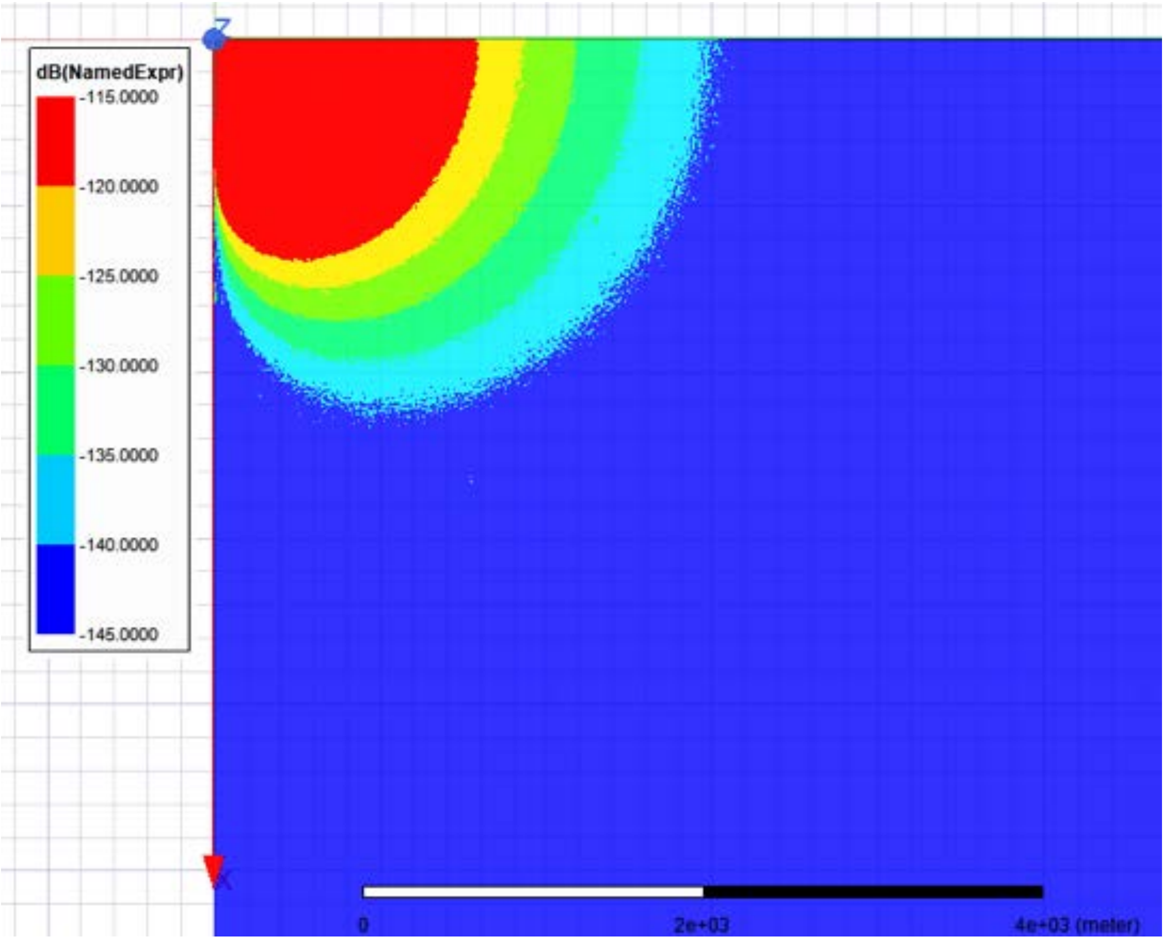

Figure 182: Simulation 10: 9kHz results

APPENDIX C – 73 kHz Simulations

73 kHz Frequency Simulations

Normal magnetic field amplitude (dBA/m) distribution over earth surface. The Green zone is the ideal DB receive distance.

Simulation 1:

Frequency: 73 kHz
Electrodes separation ~10m
Injected power ~ 3600W. Accepted power ~ 3560W.
Distance scale 100m/div.

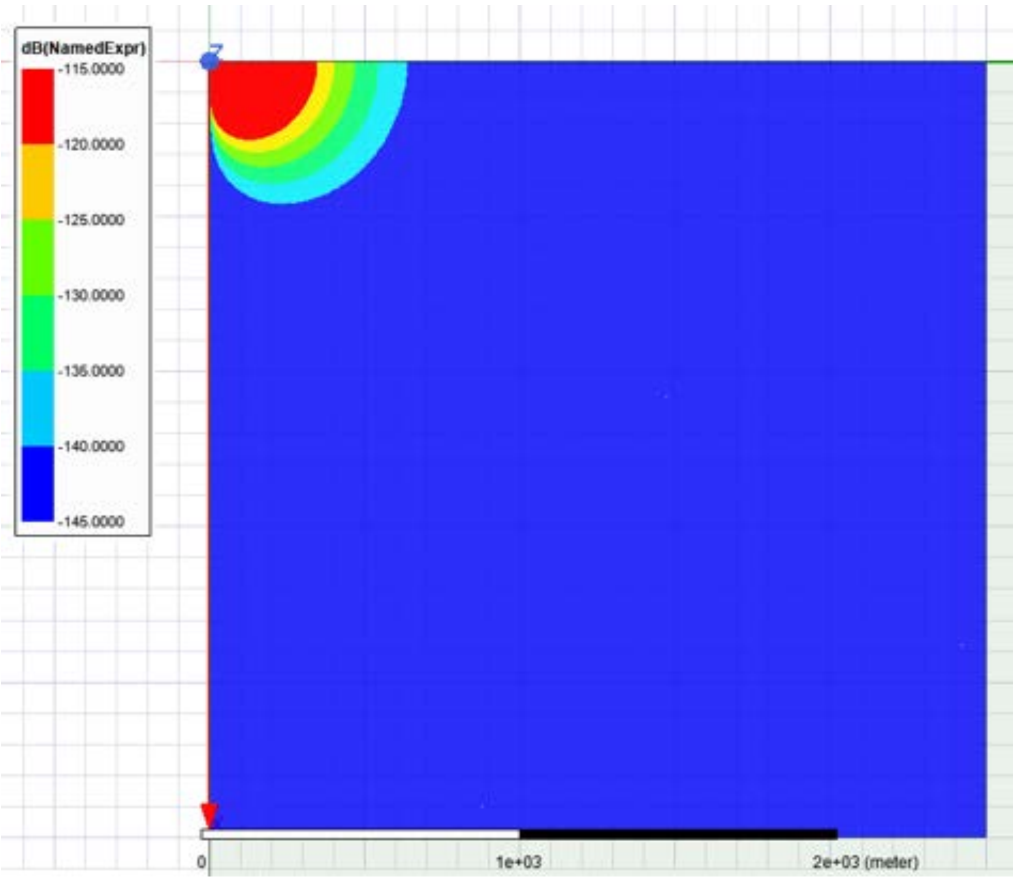

Figure 183: Simulation 1: 73kHz results

Simulation 2:

This time 1800W was chosen instead of 3600W

Frequency: 73 kHz
Electrodes separation ~10m
Injected power ~ **1800W.**
Distance scale 100m/div.

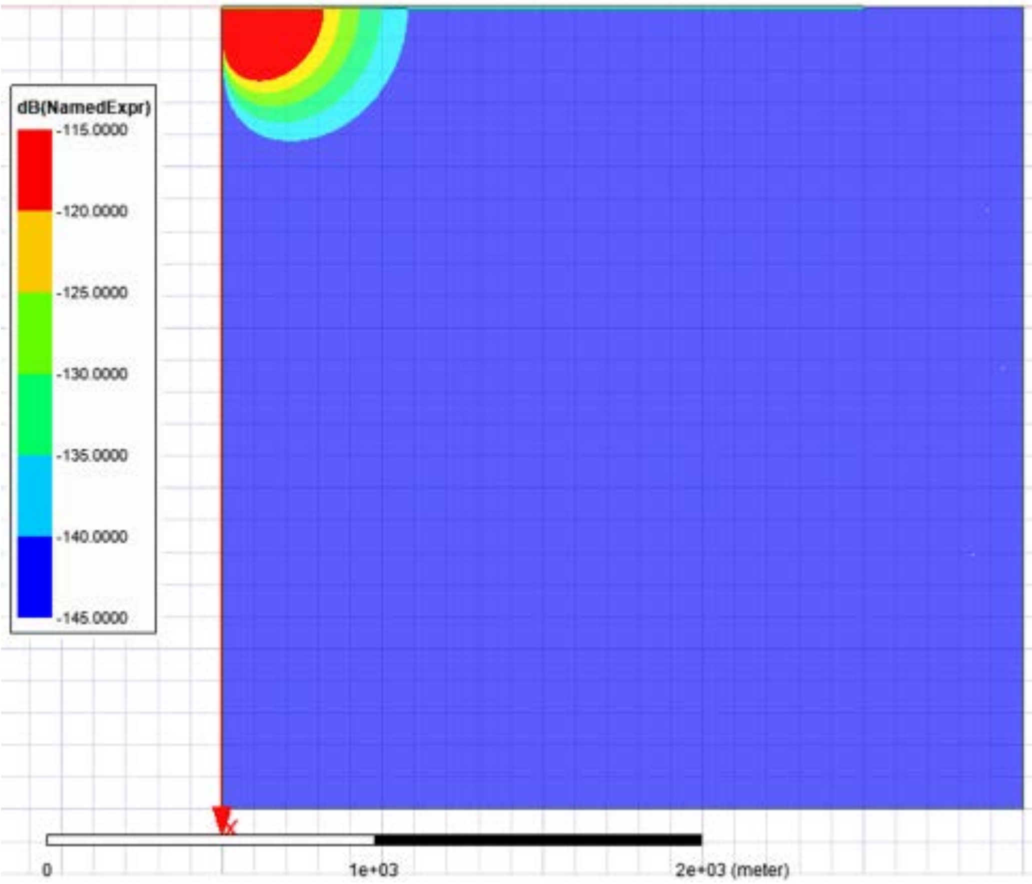

Figure 184: Simulation 2: 73kHz results

Simulation 3:

In the next simulation the TX electrodes were moved from 10 meters apart to 20 meters apart.

Frequency: 73 kHz
Electrodes separation **~20m**
Injected power ~ 3600W. Accepted power ~ 3560W.
Distance scale 100m/div.

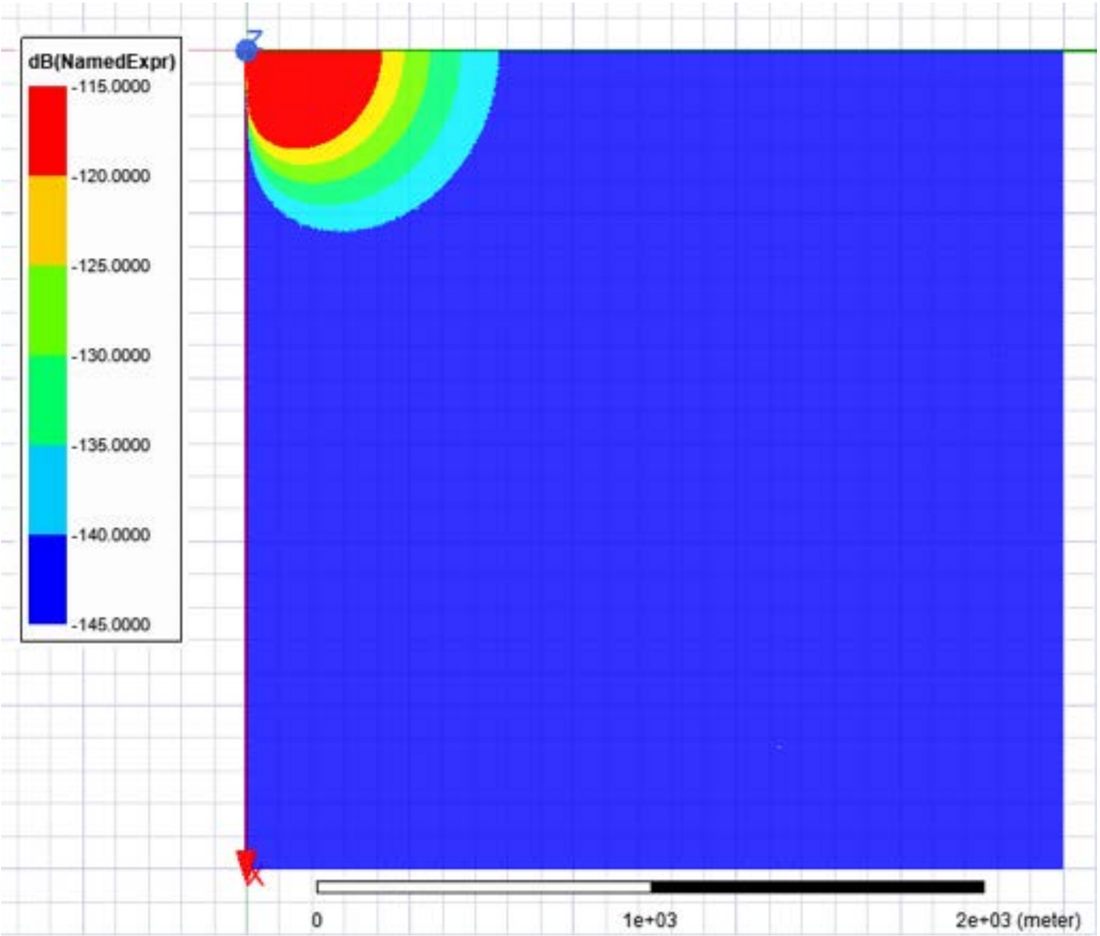

Figure 185: Simulation 3: 73kHz Results

Simulation 4:

This time 1800W was chosen instead of 3600W

Frequency: 73 kHz
Electrodes separation ~20m
Injected power ~ **1800W**.
Distance scale 100m/div.

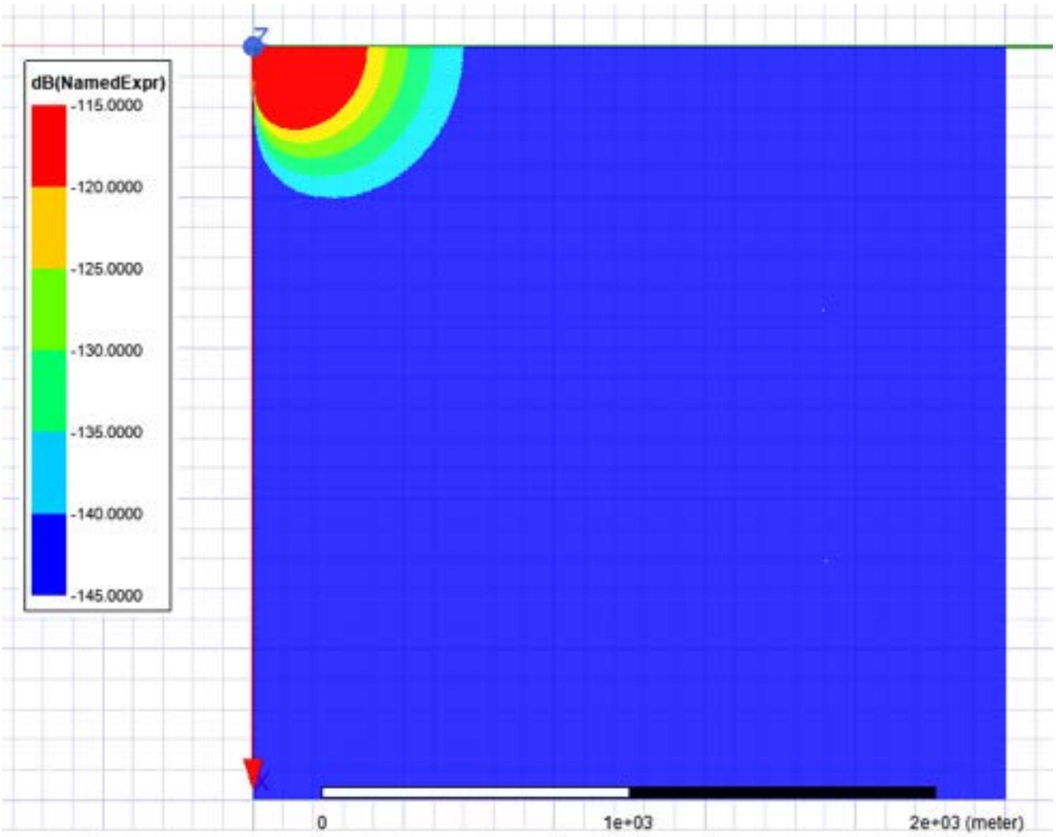

Figure 186: Simulation 4: 73kHz results

Simulation 5:

The next simulation the TX probes were increased to 50 meters apart

Frequency: 73 kHz
Electrodes separation **~50m**
Injected power ~ 3600W. Accepted power ~ 3560W.
Distance scale 100m/div.

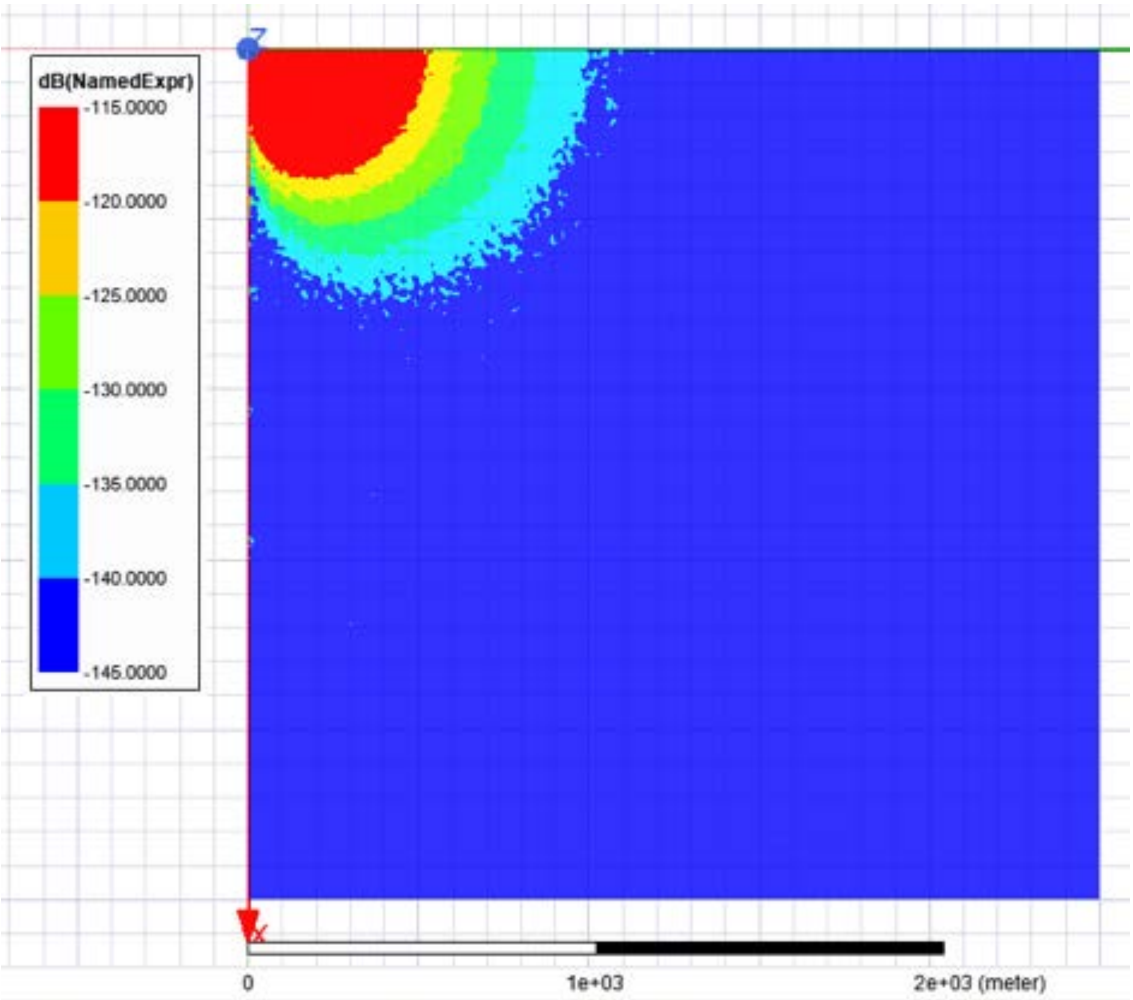

Figure 187: Simulation 5: 73kHz results

Simulation 6:

The next simulation the Watts were reduced to 1800W

Frequency: 73 kHz
Electrodes separation ~50m
Injected power ~ **1800W**.
Distance scale 100m/div.

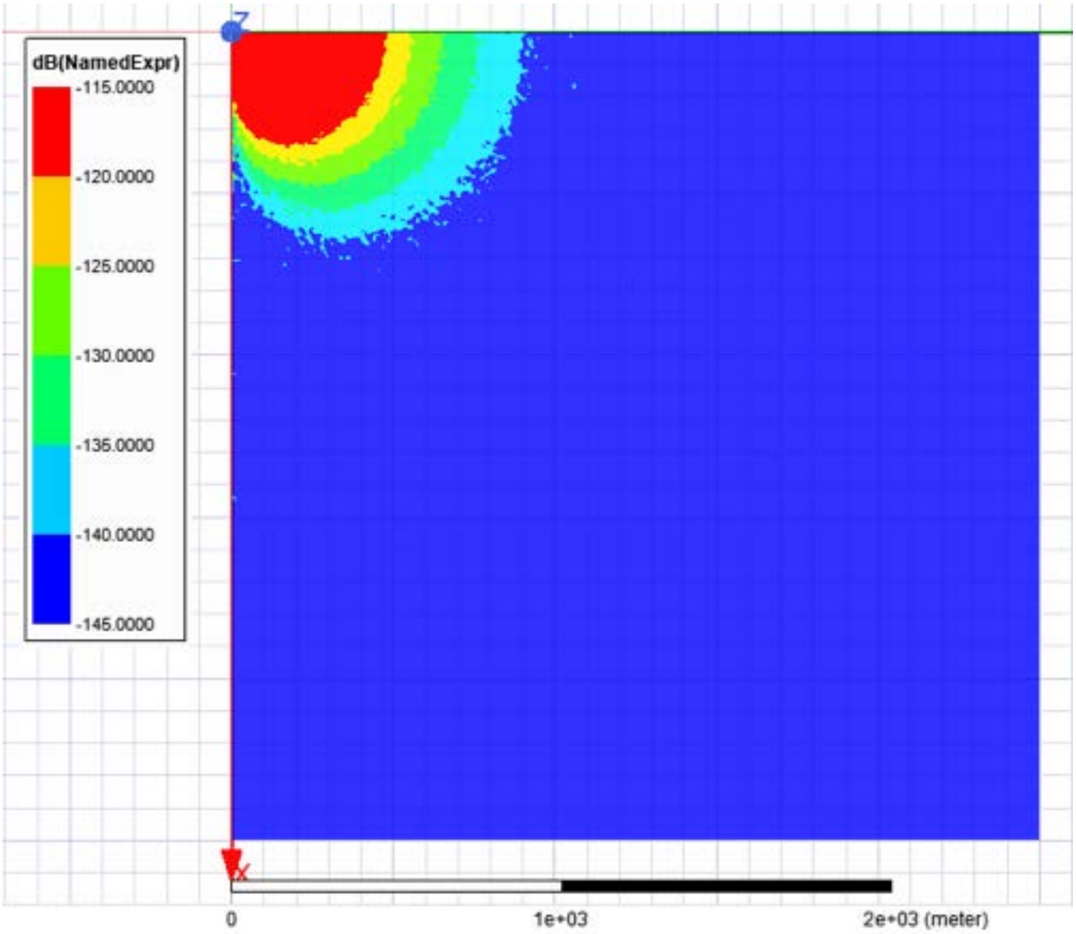

Figure 188: Simulation 6: 73kHz results

Simulation 7:

The next simulation the TX probes were increased to 100 meters apart

Frequency: 73 kHz
Electrodes separation **~100m**
Injected power ~ 3600W. Accepted power ~ 3560W.
Distance scale 100m/div.

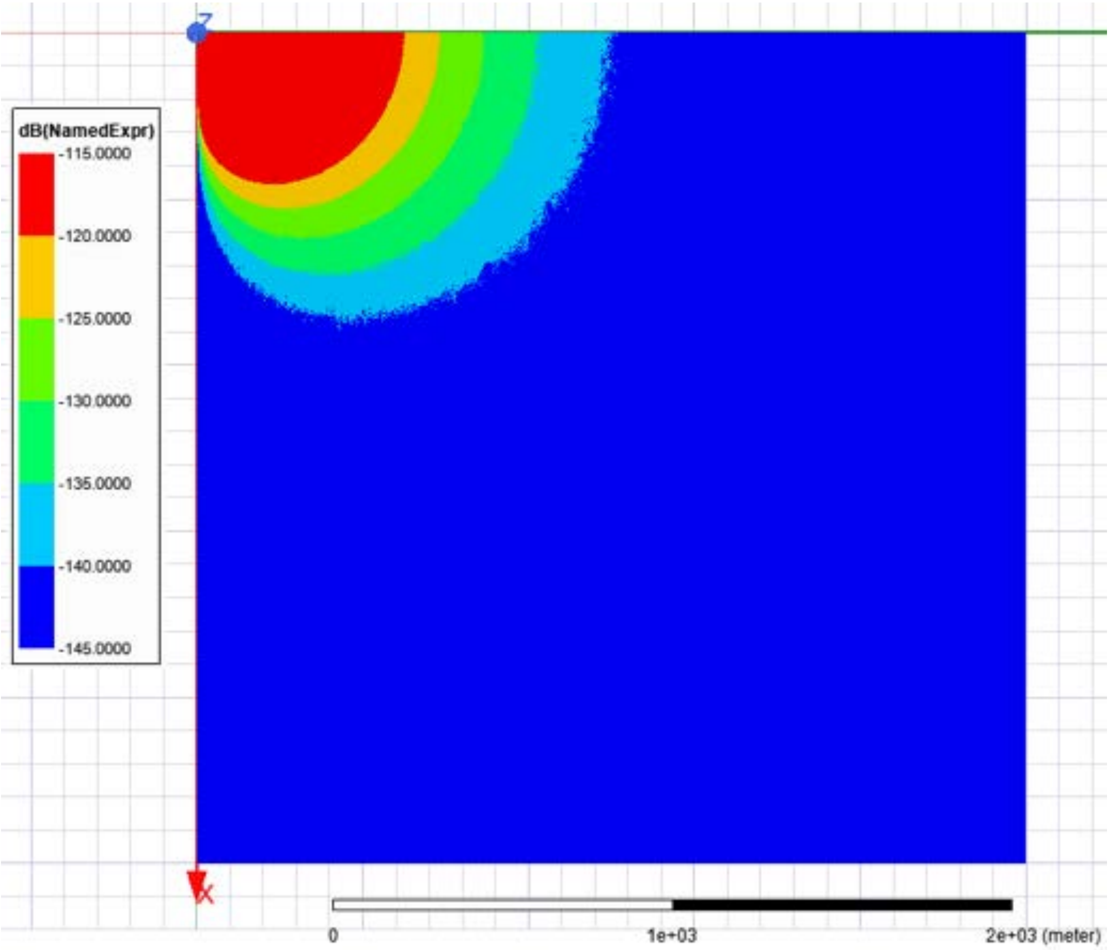

Figure 189: Simulation 7: 73kHz results

Simulation 8:

The next simulation the Watts were reduced to 1800W

Frequency: 73 kHz
Electrodes separation ~100m
Injected power ~ **1800W**.
Distance scale 100m/div.

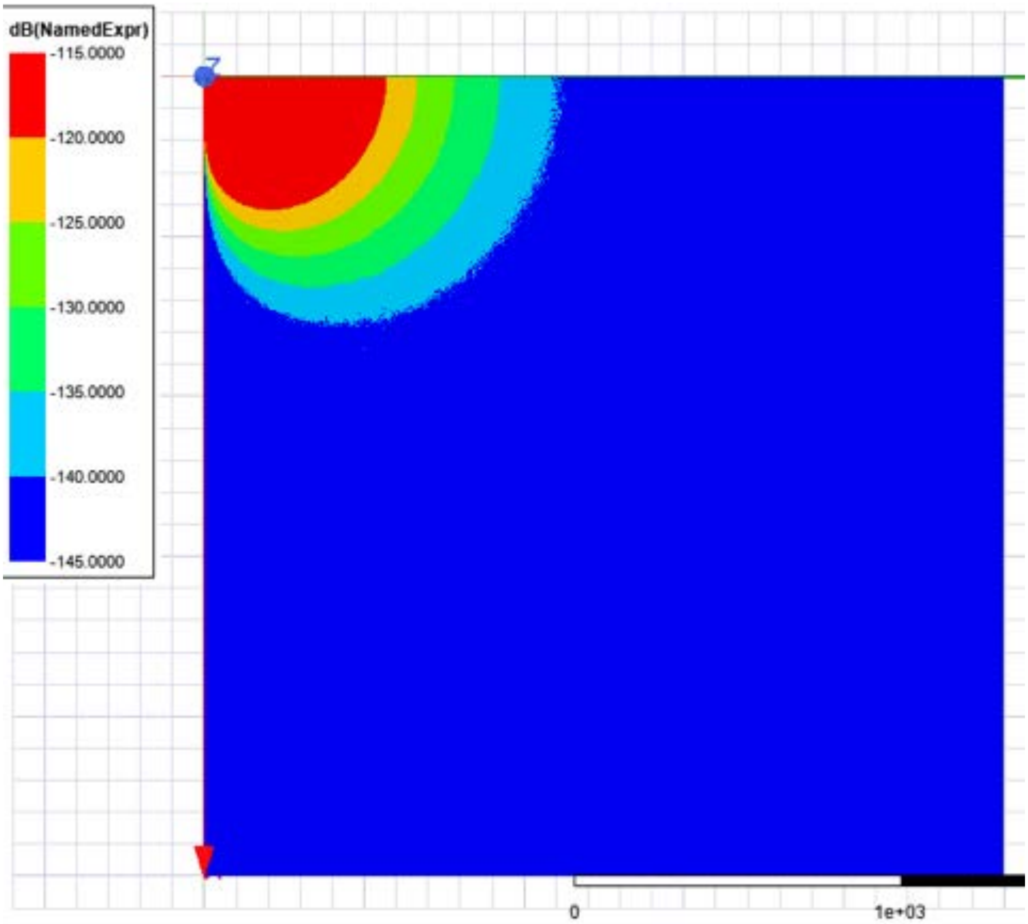

Figure 190: Simulation 8: 73kHz results

Simulation 9:

The next simulation the TX probes were increased to 1000 meters apart. <u>Notice distance scale increase to 200m/div.</u>

Frequency: 73 kHz
Electrodes separation **~1000m**
Injected power ~ 3600W. Accepted power ~ 3560W.
Distance scale **200m/div.**

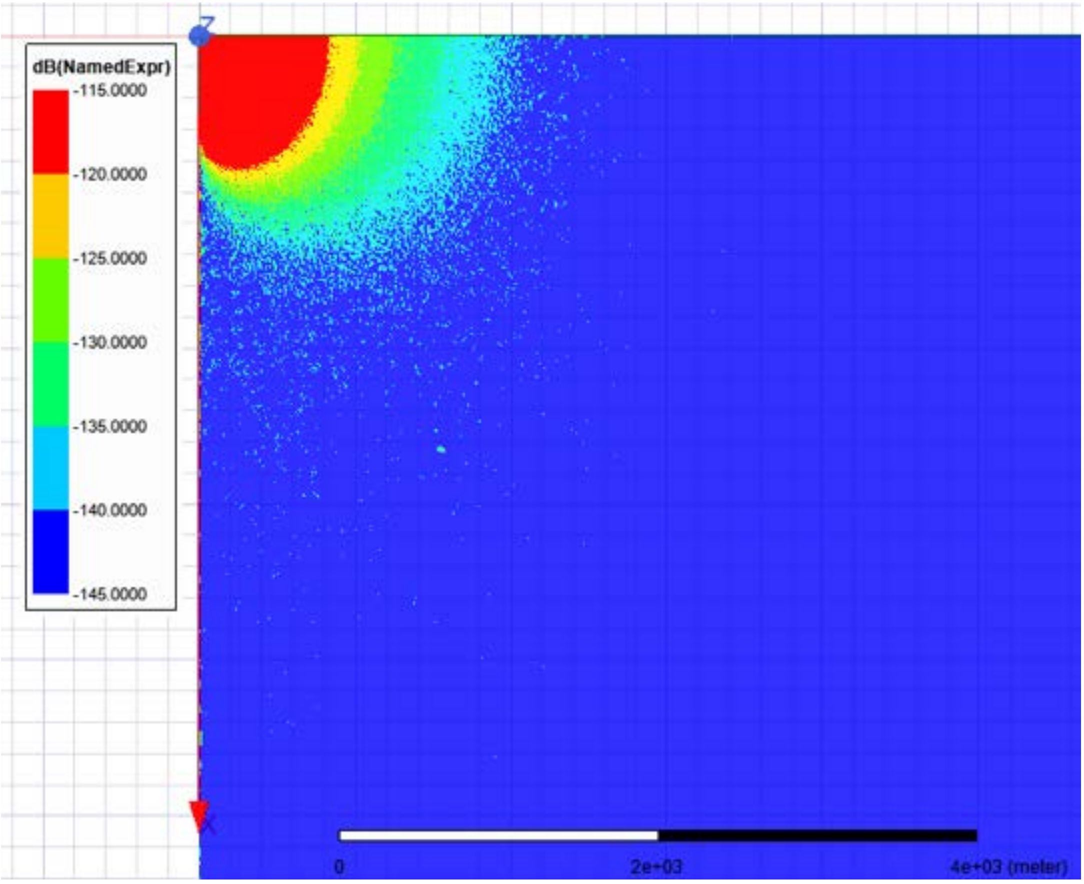

Figure 191: Simulation 9: 73kHz results

Simulation 10:

The next simulation the Watts were reduced to 1800W. <u>Notice distance scale increase to 200m div.</u>

Frequency: 73 kHz
Electrodes separation ~**1000m**
Injected power ~ **1800W**.
Distance scale **200m/div.**

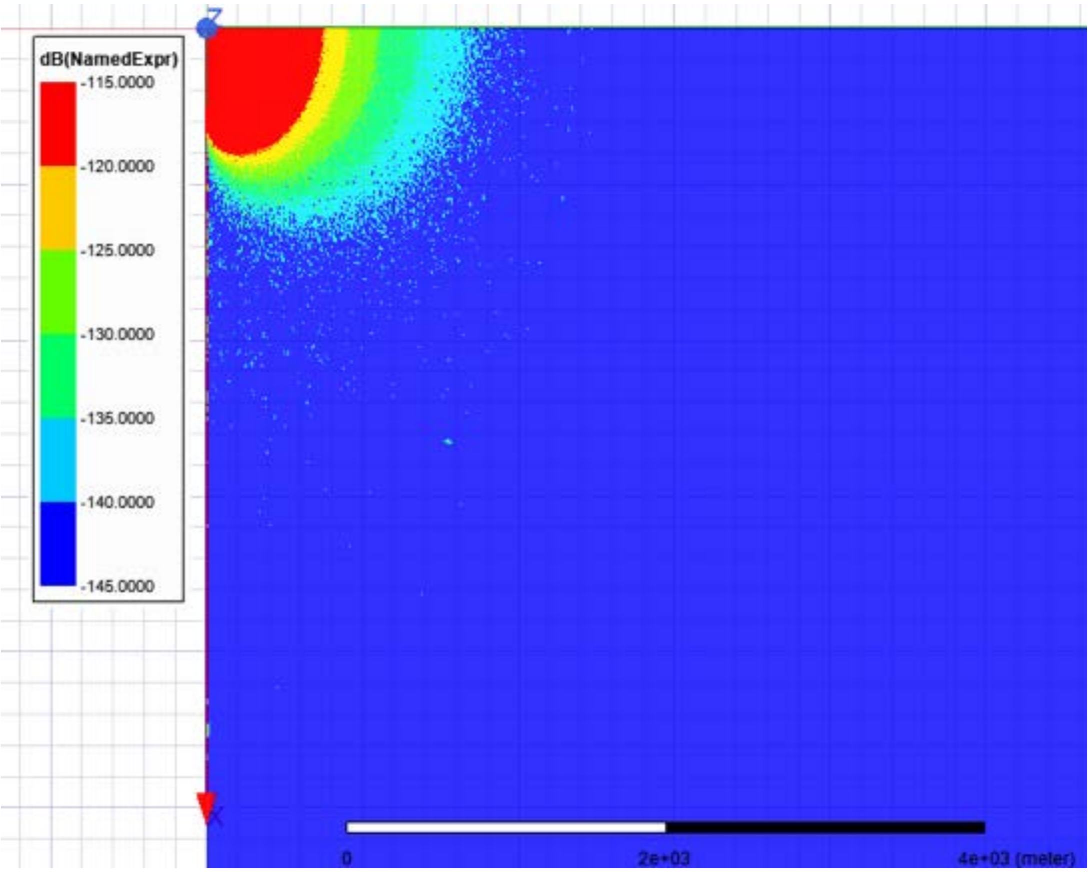

Figure 192: Simulation 10: 73kHz results

APPENDIX D – 2 kHz Simulations

2 kHz Frequency Magnetic Field Simulations

Based on what we have learnt from the simulation, EM signal and speed we can now narrow down the best frequency for data transmission whilst avoiding noise to disrupt that signal.

The simulations below are based on magnetic field distribution is represented for parameters sets Power, (20, 1800, 3600W) Tx Probe Distance (10, 20, 50 meters), Frequency (2 kHz) and Magnetic field (Normal, Tangential)

Simulation 1:

Frequency: 2 kHz
Magnetic Field: **Normal**
Electrodes separation ~**50m**
Injected power ~ **20W**
Distance scale 100m/div.

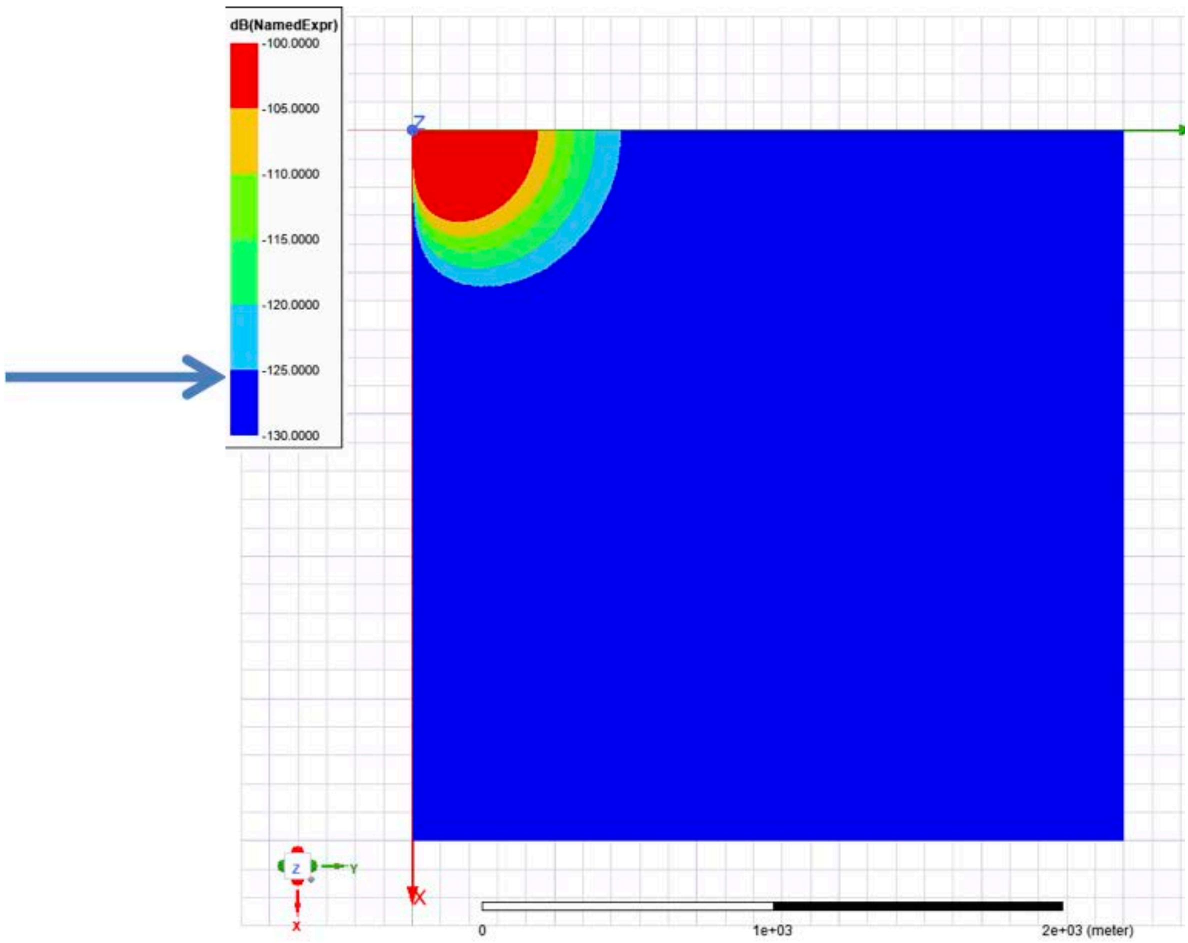

Figure 193: Simulation 1: 2kHz Normal 20W at 50m results

Simulation 2:

Frequency: 2 kHz
Magnetic Field: **Tangential**
Electrodes separation **~50m**
Injected power ~ **20W**
Distance scale 100m/div.

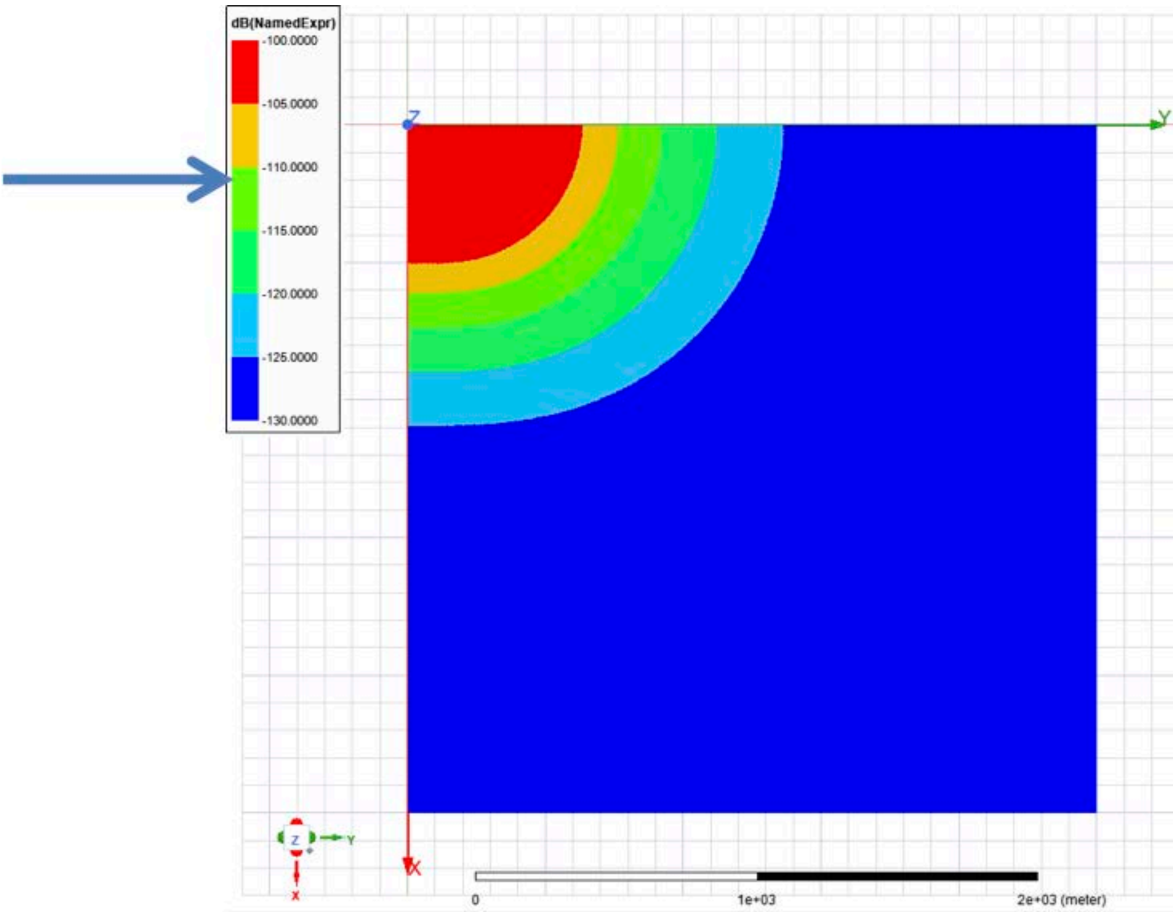

Figure 194: Simulation 2: 2kHz Tangential 20W at 50m results

Simulation 3:

Frequency: 2 kHz
Magnetic Field: **Normal**
Electrodes separation ~**20m**
Injected power ~ **20W**
Distance scale 100m/div.

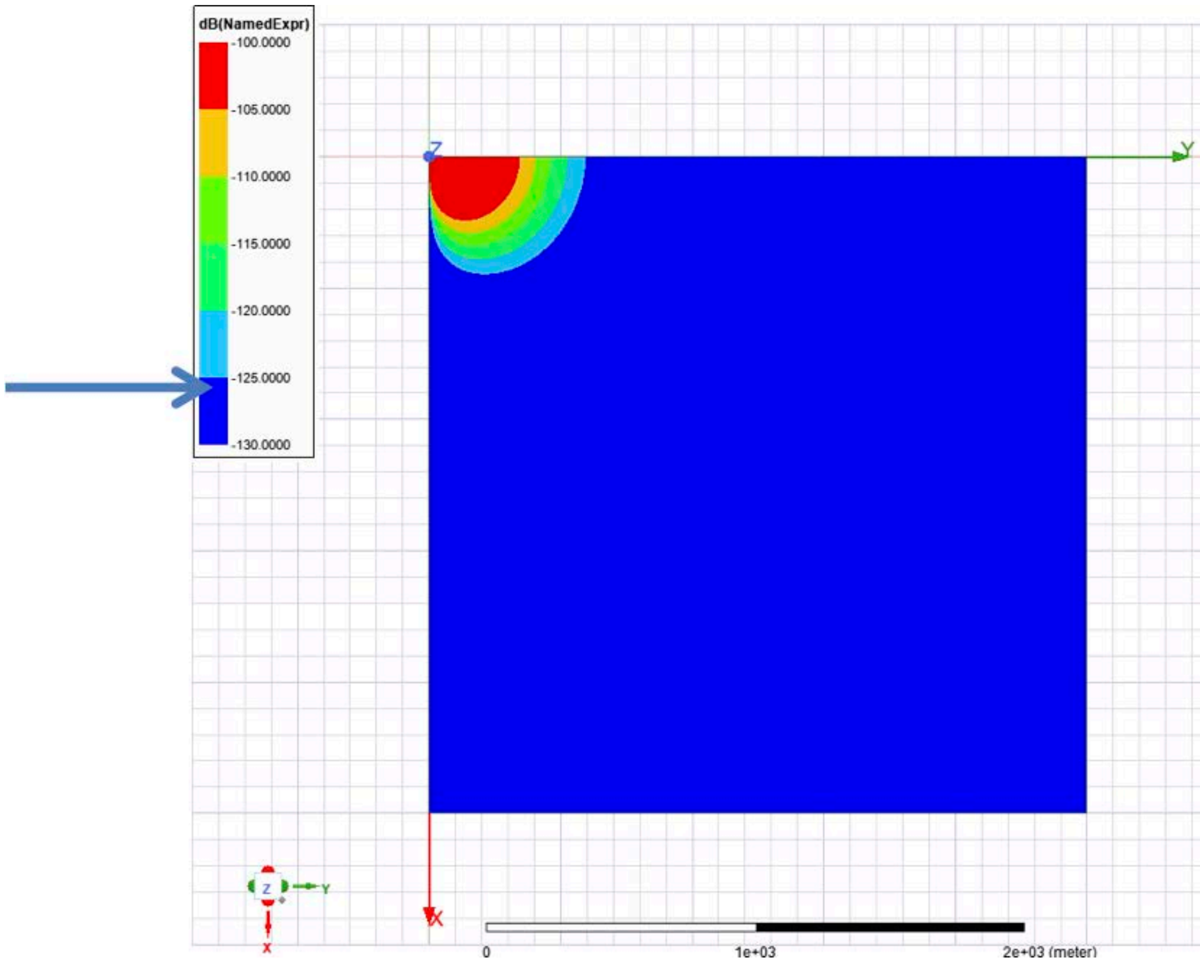

Figure 195: Simulation 3: 2kHz Normal 20W at 20m results

Simulation 4:

Frequency: 2 kHz
Magnetic Field: **Tangential**
Electrodes separation ~**20m**
Injected power ~ **20W**
Distance scale 100m/div.

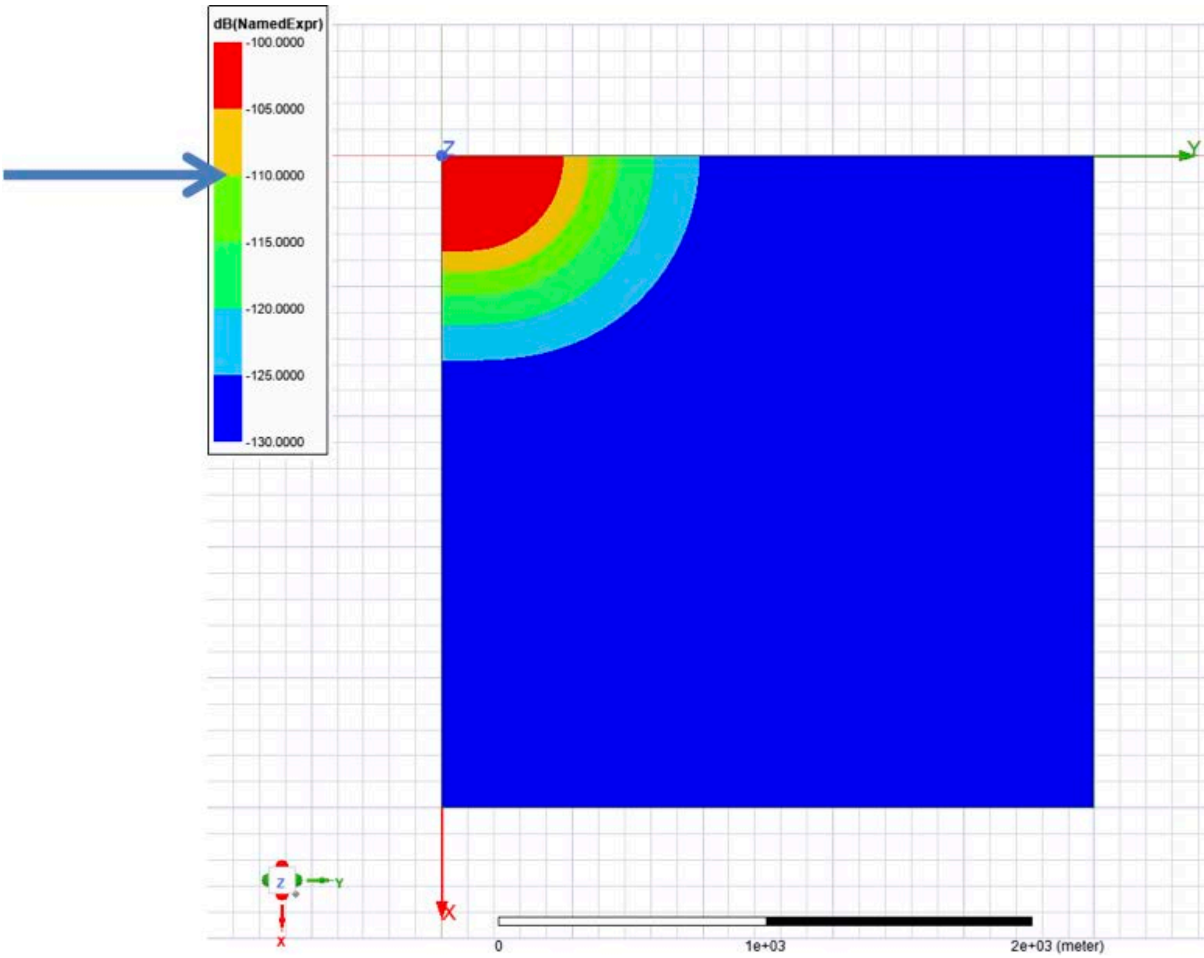

Figure 196: Simulation 4: 2kHz Tangential 20W at 20m results

Simulation 5:

Frequency: 2 kHz
Magnetic Field: **Normal**
Electrodes separation ~**10m**
Injected power ~ **20W**
Distance scale 100m/div.

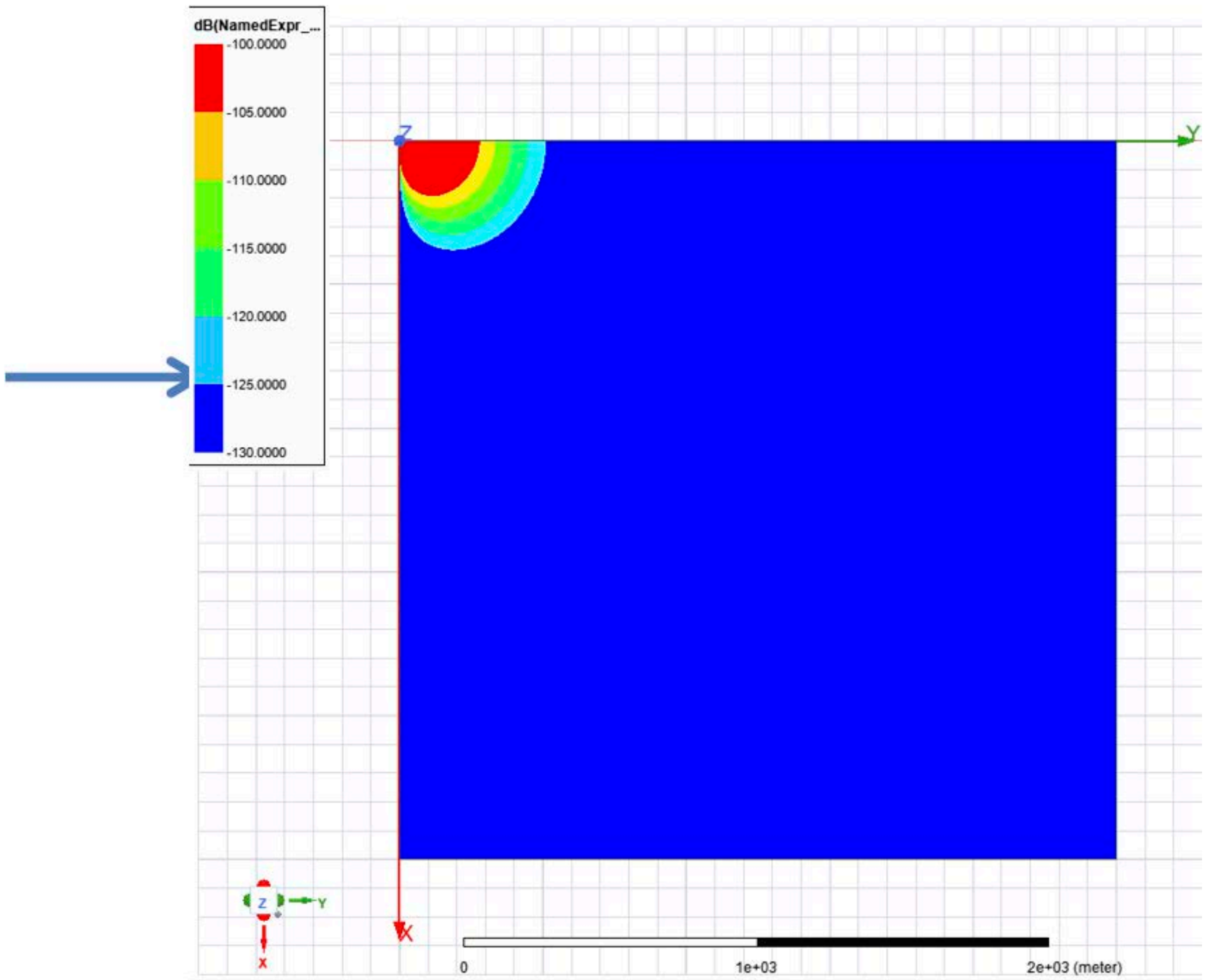

Figure 197: Simulation 5: 2kHz Normal 20W at 10m results

Simulation 6:

Frequency: 2 kHz
Magnetic Field: **Tangential**
Electrodes separation ~**10m**
Injected power ~ **20W**
Distance scale 100m/div.

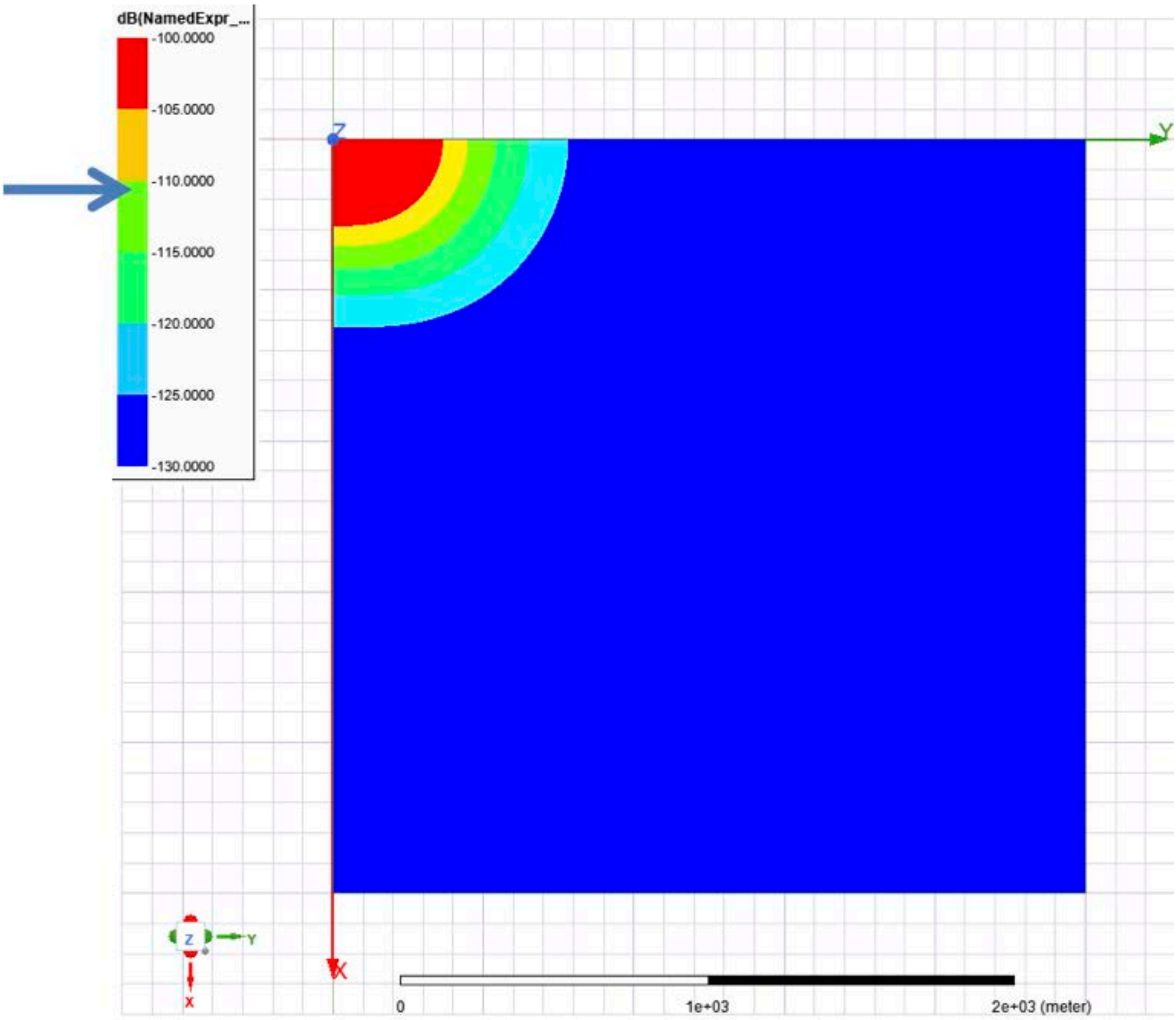

Figure 198: Simulation 6: 2kHz Tangential 20W at 10m results

Simulation 7:

Frequency: 2 kHz
Magnetic Field: **Normal**
Electrodes separation **~50m**
Injected power ~ **1800W**
Distance scale 100m/div.

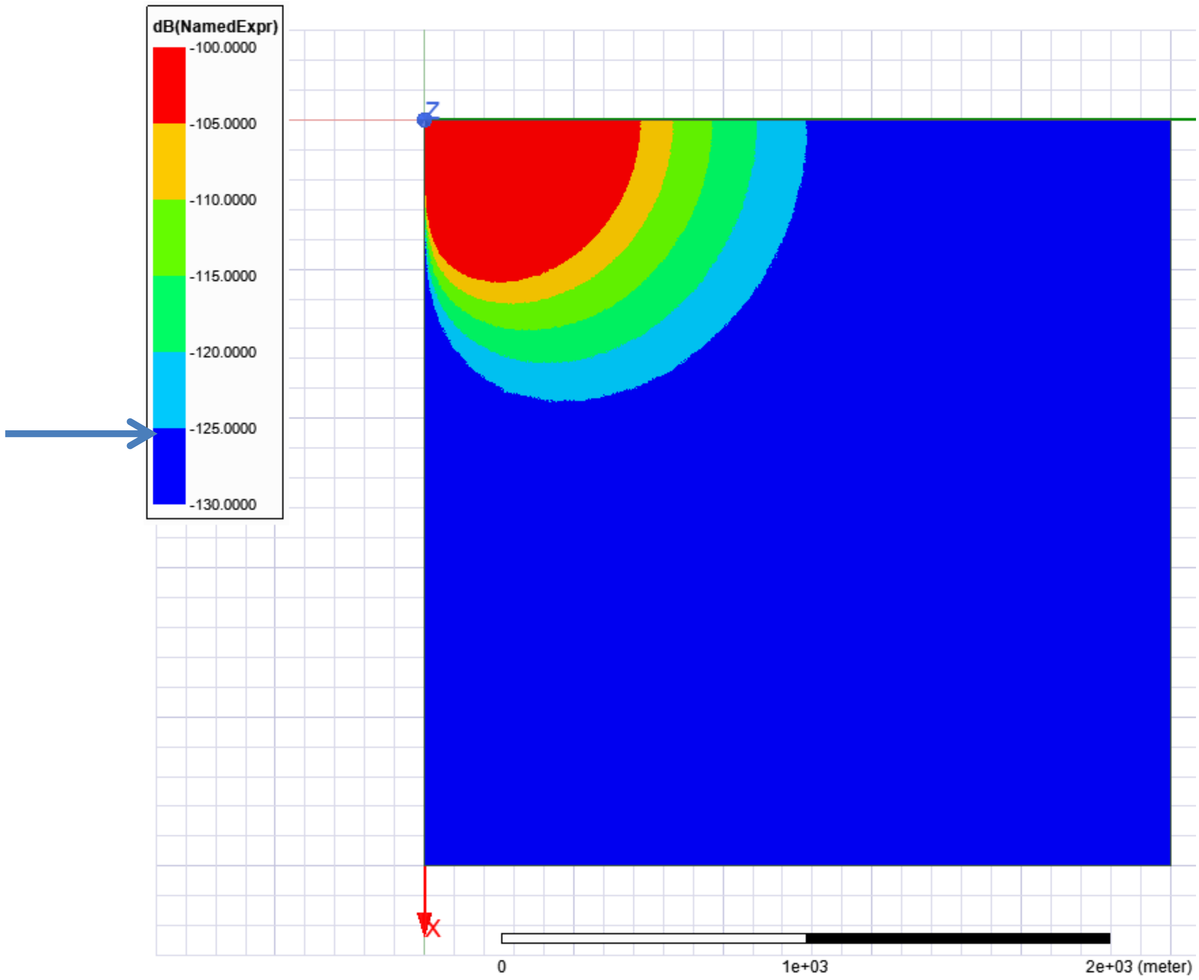

Figure 199: Simulation 7: 2kHz Normal 1800W at 50m results

Simulation 8:

Frequency: 2 kHz
Magnetic Field: **Tangential**
Electrodes separation **~50m**
Injected power ~ **1800W**
Distance scale 100m/div.

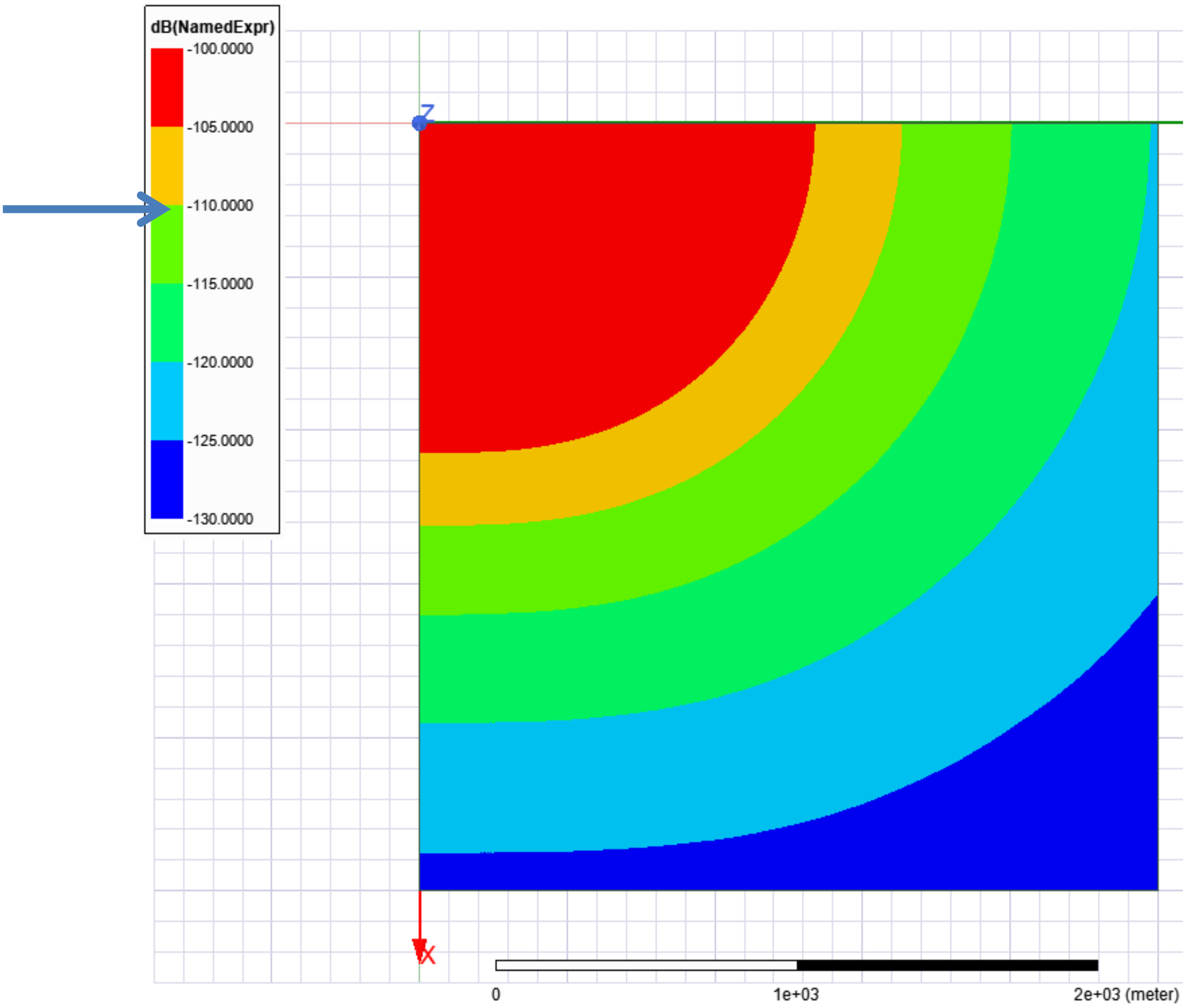

Figure 200: Simulation 8: 2 kHz Tangential 1800W at 50m results

Simulation 9:

Frequency: 2 kHz
Magnetic Field: **Normal**
Electrodes separation **~50m**
Injected power ~ **3600W**
Distance scale 100m/div.

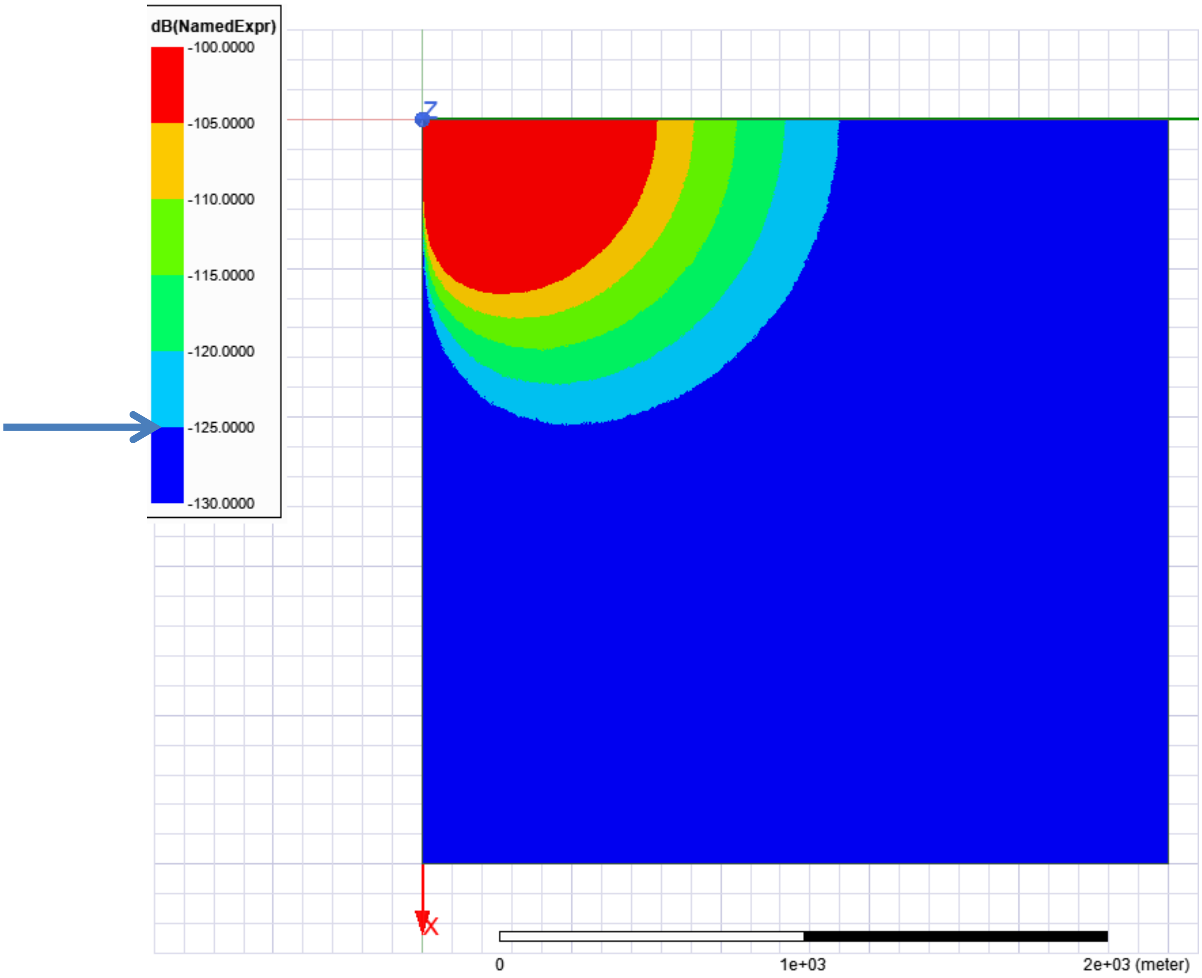

Figure 201: Simulation 9: 2kHz Normal 3600W at 50m results

Simulation 10:

Frequency: 2 kHz
Magnetic Field: **Tangential**
Electrodes separation ~**50m**
Injected power ~ **3600W**
Distance scale 100m/div.

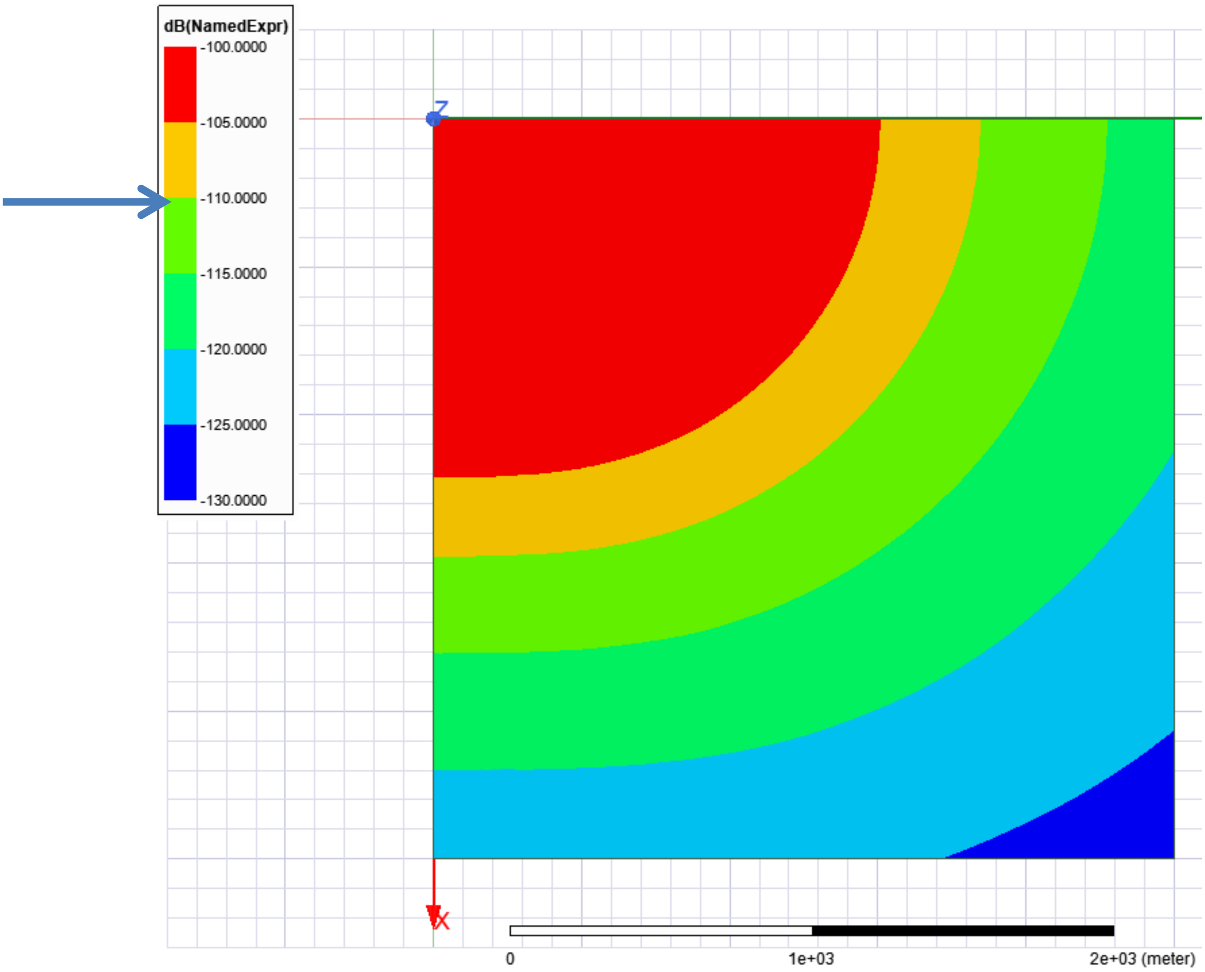

Figure 202: Simulation 10: 2kHz Tangential 3600W at 50m results

Simulation 11:

Frequency: 2 kHz
Magnetic Field: **Normal**
Electrodes separation ~**20m**
Injected power ~ **1800W**
Distance scale 100m/div.

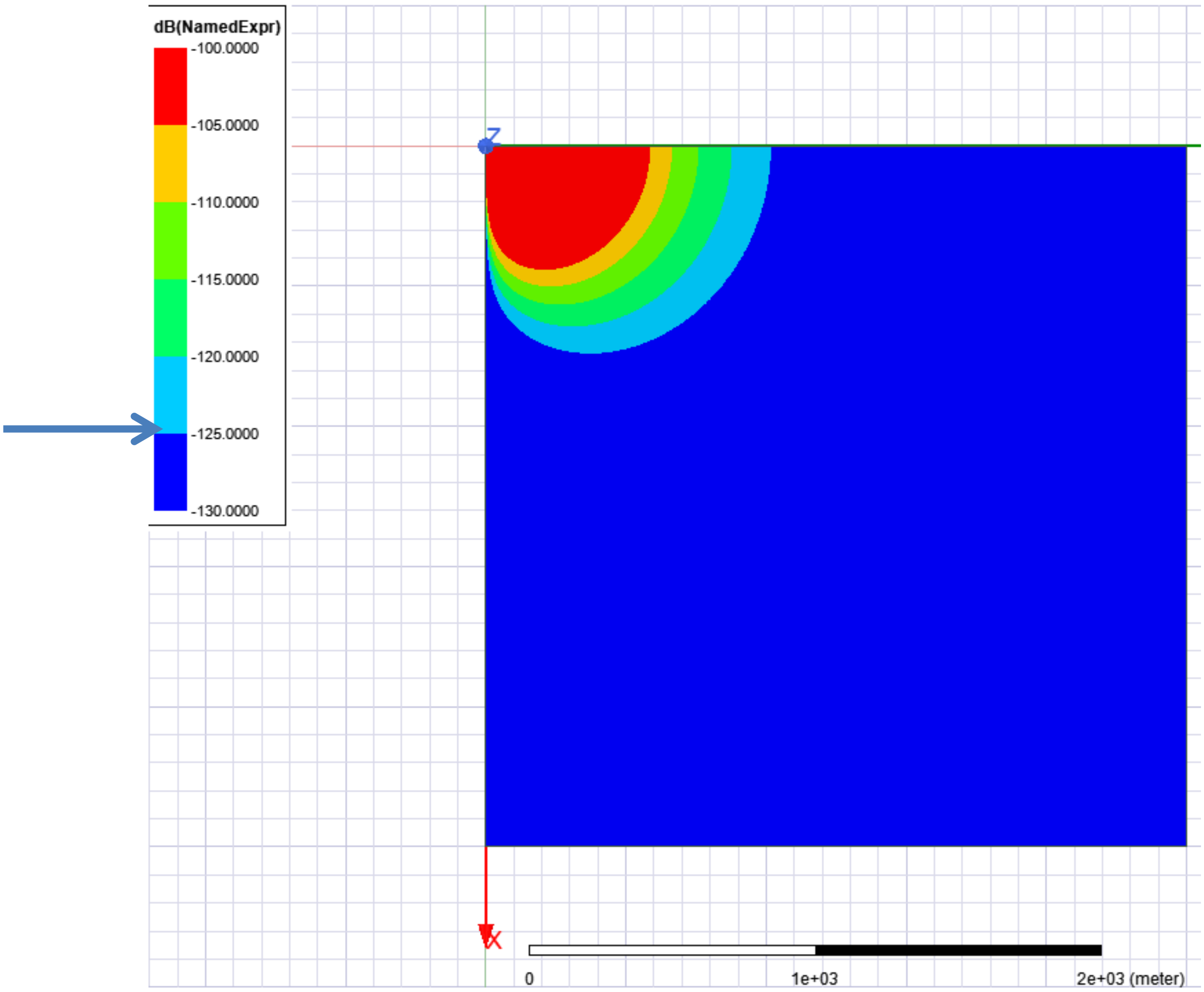

Figure 203: Simulation 11: 2kHz Normal 1800W at 20m results

Simulation 12:

Frequency: 2 kHz
Magnetic Field: **Tangential**
Electrodes separation ~**20m**
Injected power ~ **1800W**
Distance scale 100m/div.

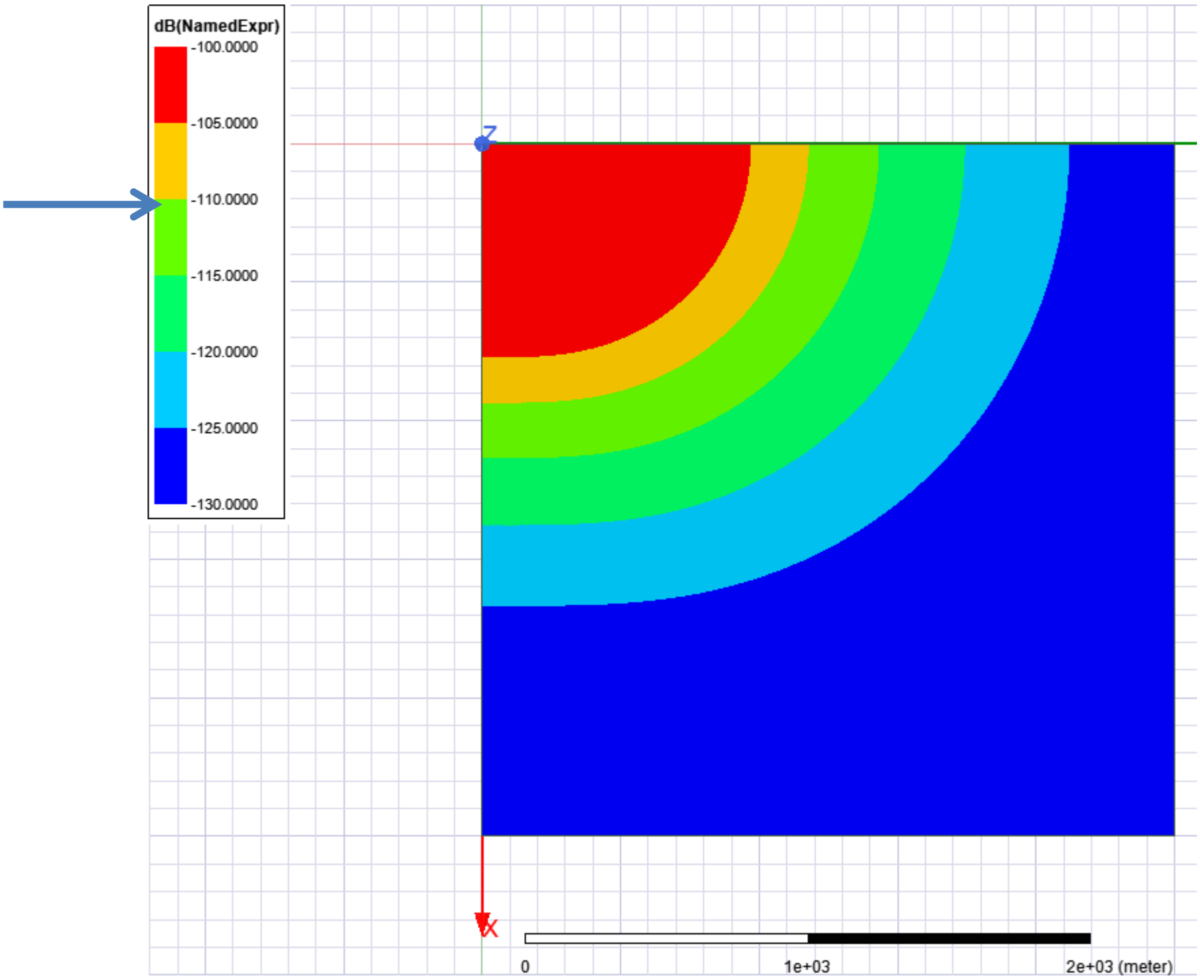

Figure 204: Simulation 12: 2kHz Tangential 1800W at 20m results

Simulation 13:

Frequency: 2 kHz
Magnetic Field: **Normal**
Electrodes separation **~20m**
Injected power ~ **3600W**
Distance scale 100m/div.

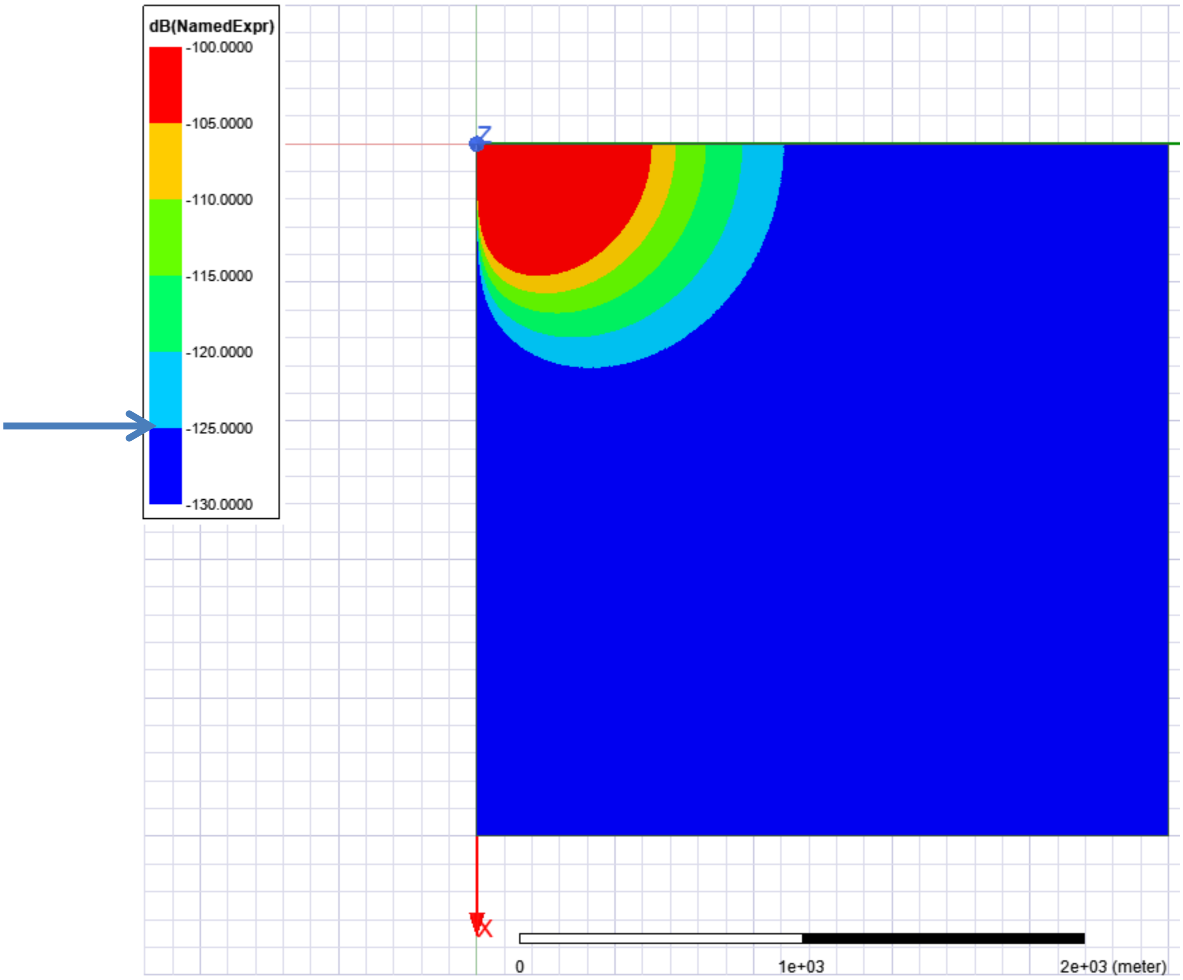

Figure 205: Simulation 13: 2kHz Normal 3600W at 20m results

Simulation 14:

Frequency: 2 kHz
Magnetic Field: **Tangential**
Electrodes separation **~20m**
Injected power ~ **3600W**
Distance scale 100m/div.

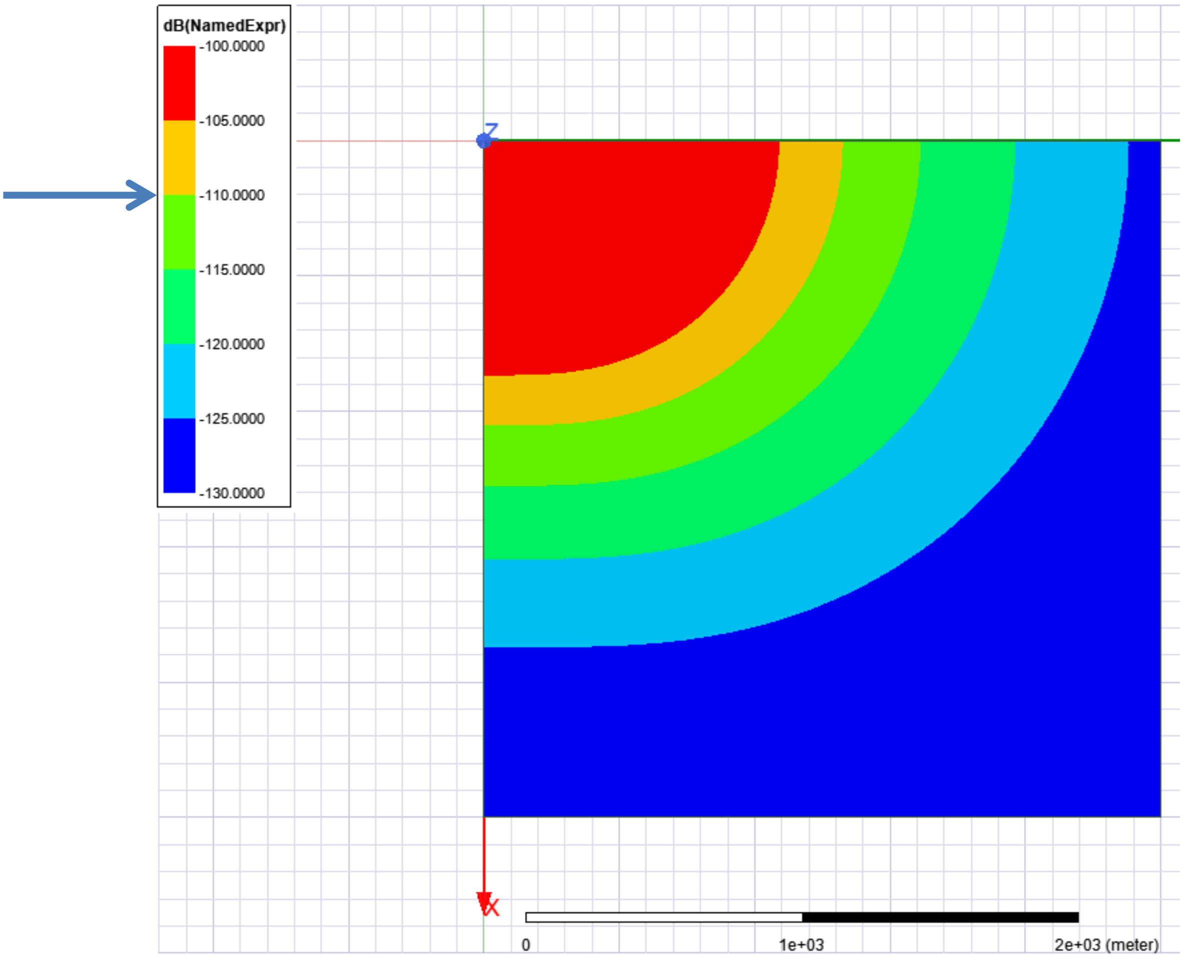

Figure 206: Simulation 14: 2kHz Tangential 3600W at 20m results

Simulation 15:

Frequency: 2 kHz
Magnetic Field: **Normal**
Electrodes separation **~10m**
Injected power ~ **1800W**
Distance scale 100m/div.

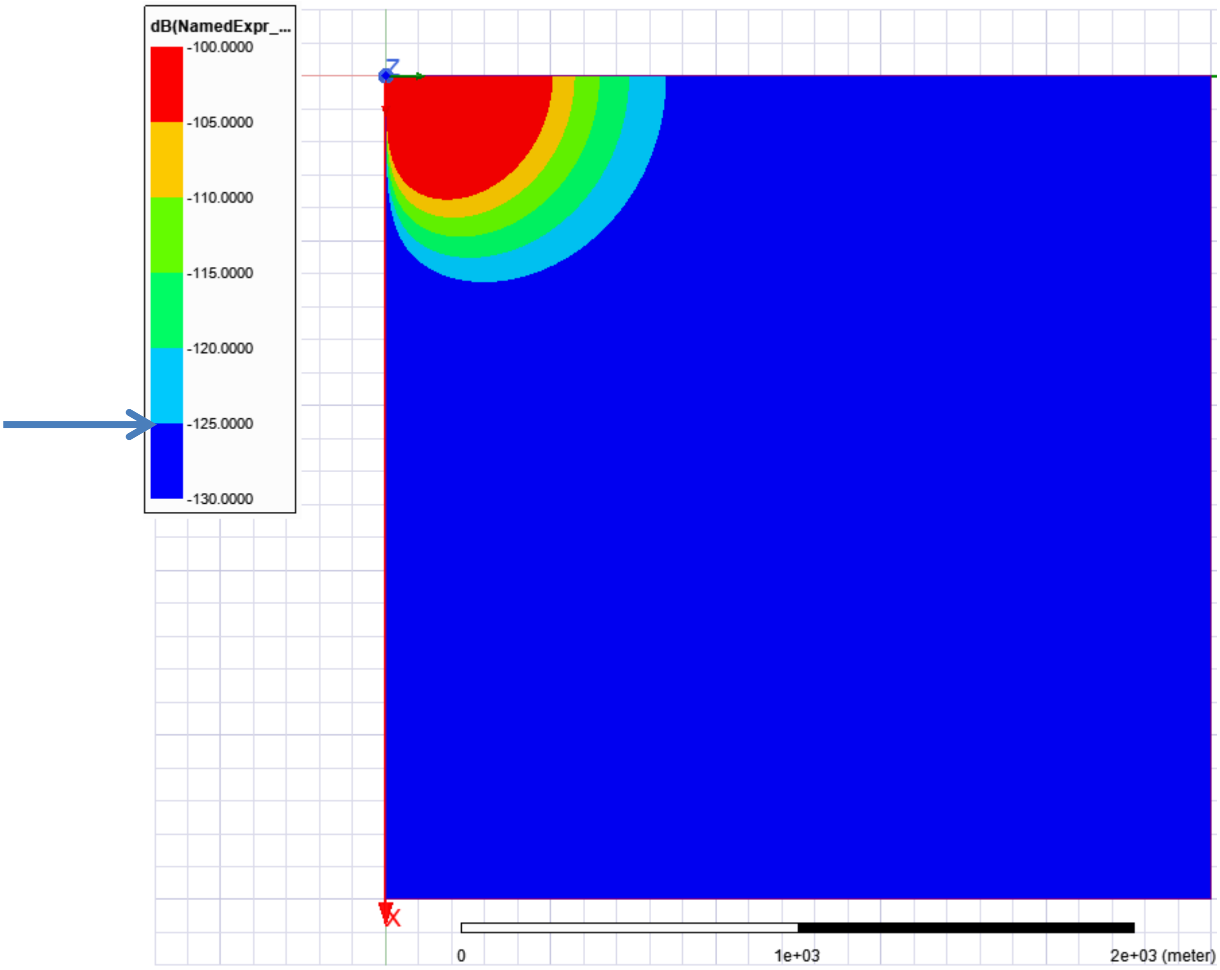

Figure 207: Simulation 15: 2kHz Normal 1800W at 10m results

Simulation 16:

Frequency: 2 kHz
Magnetic Field: **Tangential**
Electrodes separation **~10m**
Injected power ~ **1800W**
Distance scale 100m/div.

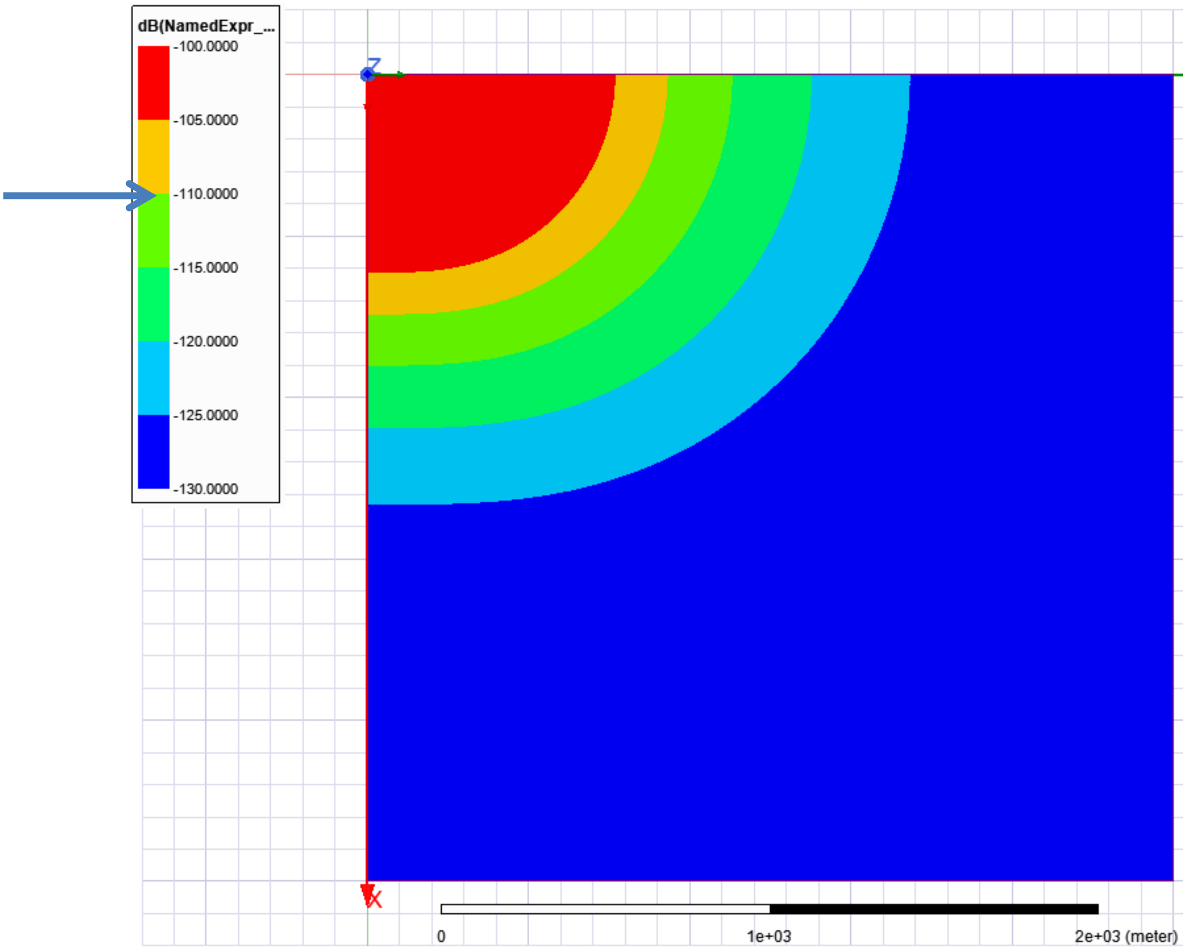

Figure 208: Simulation 16: 2kHz Tangential 1800W at 10m results

Simulation 17:

Frequency: 2 kHz
Magnetic Field: **Normal**
Electrodes separation **~10m**
Injected power ~ **3600W**
Distance scale 100m/div.

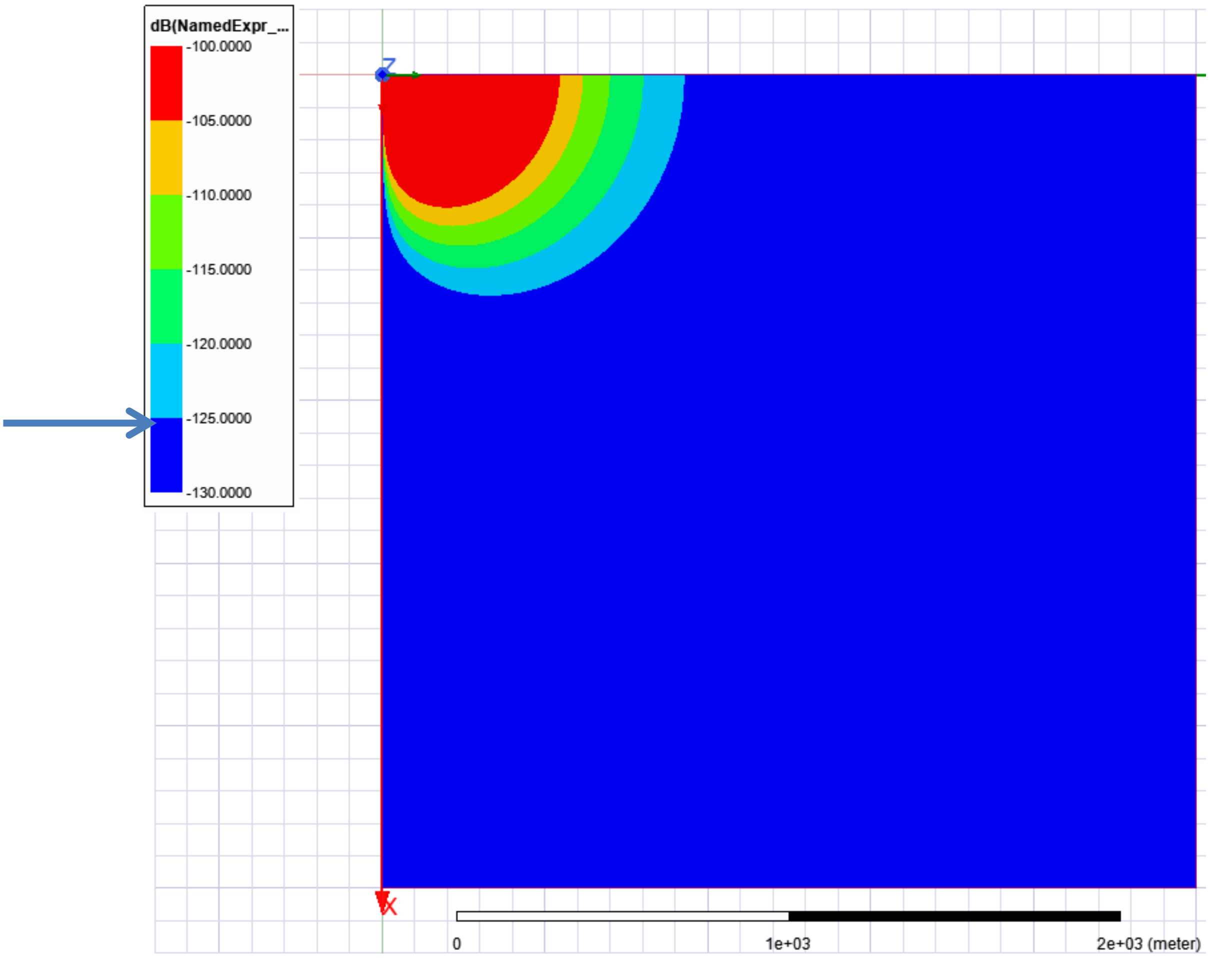

Figure 209: Simulation 17: 2kHz Normal 3600W at 10m results

Simulation 18:

Frequency: 2 kHz
Magnetic Field: **Tangential**
Electrodes separation **~10m**
Injected power ~ **3600W**
Distance scale 100m/div.

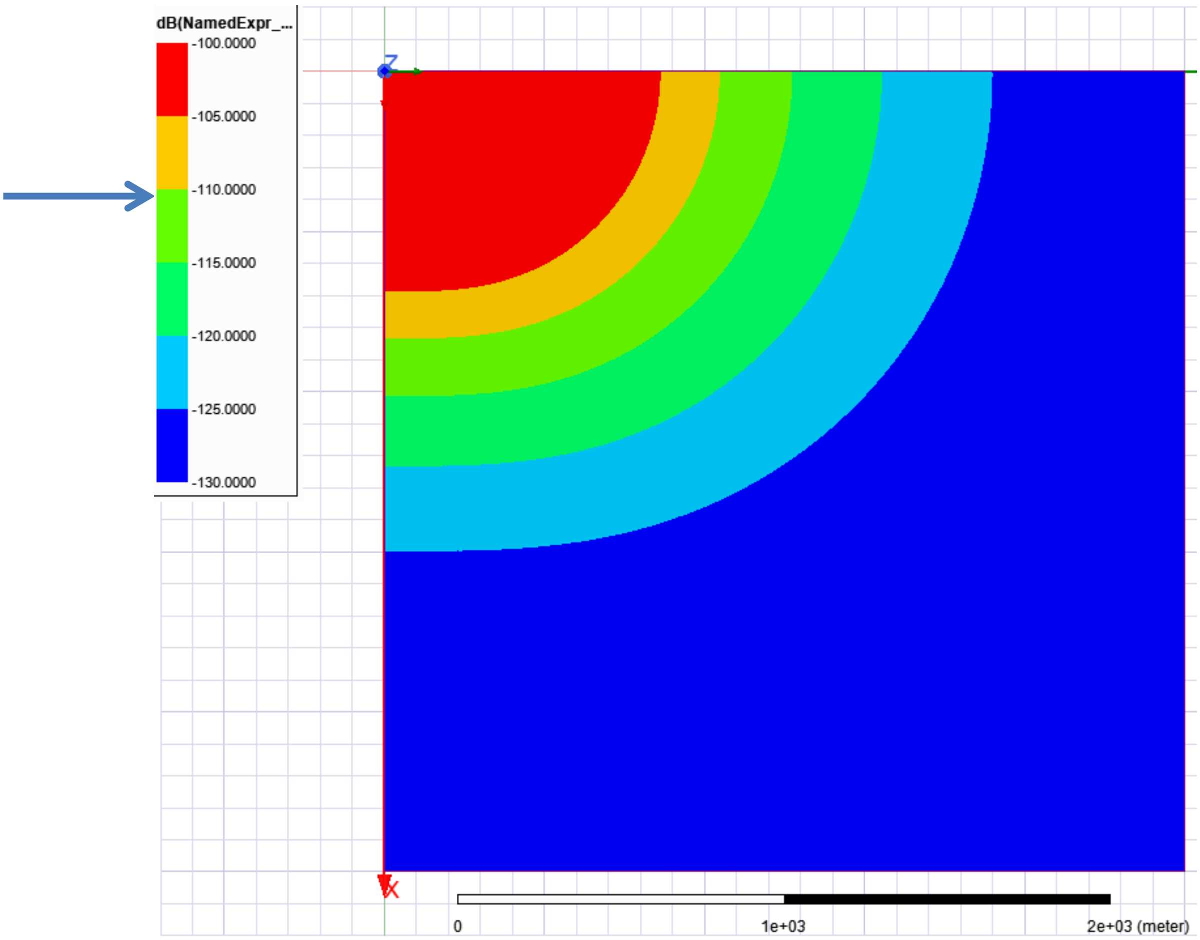

Figure 210: Simulation 18 2kHz Tangential 3600W at 10m results

APPENDIX E – 3 kHz Simulations

3 kHz Frequency Magnetic Field Simulations

Based on what we have learnt from the simulation, EM signal and speed we can now narrow down the best frequency for data transmission whilst avoiding noise to disrupt that signal.

The simulations below are based on magnetic field distribution is represented for parameters sets Power, (20, 1800, 3600W) Tx Probe Distance (10, 20,50 meters), Frequency (3 kHz) and Magnetic field (Normal, Tangential)

Simulation 1:

Frequency: 3 kHz
Magnetic Field: **Normal**
Electrodes separation ~**50m**
Injected power ~ **20W**
Distance scale 100m/div.

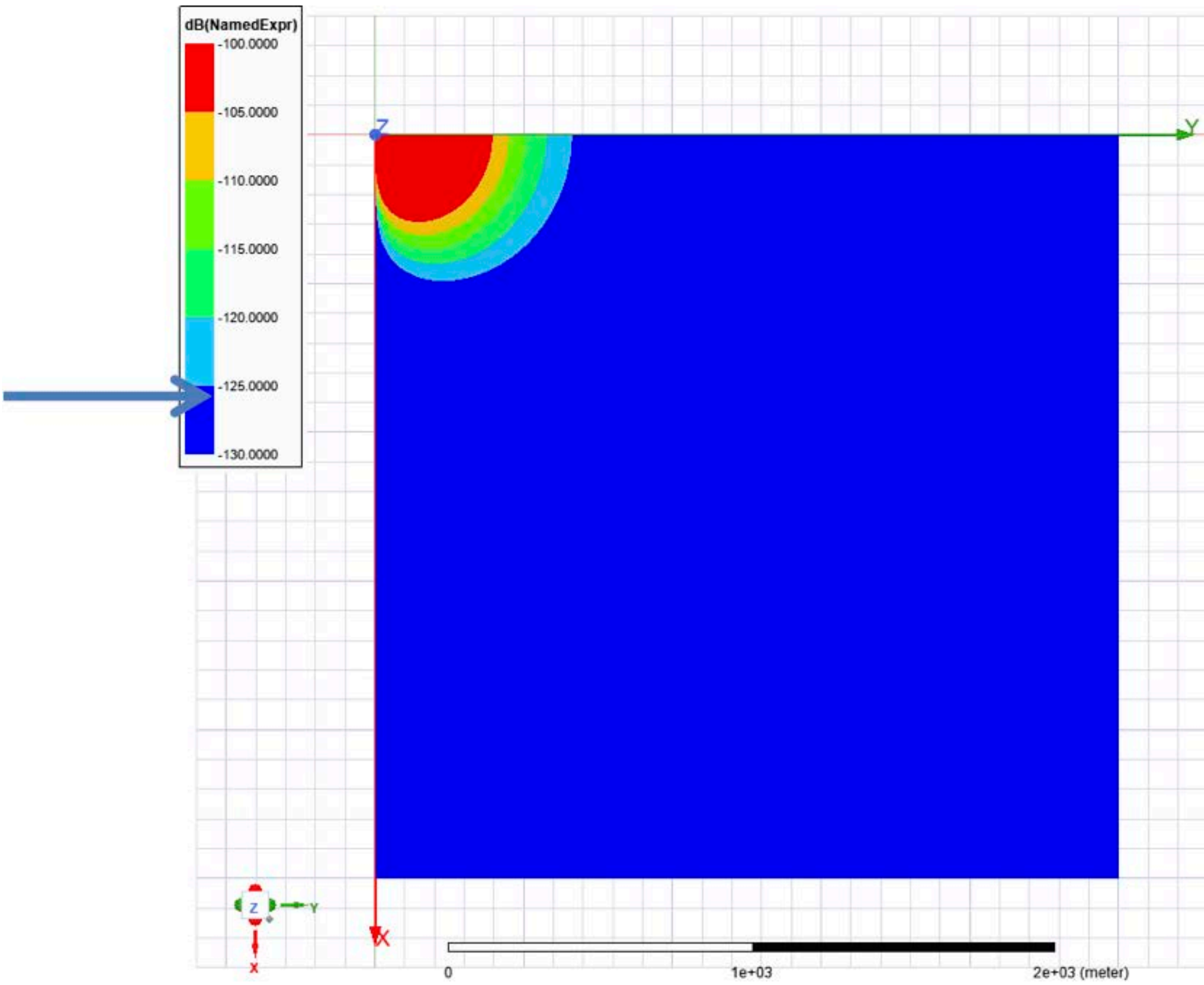

Figure 211: Simulation 1: 3kHz Normal 20W at 50m results

Simulation 2:

Frequency: 3 kHz
Magnetic Field: **Tangential**
Electrodes separation **~50m**
Injected power ~ **20W**
Distance scale 100m/div.

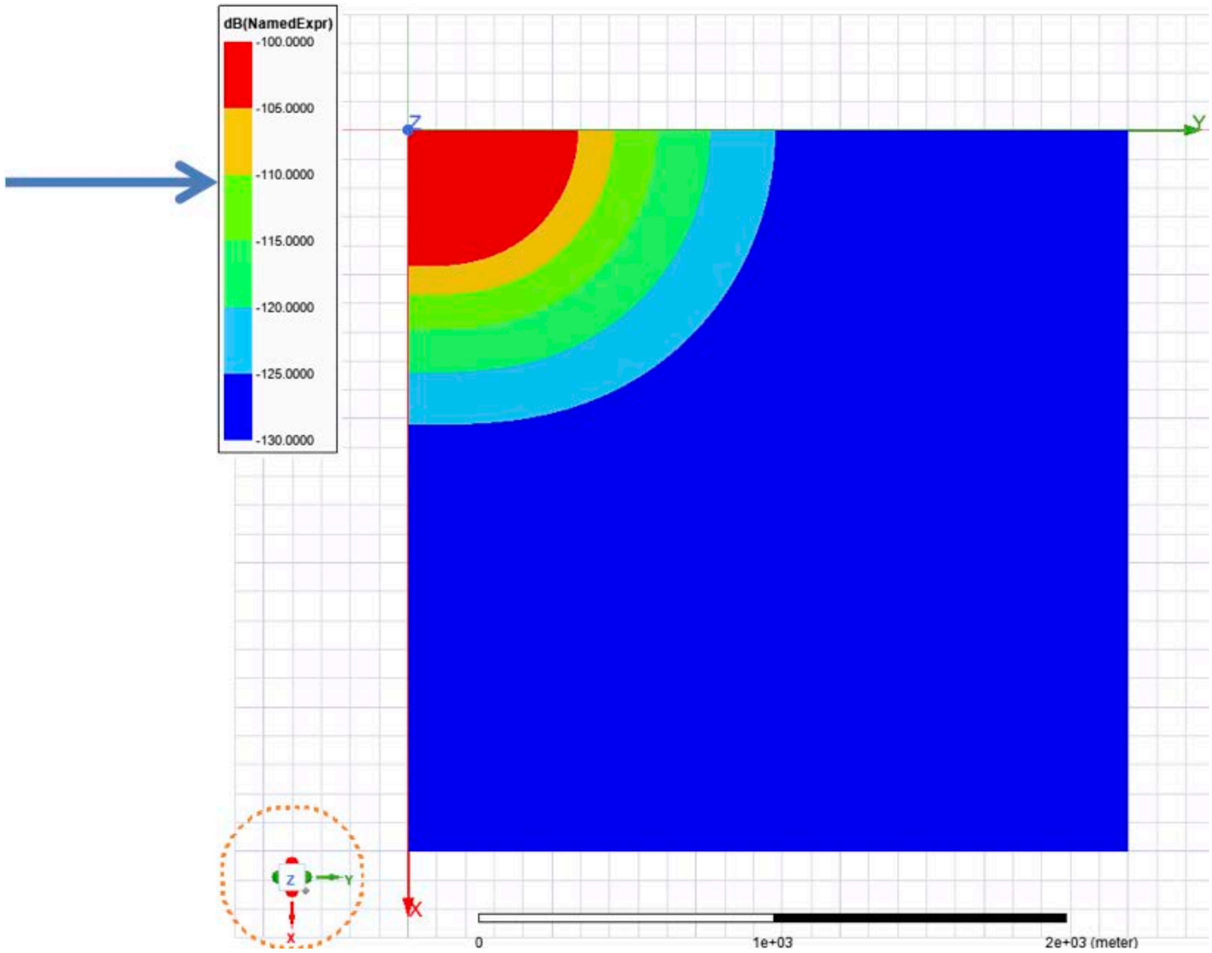

Figure 212: Simulation 2: 3kHz Tangential 20W at 50m results

Simulation 3:

Frequency: 3 kHz
Magnetic Field: **Normal**
Electrodes separation ~**20m**
Injected power ~ **20W**
Distance scale 100m/div.

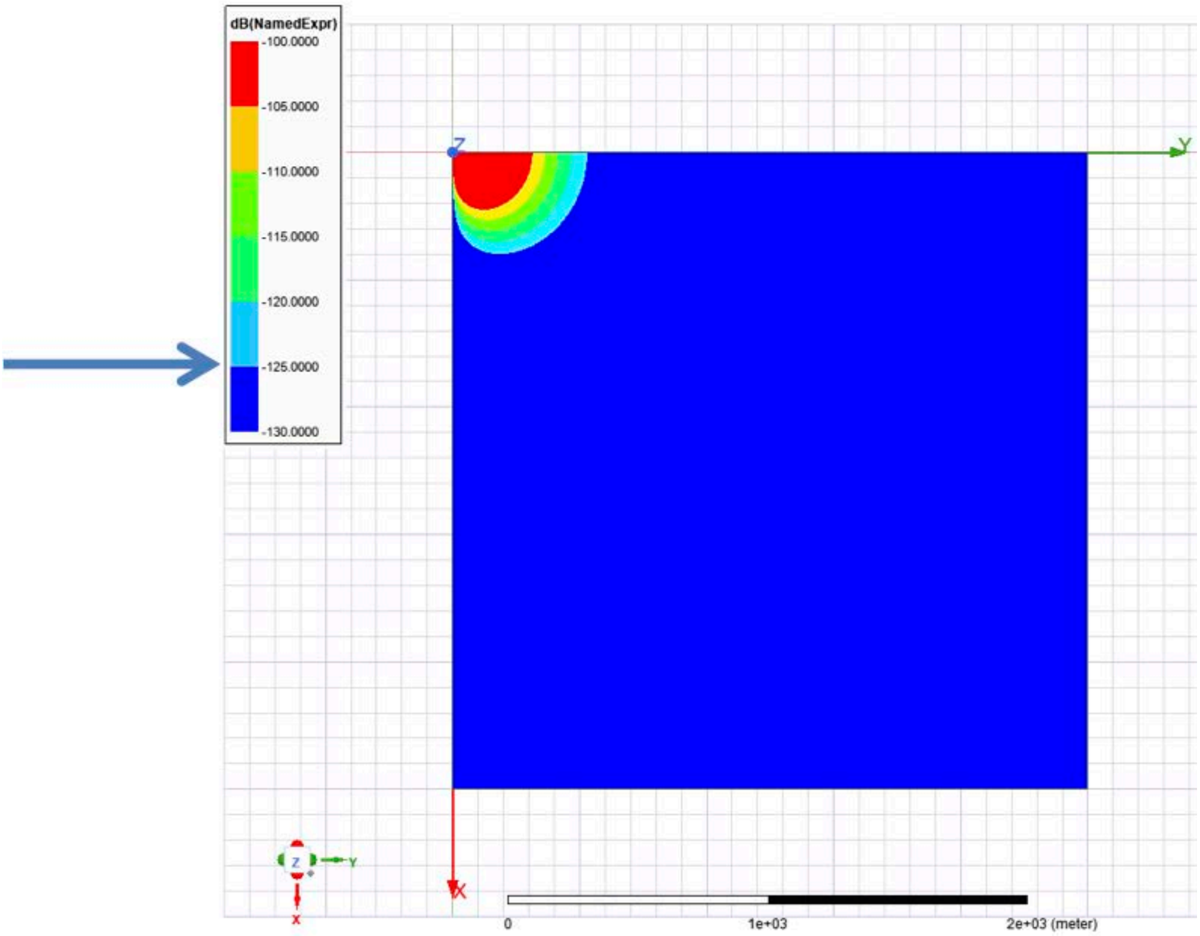

Figure 213: Simulation 3: 3kHz Normal 20W at 20m results

Simulation 4:

Frequency: 3 kHz
Magnetic Field: **Tangential**
Electrodes separation ~**20m**
Injected power ~ **20W**
Distance scale 100m/div.

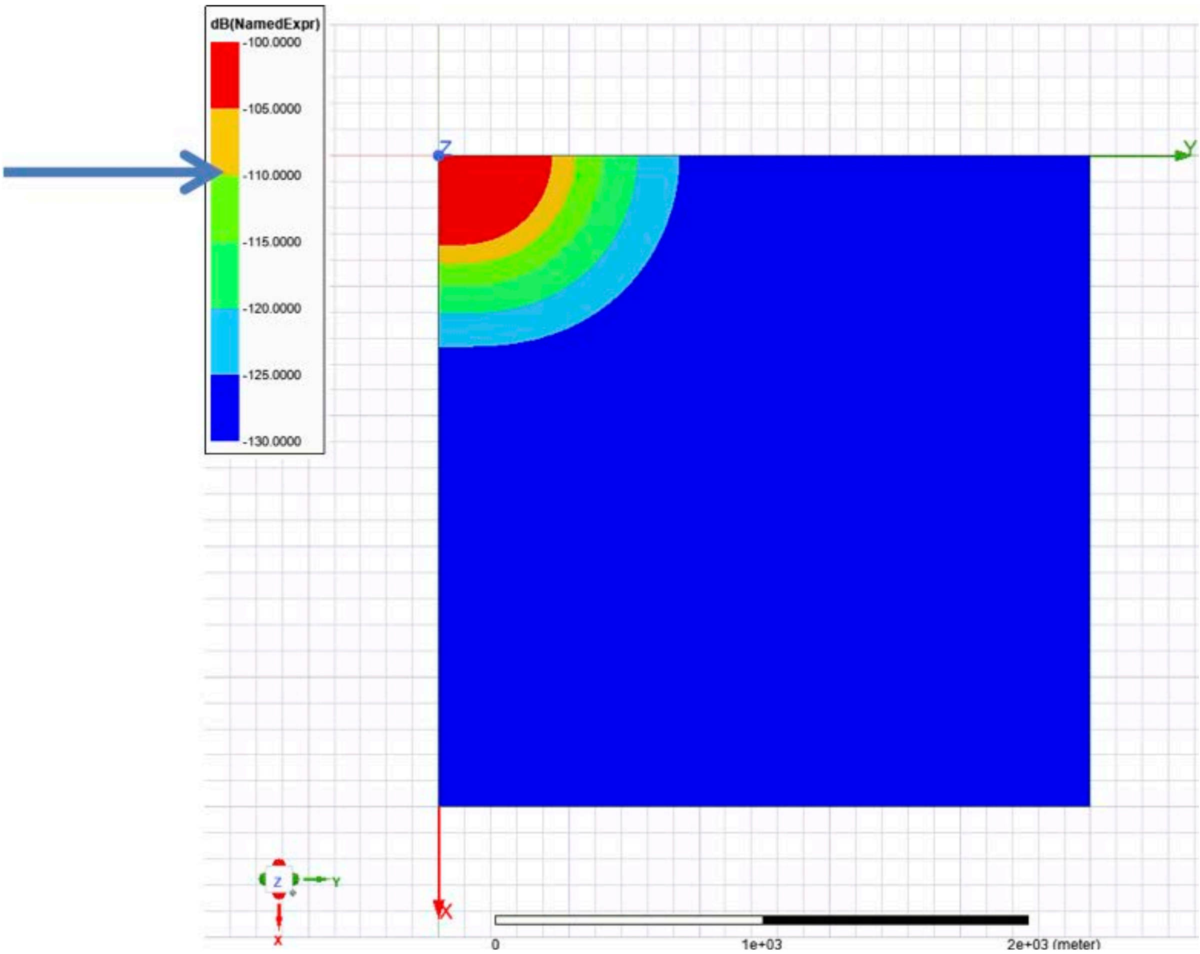

Figure 214: Simulation 4: 3kHz Tangential 20W at 20m results

Simulation 5:

Frequency: 3 kHz
Magnetic Field: **Normal**
Electrodes separation ~**10m**
Injected power ~ **20W**
Distance scale 100m/div.

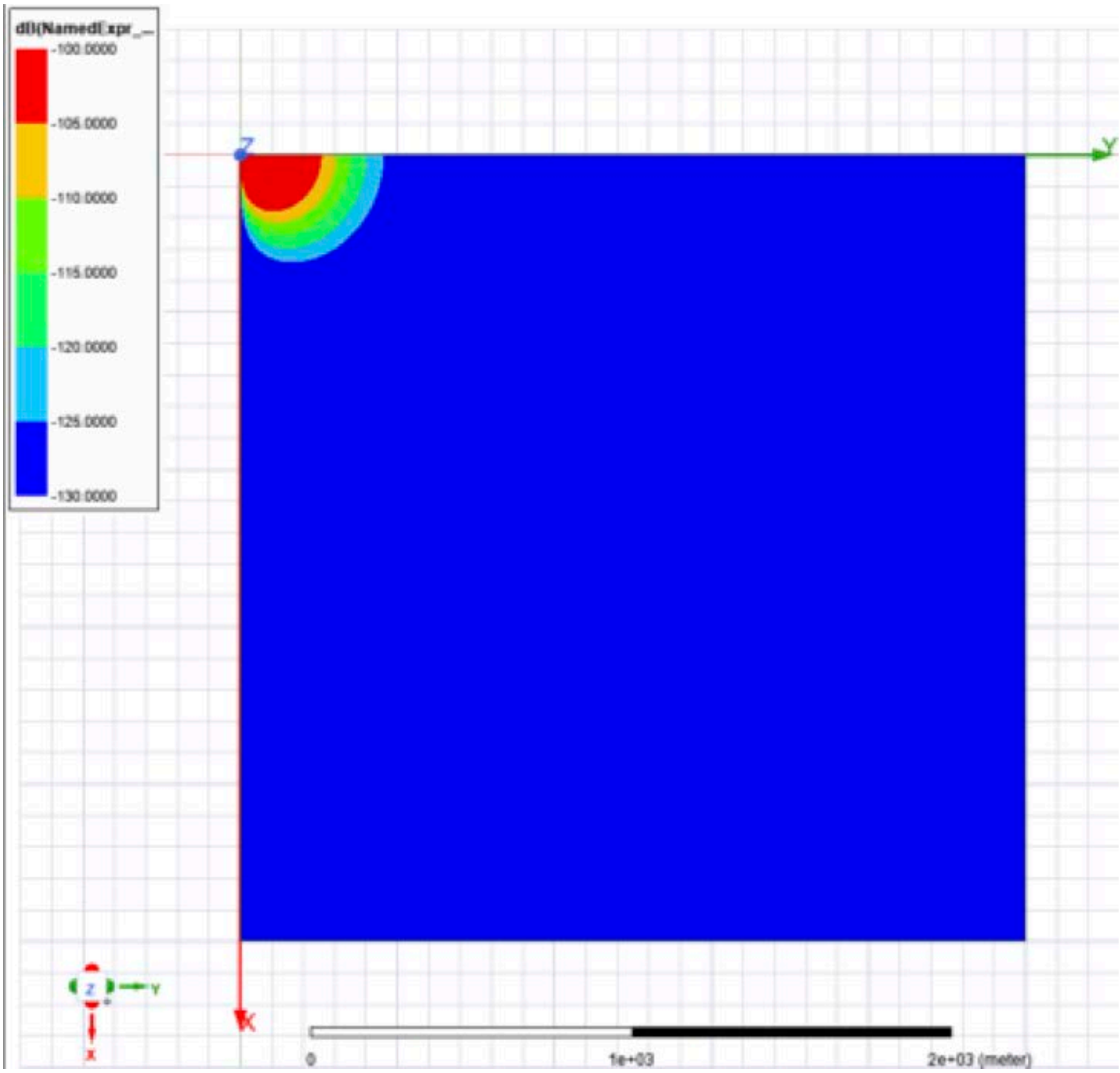

Figure 215: Simulation 5: 3kHz Normal 20W at 10m results

Simulation 6:

Frequency: 3 kHz
Magnetic Field: **Tangential**
Electrodes separation **~10m**
Injected power ~ **20W**
Distance scale 100m/div.

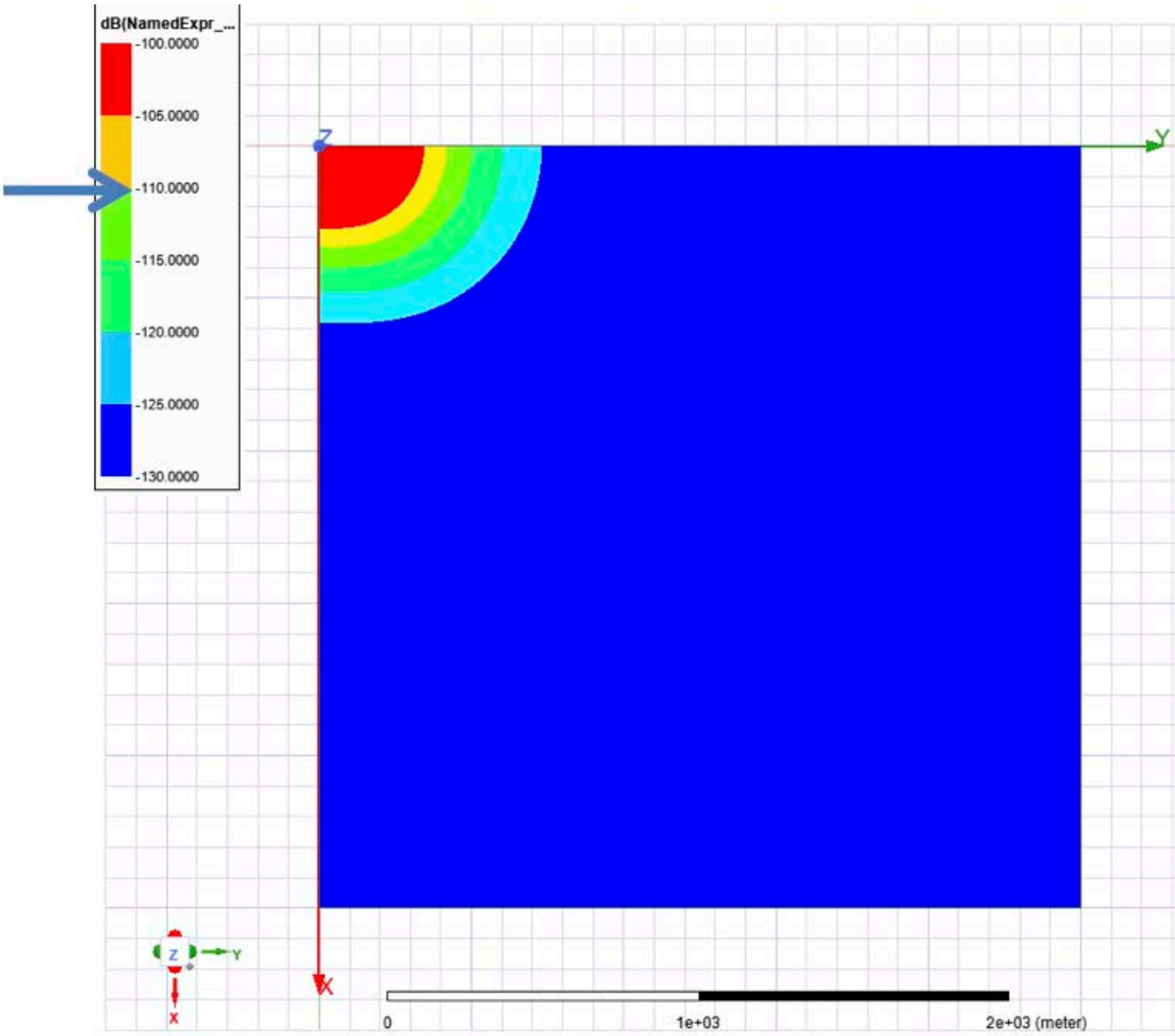

Figure 216: Simulation 6: 3kHz Tangential 20W at 10m results

Simulation 7:

Frequency: 3 kHz
Magnetic Field: **Normal**
Electrodes separation **~50m**
Injected power ~ **1800W**
Distance scale 100m/div.

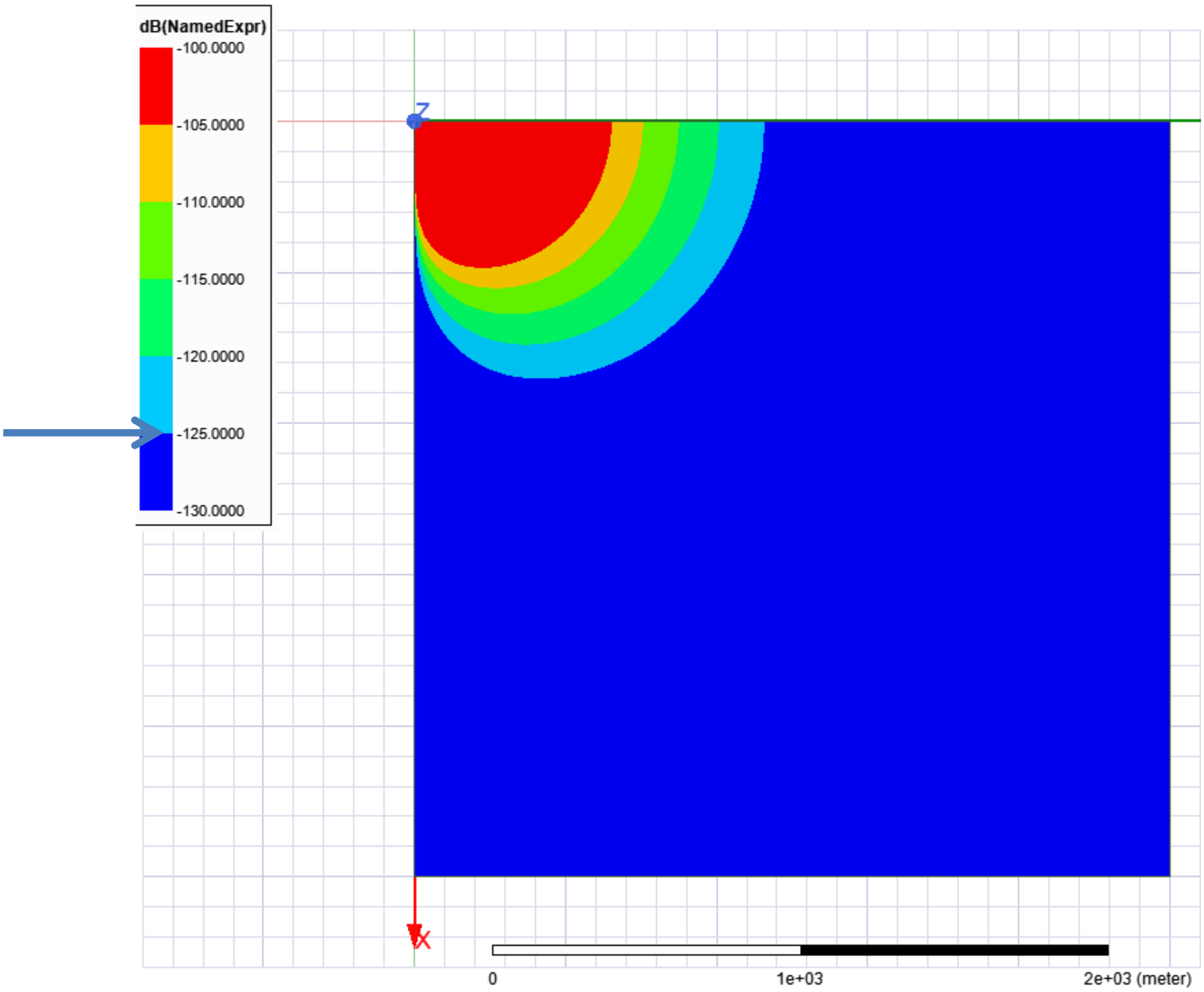

Figure 217: Simulation 7: 3kHz Normal 1800W at 50m results

Simulation 8:

Frequency: 3 kHz
Magnetic Field: **Tangential**
Electrodes separation **~50m**
Injected power ~ **1800W**
Distance scale 100m/div.

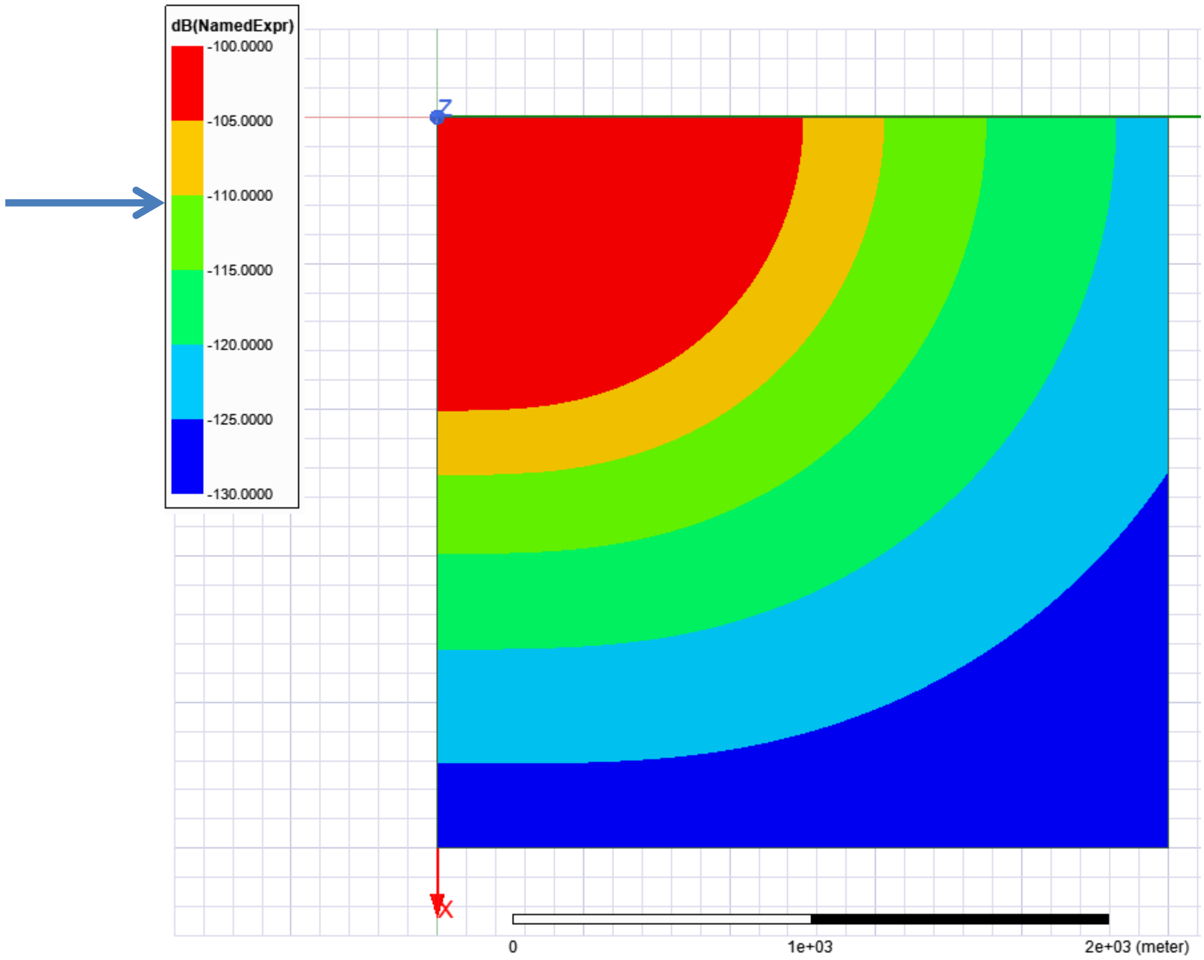

Figure 218: Simulation 8: 3kHz Tangential 1800W at 50m results

Simulation 9:

Frequency: 3 kHz
Magnetic Field: **Normal**
Electrodes separation **~50m**
Injected power ~ **3600W**
Distance scale 100m/div.

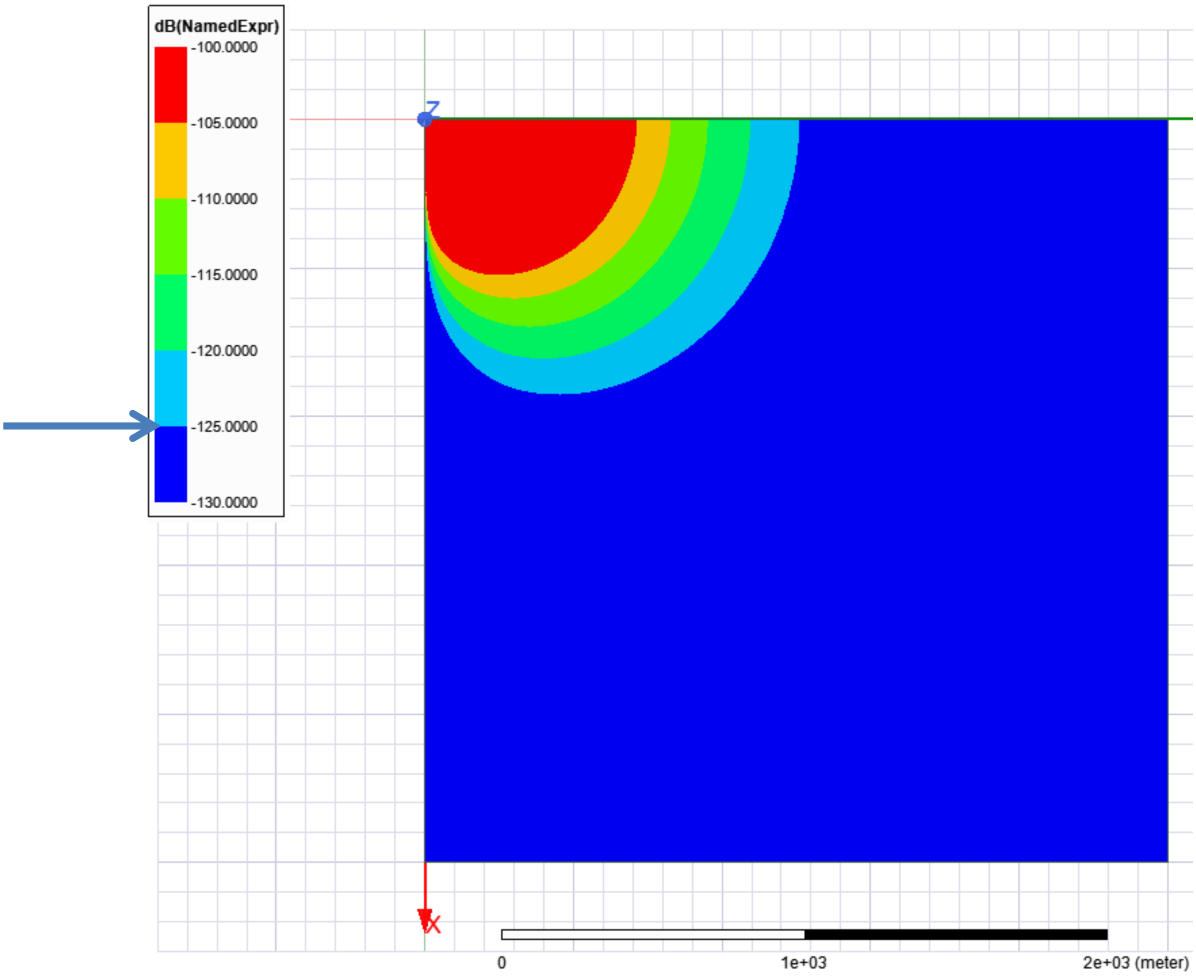

Figure 219: Simulation 9: 3kHz Normal 3600W at 50m results

Simulation 10:

Frequency: 3 kHz
Magnetic Field: **Tangential**
Electrodes separation **~50m**
Injected power ~ **3600W**
Distance scale 100m/div.

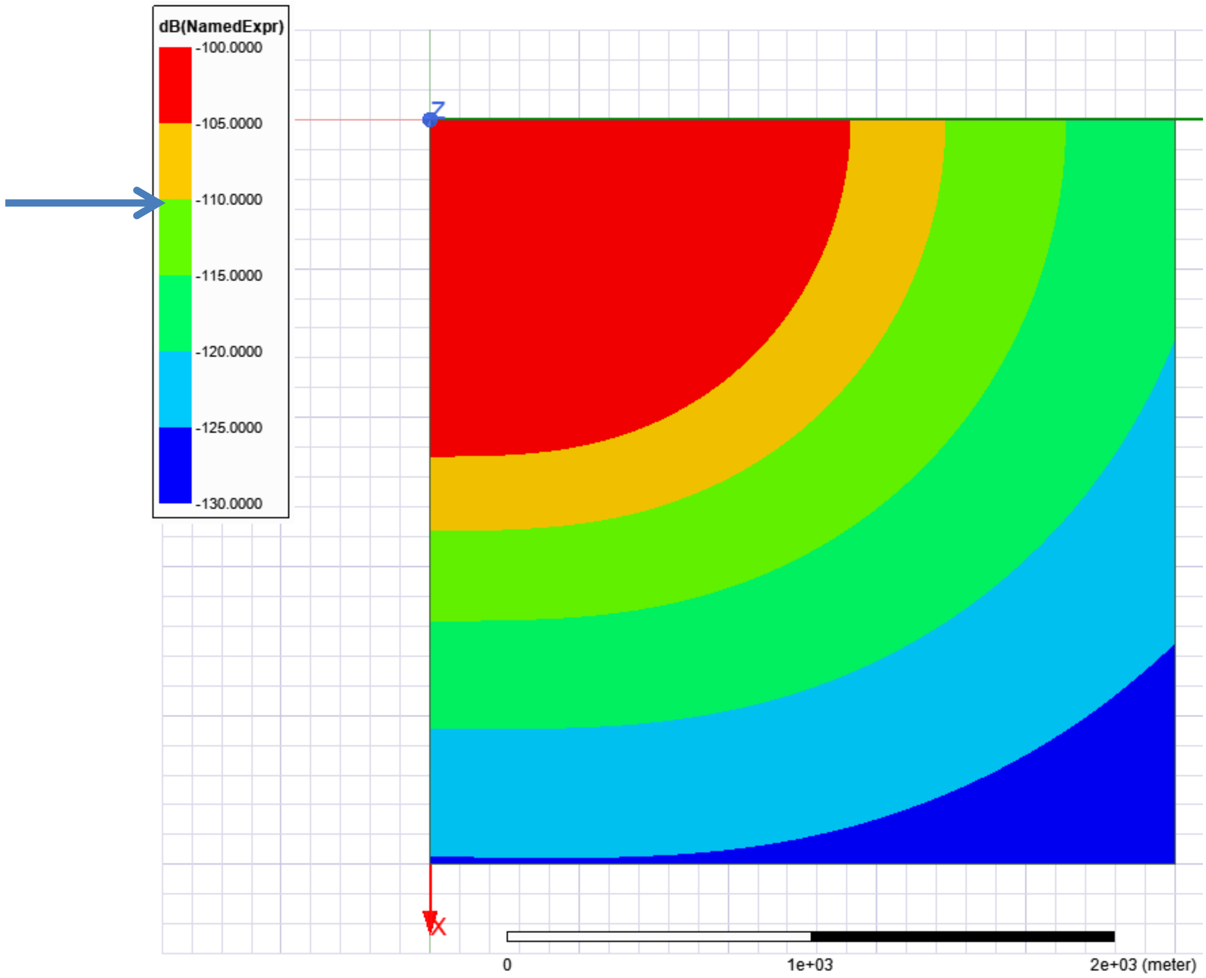

Figure 220: Simulation 10: 3kHz Tangential 3600W at 50m results

Simulation 11:

Frequency: 3 kHz
Magnetic Field: **Normal**
Electrodes separation ~**20m**
Injected power ~ **1800W**
Distance scale 100m/div.

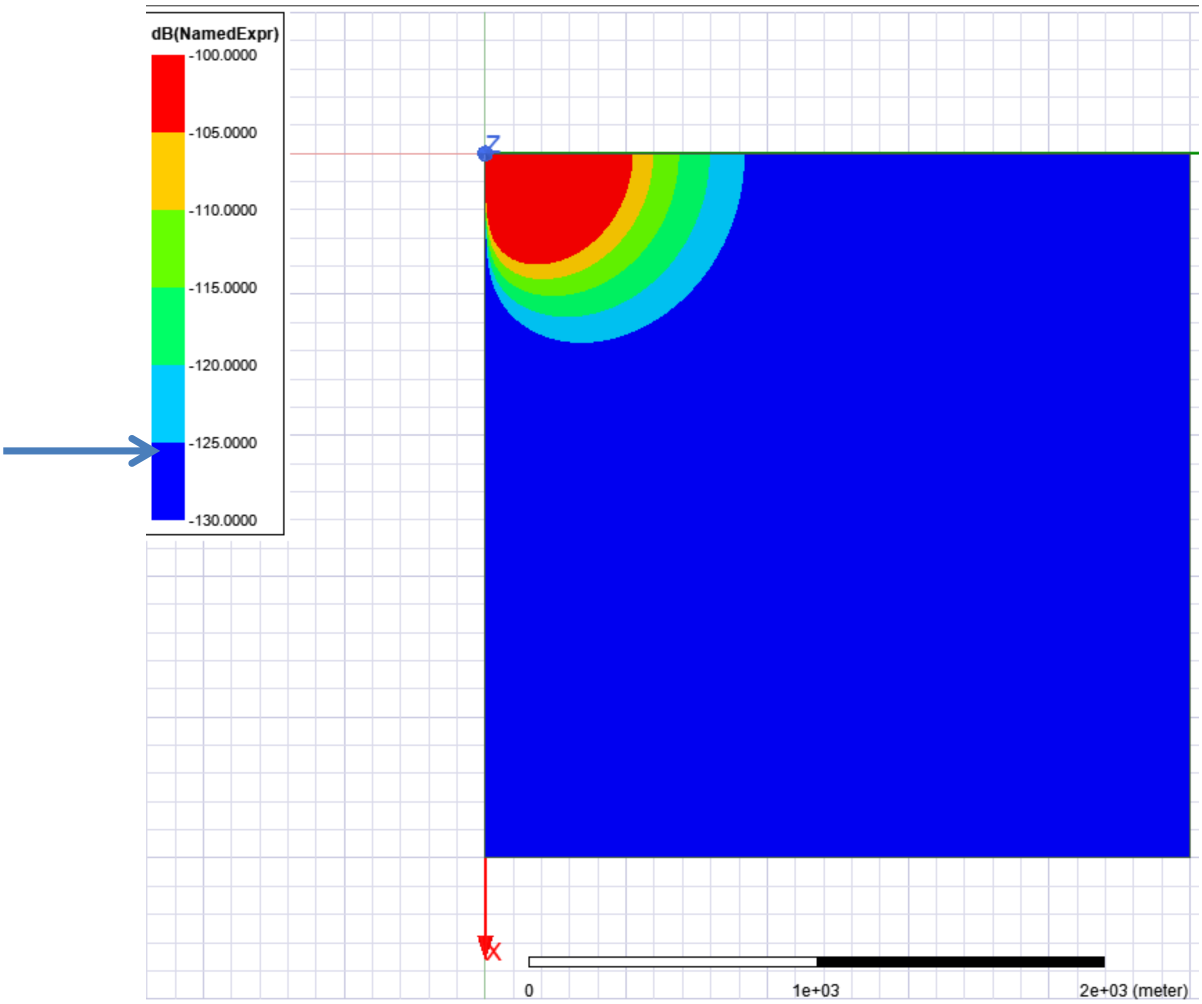

Figure 221: Simulation 11: 3kHz Normal 1800W at 20m results

Simulation 12:

Frequency: 3 kHz
Magnetic Field: **Tangential**
Electrodes separation ~**20m**
Injected power ~ **1800W**
Distance scale 100m/div.

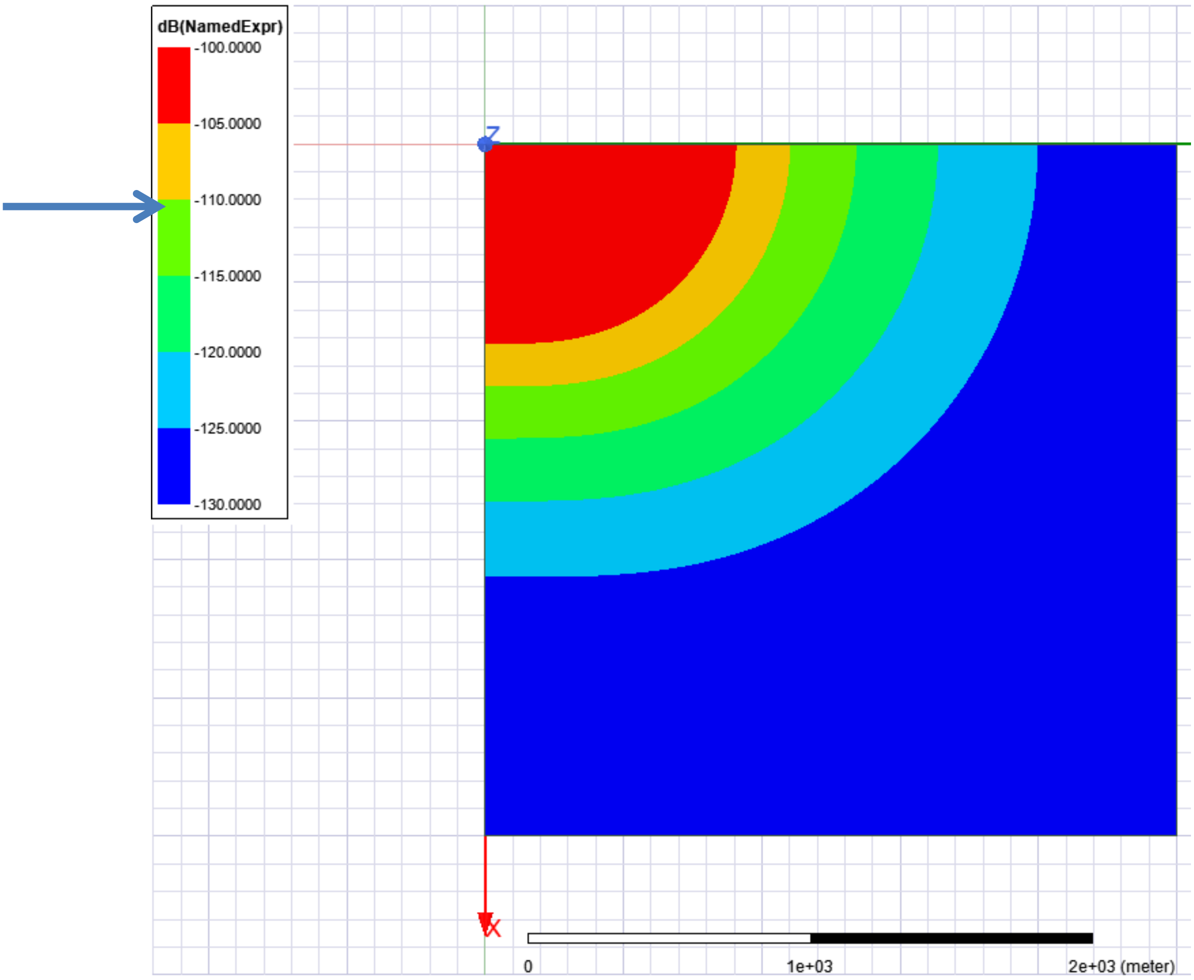

Figure 222: Simulation 12: 3kHz Tangential 1800W at 20m results

Simulation 13:

Frequency: 3 kHz
Magnetic Field: **Normal**
Electrodes separation **~20m**
Injected power ~ **3600W**
Distance scale 100m/div.

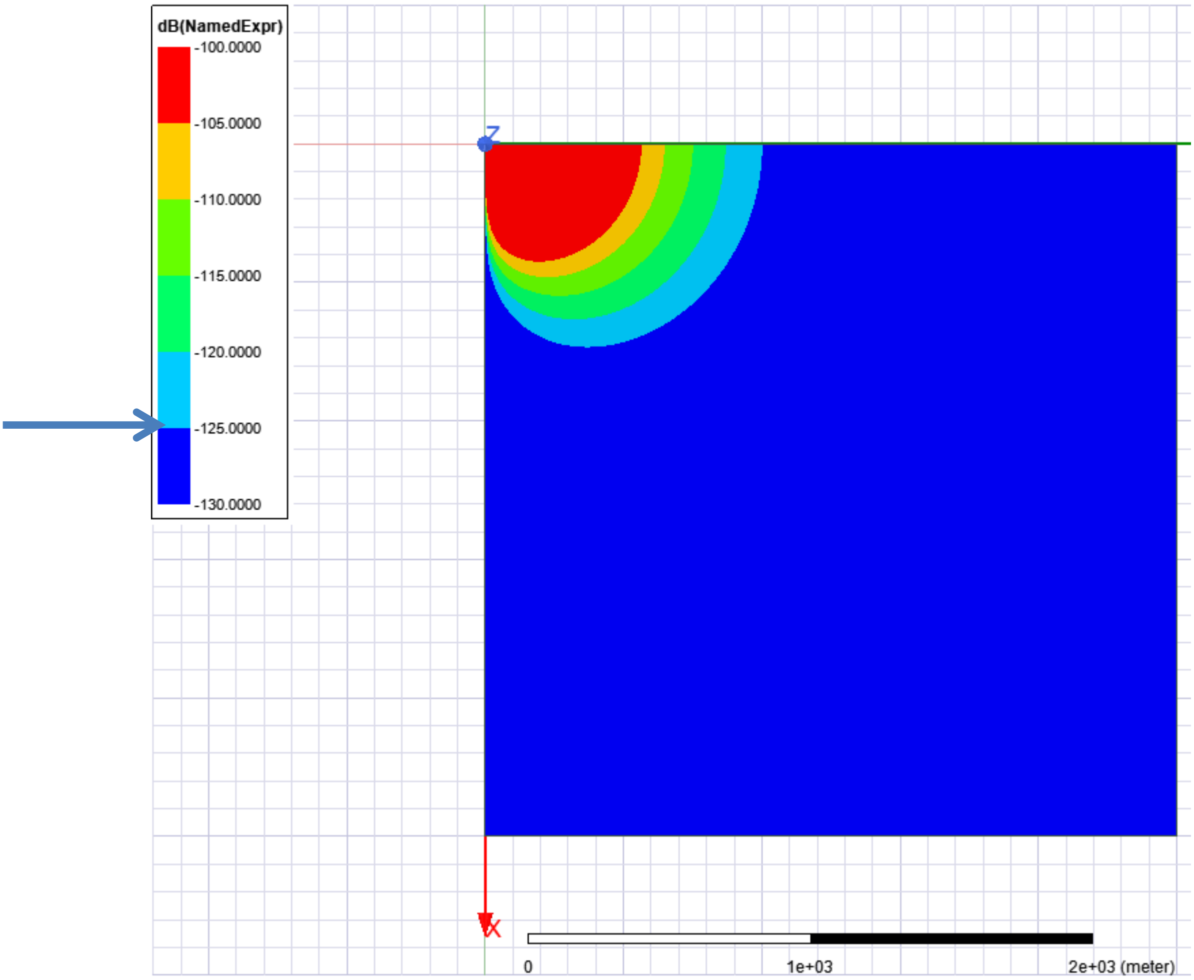

Figure 223: Simulation 13: 3kHz Normal 3600W at 20m results

Simulation 14:

Frequency: 3 kHz
Magnetic Field: **Tangential**
Electrodes separation **~20m**
Injected power ~ **3600W**
Distance scale 100m/div.

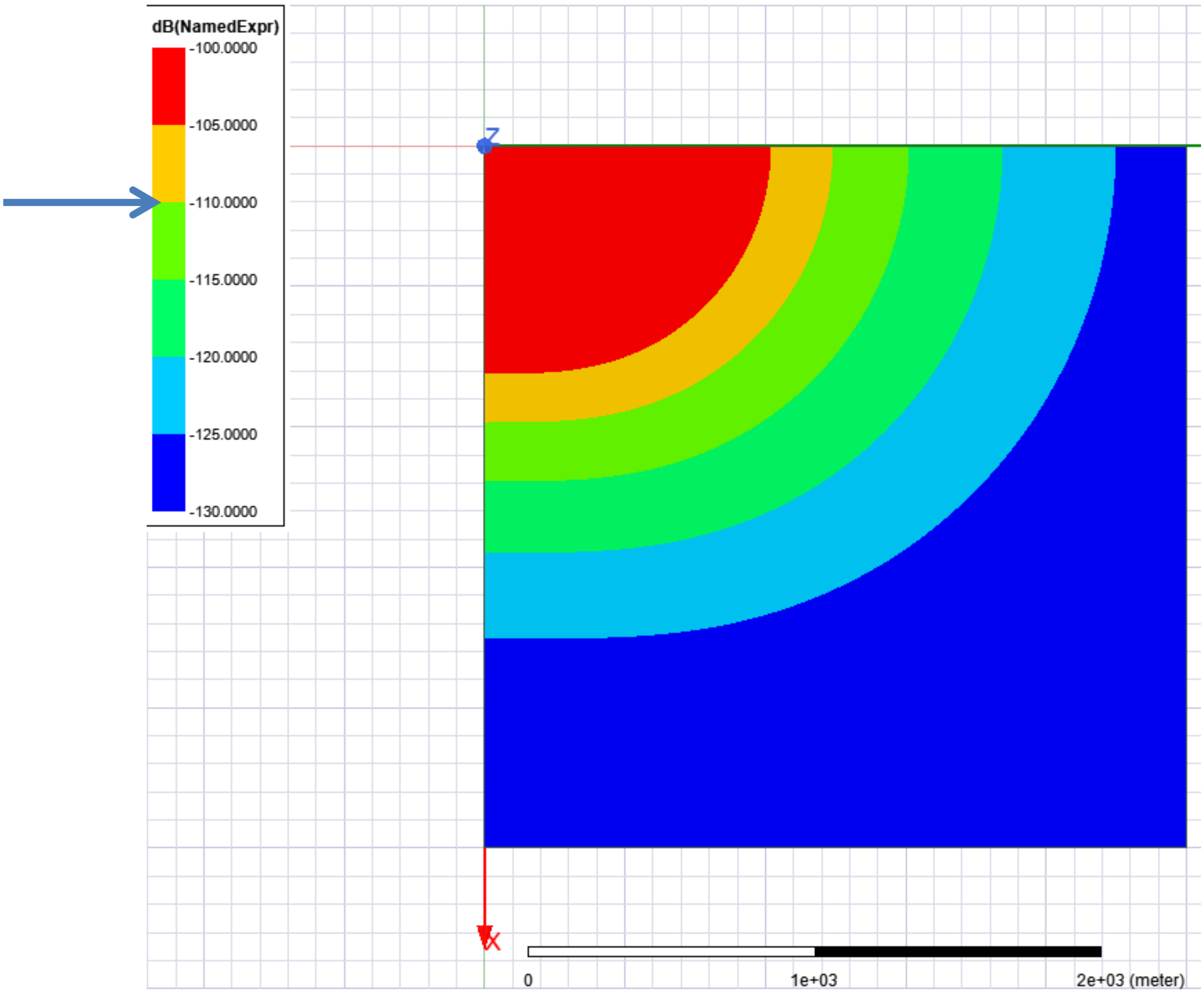

Figure 224: Simulation 14: 3kHz Tangential 3600W at 20m results

Simulation 15:

Frequency: 3 kHz
Magnetic Field: **Normal**
Electrodes separation **~10m**
Injected power ~ **1800W**
Distance scale 100m/div.

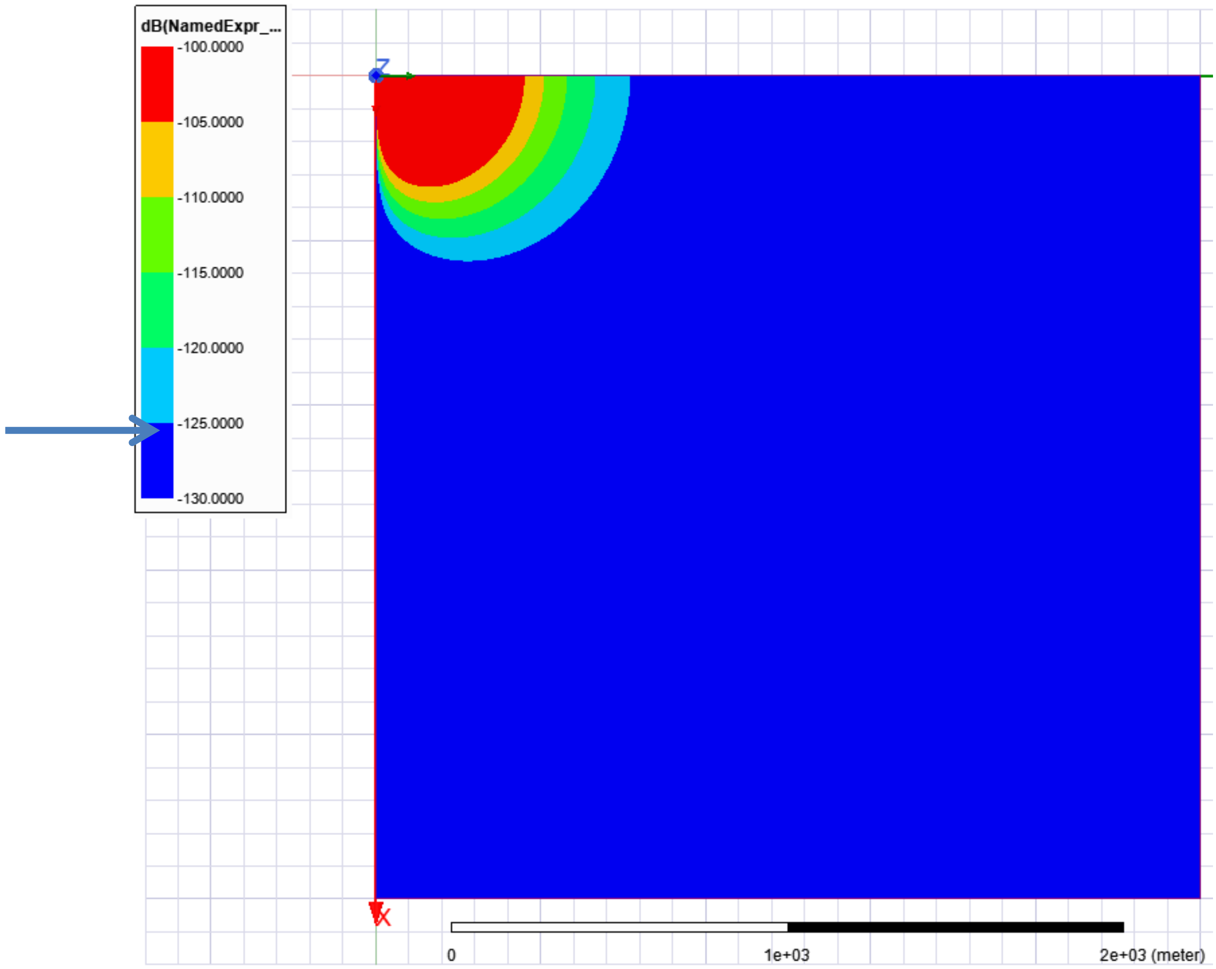

Figure 225: Simulation 15: 3kHz Normal 1800W at 10m results

Simulation 16:

Frequency: 3 kHz
Magnetic Field: **Tangential**
Electrodes separation **~10m**
Injected power ~ **1800W**
Distance scale 100m/div.

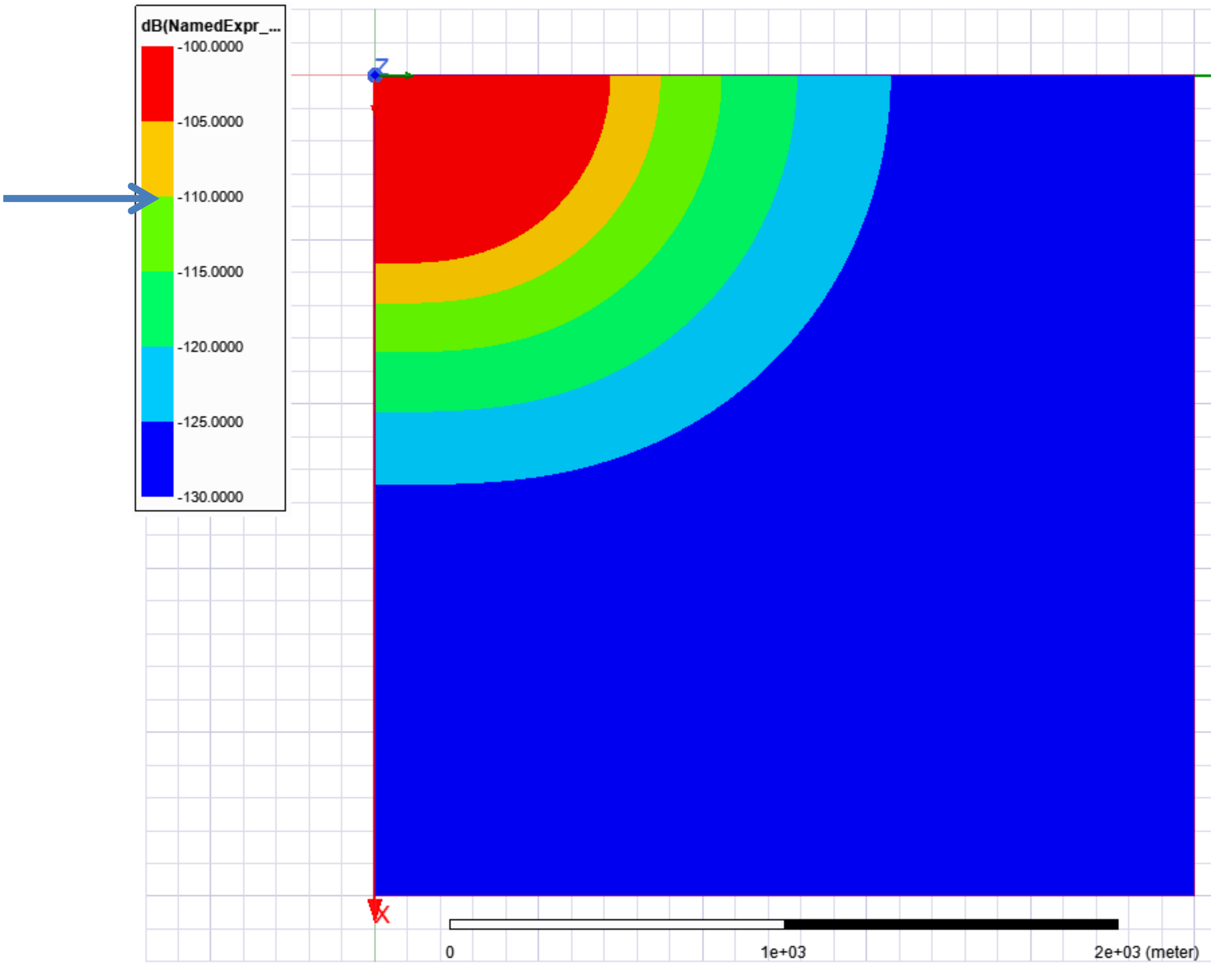

Figure 226: Simulation 16: 3kHz Tangential 1800W at 10m results

Simulation 17:

Frequency: 3 kHz
Magnetic Field: **Normal**
Electrodes separation **~10m**
Injected power ~ **3600W**
Distance scale 100m/div.

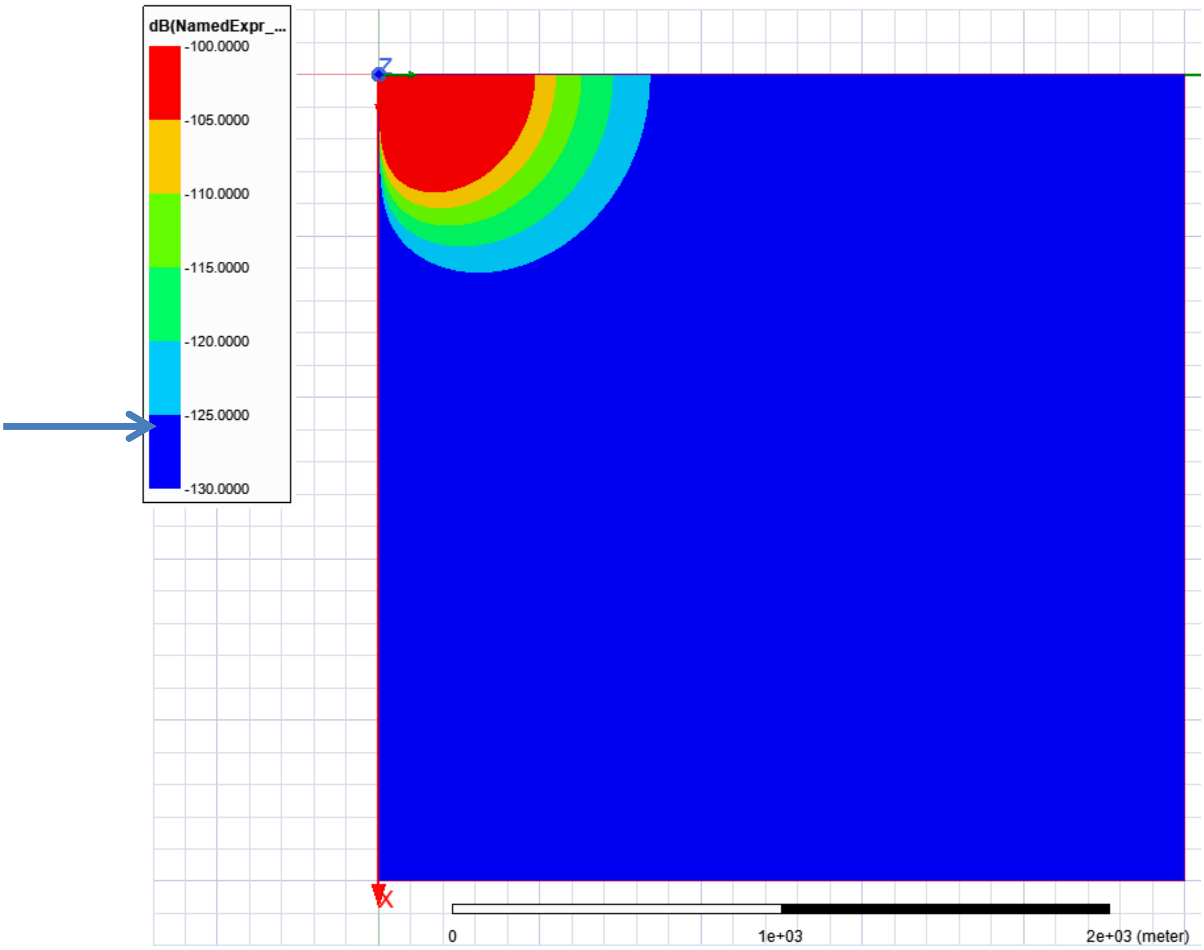

Figure 227: Simulation 17: 3kHz Normal 3600W at 10m results

Simulation 18:

Frequency: 3 kHz
Magnetic Field: **Tangential**
Electrodes separation **~10m**
Injected power ~ **3600W**
Distance scale 100m/div.

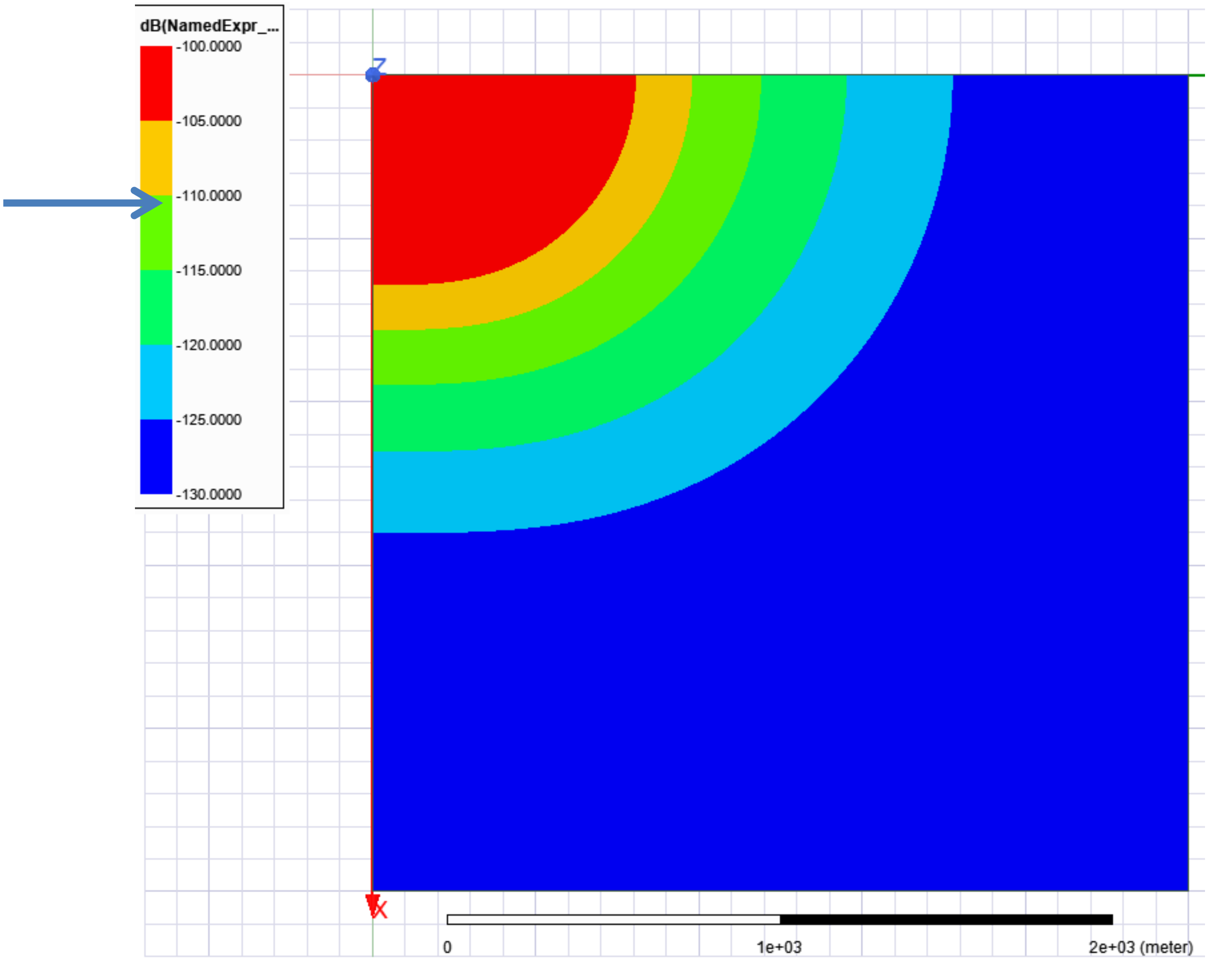

Figure 228: Simulation 18: 3kHz Tangential 3600W at 10m results

APPENDIX E – 4 kHz Simulations

4 kHz Frequency Magnetic Field Simulations

Based on what we have learnt from the simulation, EM signal and speed we can now narrow down the best frequency for data transmission whilst avoiding noise to disrupt that signal.

The simulations below are based on magnetic field distribution is represented for parameters sets Power, (20, 1800, 3600W) Tx Probe Distance (10, 20, 50 meters), Frequency (4 kHz) and Magnetic field (Normal, Tangential)

Simulation 1:

Frequency: 4 kHz
Magnetic Field: **Normal**
Electrodes separation ~**50m**
Injected power ~ **20W**
Distance scale 100m/div.

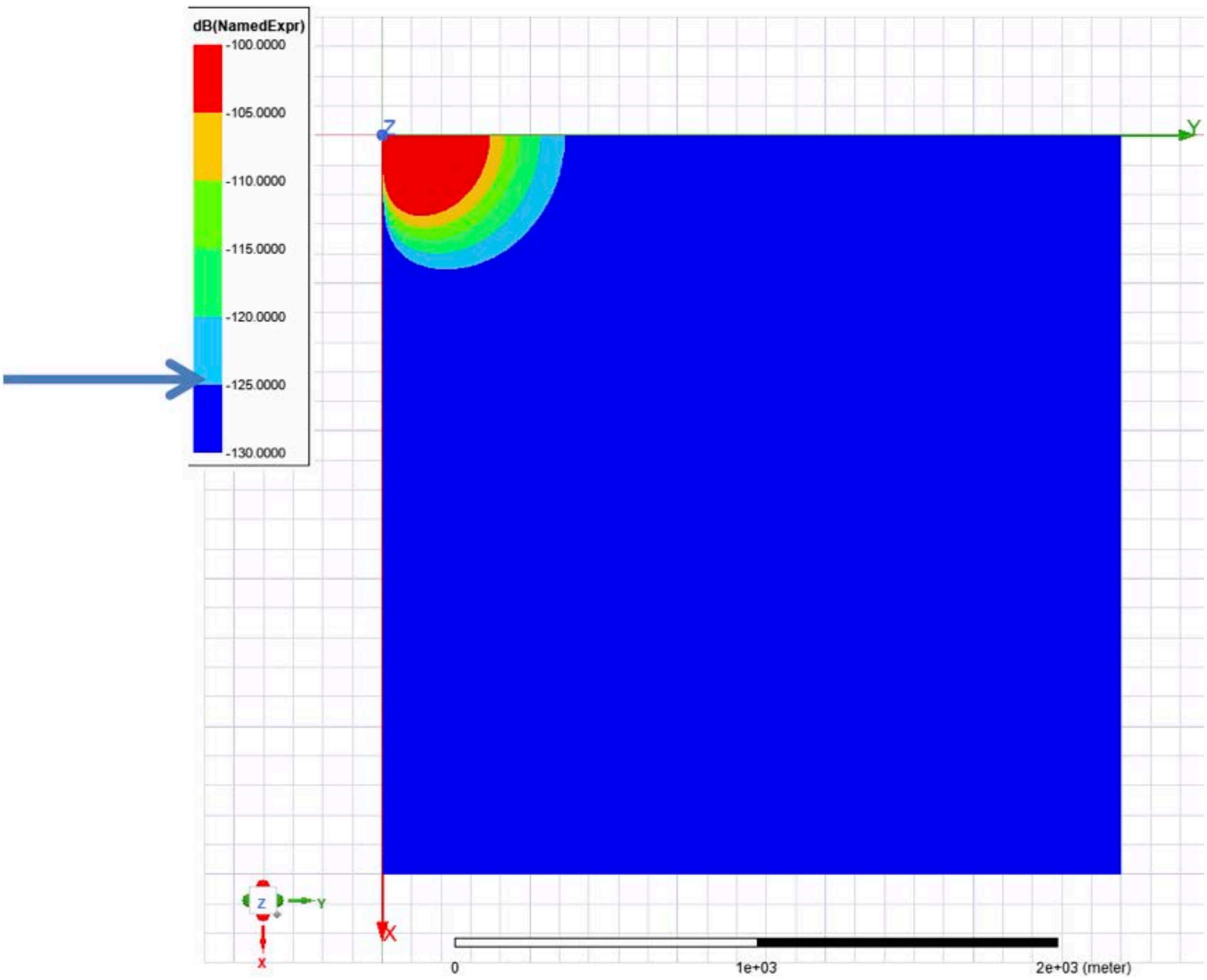

Figure 229: Simulation 1: 4kHz Normal 20W at 50m results

Simulation 2:

Frequency: 4 kHz
Magnetic Field: **Tangential**
Electrodes separation **~50m**
Injected power ~ **20W**
Distance scale 100m/div.

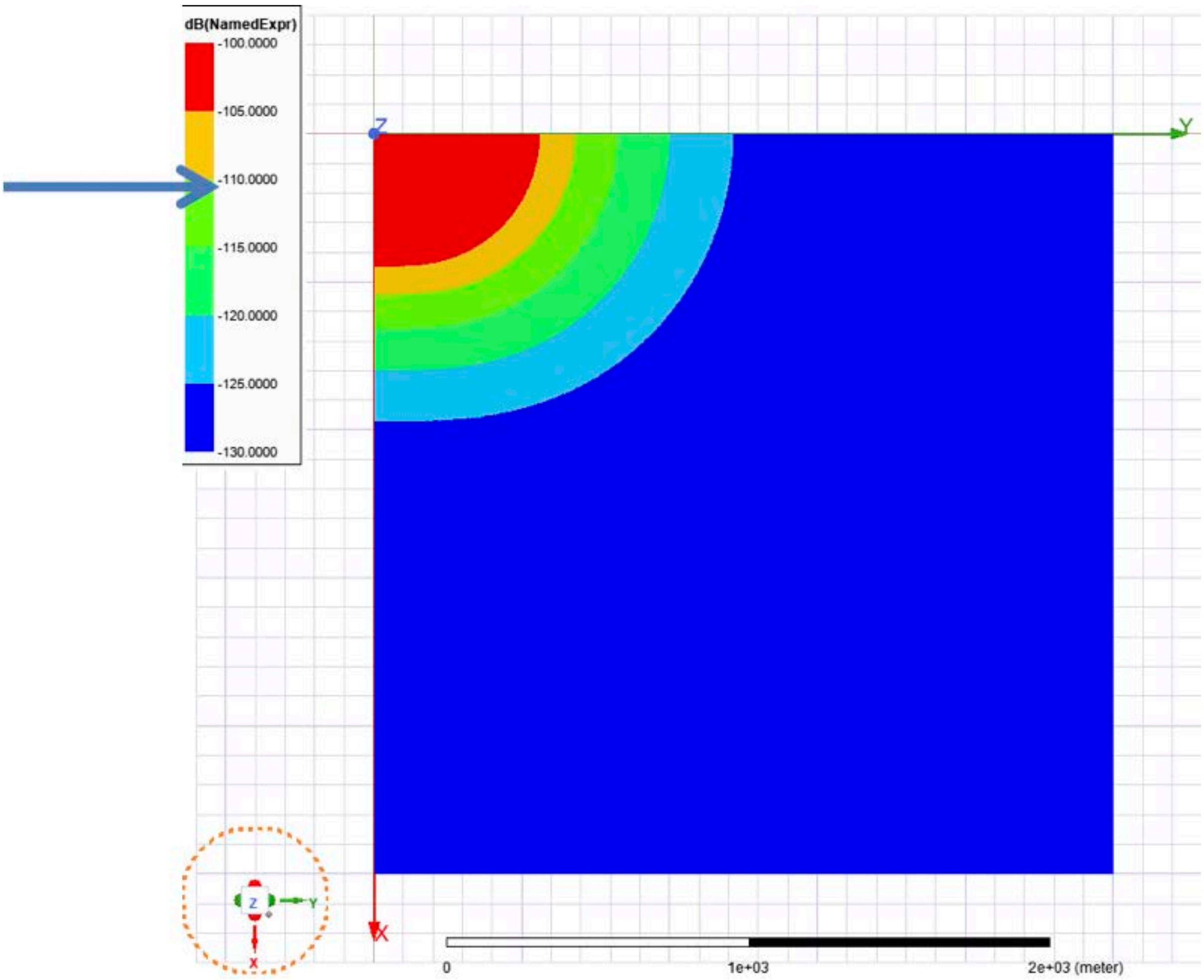

Figure 230: Simulation 2: 4kHz Tangential 20W at 50m results

Simulation 3:

Frequency: 4 kHz
Magnetic Field: **Normal**
Electrodes separation **~20m**
Injected power ~ **20W**
Distance scale 100m/div.

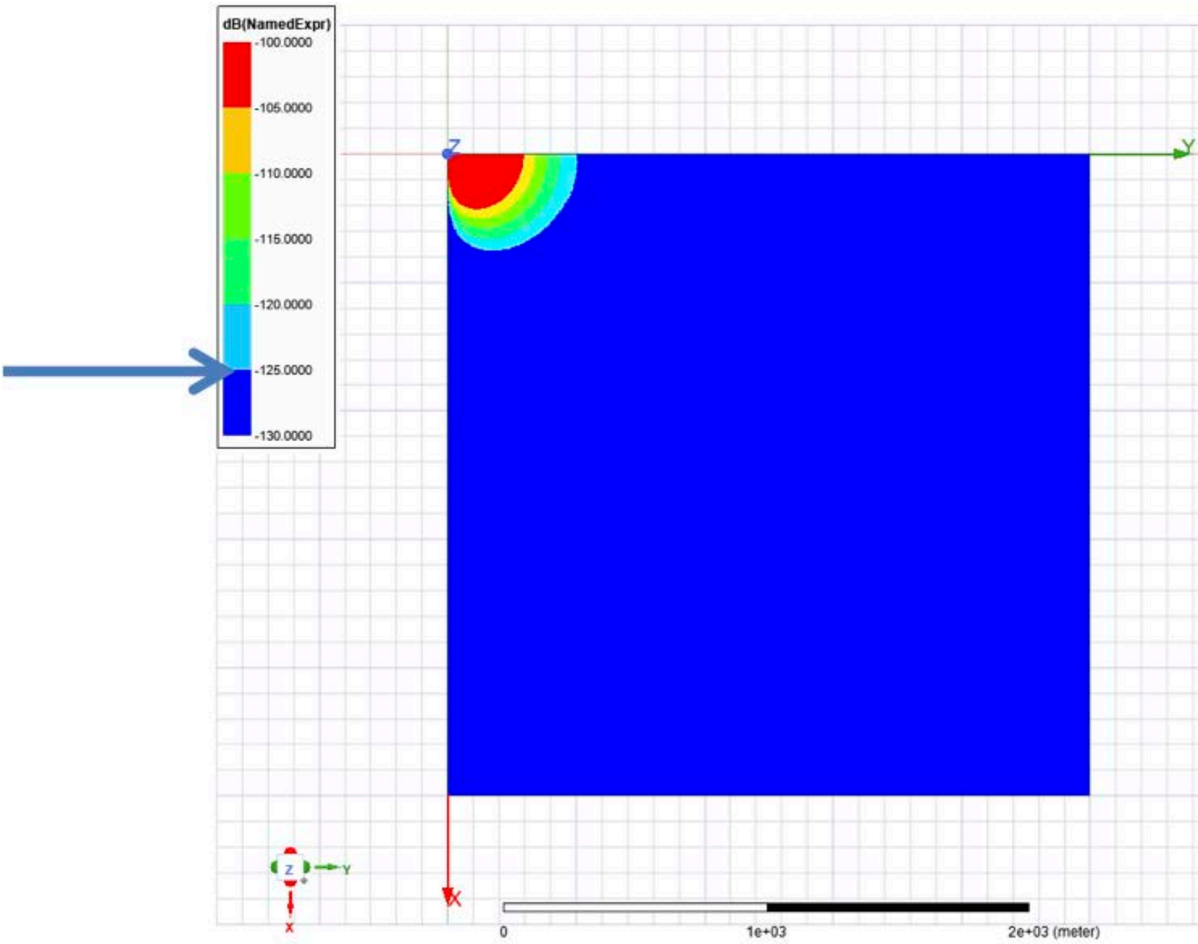

Figure 231: Simulation 3: 4kHz Normal 20W at 20m results

Simulation 4:

Frequency: 4 kHz
Magnetic Field: **Tangential**
Electrodes separation ~**20m**
Injected power ~ **20W**
Distance scale 100m/div.

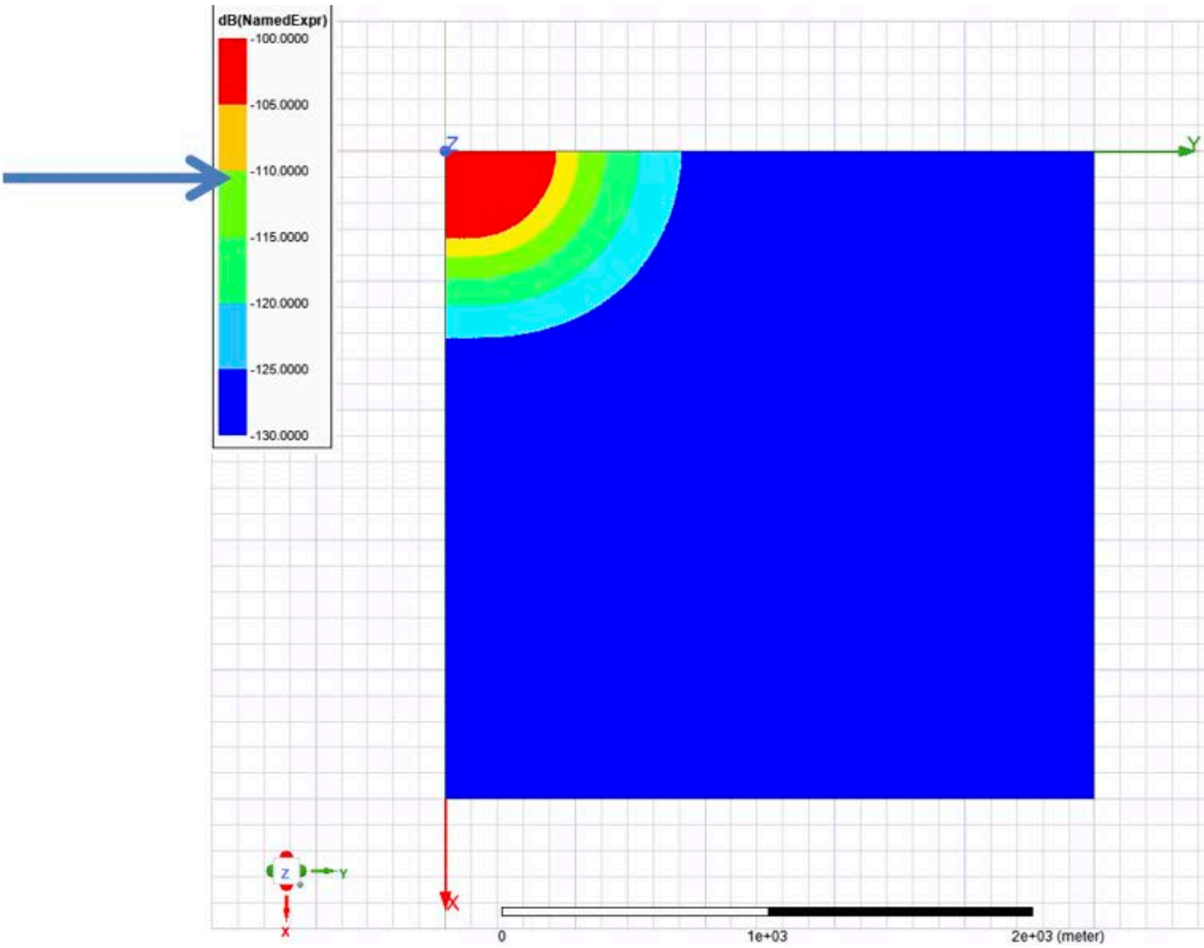

Figure 232: Simulation 4: 4kHz Tangential 20W at 20m results

Simulation 5:

Frequency: 4 kHz
Magnetic Field: **Normal**
Electrodes separation **~10m**
Injected power ~ **20W**
Distance scale 100m/div.

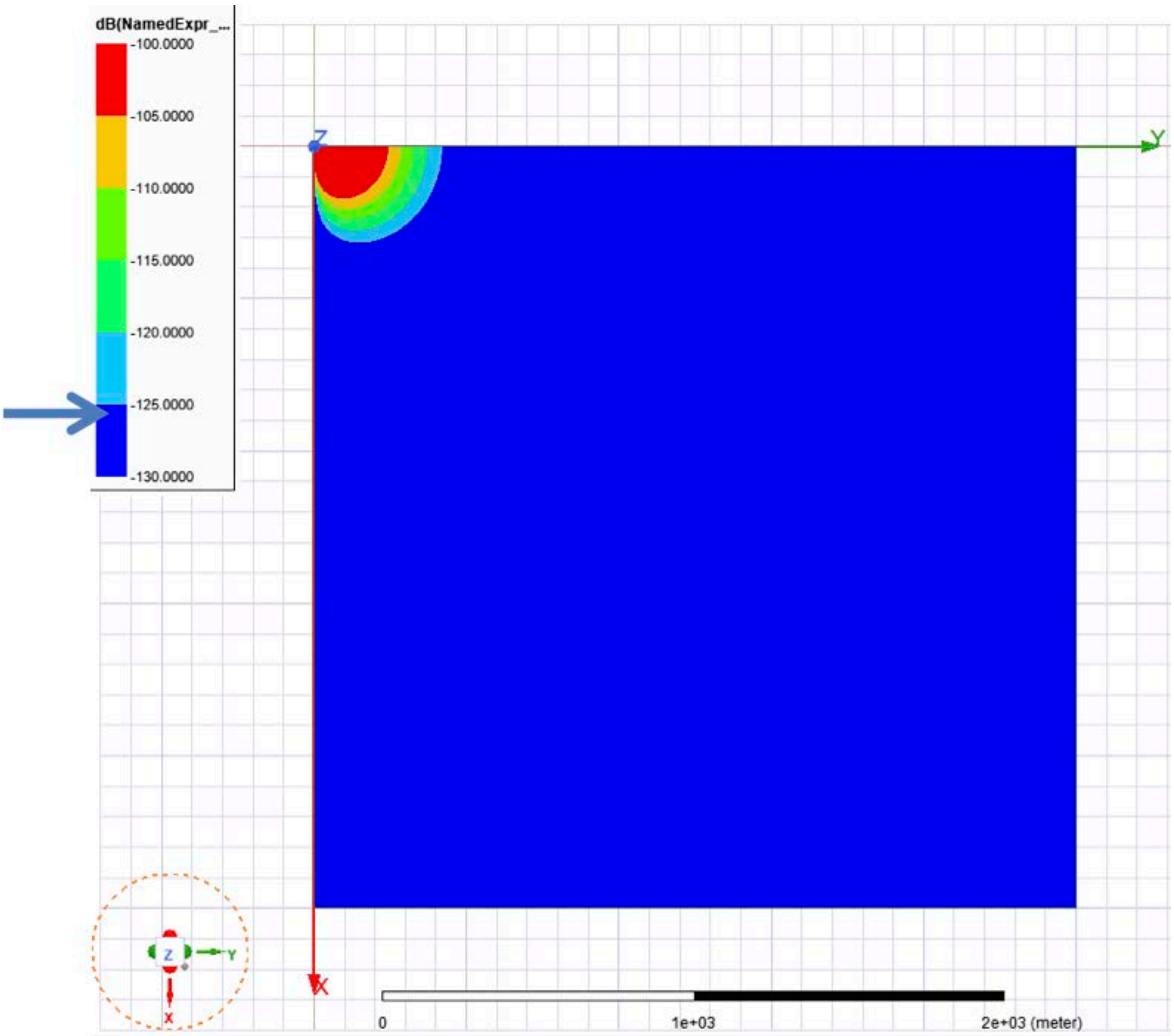

Figure 233: Simulation 5: 4kHz Normal 20W at 10m results

Simulation 6:

Frequency: 4 kHz
Magnetic Field: **Tangential**
Electrodes separation **~10m**
Injected power ~ **20W**
Distance scale 100m/div.

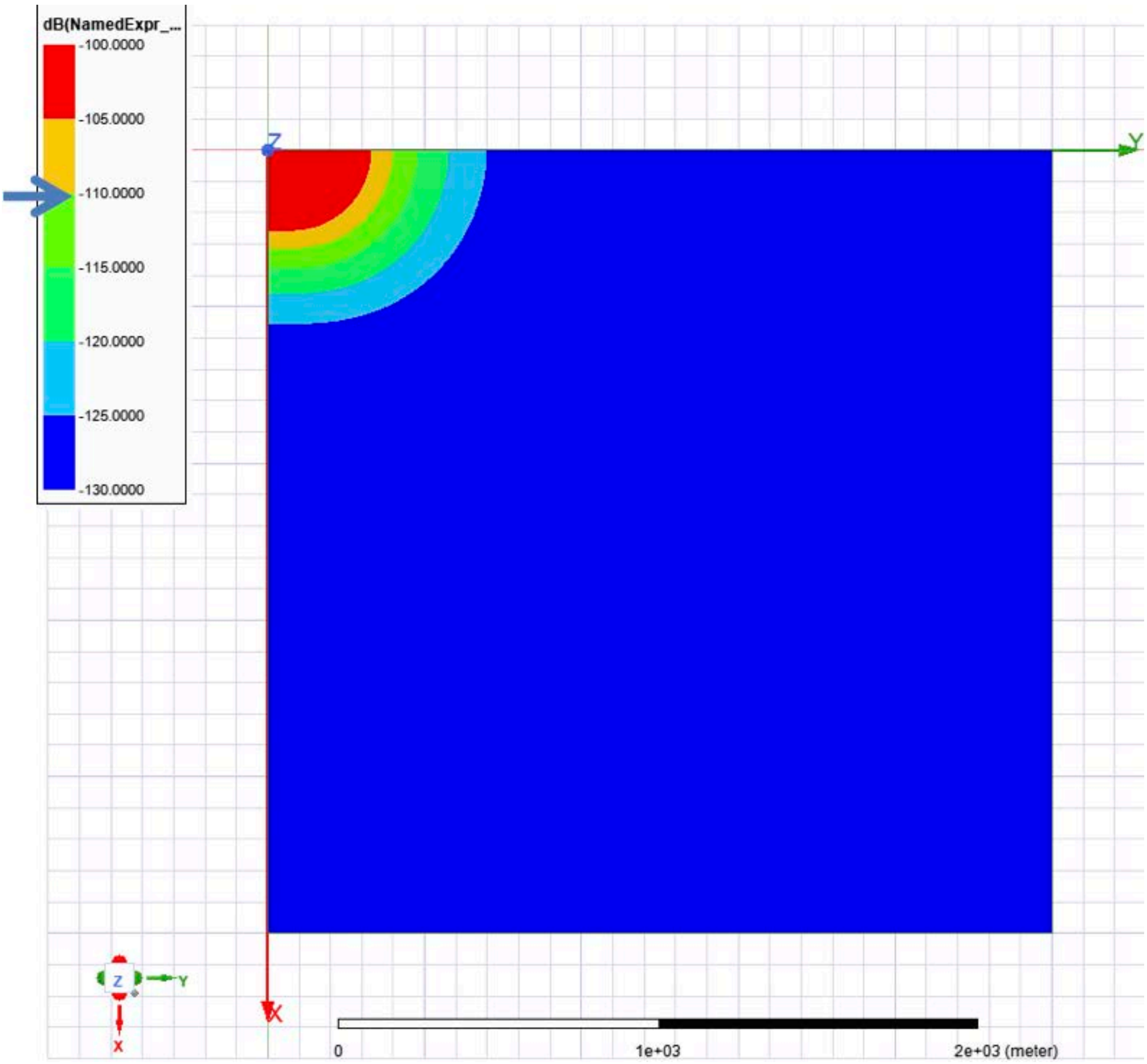

Figure 234: Simulation 6: 4kHz Tangential 20W at 10m results

Simulation 7:

Frequency: 4 kHz
Magnetic Field: **Normal**
Electrodes separation **~50m**
Injected power ~ **1800W**
Distance scale 100m/div.

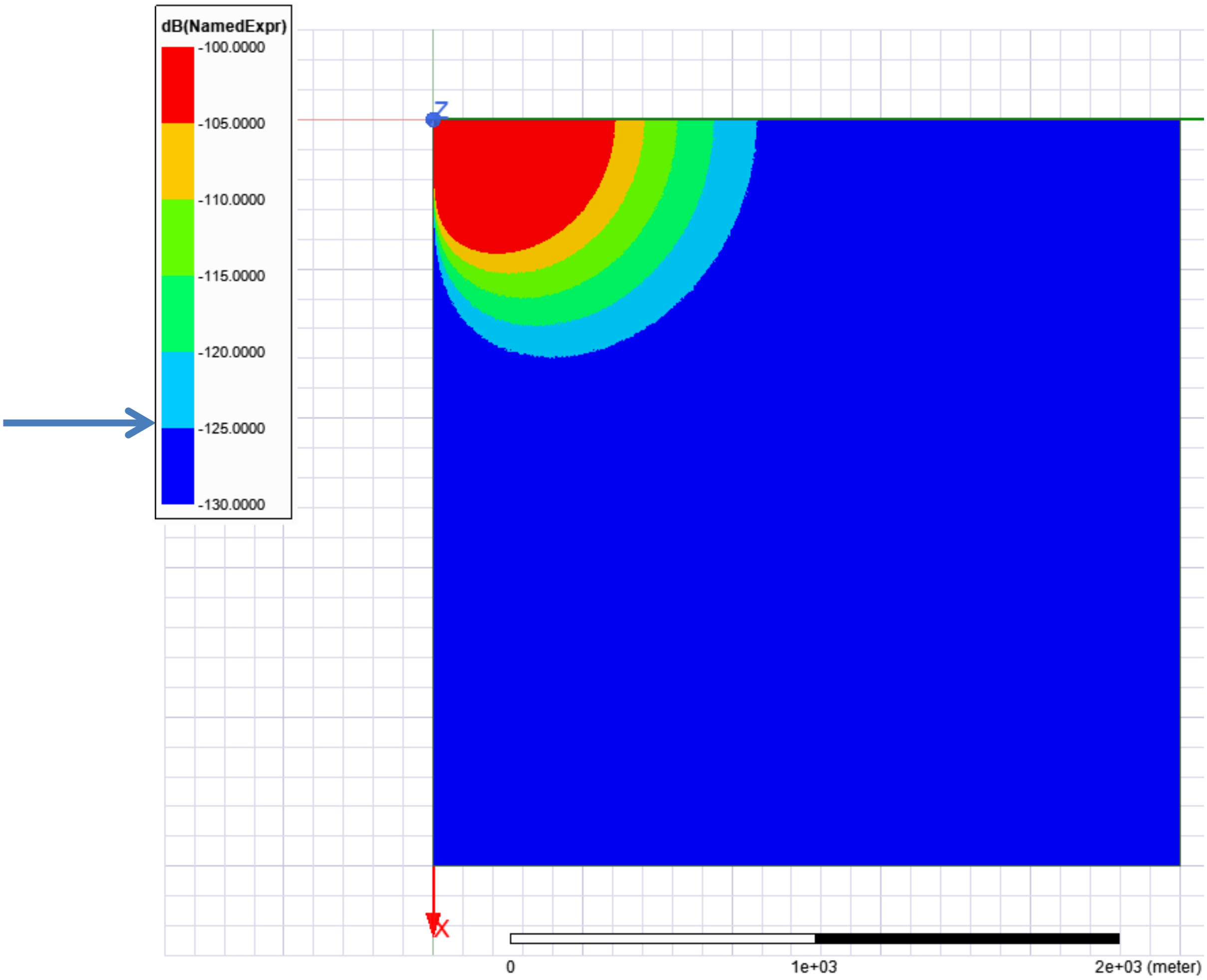

Figure 235: Simulation 7: 4kHz Normal 1800W at 50m results

Simulation 8:

Frequency: 4 kHz
Magnetic Field: **Tangential**
Electrodes separation **~50m**
Injected power ~ **1800W**
Distance scale 100m/div.

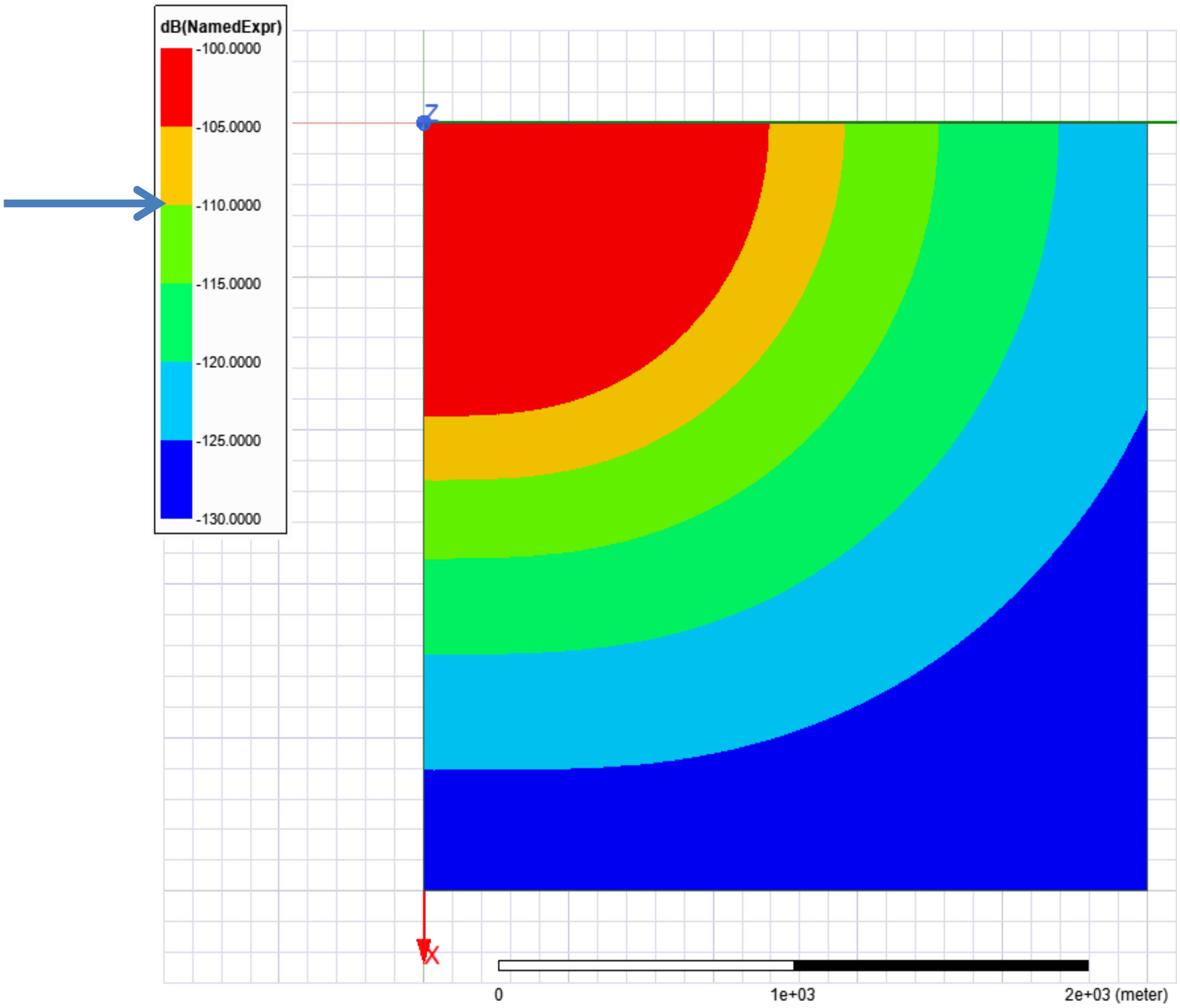

Figure 236: Simulation 8: 4kHz Tangential 1800W at 50m results

Simulation 9:

Frequency: 4 kHz
Magnetic Field: **Normal**
Electrodes separation **~50m**
Injected power ~ **3600W**
Distance scale 100m/div.

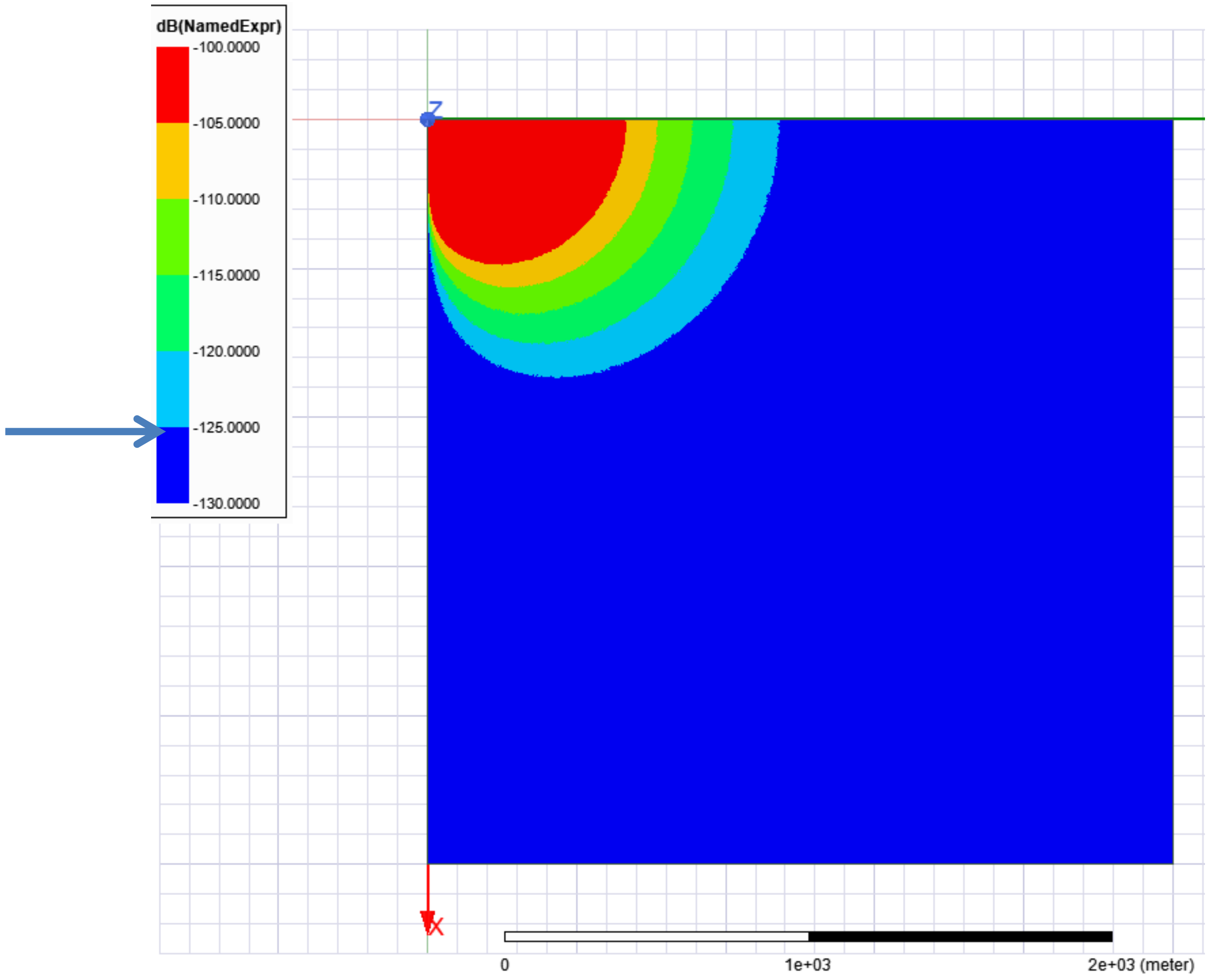

Figure 237: Simulation 9: 4kHz Normal 3600W at 50m results

Simulation 10:

Frequency: 4 kHz
Magnetic Field: **Tangential**
Electrodes separation **~50m**
Injected power ~ **3600W**
Distance scale 100m/div.

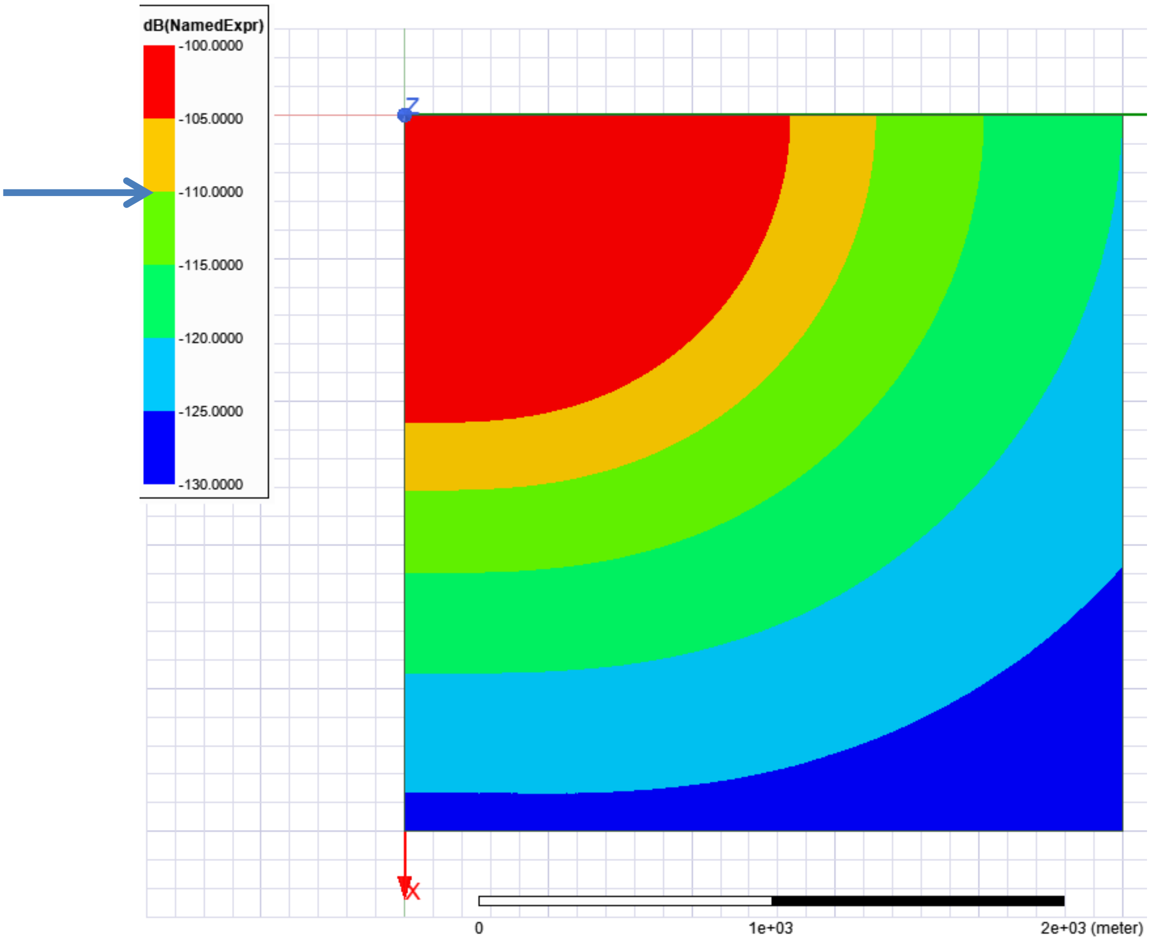

Figure 238: Simulation 10: 4kHz Tangential 3600W at 50m results

Simulation 11:

Frequency: 4 kHz
Magnetic Field: **Normal**
Electrodes separation ~**20m**
Injected power ~ **1800W**
Distance scale 100m/div.

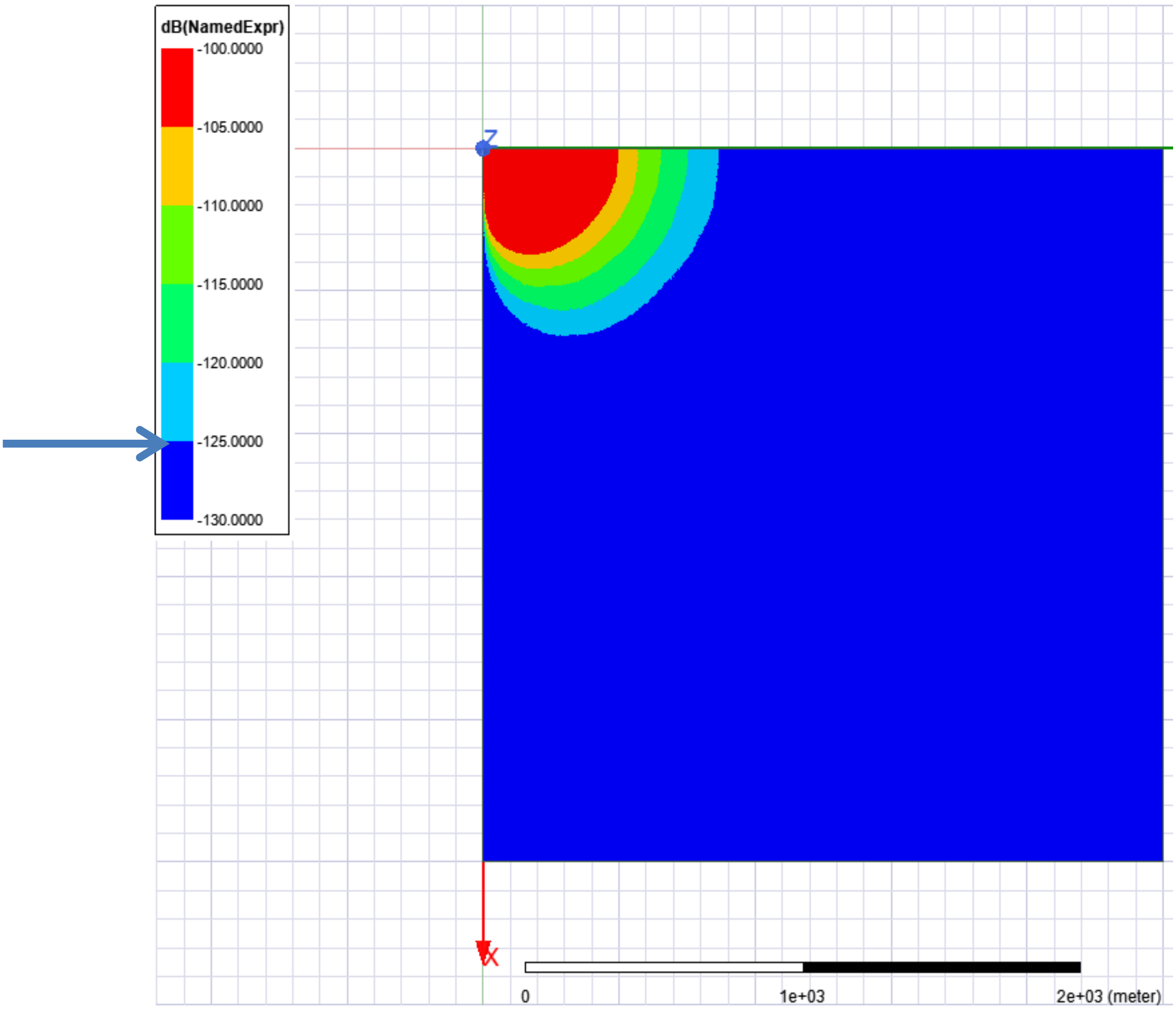

Figure 239: Simulation 11: 4kHz Normal 1800W at 20m results

Simulation 12:

Frequency: 4 kHz
Magnetic Field: **Tangential**
Electrodes separation ~**20m**
Injected power ~ **1800W**
Distance scale 100m/div.

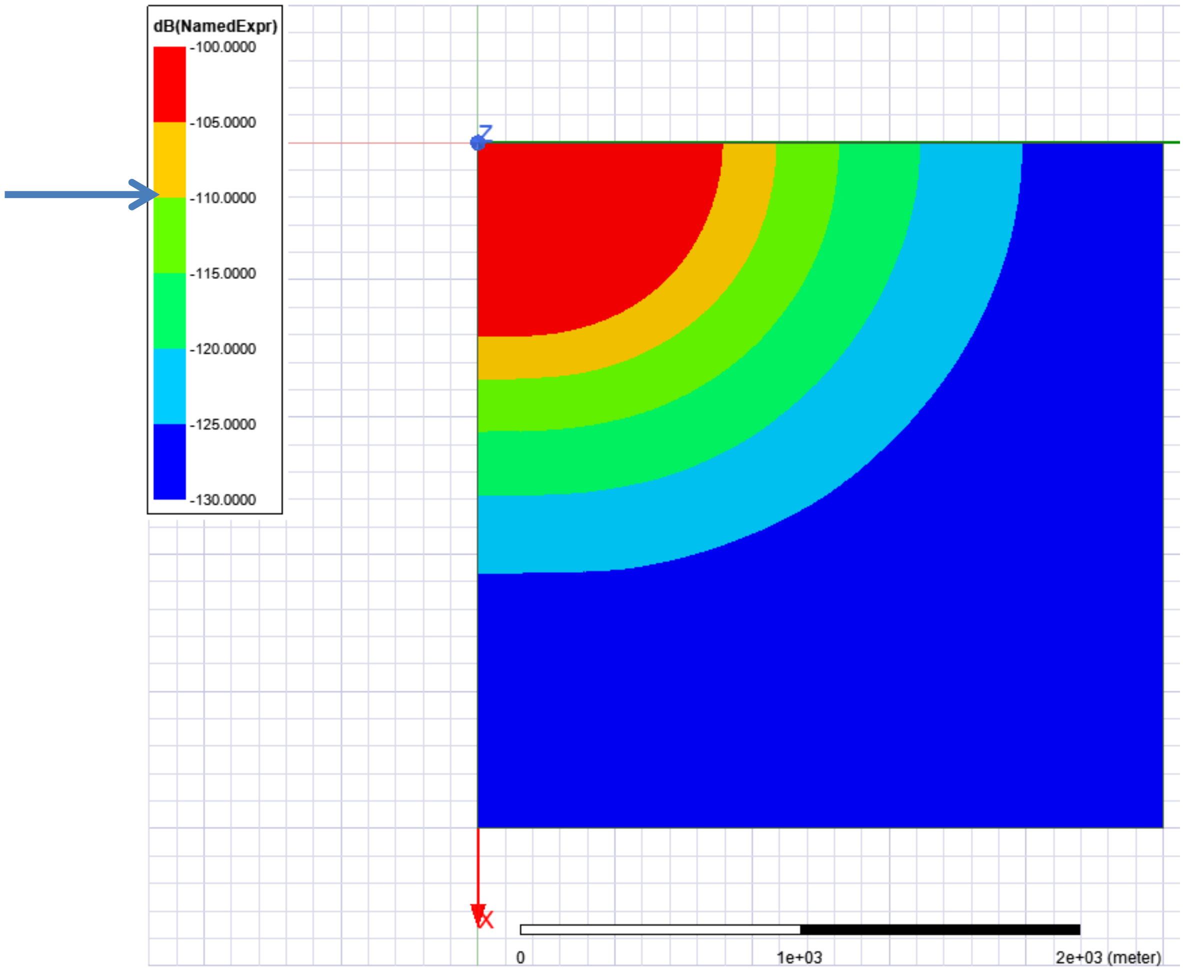

Figure 240: Simulation 12: 4kHz Tangential 1800W at 20m results

Simulation 13:

Frequency: 4 kHz
Magnetic Field: **Normal**
Electrodes separation **~20m**
Injected power ~ **3600W**
Distance scale 100m/div.

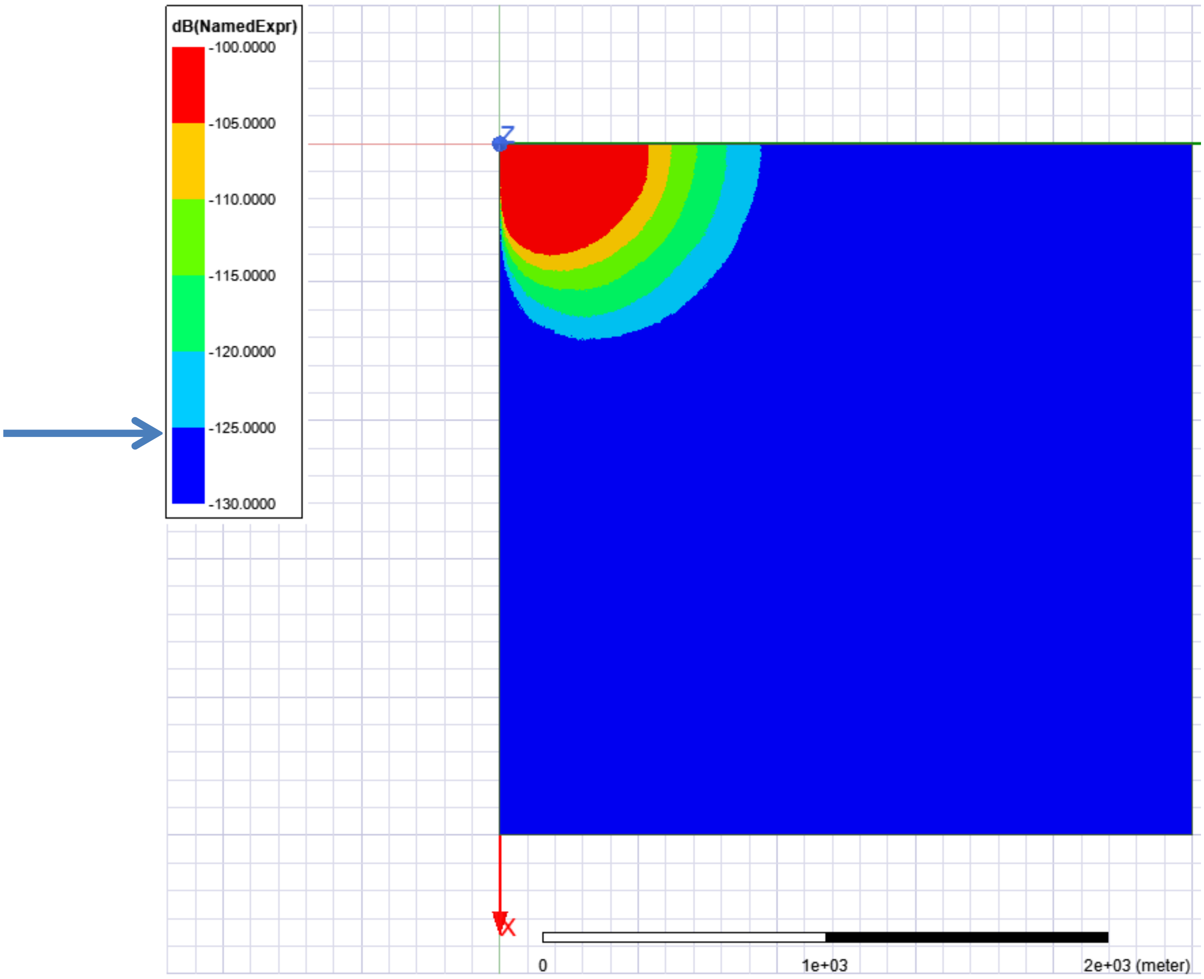

Figure 241: Simulation 13: 4kHz Normal 3600W at 20m results

Simulation 14:

Frequency: 4 kHz
Magnetic Field: **Tangential**
Electrodes separation **~20m**
Injected power ~ **3600W**
Distance scale 100m/div.

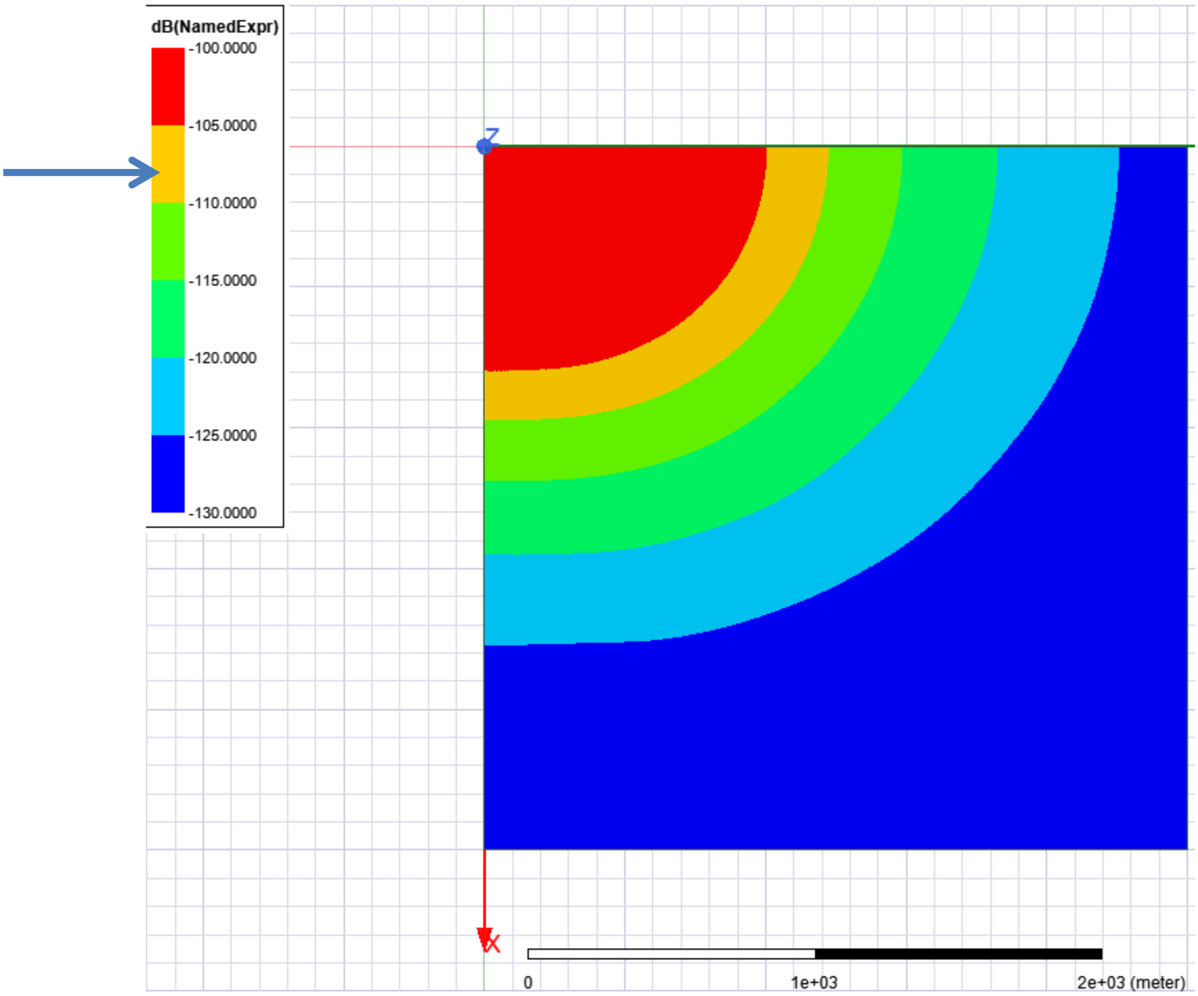

Figure 242: Simulation 14: 4 kHz Tangential 3600W at 20m results

Simulation 15:

Frequency: 4 kHz
Magnetic Field: **Normal**
Electrodes separation **~10m**
Injected power ~ **1800W**
Distance scale 100m/div.

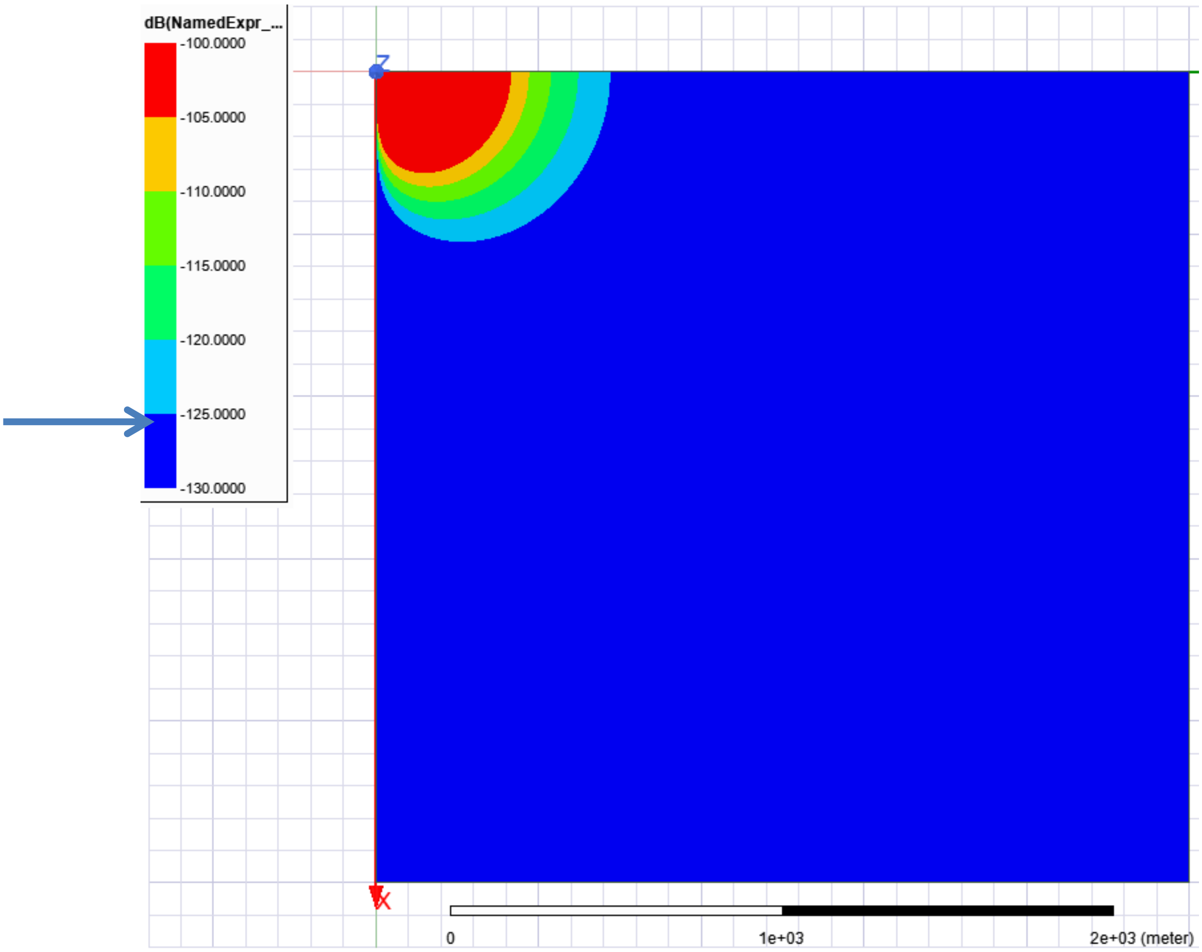

Figure 243: Simulation 15: 4kHz Normal 1800W at 10m results

Simulation 16:

Frequency: 4 kHz
Magnetic Field: **Tangential**
Electrodes separation **~10m**
Injected power ~ **1800W**
Distance scale 100m/div.

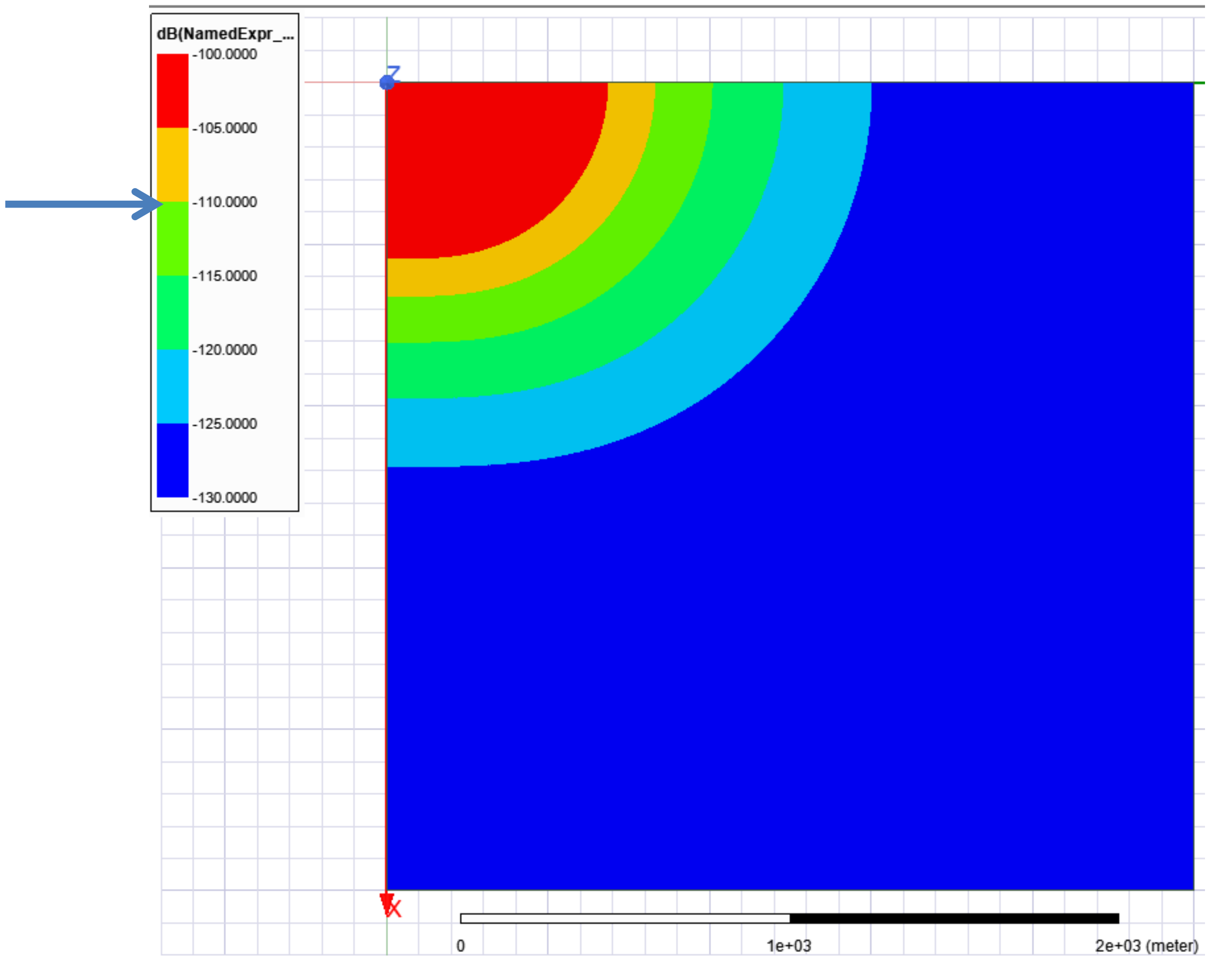

Figure 244: Simulation 16: 4kHz Tangential 1800W at 10m results

Simulation 17:

Frequency: 4 kHz
Magnetic Field: **Normal**
Electrodes separation **~10m**
Injected power ~ **3600W**
Distance scale 100m/div.

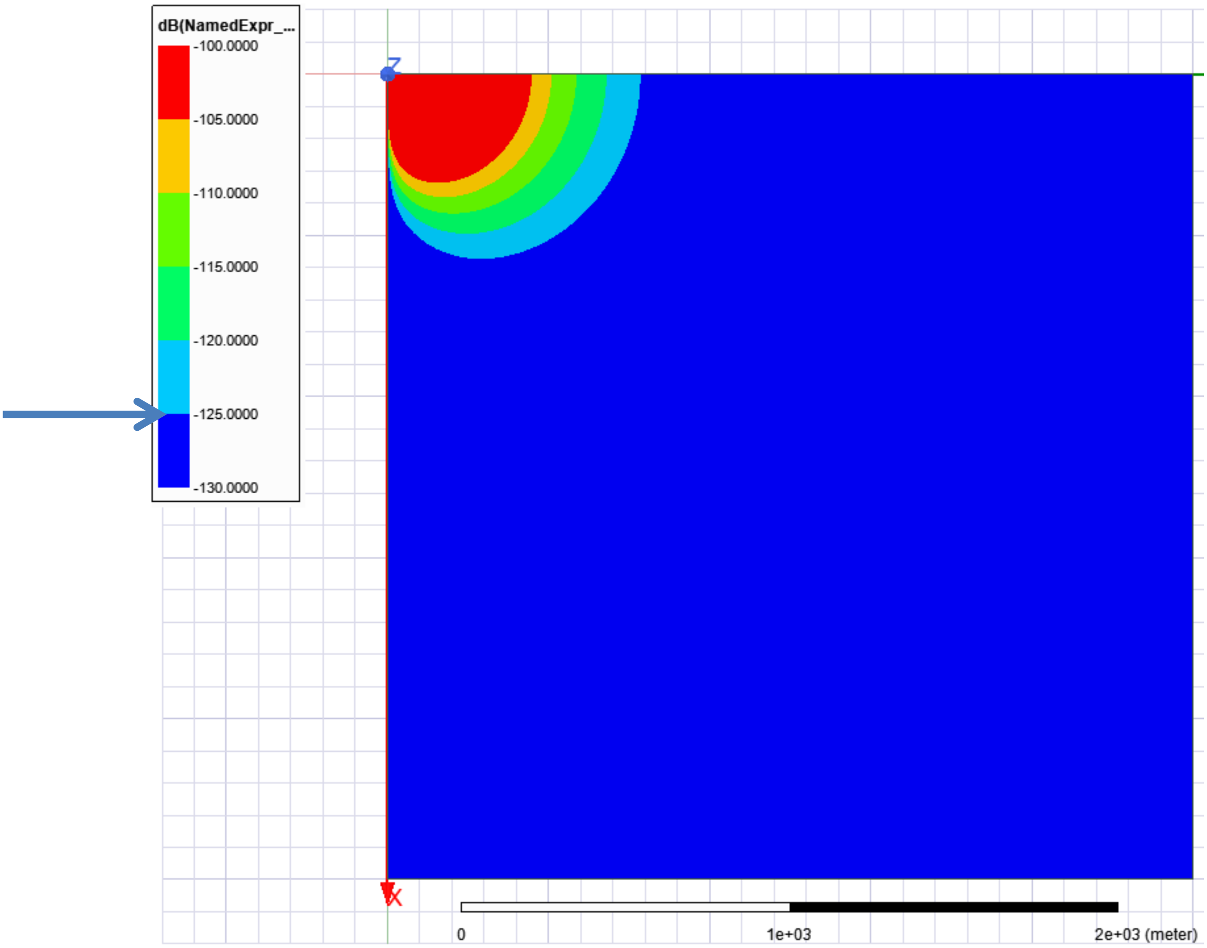

Figure 245: Simulation 17: 4kHz Normal 3600W at 10m results

Simulation 18:

Frequency: 4 kHz
Magnetic Field: **Tangential**
Electrodes separation **~10m**
Injected power ~ **3600W**
Distance scale 100m/div.

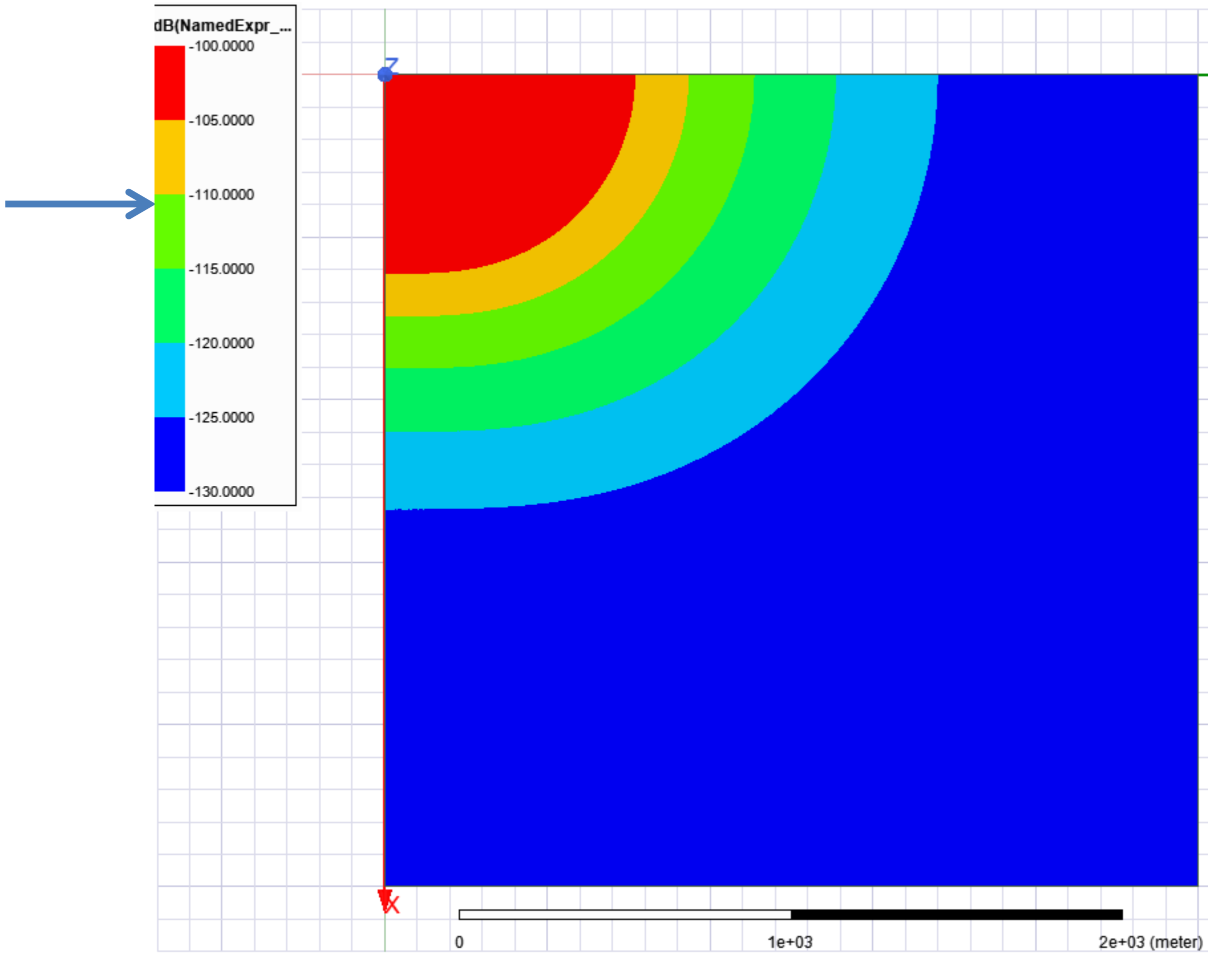

Figure 246: Simulation 18: 4kHz Tangential 3600W at 10m results